Wissenschaftszentrum Weihenstephan
für Ernährung, Landnutzung und Umwelt

Experimentelle Radioonkologie und Strahlenbiologie

Differential Protein Expression in CAIX Depleted HeLa Cells under Different Oxygen Conditions

Katharina Elisabeth Bertram

Vollständiger Abdruck der vom Wissenschaftszentrum Weihenstephan für Ernährung, Landnutzung und Umwelt der Technischen Universität München zur Erlangung des akademischen Grades eines

Doktors der Naturwissenschaften (Dr. rer. nat.)

genehmigten Dissertation.

Vorsitzende(r): Univ.-Prof. Dr. J. J. Hauner

Prüfer der Dissertation:

1. Univ.-Prof. Dr. G. Multhoff
2. Univ.-Prof. Dr. A. Görlach
3. apl. Prof. Dr. J. Graw

Die Dissertation wurde am 26.11.2015 bei der Technischen Universität München eingereicht und durch das Wissenschaftszentrum Weihenstephan für Ernährung, Landnutzung und Umwelt am 06.04.2016 angenommen.

Für E.

INDEX

Abbreviations

2DE	two-dimensional gel electro-phoresis
4E-BP	Eukaryotic translation initiation factor 4E-binding protein
4E-BP1	Eukaryotic translation initiation factor 4E-binding protein 1
A549	Lung adenocarcinoma cell line
Acc. ID	Accession IDs
ACTB	β-actin, *Homo sapiens*
Actin-rp3	Actin-related protein 3
ADAM17	ADAM metallopeptidase domain 17, *also see* TACE
ADP	adenosine diphosphate
ADRP	adipose differentiation-related protein
Akt	Serine/threonine-protein kinase Akt
ALDH	Aldehyde dehydrogenase
ARNT	Aryl hydrocarbon receptor nuclear translocator
ATF4	cAMP-dependent trans-cription factor ATF-4
ATF6	cAMP-dependent trans-cription factor ATF-6 α or Activating transcription factor 6α
ATP	adenosine triphosphate
BAPTA	1,2-bis(o-aminophenoxy)ethane-N,N,N',N'-tetraacetic acid
BAX	BCL2-associated X protein
BiP	immunoglobulin heavy-chain binding protein, *see* GRP-78
bp	Base pairs
C1qBP	Complement component 1 Q subcomponent-binding protein, mitochondrial
CA	Carbonic anhydrase
Ca^{++}	Ca^{2+}, calcium ions
CAI	CAIX inhibitor or Carbonic anhydrase I
CAII	Carbonic anhydrase II
CA9	Carbonic anhydrase 9, *Homo sapiens*
CAIX	Carbonic anhydrase IX
CA12	Carbonic anhydrase 12, *Homo sapiens*
CAXII	Carbonic anhydrase XII
cAMP	Cyclic adenosine mono-phosphate
Cdk1	Cyclin-dependent kinase 1
Chaps	3-[(3-cholamidopropyl)di-methyl-ammonio]-1-propane-sulfonate
CHOP	C/EBP homologous protein
CI-23kD	NADH dehydrogenase [ubi-quinone] iron-sulfur protein 8, mitochondrial
CO_2	Carbon dioxide
Ctr	Control
ddH_20	Aqua bidestillata
DDR	DNA damage response
DEPC	Diethylpyrocarbonate
DMOG	Dimethyloxalylglycine
DNA	Deoxyribonucleic acid
DNA-PK	DNA dependent protein kinase

ECL	Enhanced chemiluminescent reagent
EDTA	Ethylenediaminetetraacetic acid
eEF2	Eukaryotic elongation factor 2
eEF2K	Eukaryotic elongation factor 2 kinase
EF-1-δ	Elongation factor 1-δ
EGTA	Ethylene glycol tetraacetic acid
eIF2α	PRKR-like ER kinase (PERK)-eukaryotic translation initiation factor 2α or Eukaryotic translation initiation factor 2 α
eIF4A	Eukaryotic initiation factor 4A
eIF4E	Eukaryotic translation initiation factor 4E
eIF4B	Eukaryotic translation initiation factor 4B
eIF4F	Complex containing eIF4A, eIF4E and eIF4G
eIF4G	Eukaryotic translation initiation factor 4 γ
EMT	Epithelial-to-mesenchymal-transition
ER	Endoplasmic reticulum
ERAD	ER-associated protein degradation
eRF1	Eukaryotic translation termination factor 1 or Eukaryotic peptide chain release factor subunit 1
eRF3a	Eukaryotic peptide chain release factor GTP-binding subunit ERF3A
ERK	Mitogen-activated protein kinase or extracellular-signal-regulated kinases
ERp44	Endoplasmic reticulum resident protein 44
ERp46	Thioredoxin reductase 1, cytoplasmic
ERp57	Endoplasmic reticulum resident protein 57, Protein disulfide-isomerase A3
ERp72	Endoplasmic reticulum resident protein 72, Protein disulfide-isomerase A4
FDR	False discovery rate
FIH	Factor-inhibiting HIF-1
FKBP4	*see* PPIase FKBP4
GADD34	growth arrest and DNA damage-inducible protein 34
GRP-78	78 kDa glucose-regulated protein, Endoplasmic reticulum ivuminal Ca(2+)-binding protein grp78, Heat shock 70 kDa protein 5, Immunoglobulin heavy chain-binding protein
GRP94	GRP-94
GRP-94	94 kDa glucose-regulated protein, Endoplasmin
GRP-170	170 kDa glucose-regulated protein, *see* ORP-150
GTP	Guanosine-5'-triphosphate
H^+	Proton
HCO_3^-	Hydrogen carbonate
H_2CO_3	Carbonic acid
HCl	Hydrogen chloride
HDGF	Hepatoma-derived growth factor
HeLa	Cervical carcinoma cell line
HIF-1	Hypoxia-inducible factor 1

HIF-1α	Hypoxia-inducible factor 1 α
HIF-2α	Hypoxia-inducible factor 2 α
hnRNP U	Heterogeneous nuclear ribo-nucleoprotein U
HPLC	High pressure liquid chromato-graphy
HRE	Hypoxia response elements
Hsp	Heat shock protein
Hsp40	Heat shock 40 kDa protein
Hsp60	60 kDa heat shock protein, mitochondrial
Hsp70	Heat shock 70 kDa protein
Hsp90	Heat shock protein HSP 90
HX	Hypoxia
ID	Idenitification
IEF	Isoelectric focussing
$InsP_3R$	Inositol triphosphate receptor
IPG	Immobilised pH gradient gel strips
IRE1	Serine/threonine-protein kinase/endoribonuclease IRE1 or Inositol-requiring protein 1
IRS1	Insulin receptor substrate 1
JNK	JUN N-terminal kinase
kDa	Kilo Dalton
KIF	Kinesin family member
MCT	Monocarboxylate transporter
MEK	Mitogen-activated protein kinase kinase
Mnk	MAP kinase-interacting serine/ threonine-protein kinase
Mnk1	MAP kinase-interacting serine/ threonine-protein kinase 1
Mnk2	MAP kinase-interacting serine/ threonine-protein kinase 2
mRNA	Messenger ribonucleic acid
MS	Mass spectrometry
mTOR	Serine/threonine-protein kinase mTOR, Mammalian target of rapamycin
mTORC	mTOR complex protein
MW	Molecular weight
Na^+	Sodium ion
NBCe1	Na^+/HCO_3^--co-transporter e1
NBC	Na^+/HCO_3^--co-transporter
NEF	ORP-150 and nucleotide exchange factor SIL1
NF-κB	nuclear factor “kappa-light-chain-enhancer” of activated B-cells
NOX	NADPH oxidase
NUCB1	Nucleobindin-1
NUFDAF1	Complex I intermediate-associated protein 30, mito-chondrial
NX	Normoxia
ORP-150	Hypoxia up-regulated protein 1
p	Phosphorylation
p53	Cellular tumor antigen p53
PAGE	Polyacrylamide gel electro-phoresis
PAK	p21-activated kinase
PARP-1	Poly [ADP-ribose] polymerase 1
PAT	PAT protein family involving perilipin, ADRP and TIP47
PBS	Phosphate buffered saline
PCA	Principal component analysis
PCR	Polymerase chain reaction
PDCD4	Programmed cell death protein 4
PDI	Protein disulfide isomerase

PDK1	3-phosphoinositide-dependent protein kinase 1
PERK	PRKR-like endoplasmic reticulum kinase or Eukaryotic translation initiation factor 2-alpha kinase 3
pH_e	Extracellular pH
pH_i	Intracellular pH
pI	Isoelectric point
PI3K	Phosphatidylinositol 3'-kinase
PIP2	Phosphatidylinositol-4,5-bisphosphate
PIP3	Phosphatidylinositol-3,4,5-trisphosphate
PMI	Mannose-6-phosphate isomerase
PMT	Photomultiplier
PPIase	Peptidyl-prolyl cis-trans
FKBP4	isomerase FKBP4
PR	Protected region
PRAS40	Proline-rich AKT1 substrate 1, AKT1S1
PTEN	Phosphatidylinositol 3,4,5-trisphosphate 3-phosphatase and dual-specificity protein phosphatase PTEN
qPCR	Real-time polymerase chain reaction
Raf	Rapidly accelerated fibrosarcoma
Ras	Rat sarcoma
ReOX	Reoxygenation
RIDD	Regulated IRE1-dependent decay
RNAi	RNA interference
ROS	Reactive oxygen species
RSK	ribosomal s6 kinase
RTK	Receptor tyrosine kinase
RuBPS	Ruthenium(II)tris(bathophenantroline disulfonate)
S6K	Ribosomal S6 kinase
SDS	Sodium dodecyl sulphate
SERCA	sarcoplasmic/endoplasmic reticulum calcium ATPase
siCA9	siRNA directed against *CA9*
siCtr	Control siRNA
SiHa	Cervical carcinoma cell line
SIL1	nucleotide exchange factor SIL1
siRNA	Small interfering RNA
SP1	Transcription factor Sp1
SP3	Transcription factor Sp3
Src	Proto-oncogene tyrosine-protein kinase Src
SS	SameSpots software
TACE	Tumor necrosis factor-α-converting enzyme, *see* ADAM17
TBS-T	Tris buffered salt solution containing Tween-20
TCP-1-α	T-complex protein 1 subunit alpha
TEMED	Tetramethylethylenediamine
TIP47	Tail-interacting protein of 47 kDa
TMABA-DH	4-trimethylaminobutyraldehyde dehydrogenase
TRIP-5	Kinesin-like protein KIF11, TR-interacting protein 5
TRIP-13	Pachytene checkpoint protein 2 homolog, TR-interacting protein 13

Tris	Tris(hydroxymethyl)-amino-methan
Triton X-100	Polyethylene glycol p-(1,1,3,3-tetramethylbutyl)-phenyl ether
Tween-20	Polyoxyethylene (20) sorbitan monolaurate
UPR	Unfolded protein response
vs.	Versus
WB	Western blot
WebGestalt	WEB-based GEne SeT AnaLysis Toolkit
WT	Wild type
XBP1	Inositol-requiring protein 1α (IRE1α)-X-box binding protein 1
XBP1u	Uunspliced XBP1
XBP1s	Transcriptionally active XBP1

1 Abstract

Carbonic anhydrase IX (CAIX) is a pH regulating enzyme highly expressed in tumor cells. It is well established as a marker of hypoxic tumors and has been associated with poor therapeutic outcome. However, its specific role under hypoxic and reoxygenating conditions remains unclear. To identify proteins which are regulated following CAIX depletion, a differential display 2DE proteomics study was employed using RNAi to silence *CA9* in HeLa cells. A total of 25 protein functions were found to be dysregulated following of CAIX depletion. In addition, five protein functions were identified to be differentially phosphorylated when the cells were depleted of CAIX. The proteomics results support an involvement of CAIX in endoplasmic reticulum stress and the unfolded protein response. Cells depleted of CAIX showed impaired onset of the unfolded protein response. Independent of the oxygen status, CAIX was found to be involved in the regulation of cap-dependent translation. Functional assays revealed reduced viability, caspase 3/7 expression and activity in cells depleted of CAIX independent of the oxygen state. At the same time, protein levels of ERp44 and calpastatin were found to be decreased. These findings support a role of the endoplasmic reticulum and the calpain pathway in the regulation of apoptosis following CAIX depletion. Taken together, the present study suggests a role of CAIX in endoplasmic reticulum stress, the unfolded protein response and in cell survival and protection against apoptosis.

2 Introduction

Regulation of cellular pH is a prerequisite of virtually all cellular functions. Enzymes require optimal pH conditions in order to maintain their tertiary structure and fulfill their functions inside the cytosol or within different organelles. In addition, protons (H^+) are used as "energy currency" of the cell (Casey et al., 2010). The stability of the pH is important for functional maintenance of the cellular system. Changes in the mitochondrial pH can lead to apoptosis (Matsuyama and Reed, 2000) showing the fragility of the equilibrium.

The cytosolic pH can be regulated in many ways such as through alkali cation-H^+-exchangers, bicarbonate transporters or lactate-H^+ co-transporters (Aharonovitz et al., 2000; Casey et al., 2010). It is well established that the intracellular pH (pH_i) also strongly depends on the pH (pH_e) of the extracellular space (Mellergard et al., 1994). Besides ion-pumps or transporters, another important class of enzymes involved in the regulation of pH are the carbonic anhydrases.

2.1 Carbonic Anhydrase IX – Structure and Function

Carbonic anhydrases (CA) are metalloenzymes that require a zinc ion in the form of Zn(II) for their activity. They are phylogenetically highly conserved, expressed in all organs and are involved in various cellular processes such as electrolyte metabolism, gluconeogenesis and lipogenesis (Maren, 1967). However, the crucial role of carbonic anhydrases lies in their regulation of the acid-base balance and the regulation of the pH (Swietach et al., 2010).

Mammalian carbonic anhydrases are α-carbonic anhydrases and are found in a variety of cell types and tissues. A number of 16 isoforms have been identified in the cytosol or the mitochondria, some of them are transmembrane proteins and few isoforms are thought to remain inactive (Chegwidden and Carter, 2000). Carbonic anhydrases are expressed particularly in tissues and body secretions where the modulation of pH is required such as in the gastrointestinal tract (Fleming et al., 1995), the saliva (Kivela et al., 1999), the cerebrospinal fluid (Brown et al., 2004) or the bone (Riihonen et al., 2007).

Functionally, α-carbonic anhydrases catalyse the formation of the intermediate compound carbonic acid (H_2CO_3) which is the first step in the conversion from carbon dioxide (CO_2) to hydrogen

carbonate (HCO_3^-) and H^+. The proton donation to the final HCO_3^- occurs spontaneously (Breton, 2001; Gilmour, 2010). Since CO_2 is transported in the cellular system in the form of HCO_3^- this conversion is essential for the physiology of the cell.

Of particular importance among the α-carbonic anhydrases is the isoenzyme IX (CAIX). Although the isoform is known to be present in normal conditions in the stomach and the intestine (Pastorekova et al., 1997; Saarnio et al., 1998), it is mainly expressed in tumour cells (Pastorekova et al., 2004; Zavada et al., 1993). This makes CAIX unique in the group of α-CA since it is not only expressed in normal tissues, but is also needed to maintain the pathological state whereas all other α-CA isoenzymes are only necessary for "housekeeping"-activities of the cell, tissue or bodyfluids.

The hypoxic regulation of CAIX is already evident at DNA level (Wykoff et al., 2000) since the *CA9* promoter possesses hypoxia response elements (HRE) that enable transcriptional control by hypoxia-inducible factor 1α (HIF-1α). In addition, protected region (PR) elements have been identified that enable regulation by transcription factors Sp1 and Sp3 (SP1/SP3) activity. This was hypothesised to modulate *CA9* expression under different conditions and partly independent of HIF-1α by enhancing the binding of other transcription factors when higher cell density is achieved independently on the oxygenation state (Kaluz et al., 2003). In renal cancer it could be shown that hypomethylation of the CpG at -74 bp in the *CA9* promotor can regulate *CA9* expression (Cho et al., 2001).

The CAIX protein (Figure 1A) contains 459 amino acids and has a predicted isoelectric point (pI) of 4.39. The protein consists of a signal peptide (37 amino acids), an extracellular part (377 amino acids) containing the catalytical domain and proteoglycane-rich domain (Pastorekova et al., 1992), a transmembrane region (20 amino acids) and an intracellular tail of 25 amino acids (Opavsky et al., 1996). Although it has been suggested that CAIX can form trimers (Pastorekova et al., 1992), the enzyme was shown to be functional as a dimer (Hilvo et al., 2008) and to mostly occur in this form (Li et al., 2011). The crystal structure (Figure 1B) revealed that the dimer is stabilised by intermolecular disulfide bonds between two catalytic domains and pH measurements have shown that there is a clear correlation between the dimeric molecular structure and the CAIX function (Alterio et al., 2009).

The extracellular domain of CAIX is shedded under hypoxic conditions by the shedding enzyme ADAM17 (ADAM metallopeptidase domain 17, also known as tumor necrosis factor-α-converting

enzyme, TACE), but can also be shedded under basal conditions by a so far unidentified shedding enzyme (Zatovicova et al., 2005). At the molecular level, it has been suggested that the proteoglycan domain of CAIX is responsible for the sufficient hydratation of CO_2 at acidic pH_e which is a characteristic of solid tumors (Innocenti et al., 2009).

The intracellular domain has 3 putative phosphorylation sites, namely threonine443, serine448 and tyrosine449. Of these, tyrosine449 has been shown to be phosphorylated upon induction with epidermal-growth factor leading to Akt-pathway signaling (Dorai et al., 2005). Phosphorylation of threonine443 is required for the activity of CAIX under hypoxic conditions while serine448 needs to be in a dephosphorylated state (Ditte et al., 2011).

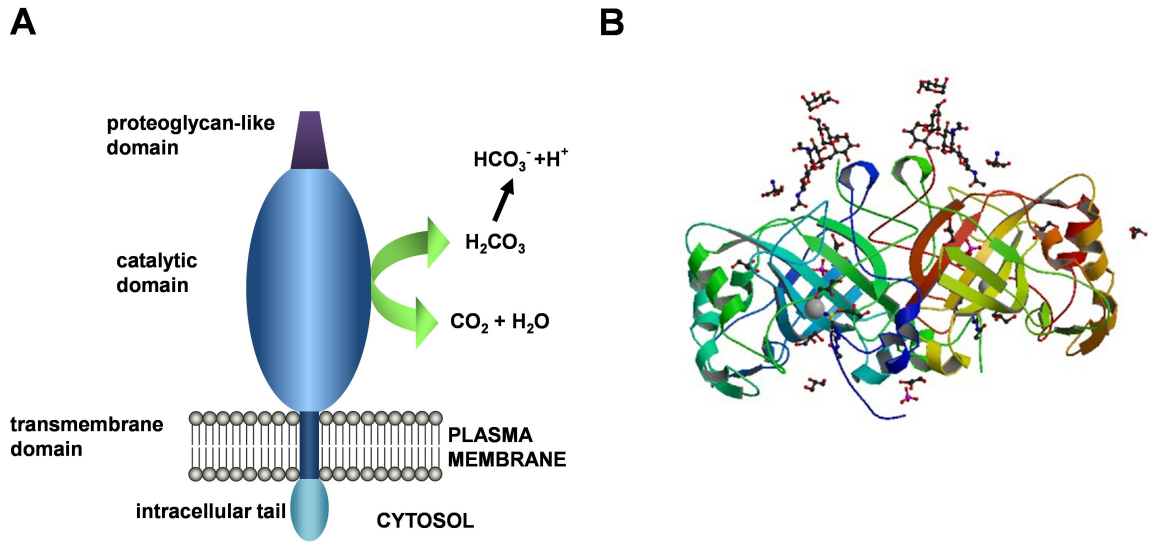

Figure 1 Carbonic anhydrase IX monomer
(A) Model of carbonic anhydrase monomer adapted from Cancer Therapy (Pastorekova and Zavada, 2004). (B) Crystal structure of the catalytic domain of CAIX, source: http://www.rcsb.org, PDB ID: 3IAI (Alterio et al., 2009; Berman et al., 2000).

CAIX is upregulated under hypoxia. This induction is mediated by HIF-1α (Kaluz et al., 2009). HIF-1 is a heterodimer composed of an oxygen sensing α-subunit and a constitutively expressed β-subunit (also reffered to as ARNT, aryl hydrocarbon receptor nuclear translocator). Under normoxic condition, the HIF-1α protein is instable, but it gets stabilised under reduced oxgyen concentrations (Semenza, 2001).

In addition to hypoxia, it has been shown that HIF-1α can be stabilised by other factors such as thrombin (Gorlach et al., 2001). Under these conditions, the regulation of HIF-1α via redox sensitive mechanisms and the generation of reactive oxygen species (ROS) by NADPH oxidases

(NOX) plays a crucial role (Gorlach et al., 2001; Gorlach and Kietzmann, 2007). It could be shown that both HIF-1α and CAIX levels are controlled by p53 (cellular tumor antigen p53) in response to DNA damage (Kaluzova et al., 2004). Being a target of HIF-1α, CAIX is not regulated by HIF-2α (Grabmaier et al., 2004). In addition, it has been shown that CAIX protein levels react to changes in the expression of FIH (factor-inhibiting HIF-1) which is a known regulator of HIF-1α and has a pivotal role in gene expression in response to the oxygen levels (Dayan et al., 2006).

In contrast to the induction under hypoxia by HIF-1α, CAIX can be expressed under normoxic conditions depending on the cell density of the culture, possibly also due to microhypoxic effects. In dense cultures, CAIX is stabilised by PI3K (phosphatidylinositol 3'-kinase) without induction by HIF-1α (Kaluz et al., 2002).

In addition, an alternative splice variant leading to a truncated CAIX protein with a reduced catalytic activity has been found to be expressed independently of the oxygen status of the cell (Barathova et al., 2008). When overexpressed, the truncated form can diminish the enzymatic capacity of the full length CAIX protein. It has been suggested that this effect can be important for adaptation to mild hypoxic conditions when cells do not need to compensate for severe acidosis with highly efficient pH control.

In order to increase efficiency, CAs can be organised in a so called "metabolon" together with transporter whose activity can contribute to meet the individual requirements of the enzymatic process (Deitmer and Becker, 2013). The same was shown to be true for CAIX. The enzyme is located in close vicinity to sodium/hydrogen carbonate (Na^+/HCO_3^-)-co-transporters (Figure 2) that can immediately transport HCO_3^- inside the cell (Parks et al., 2013).

The CAIX metabolon enhances the turnover and facilitates the acidification of the extracellular space (Morgan et al., 2007; Pastorekova and Zavada, 2004). It has been shown in rat hearts that CAIX binds to the Na^+/HCO_3^--co-transporter e1 (NBCe1) and increases its activity (Orlowski et al., 2012). In addition, it was suggested that CAs can alter the activity of transporters that facilitate lactate extrusion (Parks et al., 2013). These aspects show that CAIX function is supported by the close location to transporter systems that serve to optimize CAIX enzymatic activity (Figure 2).

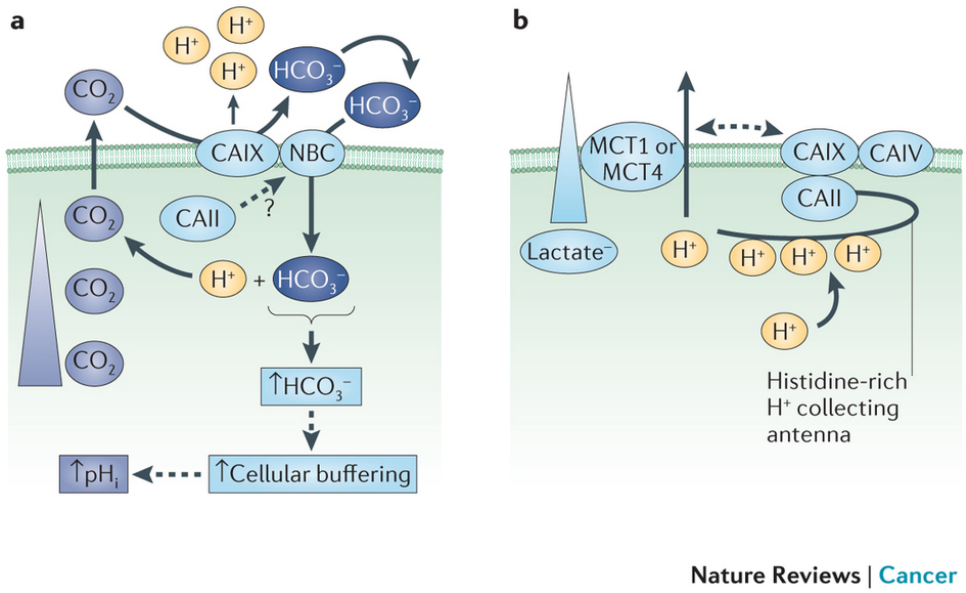

Figure 2 CAIX and its molecular function
(A) Carbonic anhydrases maintain the flux of HCO_3^- across the membrane in order to regulate the pH in and outside of the cell. Re-uptake of HCO_3^- is facilitated by Na^+/HCO_3^--co-transporters (NBCs) in cooperation with CAs to maintain the cellular buffering system functional. CAIX expression is also responsible for the diffusion of H^+ from the cellular surface. (B) By binding H^+, CAs enhance the activity of monocarboxylate transporters (MCTs) that are responsible for lactate extrusion. Possible interactions are marked by dashed arrows. Reprinted with permission from Macmillan Publishers Ltd: Nature Reviews Cancer (Parks et al., 2013), copyright 2013, licence #3595351047324.

It is known that CAIX can interact with β-catenin and controls the cell adhesion via competition with E-cadherin (Svastova et al., 2003). E-cadherin and β-catenin play a crucial role in the transition of an epithelial tumor cell to a mesenchymal phenotype (epithelial-to-mesenchymal-transition, EMT). This process is pivotal for the tumor's ability of invasion and metastasis (Kalluri and Weinberg, 2009; Yang and Weinberg, 2008). Due to the essential role of CAIX in the metabolism of the tumor cell it was hypothesised that CAIX also plays a role in EMT. It has indeed been shown in prostate carcinoma cells that CAIX expression is mandatory for EMT (Fiaschi et al., 2012).

Besides its role in EMT, CAIX is known to play a role in cell migration: embedded in the metabolon, CAIX was found to be expressed at the leading edge of lamellipodia in SiHa cervical carcinoma cells. In contrast, in non-migrating cells CAIX could only be found at cell-cell-contact sites indicating a relocation of the CAIX metabolon when cells start to migrate (Svastova and Pastorekova, 2013). In addition, gene expression profiling revealed information about CAIX being involved in focal adhesion. Cells depleted of CAIX showed impaired wound healing, supporting the role of CAIX in tumor invasion (Radvak et al., 2013).

2.2 CAIX, Tumor Hypoxia and Regulation of pH

Areas of hypoxia due to poor vascularisation are a feature of solid tumors that have been associated with malignancy, tumor progression and determination of the clinical outcome (Vaupel and Mayer, 2007). However, tumors are not characterised by a steady-state of hypoxia, rather areas of hypoxia are drifting over the tumor such that cells are exposed to cycles of hypoxia and reoxygenation. This state has been referred to as "cycling hypoxia" (Matsumoto et al., 2010).

Under hypoxia, cells produce their energy via glycolsis instead of oxidative phosphorylation. When this happens under normoxic conditions, the process is being reffered to as the "Warburg effect" (Kim and Dang, 2006; Vander Heiden et al., 2009). In the solid tumor, the lack of blood supply leads to hypoxia. Expression of HIF-1α then leads to induction of CAIX and accumulation of H^+ and thus decreased pH_e and increased pH_i (Figure 3).

What is supposed to be a metabolic disadvantage, is used by the tumor to switch to pathways which contribute to its growth: higher rate of glycolysis and acidification have been shown to be a necessary prerequisite for tumor invasiveness (Gatenby and Gillies, 2004), translated via ROS, the serine/threonine-protein kinase Akt (Akt) and nuclear factor "kappa-light-chain-enhancer" of activated B-cells, NF-κB (Gupta et al., 2014). Acidification also derives from CO_2 from the pentose phosphate pathway (Helmlinger et al., 2002). CAIX is primarily expressed in hypoxic areas of the tumor (Figure 3) contributing to the acidification of the pH_e (Airley et al., 2003).

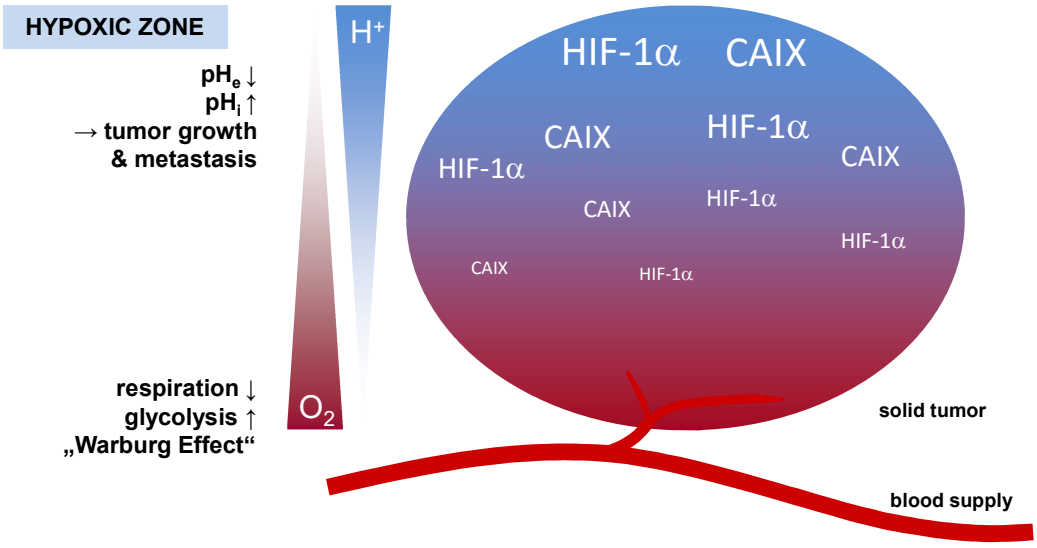

Figure 3 Metabolic role of CAIX in cancer
Expression of HIF-1α and CAIX are modulated by oxygenation of the tumor. Hypoxia leads to changes in the pH facilitated by induction of CAIX expression.

CAIX has been established as a marker protein for hypoxic tumors *in vitro* as well as *in vivo* and antibodies targeting CAIX have been developed for imaging hypoxic areas in tumors (Ahlskog et al., 2009b; Olive et al., 2001). Using these tools, it could be shown that the antibody specifically targeting CAIX accumulates in hypoxic reagions of tumor xenografts (Chrastina et al., 2003). The expression of CAIX has been correlated to poor prognosis and resistance to radio therapy (Giatromanolaki et al., 2001; Koukourakis et al., 2001; Span et al., 2003).

It was shown that CAIX – together with the CA isoform CAXII – is responsible for maintaining the pH_e acidified and the pH_i alkaline in dependence of the CO_2 levels in order to sustain cell metabolism and survival. In a xenograft model, tumor growth was impaired when cells were depleted of CAIX (Chiche et al., 2009). The same was found in spheroids (Swietach et al., 2009). When cells expressing CAIX were characterised by decreased pH_e and increased pH_i leading to an acidification of the extracellular space which favored tumor growth and invasiveness.

2.3 CAIX as Therapeutic Target

The maintenance of pH is of high importance for poorly vascularised tumors that lack supply of oxygen and other nutrients (Hulikova et al., 2011). The important role of CAIX in the regulation of the acid-base balance and the pH in the tumor makes CAIX a promising target for cancer therapy (Sedlakova et al., 2014; Swietach et al., 2010). Its expression in many types of tumors, its role also in migration and invasion have made CAIX a valuable target for anti-cancer strategies (Pastorek and Pastorekova, 2015).

Indeed, it has been shown that the pH_e in the tumor is often reduced which can favor the growth of the tumor (Svastova et al., 2004). Also, anion exchangers that can form a metabolon together with CAIX have been found to play a pivotal role during metastasis (Cardone et al., 2005). Hence, transporters and proteins involved in pH regulation have been in the focus of the search for and development of targets for cancer chemotherapy (Izumi et al., 2003).

A wide number of chemical inhibitors as well as activators have been developed (Maresca et al., 2009; Supuran, 2008). CAIX has been in the focus of research for the development of therapeutic strategies targeting the pH regulation in brain and lung tumor, melanoma or lymphoma among others (Neri and Supuran, 2011). DNA-encoded libraries have been developed to gain potentially therapeutic inhibitors in high throughput approaches (Buller et al., 2011).

CAIX inhibitors (CAI) derive from many structural families. Acetozolamide derivatives have been shown to successfully interact with CAIX in an *in vivo* xenograft model where it led to retarded growth of the tumor (Ahlskog et al., 2009a). Sulfonamides have also been shown to reduce tumor growth and metastasis (Lou et al., 2011; Pacchiano et al., 2011). The use of fluorescent labelled sulfonamide CAI could show in the xenograft model that the binding of the CAI is only possible under hypoxic conditions. When mice were brought back to normoxic atmosphere, the CAI binding to the tumor was significantly decreased (Dubois et al., 2009).

In addition, it could be shown that tumor irradiation was more successful when CAIX was simultaneously inhibited (Dubois et al., 2011). Both the use of CAIs and specific knockdown of *CA9* could enhance the effect of therapeutic treatment *in vitro* suggesting the necessity of inhibiting CAIX in anti-cancer treatment to achive better therapeutic outcome (McIntyre et al., 2012). Inhibition of CAIX by carnosine – an anti-tumorigenic agent that blocks cancer cell proliferation – led to an increase in pH_e and inhibited spheroid and xenograft growth (Ditte et al., 2014).

Another approach to inhibit CAIX function is the use of specific antibodies. An antibody has been established for a clinical trial against metastatic renal cell carcinoma for which standard therapies have been shown to have limited success (Rohrmann et al., 2005). In combination with interferon-α, it showed clinical benefit for 42% of patients and a two-year survival rate of 57% (Siebels et al., 2010). The study was terminated in the phase III in 2012 due to a lack of significant increase in the survival rate (http://www.transkript.de/nachrichten/wirtschaft/2012-04/wilex-rencarex-faellt-durch.htm, as of 23rd october 2015). A more detailed analysis of the data showed that the treatment might be beneficial in particular for patients suffering of carcinoma expressing high levels of CAIX (http://www.wilex.de/portfolio/rencarex/phase-iii-ariser/, as of 23rd october 2015).

Novel approaches to drug design also include sugar-based tails or click chemistry and are designed not only to target CAs for anticancer treatment, but are also manufactured to serve against funghi or bacteria and aim to become isoform-selective (McKenna and Supuran, 2014).

While CAIX has been well established as cancer marker and therapeutic target, not much is known about downstream targets of CAIX. Proteins that are regulated following CAIX depletion could give more insight in functions additionally to pH regulation of CAIX. Additionally, targets of CAIX could serve as therapeutic target proteins.

3 Aim of the Study

CAIX is a well-established marker protein in hypoxic tumors. Because of its association with poor prognosis, CAIX has been chosen as a target for the development of therapeutic strategies. CAIX plays a pivotal role in the pH regulation under low oxygen conditions. However, its functional role under the different oxygen conditions in a growing tumor is not clear. This study aims to identify downstream targets differentially regulated by CAIX under normoxia, hypoxia and reoxygenation. Specifically, by using an RNAi approach, the role of CAIX in controlling protein functions under these conditions in a tumor cell line shall be investigated by applying 2DE based proteomics in combination with mass spectrometry.

4 Materials and Methods

4.1 Materials

4.1.1 General Equipment

Device	Model	Company
Analytical balance	BP 3015	Sartorius, Göttingen, Germany
Autoclave (big)	KSG 116-2-ED	KSG, Bornheim, Germany
Autoclave (small)	KSG 25-2-3	KSG, Bornheim, Germany
Balance	BP 4100S	Sartorius, Göttingen, Germany
Centrifuge	Biofuge fresco/pico/stratos	Heraeus, Hanau, Germany
	Capsulefuge PMC-060	Fisher Scientific, Schwerte, Germany
	Megafuge 1.OR	Heraeus, Hanau, Germany
	Varifuge 3.OR	Heraeus, Hanau, Germany
Deep-freezer (-70°C)	Hera freeze	Heraeus, Hanau, Germany
Drying chamber	T6060	Heraeus, Hanau, Germany
Dewar	Cryolab25	Statebourne, Washington, UK
	Thermolyne 6 plus/27B	KGW Isotherm, Karlsruhe, Germany
Freezer	Comfort	Liebherr, Biberach/Riss, Germany
Fridges (various sizes)	Profi line	Liebherr, Biberach/Riss, Germany
Heating block	Thermomixer comfort	Eppendorf, Hamburg, Germany
Hypoxia workbench	Hypoxia Workstation	IUL Instruments, Königswinter, Germany
Incubator	Hera Cell	Heraeus, Hanau, Germany
Incubator for hypoxia	CB150	Binder, Tuttlingen, Germany
Laboratory dishwasher	G7783CD Mielabor	Miele, Munich, Germany
Laminar airflow cabinet	HS15	Heraeus, Hanau, Germany
Magnetic stirrer (heating)	MR3001	Heidolph, Schwabach, Germany
Magnetic stirrer	MR3000	Heidolph, Schwabach, Germany
Microscope	IX 50	Olympus, Hamburg, Germany
Microscope	Axiovert 25	Zeiss, Jena, Germany
Counting chamber	Neubauer improved	Brand, Wertheim, Germany

PCR machine	GeneAmp PCR System 9700	Applied Biosystems/Life Technologies, Darmstadt, Germany
pH meter	pH 540 GLP	WTW, Weilheim, Germany
pH electrode	InLab Expert DIN	Mettler-Toledo, Gießen, Germany
Photometer	Nano Drop 2000	Fisher Scientific, Schwerte, Germany
Platereader	Tecan Safire	Tecan, Crailsheim, Germany
Pipettes	Multipette Plus	Eppendorf, Hamburg, Germany
	Pipetus	Hirschmann Laborgeräte, Eberstadt, Germany
	Pipetman	Gilson, Limburg an der Lahn, Germany
Power supplies	Power Pac 200/300/3000	Bio-Rad, Munich, Germany
Pump	CVC 2000	Vacuubrand, Wertheim, Germany
Roller mixer	RM5 Assistent	Karl Hecht KG, Sondheim, Germany
Rotator	3000	Fröbel Labortechnik, Lindau, Germany
SDS-PAGE apparatus & WB transfer unit	Mini-Protean 3	Bio-Rad, Munich, Germany
Shaker	Duomax 1030/Polymax 1040	Heidolph, Schwabach, Germany
	IKA-Schüttler MTS2	IKA-Werke, Staufen, Germany
Spectrophotometer	Nano Drop	Thermo Fisher Scientific, Braunschweig, Germany
Thermocycler	Rotor-Gene 6000	Corbett/Qiagen, Hilden, Germany
Tip sonicator	Sonopuls	Bandelin, Berlin, Germany
Vortex	Vortex-Genie 2	Scientific Industries
Water bath	Grant	Memmert, Schwabach, Germany
Water purifying unit	Milli-Q Synthesis	Merck Millipore, Darmstadt, Germany

4.1.2 General Chemicals

Chemical Product	Company
Acetic acid	Carl Roth, Karlsruhe, Germany
Acrylamide “Gel 30 (37,5:1)”	Carl Roth, Karlsruhe, Germany
Ammonium persulfate	Carl Roth, Karlsruhe, Germany
Bromophenol blue	Sigma-Aldrich, Taufkirchen, Germany

Coumaric acid	Sigma-Aldrich, Taufkirchen, Germany
Diethylpyrocarbonate (DEPC)	Carl Roth, Karlsruhe, Germany
Dithiothreitol	Carl Roth, Karlsruhe, Germany
Ethylenediaminetetraacetic acid (EDTA)	Carl Roth, Karlsruhe, Germany
Ethanol	Merck, Darmstadt, Germany
Ethanol p.a.	CLN, Freising, Germany
Glycine	Carl Roth, Karlsruhe, Germany
Glycerol	Carl Roth, Karlsruhe, Germany
Hydrogen chloride (HCl)	CLN, Freising, Germany
Hydrogen peroxide	Merck, Darmstadt, Germany
Isopropanol	CLN, Freising, Germany
Luminol	Sigma-Aldrich, Taufkirchen, Germany
Methanol	CLN, Freising, Germany
β-Mercaptoethanol	Carl Roth, Karlsruhe, Germany
Naphthol blue black	Sigma-Aldrich, Taufkirchen, Germany
Phosphate buffered saline (PBS) tablettes	Life Technologies, Darmstadt, Germany
PonceauS	Carl Roth, Karlsruhe, Germany
Skim milk powder	Merck, Darmstadt, Germany
Sodium chloride	Carl Roth, Karlsruhe, Germany
Sodium dodecyl sulphate (SDS)	Carl Roth, Karlsruhe, Germany
Tetramethylethylenediamine (TEMED)	Carl Roth, Karlsruhe, Germany
Tris(hydroxymethyl)-amino-methan (Tris) „ultra“	Carl Roth, Karlsruhe, Germany
Polyethylene glycol p-(1,1,3,3-tetramethylbutyl)-phenyl ether (Triton X-100)	Sigma-Aldrich, Taufkirchen, Germany
Polyoxyethylene (20) sorbitan monolaurate (Tween-20)	Sigma-Aldrich, Taufkirchen, Germany

4.1.3 General Consumables

Product	Company
Aluminium foil	Carl Roth, Karlsruhe, Germany
Cell culture dishes	Sarstedt, Nümbrecht, Germany
Cell culture flasks & plates	Greiner Bio-One, Frickenhausen, Germany

Cell lifter	Corning, Munich, Germany
Cell scraper	Sarstedt, Nümbrecht, Germany
Combitips	Eppendorf, Hamburg, Germany
Cryoboxes	Kisker, Steinfurt, Germany
Cryovials	Carl Roth, Karlsruhe, Germany
Friscolyt solution	Mettler-Toledo, Gießen, Germany
Film “Fuji Super”	Fischer-Sehner Medical Imaging, Augsburg, Germany
Gloves, latex	Sempermed, Neuwied, Germany
Gloves, nitrile	Kimberly-Clark, Koblenz, Germany
Lab tape	Kisker, Steinfurt, Germany
Magnet stirring bars	Carl Roth, Karlsruhe, Germany
Membrane filter	GE Healthcare, Munich, Germany
Millex vacuum line protector, 45µm	Merck-Millipore, Darmstadt, Germany
Needle 21G	Becton, Dickinson and Company, Heidelberg, Germany
Pasteur pipettes	Carl Roth, Karlsruhe, Germany
pH buffer solutions	Mettler-Toledo, Gießen, Germany
Pipettes	Sarstedt, Nümbrecht, Germany
Pipette filter tips	Biozym Scientific, Hessisch Oldendorf, Germany
Pipette tips	Gilson, Limburg an der Lahn, Germany
Reagent reservoir	Corning, Munich, Germany
Spatulas, disposable	VWR, Darmstadt, Germany
Syringes	Braun, Melsungen, Germany
Tube openers	Kisker, Steinfurt, Germany
Tubes	Eppendorf, Hamburg, Germany Greiner Bio-One, Frickenhausen, Germany Corning, Munich, Germany Thermo Fisher Scientific, Braunschweig, Germany
Tweezers	Carl Roth, Karlsruhe, Germany
Whatman paper	GE Healthcare, Munich, Germany
Wipes	Kimberly-Clark, Koblenz, Germany

4.1.4 Materials for 2DE

4.1.4.1 *Equipment for 2DE*

Device	Model	Company
Cassette rack	Ettan Dalt	GE Healthcare, Munich, Germany
Gel clip		Bio-Rad, Munich, Germany
Gel caster	Ettan Dalt Six	GE Healthcare, Munich, Germany
Gel drying frame		GE Healthcare, Munich, Germany
Gel loading chamber	Ettal Dalt Six	GE Healthcare, Munich, Germany
Glass plates, low fluorescent		GE Healthcare, Munich, Germany
High pressure liquid chromatography (HPLC)	Easy nLC	Proxeon/Thermo Fisher Scientific, Braunschweig, Germany
IPG box	Ettan Dalt	GE Healthcare, Munich, Germany
IPGphor	Ettan IPGphor 3 isoelectric focusing unit	GE Healthcare, Munich, Germany
IPGphor manifold	Ettan Dalt	GE Healthcare, Munich, Germany
Mass spectrometer	LTQ Orbitrap XL ETD	Thermo Fisher Scientific, Braunschweig, Germany
Power pack adapter		Bio-Rad, Munich, Germany
Sterile filtering unit		Merck Millipore, Darmstadt, Germany

4.1.4.2 *Chemicals for 2DE*

Chemical Product	Company
Acetic acid	CLN, Freising, Germany
Acetonitrile	Sigma-Aldrich, Taufkirchen, Germany
Acrylamide “Plusone IEF” 40%	GE Healthcare, Munich, Germany
Agarose, low melting	Sigma-Aldrich, Taufkirchen, Germany
Ammonium biocarbonate	Sigma-Aldrich, Taufkirchen, Germany
Ammonium persulfate “Plusone”	GE Healthcare, Munich, Germany
Ammonium sulfate	Sigma-Aldrich, Taufkirchen, Germany
Bromophenol blue	Sigma-Aldrich, Taufkirchen, Germany

3-[(3-cholamidopropyl)dimethylammonio]-1-propanesulfonate (Chaps)	GE Healthcare, Munich, Germany
Coomassie brilliant blue G250	Sigma-Aldrich, Taufkirchen, Germany
DeStreak reagent	GE Healthcare, Munich, Germany
Dithiothreitol	GE Healthcare, Munich, Germany
Ethanol p.a.	CLN, Freising, Germany
Formic acid	Sigma-Aldrich, Taufkirchen, Germany
Glycine	GE Healthcare, Munich, Germany
Glycerol 87%	GE Healthcare, Munich, Germany
Hydrogen chloride (HCl)	CLN, Freising, Germany
Iodoacetamide	GE Healthcare, Munich, Germany
Methanol	CLN, Freising, Germany
N,N'-Methylene-bisacrylamide 2% „Plusone“	GE Healthcare, Munich, Germany
Pharmalyte 3-10	GE Healthcare, Munich, Germany
Phenylmethylsulfonyl fluoride	Sigma-Aldrich, Taufkirchen, Germany
Phosphoric acid 85%	Sigma-Aldrich, Taufkirchen, Germany
Ruthenium(II)tris(bathophenantroline disulfonate) (RuBPS)	RubiLAB, Burgdorf, Switzerland
Sodium acetate trihydrate	Carl Roth, Karlsruhe, Germany
Sodium dodecyl sulfate (SDS) “Plusone”	GE Healthcare, Munich, Germany
Sodium fluoride	Merck, Darmstadt, Germany
Sodium orthovanadate	Merck, Darmstadt, Germany
Spermine	Sigma-Aldrich, Taufkirchen, Germany
Sucrose	Sigma-Aldrich, Taufkirchen, Germany
Tetramethylethylenediamine (TEMED) “Plusone”	GE Healthcare, Munich, Germany
Thiourea	GE Healthcare, Munich, Germany
Trifluoroacetic acid	Sigma-Aldrich, Taufkirchen, Germany
Tris(hydroxymethyl)-amino-methan (Tris) “Plusone”	GE Healthcare, Munich, Germany
Trypsin, sequencing grade modified	Promega, Mannheim, Germany
Urea “Plusone”	GE Healthcare, Munich, Germany

4.1.4.3 *Consumables for 2DE*

Product	Company
Amberlite	GE Healthcare, Munich, Germany
Cellophan foil	Sarstedt, Nümbrecht, Germany
Cover fluid “DryStrip”	GE Healthcare, Munich, Germany
Decon90 liquid	Fisher Scientific, Schwerte, Germany
Equilibration tube set	GE Healthcare, Munich, Germany
Gel seal	GE Healthcare, Munich, Germany
Gloves, vinyl „Rotiprotect“	Carl Roth, Karlsruhe, Germany
Hair cover “Foliodress cap”	Paul Hartmann, Heidenheim, Germany
HPLC C18 separation columns	Nanoseparations, Nieuwkoop, Netherlands
IPGbox kit	GE Healthcare, Munich, Germany
Immobiline dry strip pH 4-7, 24 cm	GE Healthcare, Munich, Germany
Magnetic stirring bars	Neolab, Heidelberg, Germany
Membrane filter, 0,45µm	Neolab, Heidelberg, Germany
Microcentrifuge tubes	Kisker, Steinfurt, Germany
Paper wicks	GE Healthcare, Munich, Germany
Sample cups	GE Healthcare, Munich, Germany
Sterile filtering unit, 250 ml	Merck Millipore, Darmstadt, Germany
Strip holder cleaning solution	GE Healthcare, Munich, Germany
Tips, high recovery	Kisker, Steinfurt, Germany
Tubes	Kisker, Steinfurt, Germany
Whatman pergamin paper	VWR, Darmstadt, Germany
Wipes „Kimtech science“	Kimberly-Clark, Koblenz, Germany

4.1.5 Cell Culture Reagents and Dyes

All product were special cell culture products or cell culture tested quality.

Product	Company
Alamar Blue	AbD Serotec, Puchheim, Germany
Calcein AM	Life Technologies, Darmstadt, Germany

Dimethyl sulfoxide	Sigma-Aldrich, Taufkirchen., Germany
Dulbecco's modified Eagle's medium	PAA/GE Healthcare, Munich, Germany
Dulbecco's phosphate buffered saline solution	PAA/GE Healthcare, Munich, Germany
Fetal bovine serum	PAN-Biotech, Aidenbach, Germany
Hank's balanced salt solution with Mg and Ca	PAA/GE Healthcare, Munich, Germany
L-Glutamine	PAA/GE Healthcare, Munich, Germany
Penicillin/Streptomycin	PAA/GE Healthcare, Munich, Germany
Propidium iodide	Life Technologies, Darmstadt, Germany
Trypan blue	Sigma-Aldrich, Taufkirchen, Germany
Trypsin-EDTA	PAA/GE Healthcare, Munich, Germany

4.1.6 Kits and Ready-to-Use-Reagents

Product	Company
Homogeneous AMC Caspase - 3/7 assay kit "SensoLyte"	Anaspec, Seraing, Belgium
Lipofectamine RNAiMAX	Life Technologies, Darmstadt, Germany
Phosphoprotein gel stain „Pro-Q Diamond"	Life Technologies, Darmstadt, Germany
Phosphoprotein molecular weight marker „Peppermint Stick"	Life Technologies, Darmstadt, Germany
Proteinmarker VI, prestained	Applichem, Darmstadt, Germany
Proteinmarker unstained „PageRuler"	Fisher Scientific, Schwerte, Germany
Protein Quantitation Kit "EZQ"	Life Technologies, Darmstadt, Germany
QiaShredder Columns	Qiagen, Hilden, Germany
Reverse Transcription Kit	Applichem, Darmstadt, Germany
RNeasy Mini Kit	Qiagen, Hilden, Germany
RNase-free DNase Set	Qiagen, Hilden, Germany
SYBR Green "Quanta Perfecta"	Quanta Biosciences, Gaithersburg, Maryland, USA

4.1.7 Buffers and Solutions

4.1.7.1 *Buffers and Solutions*

Running Gel (volume for one gel)

	8%	10%	12%
ddH_20	3.4 ml	2.8 ml	2.1 ml
Acrylamide (37,5:1)	2.7 ml	3.3 ml	4 ml
1M Tris/HCl pH 8.8	3.7 ml	3.7 ml	3.7 ml
10% SDS	100 µl	100 µl	100 µl
Ammonium persulfate	80 µl	80 µl	80 µl
TEMED	10 µl	10 µl	10 µl

Stacking Gel (volume for one gel, 5% acrylamide)

2.14 ml	ddH_20
488 µl	30% Acrylamide
375 µl	1M Tris/HCl pH 6.8
30 µl	10% SDS
15 µl	Ammonium persulfate
3µl	TEMED

Laemmli Buffer (3x)

187 mM	Tris/HCl pH 6.8
6%	SDS
30%	Glycerol
0.06%	Bromophenol blue
15 mM	Dithiothreitol
60 mM	EDTA

Amido Black Staining Solution

0.1%	Naphthol blue black

50%	Methanol
10%	Acetic acid

The membrane was incubated for 2-3 min whilst slowly agitated; destaining was carried out in 50% methanol solution.

Running Buffer

25 mM	Tris
200 mM	Glycine
0.5%	SDS

Transfer Buffer

25 mM	Tris
200 mM	Glycine
20%	Methanol

Tris Buffered Salt Solution Buffer (1x TBS-T)

50 mM	Tris/HCl pH 7.5
150 mM	Sodium chloride
0.3%	Tween-20

Blocking Solution

5%	Skim milk powder in 1x TBS-T

Enhanced Chemiluminescent Reagent 1 (ECL1)

100 mM	Tris/HCl pH 8.8
2.5 mM	Luminol
0.4 mM	Coumaric acid

Enhanced Chemiluminescent Reagent 2 (ECL2)

100 mM	Tris/HCl pH 8.8
0.15%	Hydrogen peroxide

For ECL solution, ECL1 and ECL2 were mixed in 1:1 ratio and directly applied on the wet membrane using 2ml solution per membrane (8.5 x 6.5 cm).

4.1.7.2 *2DE Related Buffers and Solutions*

Bromophenol Blue Stock Solution

100 mg	Bromophenol blue
60 mg	Tris
ad 10 ml	ddH_20

Harvesting Buffer

250 mM	Sucrose
10 mM	Tris/HCl p7.4
1 mM	Phenylmethylsulfonyl fluoride
1 mM	Sodium fluoride
0.2 mM	Sodium orthovanadate

Sucrose and Tris were dissolved in ddH_20 and pH was adjusted. The solution was filtered through 0.45 µm membrane and the protein inhibitors were added maximally 1 hour before using the buffer.

Extraction Buffer

7 M	Urea
2 M	Thiourea
4%	Chaps
100 mM	Dithiothreitol

25 mM	Spermine
0.5%	Pharmalyte 3-10

Buffer was aliquoted and stored at -70°C. Pharmalyte 3-10 was added freshly before use.

Isoelectric focussing (IEF) Buffer

7 M	Urea
2 M	Thiourea
2%	Chaps
100 mM	DeStreak reagent
0.5%	Pharmalyte 3-10
0.002%	Bromophenol blue

For IPGs of 24 cm 450 µl solution were used.

Gel buffer

1.5 M	Tris/HCl pH 8.6
0.4 %	SDS

The solution was filtered through a 0.45 µm membrane and stored at 4°C.

Gel solution

115.23ml	Acrylamide 40%
61 ml	N,N'-Methylene-bisacrylamide 2%
2.2 g	Amberlite

The mixture was stirred for 1 h, then filtered through a 0.45 µm membrane.

115 ml	Gel Buffer
148.85 ml	ddH_2O
26.5 g	Glycerol 87%

The components were mixed and then added to the acrylamide mixture.

230 µl	TEMED
1.84 ml	Ammonium persulfate 10%

TEMED and ammonium persulfate were added immediately before gel casting.

Equilibration Buffer

10%	SDS
50 mM	Tris/HCl pH 8.8
0.001%	Bromophenol blue
6 M	Urea
30% (w/v)	Glycerol

A stock solution of tris was prepared and pH was adjusted. Tris, urea and glycerol were mixed in appropriate amount of water. As soon as they were dissolved completely, SDS and bromophenol blue were added. Equilibration buffer was stored at -20°C.

Directly before use, 2% dithiothreitol or 4% iodoacetamide were added as reducing or alkylating agent, respectively. The solution supplemented with iodoacetamide was strictly kept in the dark.

Low Melting Agarose Solution

1.51 g	Tris
7.21 g	Glycine
0.5 g	SDS
ad 499ml	ddH_2O

2.5 g	Agarose, low melting
heat without boiling	
1 ml	Bromophenol blue stock solution

Aliquots were stored at room temperature. Before use, agarose needed to be melted at ca. 90°C in the water bath and to be cooled down to less than 60°C before using.

Anode Buffer

25 mM	Tris
192 mM	Glycine
0.1%	SDS

Cathode Buffer

50 mM	Tris
384 mM	Glycine
0.2%	SDS

Gel Shrinking Solution

250 g	Glycerol
600 ml	Ethanol p.a.
ad 2 l	ddH_2O

4.1.7.3 *MS Related Buffers and Solutions*

Destain Solution

40%	Ethanol
50 mM	Ammonium bicarbonate

Wash Solution I

25 mM	Ammonium bicarbonate

Wash Solution II

100 mM	Ammonium bicarbonate

Shrinking Solution

50%	Acetonitrile
5 mM	Ammonium bicarbonate

Reducing Solution

100 mM	Ammonium bicarbonate
10 mM	Dithiothreitol

Alkylating Solution

100 mM	Ammonium bicarbonate
55 mM	Iodoacetamide

MS Digest Buffer

25 mM	Ammonium bicarbonate
8%	Acetonitrile

4.1.8 siRNA

Sample	siRNA Name	Order #	Target sequence (5'->3')
Negative control	siControl	SI03650325	AAT TCT CCG AAC GTG TCA CGT
Negative control	siAllStars	SI03650318	N.N.
CA9	Hs_siCA9_2	SI00023527	CTA CCT GAA GTT AAG CCT AAA
CA9	Hs_siCA9_3	SI00023534	CTG GCT GCT GGT GAC ATC CTA
CA9	Hs_siCA9_4	SI00023541	GAG GAG GAT CTG CCC AGT GAA
CA9	Hs_siCA9_5	SI03110646	TAG AGG CTG GAT CTT GGA GAA

4.1.9 qPCR-Primers

Target	Sequence (5´->3´)	Product length
CA9,	GTT GAT CCC GGC CCC TGC TC	101 bp
Homo sapiens	CCT CCT GCA TCC GGG GCA AC	
CA12,	GCA CAC ACA TGG ACG ACC CTT CC	137 bp
Homo sapiens	GAT GCC CAG ACT CAG TCC TGC CG	
ACTB,	CTG GAA CGG TGA AGG TGA CA	138 bp
Homo sapiens	AAG GGA CTT CCT GTA ACA ATG CA	

4.1.10 Antibodies

Antibodies were diluted in blocking solution in the given dilution.

Antibody	Isotype	Company	Dilution
4E-BP1	Rabbit Monoclonal	Cell Signaling, Leiden, Netherlands	1:1000
Akt	Rabbit Polyclonal	Cell Signaling, Leiden, Netherlands	1:1000
p-Akt (Thr308)	Rabbit Monoclonal	Cell Signaling, Leiden, Netherlands	1:1000
ATF4	Rabbit Polyclonal	Santa Cruz Biotechnology, Heidelberg, Germany	1:1000
CAIX	Mouse Hybridoma	Kindly provided by Prof. Pastorekova (Pastorekova et al., 1992)	1:400
Calpastatin	Rabbit Monoclonal	Cell Signaling, Leiden, Netherlands	1:1000
Cleaved Caspase 3	Rabbit Polyclonal	Cell Signaling, Leiden, Netherlands	1:1000
Cleaved Caspase 7	Rabbit Polyclonal	Cell Signaling, Leiden, Netherlands	1:1000
Cleaved Caspase 8	Rabbit Monoclonal	Cell Signaling, Leiden, Netherlands	1:1000

eIF2α	Mouse Monoclonal	Cell Signaling, Leiden, Netherlands	1:1000
p-eIF2α	Rabbit Monoclonal	Cell Signaling, Leiden, Netherlands	1:1000
eIF4E	Rabbit Monoclonal	Cell Signaling, Leiden, Netherlands	1:1000
p-eIF4E	Rabbit Monoclonal	Merck/Millipore, Darmstadt, Germany	1:1000
eIF4G	Rabbit Monoclonal	Cell Signaling, Leiden, Netherlands	1:1000
p-eIF4G	Rabbit Monoclonal	Cell Signaling, Leiden, Netherlands	1:1000
ERp44	Rabbit Monoclonal	Cell Signaling, Leiden, Netherlands	1:1000
ERp57	Rabbit Monoclonal	Cell Signaling, Leiden, Netherlands	1:1000
ERp72	Rabbit Monoclonal	Cell Signaling, Leiden, Netherlands	1:1000
Glutaredoxin-3	Rabbit Polyclonal	Sigma-Aldrich, Taufkirchen, Germany	1:1000
GRP-78	Rabbit Monoclonal	Cell Signaling, Leiden, Netherlands	1:1000
GRP-94	Rabbit Monoclonal	Cell Signaling, Leiden, Netherlands	1:1000
HIF-1α	Mouse Monoclonal	BD Biosciences, Heidelberg, Germany	1:1000
Mnk1	Rabbit Monoclonal	Cell Signaling, Leiden, Netherlands	1:1000
p-Mnk1 (Thr197/202)	Rabbit Polyclonal	Cell Signaling, Leiden, Netherlands	1:1000
p-mTOR (Ser2448)	Rabbit Polyclonal	Cell Signaling, Leiden, Netherlands	1:1000
PARP-1	Mouse Monoclonal	Cell Signaling, Leiden, Netherlands	1:1000

PDI	Rabbit Monoclonal	Cell Signaling, Leiden, Netherlands	1:1000

Secondary antibodies were used in a standard dilution of 1:10,000 in blocking solution.

Antibody	Company
Goat anti Mouse HRP conjugated	Calbiochem/Merck, Darmstadt, Germany
Goat anti Rabbit HRP conjugated	Calbiochem/Merck, Darmstadt, Germany

4.1.11 Softwares and Databases

Th following softwares and databases were used during data analysis, image analysis and pathway analysis:

Software	Company/Reference
ImageJ	NIH, Bethesda, Maryland, USA (Schneider et al., 2012)
Mascot	http://www.matrixscience.com/ (Perkins et al., 1999)
Phosphosite	http://www.phosphosite.org (Bateman et al., 2002; Li et al., 2002; Obenauer et al., 2003)
ProteomeDiscoverer	Thermo Fisher Scientific, Braunschweig, Germany
R	http://www.R-project.org (R-Development-Core-Team, 2006)
REST analysis	http://rest.gene-quantification.info (Pfaffl et al., 2002), Qiagen, Hilden, Germany
SameSpots	Nonlinear Dynamics Ltd., Newcastle upon Tyne, UK
Scaffold 4	Proteome Software Inc., Portland, Oregon, USA
SwissProt database	http://www.expasy.org/ (Bairoch and Apweiler, 2000)
Uniprot	http://www.uniprot.org/ (Uniprot-Consortium, 2014)
WEB-based GEne SeT AnaLysis Toolkit (WebGestalt)	http://bioinfo.vanderbilt.edu/webgestalt (Wang et al., 2013; Zhang et al., 2005)

4.2 Methods

4.2.1 Cell Biological Methods

4.2.1.1 *Cell Culture*

Cervical carcinoma cell line HeLa (ATCC CCL-2) was cultured in Dulbecco's modified Eagle's medium containing 4.5 g/l glucose and supplemented with 15% fetal bovine serum, penicillin (100 units/ml) and streptomycin (100 µg/ml) at 37°C in a humidified atmosphere of 5% CO_2 and 95% air. To obtain samples close to biological replicates, three different samples were allowed independently to accumulate mutations for more than eight passages (Valcu et al., 2012). For transfection, antibiotic-free medium was used.

A549 cells (ATCC CCL-185) were cultured in Dulbecco's modified Eagle's medium containing 4.5 g/l glucose and supplemented with 15% fetal bovine serum, 2 mM glutamine, penicillin (100 units/ml) and streptomycin (100 µg/ml) at 37°C in a humidified atmosphere of 5% CO_2 and 95% air.

For maintenance of the cells lines, cells were split two times per week using trypsin. Cell counting was carried out in a Neubauer counting chamber according to manufacturer's guidelines. Cell numbers were seeded as indicated.

Hypoxic incubations for maximally 24 h at 1% of oxygen and all incubations at 0.1% were carried out in the hypoxia workbench equipped with a gas mixer at 37°C with 1% O_2, 5% CO_2 and 94% N_2. For incubations longer than 24 h of hypoxia cells were incubated in an incubator at 37°C with 1% O_2, 5% CO_2 and 94% N_2.

4.2.1.2 *Transfection*

Reverse transfection was performed using Lipofactamine RNAiMAX according to the guidelines of the manufacturer. All siRNAs were purchased from the same supplier. 100 pmol of siRNA and 5 µl of Lipofectamine were used for each well of a 6well plate. For other dishes and plates the amount of siRNA and Lipofectamine was calculated according to the manufacturer's instructions.

To be able to identify effects of transfection reagent and control siRNA, control samples with untreated WT cells were included in every experiment containing transfection.

4.2.1.3 *Cell Viability Assays*

To investigate the impact of hypoxia treatment and transfection on cell viability two assays with three different dyes were performed: size exclusion assay using trypan blue dye and cell-viability assay using calcein and propidium iodide.

To determine the number of healthy cells in a suspension the size exclusion assay was carried out using trypan blue. In this staining healthy cells remain unstained while dead cells take up the dye and are therefore easily distinguished from viable cells under the microscope. After trypsinizing of the cells and adjusting the concentration of the cell suspension, 100 µl of a sterile filtered 0.4% trypan blue solution were added to 1 ml of cell suspension. An aliquot was then loaded to a Neubauer counting chamber and the number of blue stained cells as well as the total cell number were determined under the microscope.

To investigate the viability of the cells a fluorescence-based viability assay was performed using calcein and propidium iodide. The acetomethoxy derivate of calcein is cell permeable and inside the cells is converted to fluorescent calcein by an esterase. It is thus used as a marker for cell viability in biology. On the other hand, propidium iodide is cell impermeable and can only penetrate dead cells. It is commonly used to visualize necrotic cells.

After incubation, cells were washed with PBS and 3 µM calcein or 5 µM propidium iodide dissolved in prewarmed PBS were added. After incubating cells at 37°C for 30 min, the fluorescence was measured in the plate reader at 485 nm (excitation) and 535 nm (emission) for calcein and 530 nm/620 nm for propidium iodide, respectively. Cells treated with 0.2% triton X-100 were used as a positive control. Solutions without any cells served as background control.

Alamar blue dye was used as a counterstaining for standardisation in cell culture assays according to the guidelines of the manufacturer. The absorbance was measured in the plate reader at 580 nm.

4.2.1.4 *Determination of Caspase 3/7 Activity*

For the determination of activity of caspase 3 and 7, homogeneous AMC Caspase - 3/7 assay kit "SensoLyte" from Anaspec was used according to the guidelines of the manufacturer.

4.2.2 RNA-related Methods

4.2.2.1 *RNA Isolation and cDNA Synthesis*

The effiency of silencing of *CA9* in HeLa cells was tested using qPCR analysis. RNA was isolated using Qiagen RNAasy Mini Kit and QIAshredder columns. DNA digest was performed on the column with RNase-Free DNase Set. Quantification of RNA was done using NanoDrop spectrophotometer. For subsequent cDNA synthesis with reverse transcription kit, 1µg of RNA was used per sample (total volume 20 µl). Controls without enzyme, without both enzyme and RNA and with enzyme but without RNA were performed. cDNA synthesis was performed in GeneAmp PCR system 9700 using the following program: 25°C/10 min – 37°C/120 min – 85°C/5 min.

After finishing cDNA synthesis, 180 µl of ddH_2O were added to 20 µl of sample and stored at -20°C until qPCR performance.

4.2.2.2 *qPCR*

Real-time polymerase chain reaction (qPCR) analysis was performed in the Rotor-Gene 6000 using SYBR green "Quanta Perfecta" and appropriate settings. Channel settings "green" were chosen with 470 nm (source) and 510 nm (detector) wavelengths. Gain was preset to 5 and optimised at the start of the run by the device. 40 cycles were performed with a hold temperature of 95°C and a hold time of 30 s. β-actin (*ACTB*) served as control for standardisation. Triplicates were performed for each sample and primer pair. Data was analysed using REST analysis.

4.2.3 Biochemical Methods

4.2.3.1 *SDS-PAGE and Western Blot Analysis*

In order to determine protein levels in cellular extract, Western blot (WB) analysis was performed. At the end of an experiment medium was aspirated from the cell culture dish, cells were washed with PBS and subsequently frozen in liquid nitrogen. After freezing, cells were scraped in Lämmli buffer, boiled for 5 min at 96°C and allowed to cool down. In experiments with hypoxic incubation PBS washing was omitted in order to prevent the reoxygenation of hypoxic cells.

In order to destroy the contained DNA, the cell suspension was pulled through the needle (21G) three times. To estimate the protein concentration dot blot assay using amido black staining solution was carried out. 50 µg of protein was applied per lane on the denaturating polyacrylamide gel. The monomer composition of the acrylamide gel was chosen according to the size of the protein of interest.

SDS-PAGE was carried out at constant voltage of 100 V in running buffer. After the dye front had reached the end of the gel, electrophoresis was stopped and wet transfer of the proteins onto the membrane was performed. A membrane size of 6.5 x 8.5 cm and a Whatman paper size of 7.5 x 9.5 cm was chosen. Western transfer using transfer buffer was carried out at constant voltage of 100 V for 60 min in chilled conditions.

After the transfer, membranes were incubated with PonceauS solution to visualize proteins, destained with water and protein loading was recorded. Proteins were then blocked with blocking solution at room temperature for 1 h. Incubation with primary antibody was carried out at 4°C over night.

After washing the membranes in 1x TBS-T for 4x5 min, incubation in secondary antibody was carried out at room temperature for 1 h and membranes were washed again in 1x TBS-T for 4x5 min. All steps were carried out with excess buffer volume and gentle agitation to decrease background staining.

Incubation with ECL (enhanced chemiluminescent reagent) solution and subsequent exposure to photographic films resulted in chemiluminescence catalysed by the secondary antibody. Image analysis and quantification was carried out using ImageJ software.

4.2.4 Proteomics

4.2.4.1 *Sample Preparation*

Cells were cultured, counted and transfected as described above with siRNA against *CA9* or control siRNA, respectively. Wild type cells were used in parallel for validation. For each sample, three full 6well plates yielded sufficient amount of protein for the proteomic analysis. After transfection, samples were incubated under different oxygen conditions as shown in Table 1.

Table 1 Incubation conditions for the 2DE experiment

Sample	Treatment
Normoxia (NX)	48 h 21% oxygen
Hypoxia (HX)	24 h 21% oxygen – 24 h 1% oxygen
Reoxygenation (ReOX)	16 h 21% oxygen – 24 h 1% oxygen – 8 h 21% oxygen

Cells were washed two times with 1 ml of prechilled harvesting buffer. After washing, cells were gently scraped in 800 µl buffer/well. Harvesting of hypoxic samples was carried out under hypoxic conditions with equilibrated buffer. Cells were pelleted at 1,500 rpm for 5 min at 4°C and pellets were immediately frozen in liquid nitrogen and stored at -70°C until protein extraction.

For protein extraction, cell pellets were resuspended in 0.5-1 ml of extraction buffer depending on the pellet size and incubated on ice for 60 min. To enhance extraction, samples were sonicated on ice with a tip sonicator (90%/70% power) for 5 cycles of 30 s interrupted by 30 s breaks between cycles.

Quantification of protein content was carried out using protein quantitation kit “EZQ” according to manufacturer’s guidelines. After quantification, 50 µg protein per sample were subjected to WB analysis to verify the silencing of *CA9* and the hypoxic induction of HIF-1α.

4.2.4.2 *Isoelectric Focussing*

For the isoelectric focussing (IEF), immobilised pH gradient gel strips (IPGs) with a pH range from 4 to 7 were rehydrated over night in IEF buffer at constant temperature (16-20°C). Rehydrated IPGs were placed in a ceramic manifold under 108 ml “DryStrip” cover fluid. Paper wicks

(prewetted with 150 µl MilliQ water each), electrodes and sample cups were positioned according to the guidelines of the manufacturer with the cup placed at the cathode. An aliquot containing 500 µg of protein was equilibrated for 10 min at room temperature, then mixed with IEF buffer to a final volume of 150 µl and incubated at room temperature for another 10 min. After loading the samples into the cups, IEF was carried out over night using the current protocol showed in Table 2.

Table 2 IEF running conditions

Step	Hold/Gradient	Voltage	Total kVhr
S1	Gradient	300 V	0.6 kVhr
S2	Gradient	600 V	1.2 kVhr
S3	Gradient	1000 V	2.0 kVhr
S4	Gradient	8000 V	13.5 kVhr
S5	Hold	8000 V	46.7 kVhr

After completion of IEF, IPGs were stored at -70°C until the second dimension.

4.2.4.3 *2DE Gel Electrophoresis*

For the second dimension, 10% polyacrylamide gels were cast in a gel caster. Gels were overlaid with 1 ml of 0.1% SDS solution per gel. Polymerisation was carried out for 3 h at room temperature, silent polymerisation was allowed to take place over night at 10-20°C. To prevent the drying of the gel surface gels were over laid with appropriately diluted gel buffer and kept over night in a sealed box.

Prior to the second dimension, IPGs were thawed and equilibrated in equilibration buffer containing subsequently 2% dithiothreitol and 4% iodoacetamide, in order to reduce and alkylate the focussed proteins. 10 ml of equilibration buffer were used per IPG and each incubation was carried out for 15 min under gentle agitation. Alkylation with iodoacetamide was carried out in the dark.

Equilibrated IPGs were sealed on the top of the polyacrylamide gel with low melting agarose solution. The second dimension was carried out in an „Ettal Dalt Six“ gel loading chamber at 16°C. The run was stopped when the bromophenol blue front had reached the end of the gel. The current protocol is displayed in Table 3.

Table 3 SDS-PAGE running conditions

Step	Current	Voltage	Power	Duration
S1	30 mA	150 V	12 W	2 h
S2	48 mA	150 V	12 W	2 h
S3	60 mA	150 V	12 W	8 h
S4	95 mA	150 V	12 W	Variable (*)

(*) final duration has been recorded

4.2.4.4 *Staining and Scanning of Gels*

After the second dimension, gels were carefully removed from the glass plates. Further treatment of the gels depended on the staining. Staining with ruthenium(II)tris(bathophenantroline disulfonate) (RuBPS) was carried out in the dark (Lamanda et al., 2007) as well as staining with „Pro-Q Diamond“ phosphoprotein gel stain, both under gentle shaking. Up to six gels were stained in one tray using 200 ml of solution per gel. For „Pro-Q Diamond“ phosphoprotein staining two gels were placed together in one tray with 500 ml of solution for each gel.

Gels stained with RuBPS fluorescent stain (Table 4) were scanned in a Typhoon Trio using the green laser (528 nm) at 610 nm and sensitivity set to “normal”. After prescanning at 1000 microns, final scans were obtained at 100 microns resolution and with a photomultiplier (PMT) voltage around 600 V (optimised PMT voltage was recorded).

For the visualisation of phosphorylated proteins, gels stained with „Pro-Q Diamond“ phosphoprotein gel stain (Table 4) were scanned using the green laser (528 nm) at 610 nm, normal sensitivity and with a PMT voltage of 750 V. After scanning, gels were stained with RuBPS in order to visualize all proteins and scanned with the appropriate settings.

Preparative gels were stained with colloidal coomassie (Table 4). After spots had been cut, the gels were shrunk 8-10 min in gel shrinking solution, then dried and preserved for further reference.

Table 4 summarises the staining conditions.

Table 4 Synopsis of staining protocols

	RuBPS		Phophor Stain		Colloidal Coomassie	
	Solution	**Time**	**Solution**	**Time**	**Solution**	**Time**
Fixation	-	-	50% methanol 10% acetic acid	30-60 min	50 % methanol 3% phosphoric acid	3 h
Washing	-	-	ddH_2O	3x15 min	ddH_2O	3x30 min
Prestain	-	-	-	-	50 % methanol 3% phosphoric acid 17% ammoniumsulfate	1 h
Stain	40% ethanol 10% acetic acid 1 mM RuBPS	1 h	"ProQ-Diamond" phosphoprotein gel stain	2 h	addition of 0.35 g/l coomassie brilliant blue G-250	4-5 d
Destain	40% ethanol 10% acetic acid	24-48 h	20% acetonitrile 50mM sodium acetate, pH 4.0	3x35 min	ddH_2O	var. (*)
Wash	ddH_2O	40 min	ddH2O	2x10 min		

(*) until background has been removed

4.2.4.5 *Image and Data Analysis*

2DE image analysis was performed with Progenesis SameSpots software. Spot parameters were exported from SameSpots. Log_e-transformed normalised spots volumes were computed by the software and exported for further statistical analysis (Valcu et al., 2012). Statistical analysis was performed with R (R-Development-Core-Team, 2006) using the following packages: lme4 (Bates et al., 2014) effects (Fox, 2006) and multcomp (Hothorn, 2011). Model estimates were visualised using the R package ggplot2 (Wickham, 2009).

To test whether the replicate explained significant variation of the log_e-transformed normalised spot volumes, two linear mixed effect models were applied for each spot, with either only treatment (NX vs. HX vs. ReOx; Model 1) or treatment and replicate (Model 2) as random factors.

Model 1 = lmer(log(Normalised Volume) ~ 1 + (1|Treatment), data)
Model 2 = lmer(log(Normalised Volume) ~ 1 + (1|Replicate) + (1|Treatment), data)

A likelihood ratio test was applied to compare the two models and the p-values of the Chi^2 tests were saved for all spots. A false discovery rate (FDR) correction was then applied (Benjamini and Hochberg, 1995).

A similar procedure was applied in order to determine whether the 2DE run explained significant variation of the log_e-transformed normalised spot volumes.

Model 1 = lmer(log(Normalised Volume) ~ 1 + (1|Treatment), data)
Model 2 = lmer(log(Normalised Volume) ~ 1 + (1|2DE run) + (1|Treatment), data)

Statistical analysis was performed on log_e-transformed normalised spot volumes computed by SameSpots (SS) software. For each spot a linear model was fitted with log_e-transformed normalised spot volume as dependent variable and treatment (NX vs. HX vs. ReOX) and cell line (WT vs. siCtr vs. siCA9) as predictors. The full model included the interaction between factors (i.e. treatment x cell line). To choose the minimal adequate model for each spot, the full model was simplified using an Akaike information criterion based stepwise backward elimination algorithm. Depending on the spots, the minimal models either retained 1 (intercept only), 3 (cell line or treatment), 5 (cell line and treatment) or 9 (cell line in interaction with treatment) parameters.

To test for differential spot abundance between cell lines and treatments, an FDR corrected posthoc test (Bretz et al., 2010) was performed on each minimal model. Spots which exhibited simultaneously a statistically significant difference between siCA9 and siCtr samples and a statistically non-significant (or an order of magnitude weaker) difference between siCtr and nontransformed WT HeLa cells were selected as being differentially regulated.

„Pro-Q Diamond“ phosphoprotein gel stain-treated gel images and RuBPS images obtained from the same gels were imported in SameSpots and aligned to a reference RuBPS stained gel. Differentially stained phosphorylated proteins were identified visually.

4.2.4.6 *Spot Preparation for Mass Spectrometry*

Spots for be analysed using mass spectrometry were manually excised from colloidal coomassie stained gels and stored at 4°C until further processing.

Gel plugs were incubated (with occasional vortexing) in destain solution until colorless. The solution was exchanged several times if needed. Destained gel plugs were washed in wash solution I for 3x15 min and incubated in shrinking solution for 2x3 min. Gel plugs were dehydrated in 100% acetonitrile for 10 min, then dried in the speed vac for 30 min and kept at -20°C until further processing.

The proteins were reduced in gel for 30 min at 56°C in reducing solution. After cooling down to room temperature, the solution was exchanged to alkylating solution. Incubation was carried out at room temperature in the dark for 45 min. Gel plugs were then washed for 15 min with 200 µl wash solution II and dehydrated with 100% acetonitril for 10 min. After reswelling in 100 µl wash solution II for another 10 min, gel plugs were shrunk again in 100% acetonitrile and dried in the speed vac for 10 min. Until further treatment, dried plugs were kept at -20°C.

For trypsin digest, gel plugs were rehydrated in 30 µl 2.5 ng/µl trypsin dissolved in 1 mM HCl. Excess supernatant was removed upon full swelling of the gel plugs and 30 µl MS digest buffer was added before the digst was carried out over night. Extraction of the peptides was carried out using 50 µl of 0.1 % trifluoroacetic acid in 33 % acetonitrile and a second step with 100 µl of 75% acetonitrile.

After removal of the solvent in the speed vac, samples were reconstituted in 20 µl of 5% acetonitrile in 0.1% formic acid. Analysis of samples was carried out in a nano-HLPC system (Easy nLC) using a 100 µm x 2 cm trapping column and a 75 µm x 10 cm C18 separation column with 5 µm particles. Elution was persued with an increasing gradient from 5% to 38% acetonitrile in 0.1% formic acid over 90 min.

4.2.4.7 *Mass Spectrometry*

MS analysis of gel plugs was carried out by Dr. Karl-Heinz Gührs from Friedrich Schiller University Jena as described below. The HPLC eluted fractions were sprayed into the sample inlet of a LTQ Orbitrap XL ETD mass spectrometer operating with a data dependent measuring scheme.

Measurements of up to three collision-induced dissociation spectra in the ion trap (Top3) were persued after a full scan at 60,000 resultion. Analysis of the spectra was carried out by ProteomeDiscoverer software, spectra search was performed by Mascot against the SwissProt

database. Fixed modifications were carbamidomethylation, whereas oxidation of methionine and phosphorylation of serine and threonine were set as variable modifications.

For analysis of phosphorylated proteins, settings were chosen accordingly in order to be able to select for phosphorylated proteins. At least three peptides were fixed as requirement for a positive identification within Mascot ion scores of at least 20 each or two spectra with scores higher than 40.

4.2.4.8 *Protein Identifications*

MS results were analysed using Scaffold 4 software. Spots with multiple hits were resolved by comparing spectral counts and spectral abundance factors (Shevchenko et al., 2009).

Information about protein features – such as molecular weight, isoelectric point and protein function – was acquired from the open access databases Phosphosite and Uniprot.

5 Results

Carbonic anhydrase IX (CAIX) is responsible for the regulation of pH in the cells. The protein has been established as a marker protein for hypoxic tumors that are resistent to radiotherapy and its presence has been associated with poor prognosis (Chia et al., 2001). Since there is only limited knowledge about further effects of CAIX on the cellular level, a proteomic screen was employed to identify potential downstream target proteins that are regulated following CAIX depletion.

5.1 CAIX Expression and Silencing of *CA9* in HeLa cells

For studying CAIX, the cervix carcinoma cell line HeLa has been selected, one of the classical tumour cell lines used in the literature. For all cell culture experiments three biological replicates were performed.

Being a target of HIF-1α transcription factor, CAIX protein is increasingly abundant with increasing cell density due to the microhypoxic environment created by increasing cell number (Chrastina, 2003). Hence it was important to determine the optimal conditions for all experimental procedures that would prevent cell density dependent CAIX induction while still providing sufficient biological material for analysis. To this aim HeLa cells were seeded at different densities and the level of CAIX protein expression was assessed by Western blot (WB) analysis. Indeed, CAIX protein levels were directly dependent on cell density (Figure 4).

The increase in HIF-1α protein was significant at a density of 40,000 ($z=3.803$, $N=3$, $p<0.001$ vs. 2,500) and 50,000 ($z=4.731$, $N=3$, $p<0.001$ vs. 2,500) cells/cm^2 whereas the increase in CAIX protein levels reached statistical significance at densities of 20,000 ($z=3.222$, $N=3$, $p=0.007$ vs. 2,500), 30,000 ($z=6.664$, $N=3$, $p<0.001$ vs. 2,500), 40,000 ($z=9.339$, $N=3$, $p<0.001$ vs. 2,500) and 50,000 ($z=12.744$, $N=3$, $p<0.001$ vs. 2,500) cells/cm^2 (Figure 4).

For further experiments a starting cell density of 10,000 cells per cm^2 was chosen for experiments of 48 h or shorter since the level of CAIX protein was indistinguishable from initial conditions ($z=2.158$, $N=3$, $p=0.136$ vs. 2,500). For longer incubation times, cell numbers were adjusted accordingly.

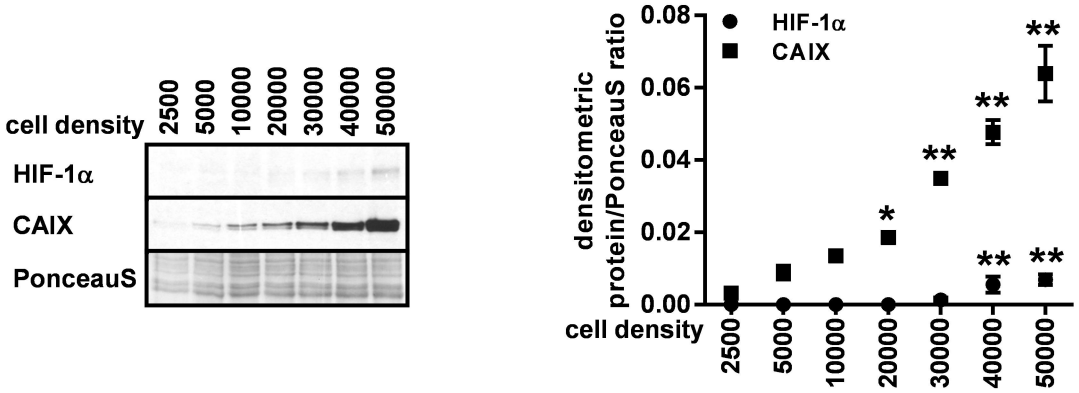

Figure 4 CAIX expression is dependent on cell density
HeLa cells were seeded at different cell densities (indicated are number of cells per cm^2) and allowed to grow for 48 h. CAIX and HIF-1α levels were determined by WB analysis using specific antibodies (left). PonceauS staining served as loading control. The figure (right) displays densitometric analysis (ImageJ) of WB data normalised to PonceauS (n=3, mean±SEM, *p<0.01 vs. 2,500, **p<0.001 vs. 2,500).

To investigate the role of CAIX in HeLa cells, a RNA interference (RNAi) approach was set up for silencing *CA9*. CAXII is another member of the family of α-carbonic anyhydrases known as the major enzyme responsible for regulating intracellular pH together with CAIX. The expression of CAXII is known to increase in response to *CA9* silencing (Chiche et al., 2009). Although CAXII expression could not previously be detected in HeLa cells (Wykoff et al., 2000) this had to be confirmed in order to decide whether a double knock down was necessary. HeLa cells were therefore exposed for 24 h to hypoxia (1% oxygen) in order to stimulate potential CAXII expression. A549 cells were used as positive controls since they are known to contain both *CA12* mRNA and CAXII protein (Wykoff et al., 2000). Using a qPCR approach it could be shown that *CA12* is not expressed in HeLa cells (Figure 5A). Therefore, silencing of *CA12* was not required when silencing *CA9* in HeLa cells.

For *CA9* silencing four different commercially available siRNAs specific for human *CA9* and two negative control siRNAs were tested (see 4.1.8 and 4.2.1.2). To exclude any influence of the transfection reagent, a mock transfection was performed. To monitor the silencing effect of the siRNAs, cells were seeded at 70% density sufficient to achieve full confluency at the time point of harvesting in order to induce CAIX expression to a level that could be reliably measured. Silencing efficiency was tested on mRNA level using qPCR as well as on protein level by WB analysis.

Among the negative control siRNAs, siControl_1 expression was in average closer to the mock treatment, but its variation was higher (Figure 5 B and C) whereas siAllStars showed a significant diferrence to mock levels on mRNA level (log ratio=-0.179, p=0.021 vs. mock). At protein level, the variance of siAllStars was closer to the variance of mock treated samples hence it was chosen as negative control siRNA in subsequent experiments. All siRNA duplexes tested showed

significant knock down of *CA9* and CAIX (Figure 5 B and C) as compared to control conditions (siCA9_2: log ratio=-2.894, p=0.003 vs. mock for RNA, z=-12.177, N=3, p<0.001 vs. mock, z=-13.866; N=3, p<0.001 vs. siAllStars for protein; siCA9_4: log ratio=-1.861, p=0.001 vs. mock for RNA, z=-11.295, N=3, p<0.001 vs. mock, z=-12.984, N=3, p<0.001 vs. siAllStars for protein; siCA9_5: log ratio=-2.518, p=0.044 vs. mock for RNA, z=-11.380, N=3, p<0.001 vs. mock, z=-12.809; N=3, p<0.001 vs. siAllStars for protein). Gene specific siRNA siCA9_3 showed the highest silencing effect on CAIX protein (z=12.655, N=3, p<0.001 vs. mock, z=14.084, N=3, p<0.001 vs. siAllStars) and the second highest at mRNA level (log ratio=-2.816, p=0.002 vs. mock) and was therefore selected for further experiments. In the following experiments, siCA9_3 is referred to as siCA9 and siAllStars as siCtr.

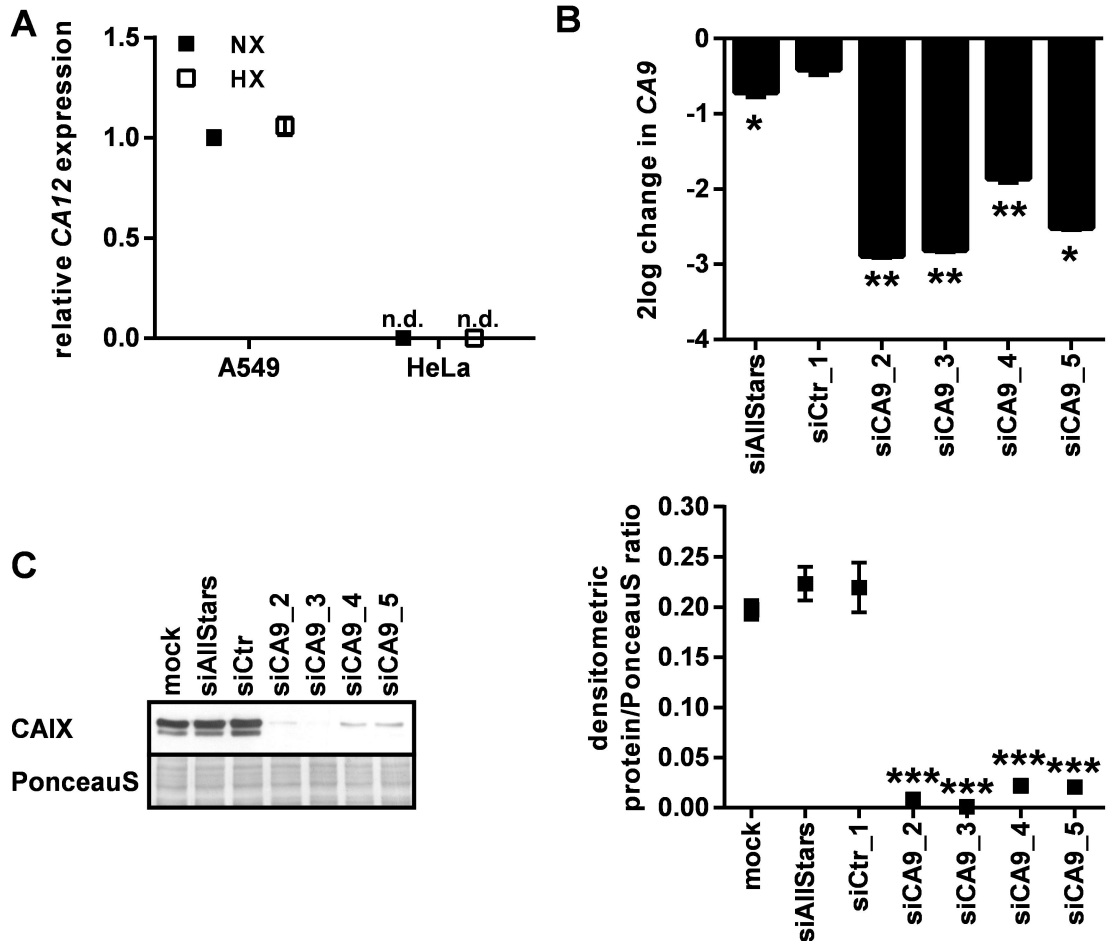

Figure 5 Silencing of *CA9* using specific siRNA
(A) A549 and HeLa cells were grown at 1% oxygen for 48 h. RNA was isolated for qPCR analysis. Relative *CA12* mRNA expression is shown after normalisation to *ACTB* (n=3, mean±SD, n.d. = not detectable). (B+C) HeLa cells were transfected using four specific siRNAs against *CA9* (siCA9_2, siCA9_3, siCA9_4, siCA9_5) and two unspecific control siRNAs (siAllStars, siCtr_1) or transfection reagent only (mock). Cells were harvested 48 h posttransfectionally and either RNA for qPCR (B) or protein for WB analysis (C) was isolated. (B) Relative *CA9* mRNA expression after normalisation to *ACTB* is shown as 2-log regulation. (C) WB analysis of CAIX using an specific antibody against CAIX is shown. PonceauS staining served as loading control. Graph shows densitometric analysis (ImageJ) of CAIX protein levels after normalisation to PonceauS (n=3, mean±SEM, *p<0.05 vs. mock, **p<0.01 vs. mock, ***p<0.001 vs. mock/siAllStars/siCtr_1).

5.2 Regulation of CAIX in HeLa Cells

Since CAIX is a marker for hypoxic tumours (Loncaster et al., 2001) hypoxia was used as a stimulus in order to investigate the role of CAIX in the chosen tumour model of HeLa cells. To determine the best time point for studying CAIX under the control of hypoxia, cells were exposed to 1% oxygen for different time periods and the expression of CAIX protein was investigated (Figure 6) using WB analysis. The expression of HIF-1α as the main transcription factor regulating CAIX was also assessed. In order to avoid induction of CAIX due to cell density, different starting cell numbers were chosen depending on the duration of the incubation such that all samples reached the same density at the end of the incubation period.

As expected, CAIX protein levels were significantly increased after 16 h incubation at 1% oxygen ($z=4.559$, $N=3$, $p<0.001$ vs. Ctr) and were still statistically significant at 24 h ($z=7.085$, $N=3$, $p<0.001$ vs. Ctr) and 48 h ($z=7.037$, $N=3$, $p<0.001$ vs. Ctr; Figure 6).

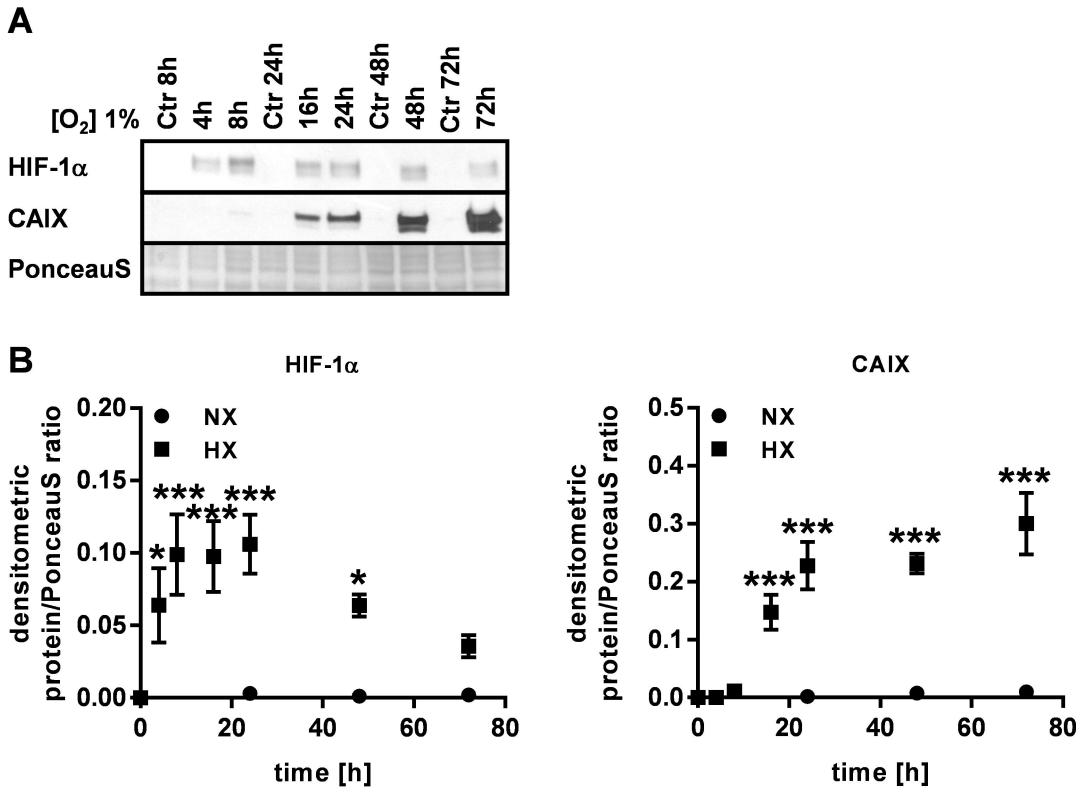

Figure 6 Sustained hypoxia induces CAIX in HeLa cells
HeLa cells were exposed to 1% oxygen for indicated time periods. (A) Levels of HIF-1α and CAIX were determined by WB analysis using specific antibodies. PonceauS staining served as loading control. (B) Densitometric analysis (ImageJ) of protein levels of HIF-1α and CAIX as ratio to PonceauS (n=3, mean±SEM, *p<0.05 vs. Ctr, ***p<0.001 vs. Ctr).

HIF-1α levels showed an increase starting from 4 h (4 h: z=3.138, N=3, p=0.010 vs. Ctr; 8 h: z=4.852, N=3, p<0.001 vs. Ctr; 16 h: z=4.644, N=3, p<0.001 vs. Ctr) peaking at 24 h of hypoxia (24 h: z=5.066, N=3, p<0.001 vs. Ctr; 48 h: z=3.068, N=3, p=0.013 vs. Ctr), while CAIX further increased until 72h of hypoxia (z=9.126, N=3, p<0.001 vs. Ctr; Figure 6). Given the rapid proliferation of HeLa cells and the dependence of CAIX expression on the cell number and density, a 24 h hypoxic treatment was selected for further investigations of CAIX.

Since HIF-1α is sensitive to reoxygenation and CAIX is a HIF-1α target protein, the effect of reoxygenation on CAIX was further investigated. Following 24 h at 1% oxygen cells were exposed to normoxia (21% oxygen) for different time periods and CAIX and HIF-1α protein levels were assessed by means of WB analysis (Figure 7).

After a fast induction under hypoxic conditions, HIF-1α protein (z=7.162, N=3, p<0.001 vs. Ctr) was highly unstable after reoxygenation resulting in a complete reduction within one hour of reoxygenation (z=-7.162, N=3, p<0.001 vs. 0h ReOX; Figure 7).

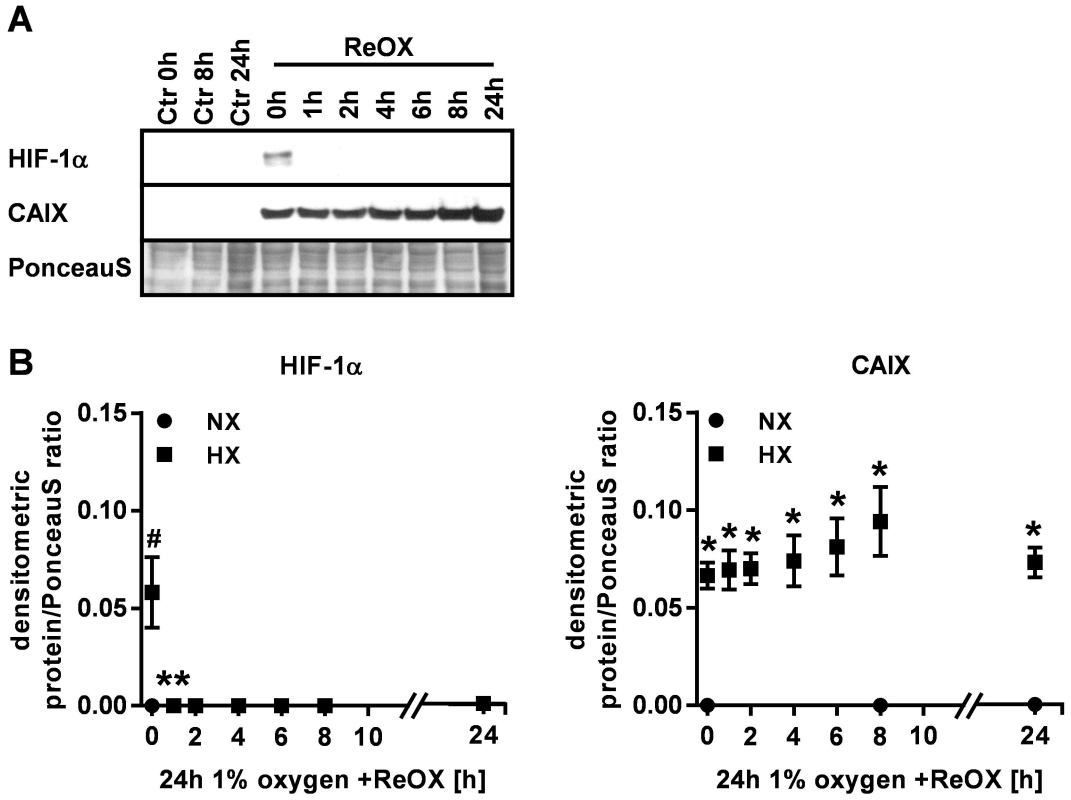

Figure 7 CAIX is stable during the first 24 h of reoxygenation
HeLa cells were exposed to 1% oxygen for 24 h and subsequently reoxygenated for the indicated time points. (A) HIF-1α and CAIX levels were determined by WB analysis using specific antibodies. PonceauS staining served as loading control. (B) Densitometric analysis (ImageJ) of protein levels of HIF-1α and CAIX as ratio to PonceauS (n=3, mean±SEM, #p<0.001 0h ReOX vs. Ctr, *p<0.001 ReOX vs. Ctr, **p<0.001 vs. 0h ReOX).

However, CAIX levels were significantly upregulated after 24 h of hypoxia as compared to control condition ($z=6.725$, $N=3$, $p<0.001$ vs. Ctr), then remained stable until after 24 h of reoxygenation (1h: $z=7.023$, $N=3$, $p<0.001$ vs. Ctr; 2h: $z=7.077$, $N=3$, $p<0.001$ vs. Ctr; 4 h: $z=7.483$, $N=3$, $p<0.001$ vs. Ctr; 6 h: $z=8.212$, $N=3$, $p<0.001$ vs. Ctr, 8 h: $z=9.534$, $N=3$, $p<0.001$ vs. Ctr; 24 h: $z=7.370$, $N=3$, $p<0.001$ vs. Ctr; Figure 7).

Based on these results, for all further experiments, the hypoxic induction had a duration of 24 h and the cells were subsequently subjected for 8 h to normoxic conditions for reoxygenation.

5.3 Proteomic Profiling of CAIX Depleted HeLa Cells

A proteomic study was undertaken to investigate the role of CAIX in the response of HeLa cells to fluctuating oxygen concentrations which are known to occur in tumors (Kimura et al., 1996; Matsumoto et al., 2010). Specific siRNA against *CA9* was used to silence CAIX expression in HeLa cells, which were subsequently subjected to hypoxia and reoxygenation.

This setup was chosen to maximize the output information on the effect of *CA9* silencing under different oxygen concentrations at proteome level. The combination of CAIX induction during hypoxia and CAIX stability during reoxygenation which contrasts to the expression of HIF-1α aimed to facilitate the identification of cellular processes that are controlled by CAIX and to gain further insights in the crucial role of CAIX in cancer.

To this end, *CA9* was silenced in HeLa cells and CAIX depleted cells were exposed to 24 h hypoxia or 24 h hypoxia followed by 8 h of reoxygenation. Treated cells were compared to normoxic cells as shown in Figure 8. HeLa cells transfected with siCtr and untreated wild type HeLa cells (WT) were used as controls under all experimental conditions. The latter allowed to identify and exclude the effects of the transfection and the control siRNA. The experimental setup consisted thus of 9 experimental conditions. In order to minimize the confounding effects of cell growth and density, all cells were harvested at the same time point, 48 h after the start of the experiment (Figure 8).

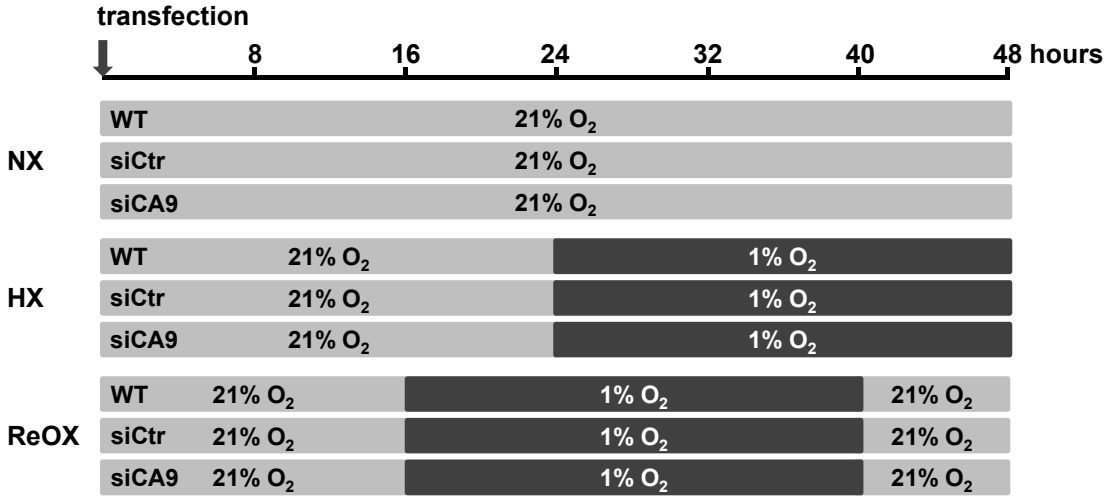

Figure 8 Experimental setup of the 2DE experiment
Displayed is the experimental outline. Cells were treated using siRNA against *CA9* (siCA9) or control siRNA (siCtr) or left untransfected (WT) followed by either treatment with 48 h of normoxia (NX), 24 h of normoxia followed by 24 h of hypoxia (1% oxygen; HX) or 16 h of normoxia followed by 24 h hypoxia (1% oxygen) and 8 h of normoxia (21% oxygen; ReOX).

5.3.1 Validation of the Experimental System

Proteins were isolated for proteomics analysis according to the protocol described in section 4.2.4.1. Protein levels of HIF-1α and CAIX were verified by WB analysis prior to 2DE analysis. The induction of HIF-1α and CAIX due to hypoxic treatment and the silencing of *CA9* could thus be validated (Figure 9).

The increase in protein levels due to hypoxic treatment was significant for HIF-1α and CAIX in WT cells (HIF-1α: $z=3.688$, $N=3$, $p<0.001$ vs. NX; CAIX: $z=5.626$, $N=3$, $p<0.001$ vs. NX) and in cells transfected with siCtr (HIF-1α: $z=5.832$, $N=3$, $p<0.001$ vs. NX; CAIX: $z=10.85$, $N=3$, $p<0.001$ vs. NX), respectively. For CAIX, the induction was maintained during reoxygenation (WT: $z=10.537$, $N=3$, $p<0.001$ vs. NX; siCtr: $z=15.44$, $N=3$, $p<0.001$ vs. NX). Silencing of *CA9* resulted in significantly reduced CAIX levels under hypoxic ($z=-6.723$, $N=3$, $p<0.001$ vs. WT; $z=-7.920$, $N=3$, $p<0.001$ vs. siCtr) as well as under reoxygenating conditions ($z=-22.78$, $N=3$, $p<0.001$ vs. WT; $z=-20.23$, $N=3$, $p<0.001$ vs. siCtr; Figure 9). Silencing of *CA9* did not significantly influence levels of HIF-1α under hypoxic conditions ($z=-1.388$, $N=3$, $p=0.280$ vs. WT; $z=-1.750$, $N=3$, $p=0.142$ vs. siCtr).

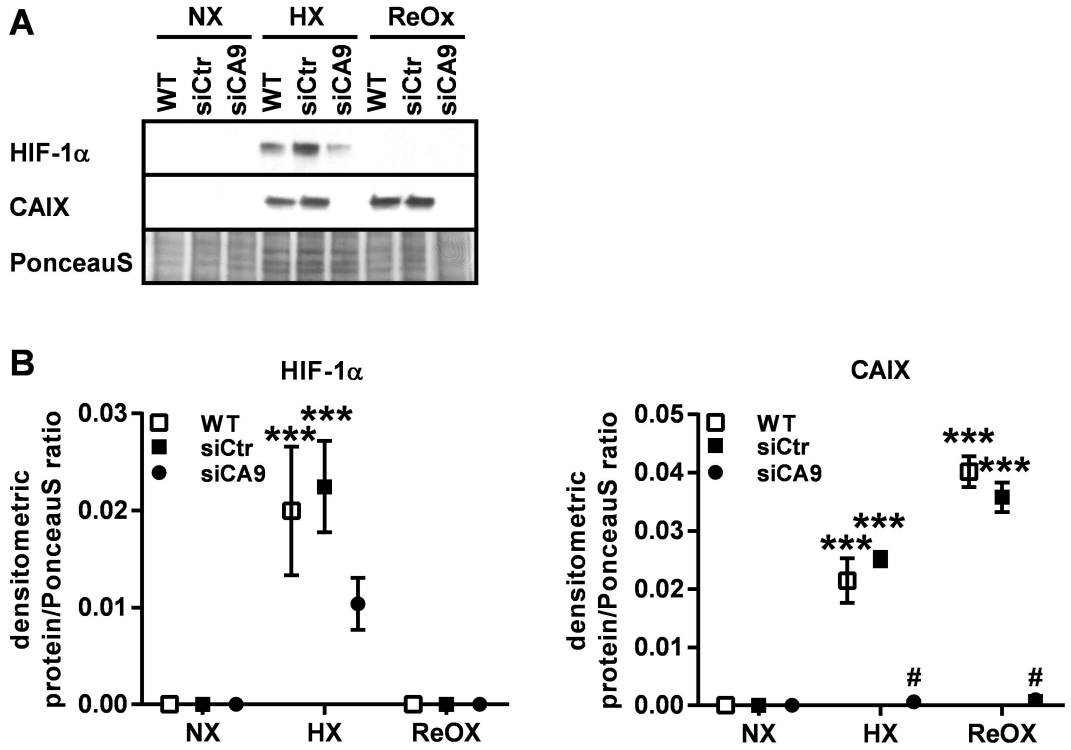

Figure 9 Levels of CAIX and HIF-1α in protein extracts for the 2DE study
HeLa cells used for 2DE analysis were reversely transfected with siRNA against *CA9* (siCA9) or control siRNA (siCtr) or left untransfected (WT). Cells were exposed to either 48 h normoxia (NX), 24 h normoxia followed by 24 h 1% oxygen (HX) or 16 h normoxia, 24 h hypoxia (1% oxygen) followed by 8 h normoxia (ReOX). Cells were harvested and protein extracts were prepared for 2DE analysis. (A) In addition, protein levels of HIF-1α and CAIX were analysed using WB analysis with specific antibodies. PonceauS staining served as loading control. (B) Densitometric analysis (ImageJ) of protein levels of HIF-1α and CAIX as ratio to PonceauS (n=3, mean±SEM, ***p<0.001 vs. NX, #p<0.001 vs. WT/siCtr).

5.3.2 Data Quality Control

2DE experiments were performed in three independent replicates as described in section 4.2.4 and allowed the reproducible identification and quantification of 2,331 spots in total. Two linear mixed effect models were applied for every spot: with either only treatment (NX vs. HX vs. ReOx; Model 1) or with treatment and replicate (Model 2) as random factors in order to determine whether the replicate explained significant variation of the spot volumes (see 4.2.4.5).

Statistical models were applied as described in section 4.2.4.5. Including the replicate as random factor improved the fit of the model for only 0.3% of the spots (seven out of 2,331 spots) while including the 2DE run as random factor did not improve the fit of the model for any of the 2,331 analysed spots, which indicates a high technical reproducibility of the 2DE analysis. The replicate and the 2DE run were therefore not included as factors in further analyses.

5.3.3 Protein Expression Pattern under Different Oxygen Conditions

Principal component analysis (PCA) of normalised spot volumes in SameSpots software allowed differentiating the gels according to the treatment applied. 2DE gels from hypoxia treated samples clustered away from those from samples subjected to normoxia or reoxygenation (Figure 10).

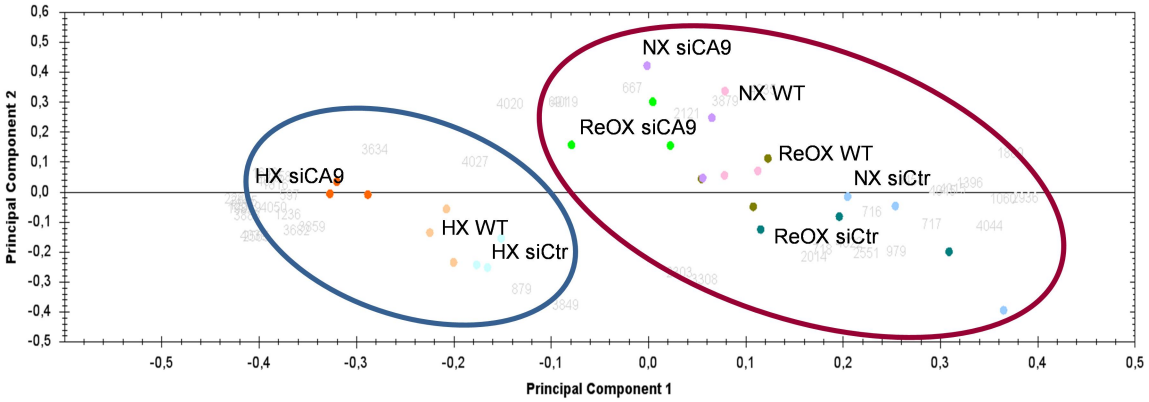

Figure 10 Principal component analysis of 2DE gels
The analysis shows a clear distinction between hypoxia treated samples (circled in blue) and those treated with normoxia or reoxygenation (circled in red). PCA was carried out in SameSpots software.

5.3.4 Differential Expression of Proteins in CAIX Depleted HeLa Cells under Different Oxygenation Conditions

Image analysis was performed using SameSpots software. Normalised spot volumes were exported from SameSpots and $\log_e$-transformed towards a Gaussian distribution before further statistical analysis (Valcu et al., 2012). Statistical analysis of $\log_e$-transformed normalised spot volumes was carried out using different statistical models in order to identify differential expression of 2DE protein spots under different treatments (NX vs. HX vs. ReOX) and/or in different cell lines (WT vs. siCtr vs. siCA9) as described in section 4.2.4.5.

The minimal model retained 1 (intercept only), 3 (cell line or treatment), 5 (cell line and treatment) or 9 (cell line in interaction with treatment) parameters for 384, 1,168, 345 and 434 spots, respectively. An FDR corrected posthoc test (Bretz et al., 2010) was used to test for differential spot abundance between cell lines and treatments. Spots that showed a statistically significant difference between siCA9 and siCtr samples and at the same time a statistically non-significant (or at least an order of magnitude weaker) difference between siCtr and WT HeLa cells were selected as being differentially regulated. A few additional spots which partly fulfilled these requirements

(e.g. with marginally significant differences between siCtr and siCA9 [#30, 41], significant differences between siCtr and WT [#26] and/or appearing on the 2DE gel to be isoforms of already selected spots possibly carrying different post translational modifications [#1, 26, 30]) were also retained in the data set.

Among the spots differentially expressed in siCA9 cells, nine had similar expression profiles under all conditions of oxygenation tested (Figure 11), 35 were differentially regulated under different experimental variants (NX vs. HX vs. ReOx, Figure 12) and three displayed complex expression profiles with interaction between factors (Figure 13). In total, 47 spots were selected as differentially expressed (Figure 15). P-values for each spot and the models applied are summarised in Supporting Table 1 (see 8.4).

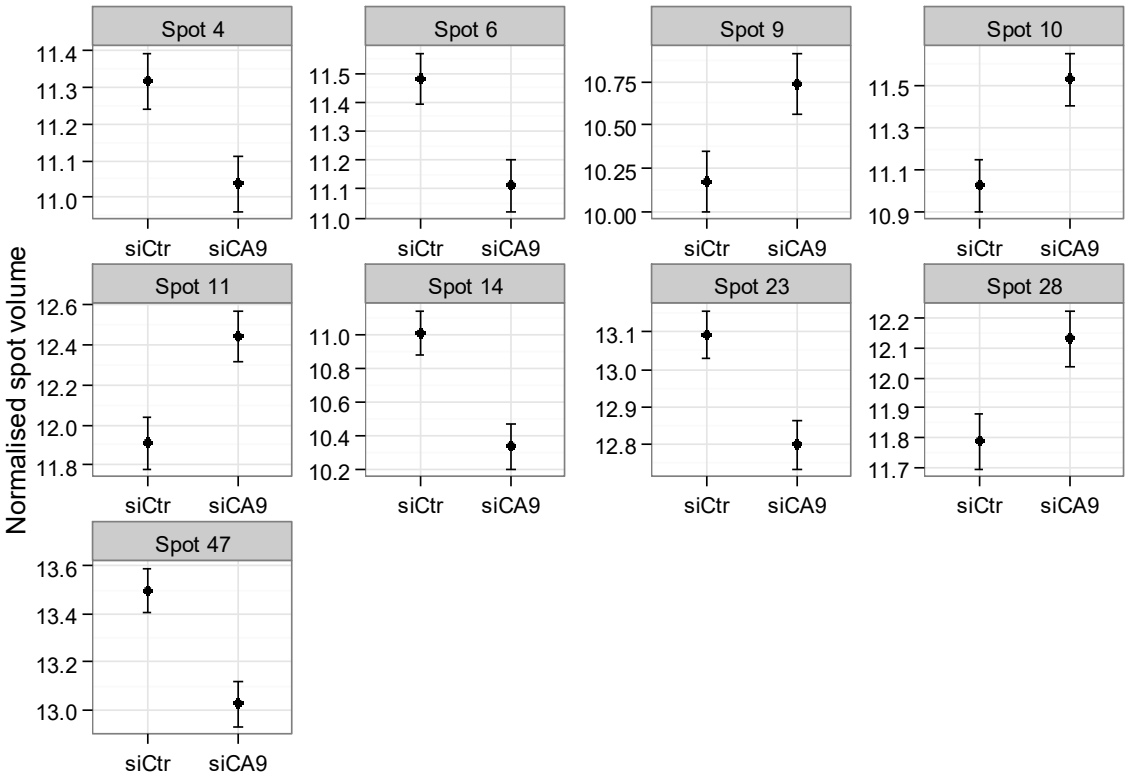

Figure 11 2DE spots differentially expressed in siCA9 vs. siCtr HeLa cells
Given are normalised spot volumes for the selected conditions. Error bars show standard deviation.

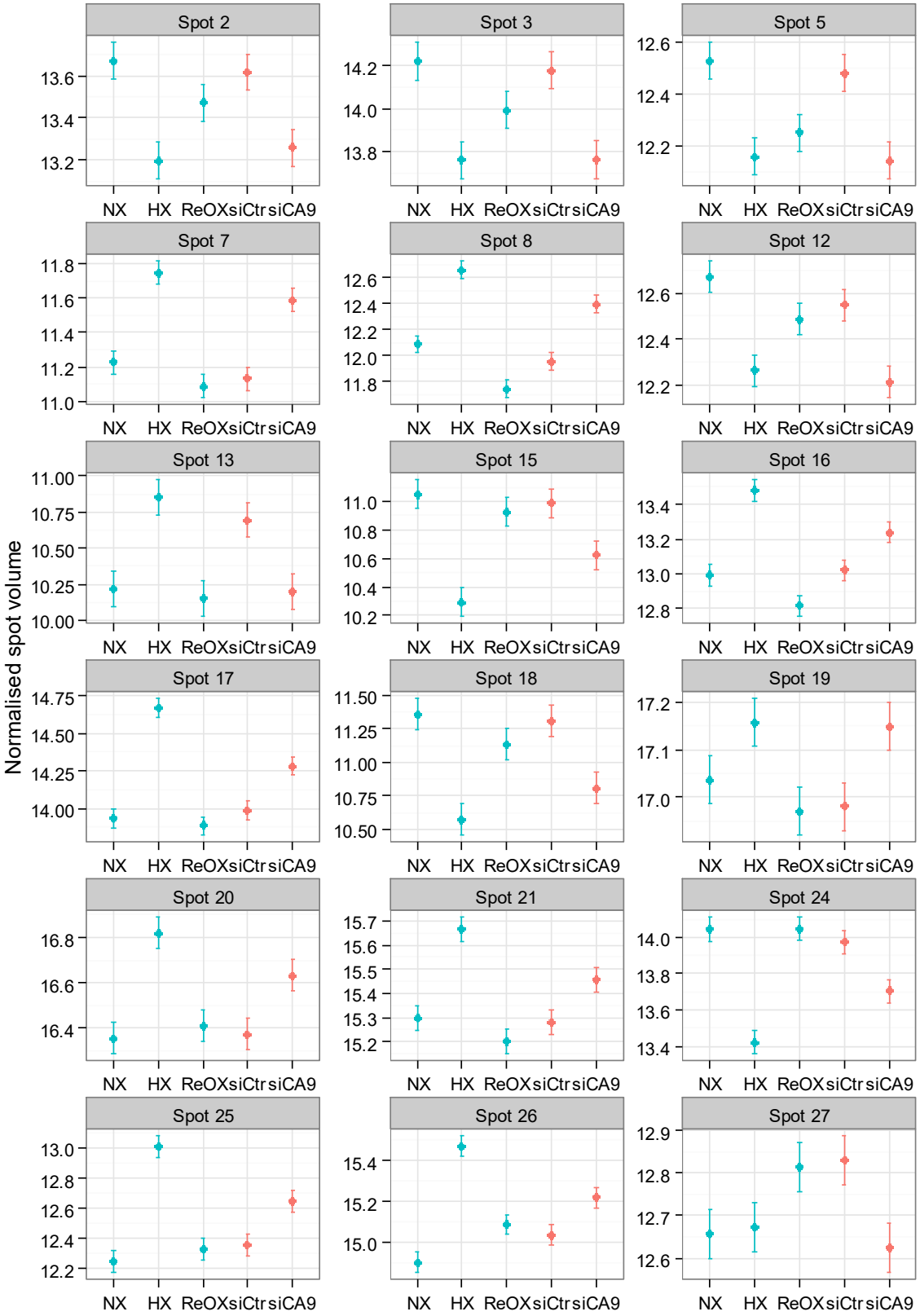

continued on next page…

Figure 12 2DE spots differentially expressed in siCA9 vs. siCtr HeLa cells and under different oxygenation conditions
Given are normalised spot volumes for the selected conditions. Error bars indicate standard deviation.

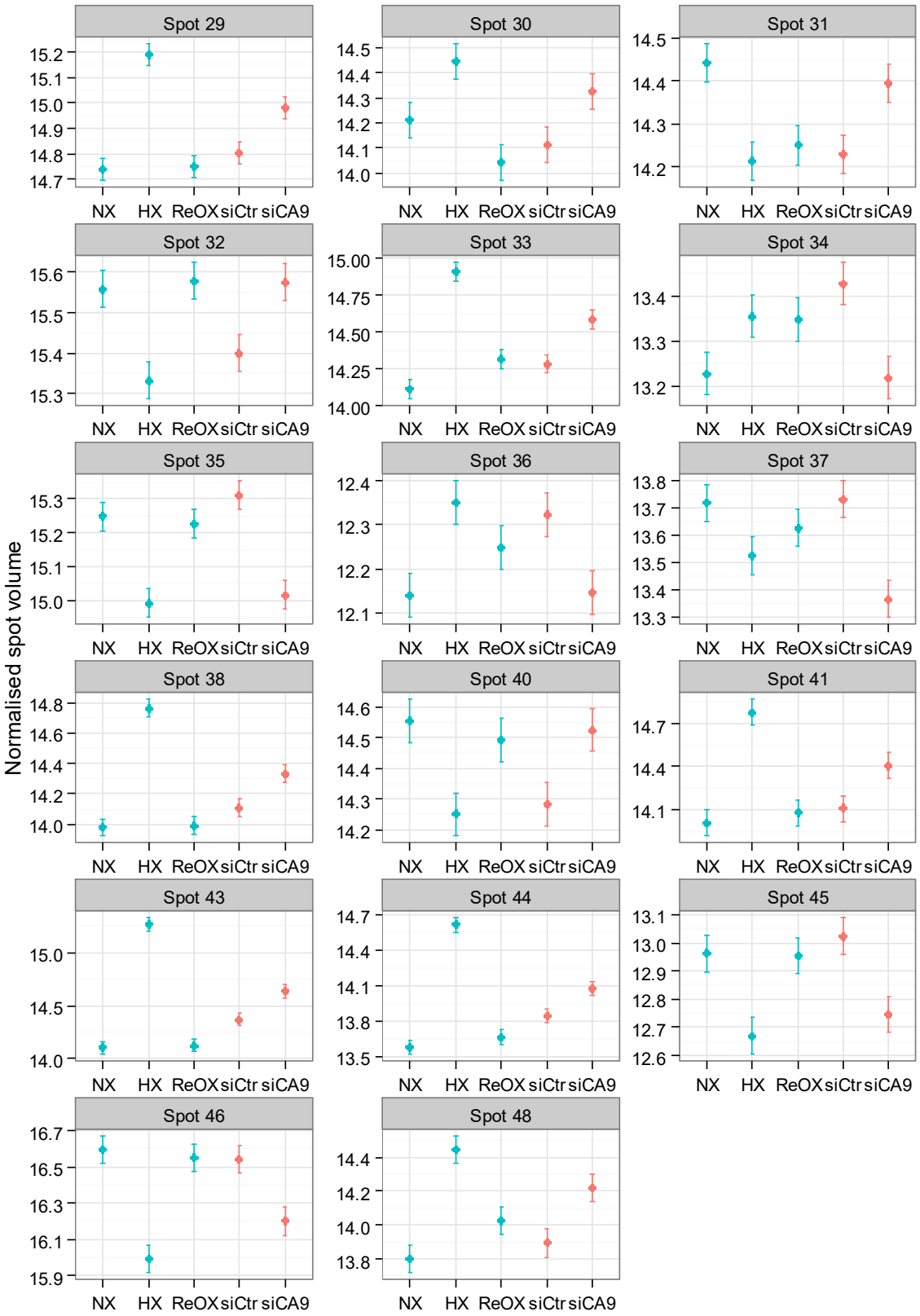
Normalised spot volume
Spot 29
Spot 30
Spot 31
Spot 32
Spot 33
Spot 34
Spot 35
Spot 36
Spot 37
Spot 38
Spot 40
Spot 41
Spot 43
Spot 44
Spot 45
Spot 46
Spot 48
NX
HX
ReOX
siCtr
siCA9

...continued.

Spots #1, #22 and #39 displayed more complex behaviours, with significant interactions between factors, i.e. oxygenation**CA9* silencing (Figure 13). In these cases, spot regulation in siCtr samples is different from the regulation of siCA9 samples for this particular spot.

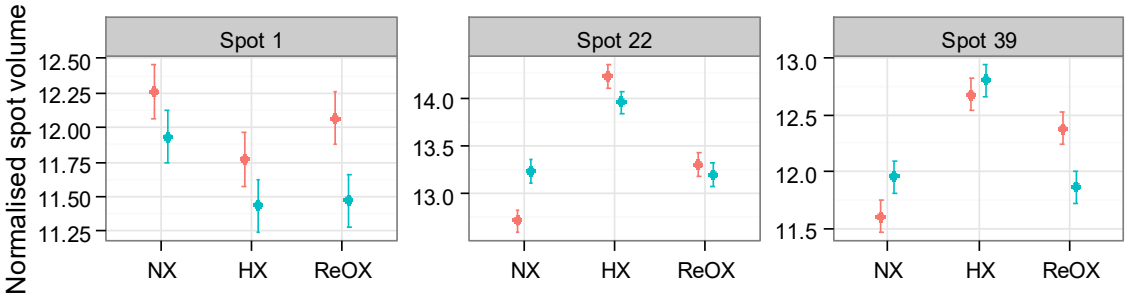

Figure 13 2DE spots differentially expressed in siCA9 vs. siCtr HeLa cells and under different oxygenation conditions which displayed interaction between factors
Given are normalised spot volumes for siCtr (red) and siCA9 (green). Error bars indicate standard deviation.

The majority of the protein spots (53.2%, i.e. 25 spots) identified by 2DE analysis showed increased volumes after silencing of *CA9* (Figure 14, all labelled in red colour). Of those, 29.8% (14 spots) displayed in addition changed volumes upon treatment with hypoxia. 10.6% (five spots) also changed their abundance following reoxygenation and in comparison to normoxic treatment. In contrast to this, only single 2DE spots decreased their volumes in response to hypoxia or to hypoxia and reoxygenation, respectively.

42.6% (20 spots), showed smaller spot volumes in 2DE gels obtained from CAIX depleted cells (Figure 14, all labelled in blue colour). 12.8% (six spots) did not display any dependence on oxygen concentration, whereas the volumes of 27.7% (13 spots) significantly changed upon hypoxic incubation and 2.1% (one spot) also upon reoxygenation. Three spots (6.4%) showed unique regulation. In these cases, the regulation of spot volumes was different under siCtr conditions in comparison to siCA9 treatment.

Overall, 23.4% of the spots (11 spots) were only regulated by CAIX depletion, 57.4% (27 spots) were additionally regulated by hypoxia and 12.8% (six spots) were regulated by CAIX and reoxygenation. Figure 14 visualizes these regulation pattern showing a strong relation of upregulation by siCA9 and hypoxia.

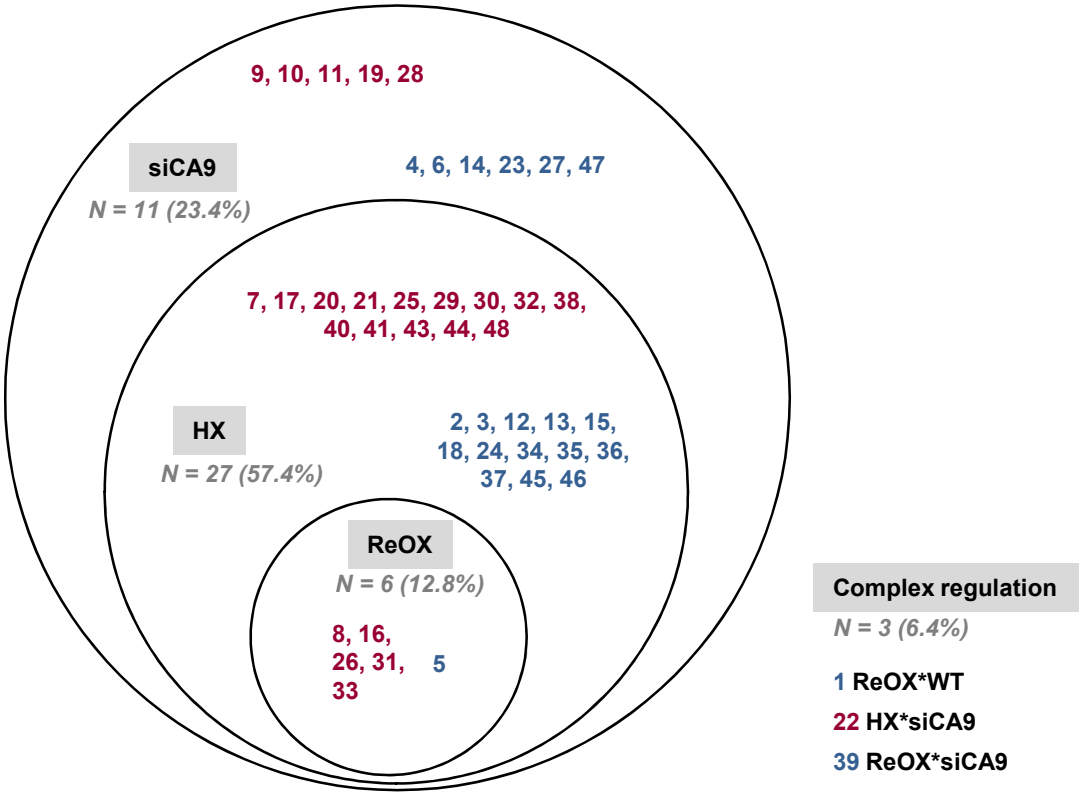

Figure 14 Regulation of spot volumes
Displayed are regulation patterns of spot volumes identified by 2DE analysis using calculated percantages. Red = upregulated spot/blue = downregulated spot when cells were depleted of CAIX, HX = hypoxia, ReOX = reoxygenation, siCA9 = transfection with specific siRNA against *CA9*.

Summarizing all the above findings, Figure 15 shows all regulated spots on a representative 2DE gel presenting the spot number and the regulation pattern.

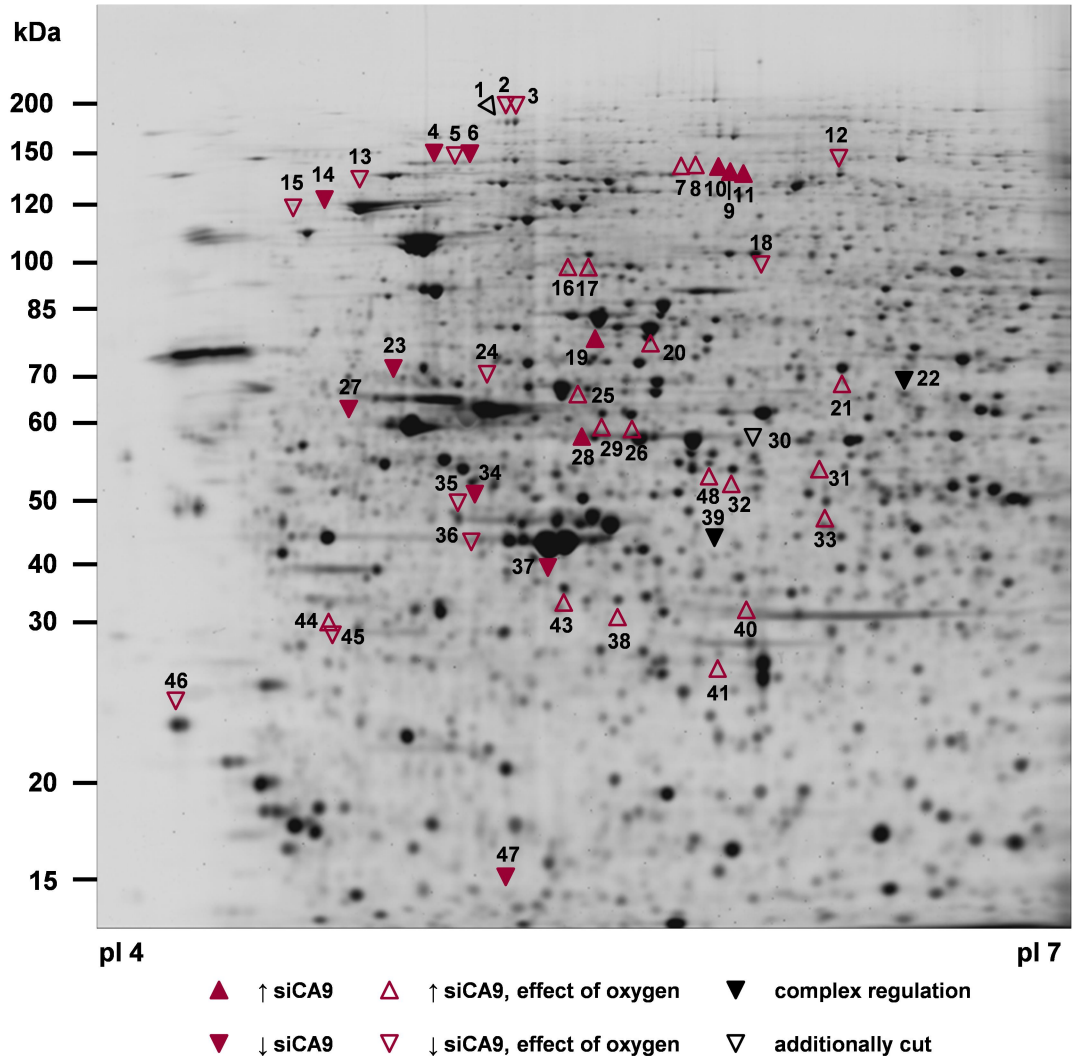

Figure 15 Spots identified by 2DE as being differentially regulated
Dysregulated spots are displayed on a representative 2DE gel. Markers for isoelectric points (pI 4 and pI 7) are given below the gel, marker protein sizes (in kDa) are given on the left.

Detailed images for all regulated spots under all different conditions are presented in Supporting Figure 1 in section 8.4.

5.3.5 Identification of the Proteins Differentially Expressed in CAIX Depleted HeLa Cells under Different Oxygenation Conditions

The spots identified as differentially expressed were excised from coomassie-stained preparative gels obtained from two experimental variants (cell line and treatment) which displayed minimal and maximum spot abundance, respectively. The eluted and digested protein content underwent MS analysis. MS analysis was carried out in the lab of a collaboration partner as described in section 4.2.4.7.

MS analysis successfully identified the proteins contained within 43 spots. Among these, four spots contained single proteins while the rest contained mixtures of two or more proteins. For 24 of these spots, the dysregulated protein could be identified by comparing spectral counts and spectral abundance factors of the different proteins identified in the plugs excised from siCA9 vs. siCtr gels (Shevchenko et al., 2009).

Taken together, MS analysis unambigously identified 25 dysregulated protein functions from 37 spots. All protein functions are listed in Table 5. Besides the identification numbers from SameSpots analysis and MS analysis, the molecular weights and isoelectric points determined by 2DE analysis are displayed together with the direction of their regulation. Further information such as number of peptides and sequence coverage are given in section 8.4 (Supporting Table 2 and Supporting Table 3).

Table 5 Regulated protein containing spots identified by MS

Given are spot IDs from SameSpots software (SS) and MS analysis (MS), molecular weight (MW) and isoelectric point (pI) as identified on 2DE gels and the identified protein functions. For the regulation of spot volumes fold regulation (fold reg.), direction of regulation (up/down) and significance levels (°p<0.1,*p<0.05, **p<0.01, ***p<0.001) are presented. Accession IDs from Uniprot database (Acc. ID) are listed for each protein. siCA9 = transfection with specific siRNA against *CA9*, HX = hypoxia, ReOX = reoxygenation, A*B indicates complex regulation by interplay of two factors (A,B).

Spot ID		MW	pI	Protein Identified	Abbreviation (Uniprot)	Acc. ID	siCA9 vs. siCtr			HX vs. NX			ReOX vs. NX		
MS	SS						fold reg.	dir.	p	fold reg.	dir.	p	fold reg.	dir.	p
2	4015	145	5.1	Hypoxia up-regulated protein 1	ORP-150	Q9Y4L1	0.70	▼	*	0.62	▼	**			
3	4045	145	5.1	Hypoxia up-regulated protein 1	ORP-150	Q9Y4L1	0.66	▼	**	0.80	▼	**			
4	716	119	4.9	Calpastatin	Calpastatin	P20810	0.76	▼	*						
5	717	119	5	Calpastatin	Calpastatin	P20810	0.71	▼	**	0.69	▼	**	0.76	▼	*
6	718	119	5	Calpastatin	Calpastatin	P20810	0.69	▼	*						
7	4017	127	5.6	Heterogeneous nuclear ribonucleoprotein U Kinesin-like protein KIF11	hnRNP U TRIP-5	Q00839 P52732	1.58	▲	***	1.68	▲	***			
8	597	128	5.6	Heterogeneous nuclear ribonucleoprotein U	hnRNP U	Q00839	1.55	▲	***	1.77	▲	***	0.71	▼	**
10	667	123	5.7	Heterogeneous nuclear ribonucleoprotein U Kinesin-like protein KIF11	hnRNP U TRIP-5	Q00839 P52732	1.65	▲	*						
11	691	122	5.8	Heterogeneous nuclear ribonucleoprotein U	hnRNP U	Q00839	1.70	▲	*						
13	879	111	4.7	Endoplasmin	GRP-94	P14625	0.61	▼	*	1.89	▲	**			
16	1236	92	5.3	Eukaryotic pept. chain release fact. GTP-bind. subunit ERF3A	eRF3a	P15170	1.25	▲	*	1.63	▲	***	0.84	▼	°
17	1237	92	5.3	Eukaryotic pept. chain release fact. GTP-bind. subunit ERF3A	eRF3a	P15170	1.34	▲	**	2.09	▲	***			
18	1396	84	5.8	78 kDa glucose-regulated protein	GRP-78	P11021	0.61	▼	*	0.45	▼	***			
19	3634	74	5.4	78 kDa glucose-regulated protein	GRP-78	P11021	1.18	▲	*						
20	1649	73	5.5	78 kDa glucose-regulated protein	GRP-78	P11021	1.30	▲	*	1.59	▲	***			
21	1816	65	6	T-complex protein 1 subunit alpha	TCP-1-α	P17987	1.19	▲	*	1.44	▲	***			
23	4022	62	4.8	Programmed cell death protein 4	PDCD4	Q53EL6	0.74	▼	**						
24	1889	61	5.1	Nucleobindin-1	Nucleobindin-1	Q02818	0.76	▼	*	0.53	▼	***			
25	3665	63	5.3	60 kDa heat shock protein, mitochondrial	Hsp60	P10809	1.33	▲	*	2.14	▲	***			
26	4049	57	5.5	Peptidyl-prolyl cis-trans isomerase FKBP4	PPIase FKBP4	Q02790	1.20	▲	*	1.77	▲	***	1.21	▲	*
27	2014	56	4.7	Tubulin β-4A chain	Tubulin β-4A chain	P04350	0.81	▼	*						
28	4027	55	5.3	Tubulin β-4A chain	Tubulin β-4A chain	P04350	1.41	▲	*						
29	1987	57	5.4	Peptidyl-prolyl cis-trans isomerase FKBP4	PPIase FKBP4	Q02790	1.19	▲	*	1.57	▲	***			
30	4030	51	5.8	4-trimethylaminobutyraldehyde dehydrogenase	TMABADH	P49189									
31	2121	51	6	4-trimethylaminobutyraldehyde dehydrogenase	TMABADH	P49189	1.18	▲	*	0.80	▼	**	0.83	▼	*
32	4035	48	5.7	Actin-related protein 3	Actin-related protein 3	P61158	1.19	▲	*	0.80	▼	**			
33	2285	43	6	Pachytene checkpoint protein 2 homolog	TRIP-13	Q15645	1.35	▲	**	2.22	▲	***	1.23	▲	°
35	3820	41	5	Endoplasmic reticulum resident protein 44	ERp44	Q9BS26	0.74	▼	***	0.77	▼	***			
38	3888	29	5.4	Glutaredoxin-3	Glutaredoxin-3	O76003	1.25	▲	*	2.19	▲	***			
41	4050	27	5.7	Elongation factor 1-δ	EF-1-δ	P29692	1.35	▲	°	2.17	▲	***			
43	2565	30	5.3	Serpin B6	Serpin B6	P35237	1.30	▲	*	3.21	▲	***			
44	4039	29	4.6	Endoplasmin Hepatoma-derived growth factor	GRP-94 HDGF	P14625 P51858	1.26	▲	*	2.81	▲	***			
46	2936	25	4.2	Complement comp. 1 Q subcomponent-binding protein, mitochondrial	C1qBP	Q07021	0.71	▼	**	0.55	▼	***			
47	3308	17	5.1	NADH dehydrogenase [ubiquinone] iron-sulfur protein 8, mitochondrial	CI-23kD	O00217	0.62	▼	**						

Spot ID		MW	pI	Protein Identified	Abbreviation	Acc. ID	ReOX*WT			HX*siCA9			ReOX*siCA9		
MS	SS						fold reg.	dir.	p	fold reg.	dir.	p	fold reg.	dir.	p
1	4014	145	5.1	Hypoxia up-regulated protein 1	ORP-150	Q9Y4L1									
22	3682	60	6.2	Thioredoxin reductase 1, cytoplasmic	ERp46	Q8NBS9				2.05	▲	*	0.90	▼	°
39	3859	34	5.7	Mannose-6-phosphate isomerase	PMI	P34949							0.59	▼	*

All protein identifications of spots being significantly regulated including the specific regulation of each spot and the identified protein functions are displayed in Figure 16.

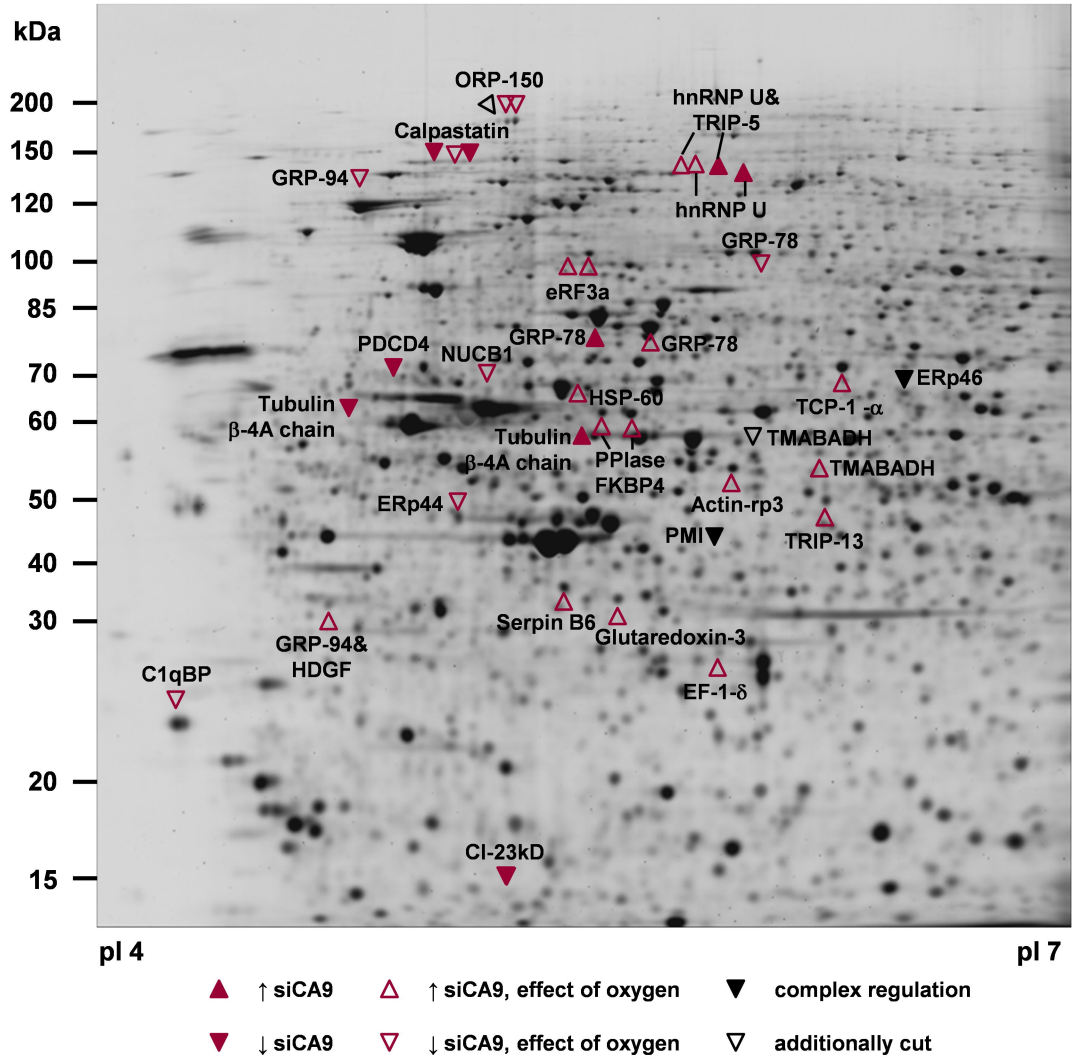

Figure 16 Protein functions and their regulation identified by 2DE and MS analysis
Shown are all spots differentially regulated with the specific pattern of regulation as indicated. All identified protein functions are as given in Table 5. Markers for isoelectric points (pI 4 and pI 7) are given below the gel, marker protein sizes (in kDa) are given on the left. Abbreviations (different to those in Table 5): Actin-rp3 = Actin-related protein 3, NUCB1 = Nucleobindin-1.

5.3.6 Validation of the Differential Protein Expression

A number of five proteins which were present in 2DE spots in complex mixtures with other proteins and identified as regulated through spectral counts analysis were selected for validation by means of WB analysis. The spectral counts analysis has confirmed the direction of regulation apparent on the 2DE gels for two of these proteins (endoplasmic reticulum resident protein 44 [ERp44] and glutaredoxin-3) while in the case of the other three proteins (calpastatin, endoplasmin [GRP-94] and 78 kDa glucose-regulated protein [GRP-78]) the analysis was not conclusive. Aliquots of the same samples that were used for the 2DE analysis underwent WB analysis.

ERp44 (the most abundant of the nine proteins identified in spot #35) and glutaredoxin-3 (the most abundant of the 23 proteins identified in spot #38) were found to be the dysregulated components in their spots by means of spectral counts analysis, which also confirmed the direction of regulation observed on the 2DE gels. In order to validate the regulation of these two proteins as a proof of principle, they were subjected to WB analysis. Figure 17 shows the WB analysis of these two proteins and the corresponding densitometric analysis of the bands normalised to the PonceauS staining. The conditions that were chosen for MS analysis of the excised spots are highlighted in red. For both ERp44 and glutaredoxin-3, WB analysis revealed similar patterns of protein regulation as measured on 2DE gels and calculated based on spectral counts, thus validating the experimental procedure.

ERp44 protein levels showed a statistically significant difference between HX siCA9 and NX siCtr ($z=-4.747$, $N=3$, $p<0.001$) with decreased ERp44 levels under HX siCA9 condition in comparison to NX siCtr. Therefore, WB analysis validated the spectral counting for ERp44.

Glutaredoxin-3 showed a general increase in abundance under hypoxia (WT: $z=9.603$, $N=3$, $p<0.001$ vs. NX; siCtr: $z=11.92$, $N=3$, $p<0.001$ vs. NX; siCA9: $z=8.386$, $N=3$, $p<0.001$ vs. NX) and under reoxygenation (WT: $z=3.665$, $N=3$, $p<0.001$ vs. NX; siCtr: $z=5.083$, $N=3$, $p<0.001$ vs. NX; siCA9: $z=4.876$, $N=3$, $p<0.001$ vs. NX). In contrast to the identified spot regulation (Table 5) the WB analysis did not show influence of CAIX depletion on glutaredoxin-3 levels.

Calpastatin was found in spots #5 and #6 (both with decreased abundance on the 2DE maps of siCA9 samples) and spectral counts analysis was not decisive for validation as the dysregulated protein in these spots. Another neighboring spot (#4, also downregulated in siCA9 samples) contained calpastatin as the most abundant protein but spectral counts could not be used to verify the regulation of the protein because gel plugs were available only from one sample. The protein

was therefore selected for validation. The differences that were expected from spot regulation and spectral counts did not match the results from WB analysis (siCtr: z=1.124, N=3, p=0.499 HX vs. NX, z=1.422, N=3, p=0.330 ReOX vs. HX, z=0.298, N=3, p=0.952 ReOX vs. NX). However, WB analysis confirmed the regulation pattern observed on 2DE maps for this protein, with calpastatin showing a trend to be less abundant in siCA9 samples (Figure 17).

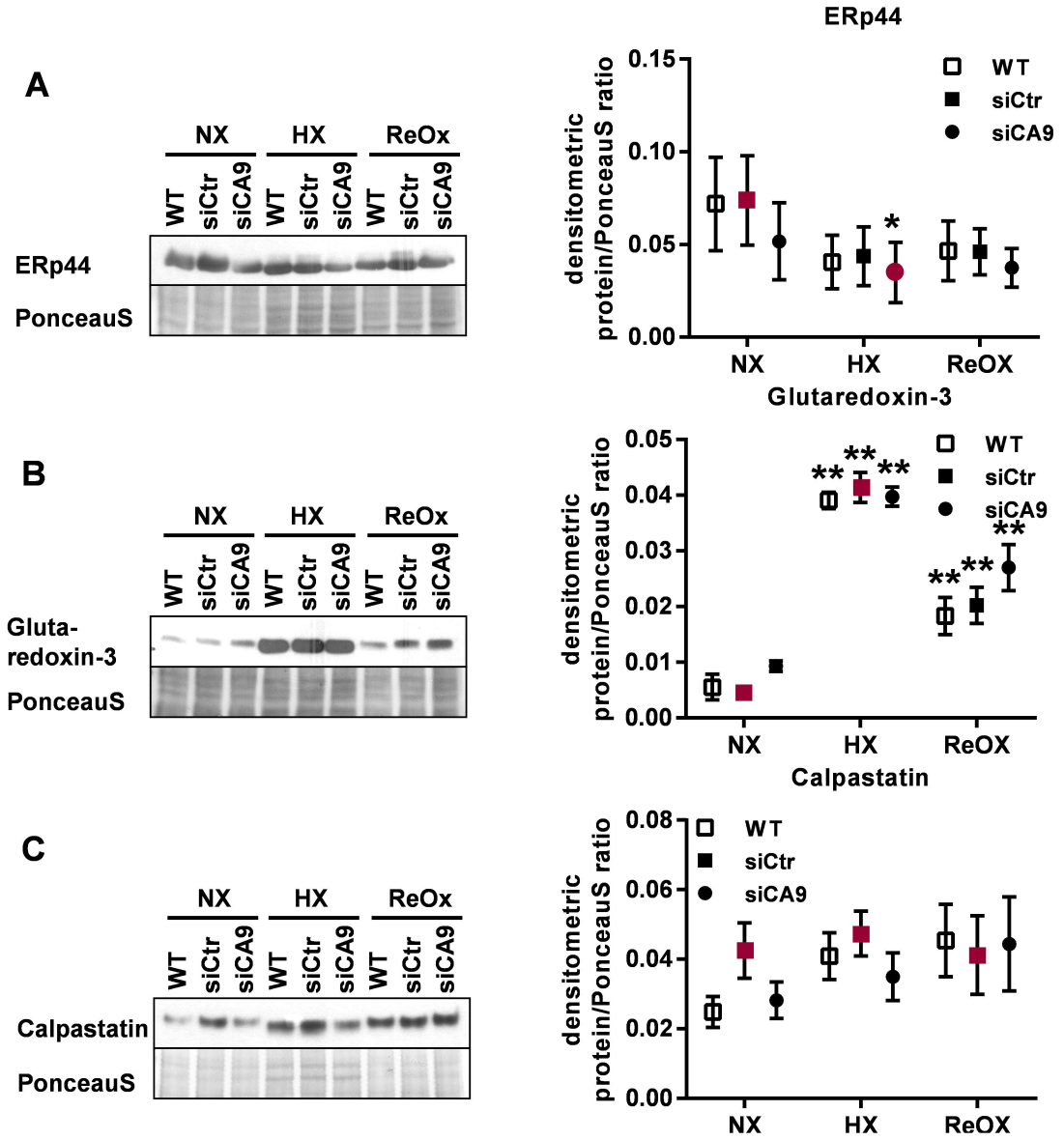

Figure 17 Validation of selected spot after 2DE/MS analysis I
HeLa cells used for 2DE analysis were reversely transfected with siRNA against *CA9* (siCA9) or control siRNA (siCtr) or left untransfected (WT). Cells were exposed to either 48 h normoxia (NX), 24 h normoxia followed by 24 h 1% oxygen (HX) or 16 h normoxia, 24 h hypoxia (1% oxygen) followed by 8 h normoxia (ReOX). Cells were harvested and protein extracts were prepared for 2DE/MS analysis. For selected proteins WB analysis was performed using specific antibodies to validate MS analysis. PonceauS staining served as loading control. Graphs show densitometric analysis (ImageJ) of protein levels of ERp44 (A), Glutaredoxin-3 (B) and Calpastatin (C) as ratio to PonceauS (n=3, mean±SEM, *p<0.001 HX siCA9 vs. NX siCtr, **p<0.001 NX). Displayed in red are the conditions that were used in MS analysis.

GRP-94 (92 kDa) was the most abundant of the three proteins identified in spot #13 (around 110 kDa estimated on the 2DE gel). The spot is more abundant in HX siCtr samples as compared to ReOX siCtr samples, but the spectral counts analysis was not conclusive regarding the direction of the regulation. The protein was also present in spot #44 (around 30 kDa estimated on the 2DE gel), in mixture with 23 other proteins. Spectral counts analysis suggested that GRP-94 and hepatoma-derived growth factor (HDGF) would be the regulated components of spot #44.

However, the low apparent MW of the spot on the 2DE gel did not match the MW of the protein, suggesting that spot #44 might contain a degradation product of GRP-94. Since the gel plugs used for the MS analysis of spots #13 and #44 originated from different pairs of samples, a direct comparison was not possible and therefore GRP-94 was selected for validation through WB analysis (Figure 18).

WB analysis did not confirm the regulation patterns observed for this protein on 2DE maps obtained from samples under different oxygenation regimes, showing no significant changes in protein levels (siCtr: $z=-0.596$, $N=3$, $p=0.551$ HX vs. ReOX) in the two conditions where differences were detected by spectral counting. Nevertheless, the densitometric analysis confirmed a tendency for GRP-94 to decrease in abundance in NX siCA9 samples (Figure 18). It may be speculated that GRP-94 was degraded in siCA9 samples with the higher molecular spot containing the full length protein and the lower molecular weight spot containing a proteolysis product of this protein. Generally, GRP-94 was found to be decreased in hypoxic samples in comparison to normoxia (WT: $z=-3.062$, $N=3$, $p=0.002$ vs. NX; siCtr : $z=-2.931$, $N=3$, $p=0.007$ vs. NX; siCA9: $z=-4.845$, $N=3$, $p<0.001$ vs. NX).

GRP-78 was found in three spots (#18, #19 and #20), all of them containing mixtures of six to 18 proteins. The protein could be identified as the regulated component of spots #18 and #20 based on spectral counts analysis and was the most abundant protein in spot #19. Spots #19 and #20 were neighboring spots of similar intensity on the 2DE gel while spot #18 was further apart, at a higher MW and significantly weaker (Figure 15). Moreover, spot #18 displayed opposite regulation as compared to spots #19 and #20 (Figure 12). Spectral counting supported the direction of regulation apparent on the 2DE gel for all three spots. Taken together, the positions, intensities and regulation profiles of these spots suggested that spot #18 might contain a precursor of the mature protein contained by spots #19 and #20. This interesting context prompted further analysis of GRP-78, therefore the protein was selected for validation through WB analysis.

As for GRP-94, WB analysis did not confirm the patterns of regulation of GRP-78 under different oxygenation conditions (siCtr: z=-0.965, N=3, p=0.335 HX vs. NX), but showed that GRP-78 has a tendency to be more abundant in siCA9 samples. These results were also compatible with the above interpretation of 2DE and MS results, with spots #19 and #20 containing the mature GRP-78 protein and spot #18 containing a precursor of this protein.

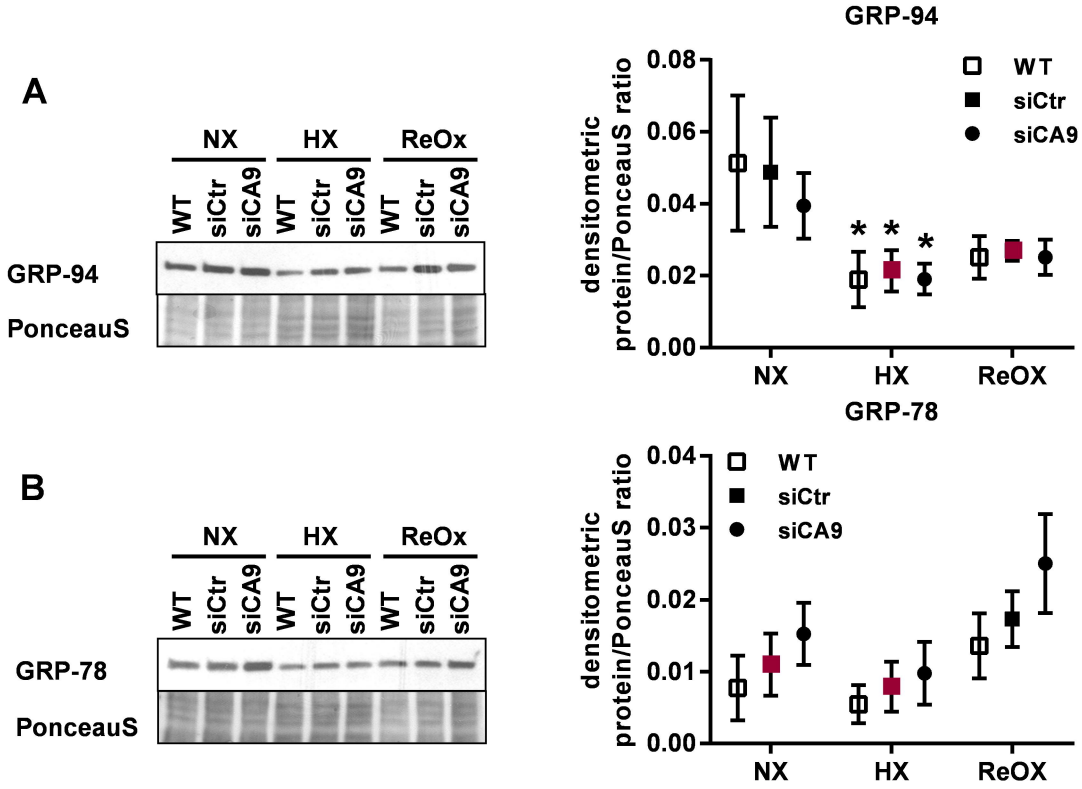

Figure 18 Validation of selected spot after 2DE/MS analysis II
HeLa cells used for 2DE analysis were reversely transfected with siRNA against *CA9* (siCA9) or control siRNA (siCtr) or left untransfected (WT). Cells were exposed to either 48 h normoxia (NX), 24 h normoxia followed by 24 h 1% oxygen (HX) or 16 h normoxia, 24 h hypoxia (1% oxygen) followed by 8 h normoxia (ReOX). Cells were harvested and protein extracts were prepared for 2DE/MS analysis. For selected proteins WB analysis was performed using specific antibodies to validate MS analysis. PonceauS staining served as loading control. Graphs show densitometric analysis (ImageJ) of protein levels of GRP-94 (A) and GRP-78 (B) as ratio to PonceauS (n=3, mean±SEM, *p<0.01 NX). Displayed in red are the conditions that were used in MS analysis.

5.3.7 Identification of Proteins Differentially Phosphorylated in CAIX Depleted HeLa Cells under Different Oxygenation Conditions

In order to identify differentially phosphorylated proteins in addition to differentially regulated proteins, a highly sensitive staining specific for phosphorylated proteins was employed. Staining and scanning of the gels stained with "Pro-Q Diammond" phosphoprotein gel stain was carried out as described in 4.2.4.4 and data analysis was performed as described in 4.2.4.5.

siCtr and siCA9 samples were analysed in one replicate each due to limitations imposed by the staining procedure. Following the staining process with „Pro-Q Diamond" phosphoprotein gel stain, the gels were counterstained with RuBPS staining in order to visualize protein load and to facilitate comparison of the gels and avoid false positive identifications.

The identification of differentially phosphorylated proteins was carried out by visual comparison following gel alignment in SameSpots software. To this end, spots from phosphoprotein-stained gels were compared to those from the according RuBPs stained gels to take into account the protein load. Also, the spots have been compared to spots from gels that only have been stained with RuBPs and were available for three replicates per sample in order to confirm that the spot was regulated and to exclude putative technical artefacts.

The analysis of the phosphoprotein-stained gels revealed 25 spots (numbered #101 to #125) stained with different intensity in siCA9 vs. siCtr and hypoxic or reoxygenated vs. normoxic samples. Of them, 20 gel plugs could be unambiguously matched and excised from preparative gels stained with colloidal coomassie. Spot preparation followed the protocol described in section 4.2.4.6, MS analysis was carried out as in 4.2.4.7. The MS analysis successfully identified the phosphorylated protein in five of the analysed spots. Figure 19 displays the staining intensity of the identified protein spots depending on the treatment.

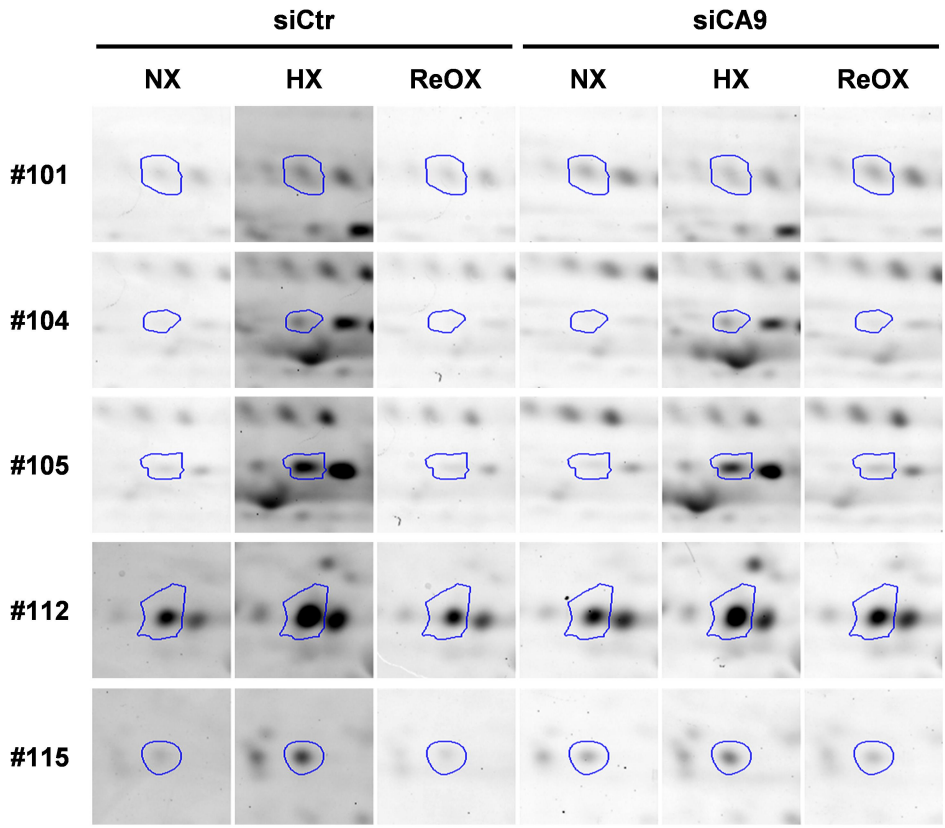

Figure 19 2DE spots differentially phosphorylated upon different oxygen and transfection conditions in HeLa cells
Displayed are magnified sections of 2DE gels for each spot differentially phosphorylated by treatment with 21% oxygen for 24 h (normoxia; NX), 1% oxygen for 24 h (hypoxia; HX) or 1% oxygen for 24 h and 21% oxygen for 8 h (reoxygenation; ReOX) and/or different conditions of transfection. Spot IDs are given according to IDs for MS analysis.

MS analysis was carried out in order to validate the phosphoprotein staining results and identify the phosphorylation sites (Figure 20). Among the five spots shown in Figure 19 the phosphorylated proteins could be clearly identified as single hits in four spots. For spot #101, MS analysis returned multiple hits which could be resolved by means of spectral counting. The dysregulated and phosphorylated proteins were sequestosome-1 and programmed cell death protein 4 (PDCD4), both also identified in spot #23. In addition, spot #23 is located in the close vicinity of spot #101 on the 2DE gel and spectral counting indicated PDCD4 as the regulated protein for spot #23. Figure 20 shows the identified peptides and phosphorylation sites identified by MS analysis.

Figure 20 MS identifications for phosphoprotein containing spots
Shown are the MS results viewed in Scaffold Software. Spot IDs are given according to IDs for MS analysis. Identified peptides are coloured yellow, phosphorylated amino acids are indicated in red.

All identifications are summarised in Table 6. The regulation pattern identified by phosphoprotein staining is listed: “siCA9” refers to the visually identified regulation in dependence to CAIX expression levels, “HX” indicates a potential under hypoxia. In addition, the direction of the regulation is presented. All of the identified spots are differentially phosphorylated in CAIX depleted cells, spot #105 only showed regulation under hypoxia, but was cut in addition due to close vicinity to #104 and appearing on the gel to be a possible isoform of #104. Indeed, for both #104 and #105 the same protein could be identified to be differentially phosphorylated, vimentin.

Table 6 Regulated phopsphoprotein containing spots identified by MS
Given are spot IDs, molecular weight (MW) and isoelectric point (pI) as identified on 2DE gels and the identified protein functions.

Spot ID MS	Spot ID SS	Protein Identified	Abbreviation	Accession ID	siCA9 vs. siCtr	HX vs. NX
101	1743	Sequestosome-1 Programmed cell death protein 4	Sequestosome-1 PDCD4	Q13501 Q53EL6	▲	
104	1891	Vimentin	Vimentin	P08670	▲	▲
105	1897	Vimentin	Vimentin	P08670		▲
112	2412	Perilipin-3	Perilipin-3	O60664	▲	▲
115	2719	Elongation factor 1-δ	EF-1-δ	P29692	▲	▲

The position of the regulated spots on a representative phosphorstained gel are shown in Figure 21.

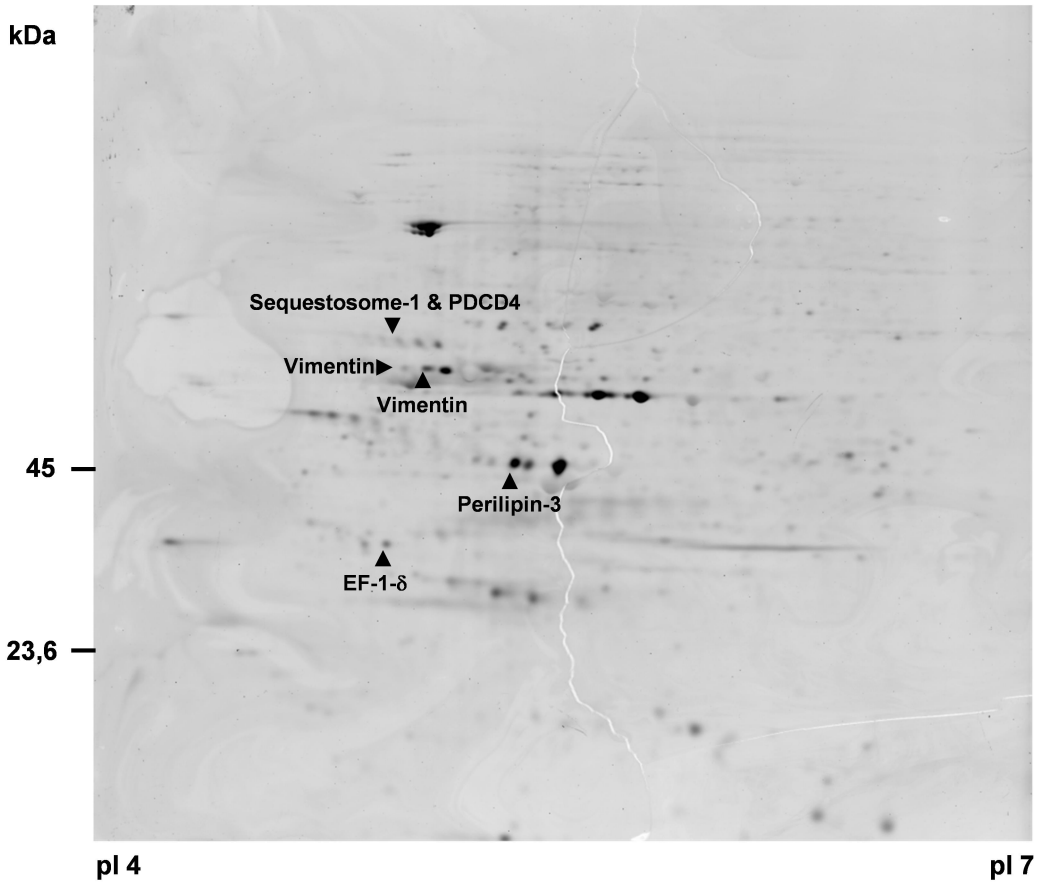

Figure 21 Regulated phosphoprotein containing spots identified by 2DE/MS
Displayed is a representative 2DE gel stained with „Pro-Q Diamond“ phosphoprotein gel stain. Spot IDs are given according to IDs for MS analysis.

Further information on the MS identifications such as sequence coverage and identified peptides are presented in Supporting Table 2 and Supporting Table 3 in section 8.4.

5.4 Profiling of Regulated Protein Functions

Pathway analysis was carried out in order to uncover the cellular function of CAIX on the basis of proteins identified through 2DE analysis as being dysregulated in siCA9 cells. To this aim the free accessible online tool WebGestalt was used. All identified protein functions including differentially phosphorylated proteins and CAIX and HIF-1α were submitted for the following analyses with WebGestalt: GO enrichment analysis, KEGG pathway analysis and Pathway Commons analysis.

GO enrichment analysis is a tool that identifies over- or under-represented gene clusters in the genome of a species based on the submitted data set. This analysis revealed that most of the genes corresponding to the identified protein functions were connected to the area of protein folding, unfolded protein response and the endoplasmic reticulum (ER; Table 7). In addition, some proteins were also found to be associated with nuclease activity and its regulation.

The over-represented molecular functions and cellular compartments were identified with the same tool (Table 7). The results showed that several targets were involved in (ribo)nucleotide and (ribo)nucleoside binding. Most of the identified proteins were located in the cytosol or in the ER. A number of 13 proteins could be identified as being part of macromolecular complexes.

The protein identities in all affected clusters are listed in Table 7.

Table 7 Results of GO enrichment analysis

Biological Process	Proteins Involved
response to topologically incorrect protein	ORP-150, ERp44, GRP-94, Hsp60, HDGF, GRP-78
response to unfolded protein	ORP-150, ERp44, GRP-94, Hsp60, HDGF, GRP-78
protein folding	Tubulin β-4A chain, ERp44, TCP-1-α, GRP-94, Hsp60, PPIase FKBP4, GRP-78
positive regulation of nuclease activity	ORP-150,GRP-94, HDGF, GRP-78
activation of signaling protein activity involved in unfolded protein response	ORP-150,GRP-94, HDGF, GRP-78
regulation of nuclease activity	ORP-150,GRP-94, HDGF, GRP-78
cellular protein complex assembly	Tubulin β-4A chain, CI-23kD, TCP-1- α, Hsp60, PPIase FKBP4, Actin-related protein 3
cellular response to unfolded protein	ORP-150,GRP-94, HDGF, GRP-78
endoplasmic reticulum unfolded protein response	ORP-150,GRP-94, HDGF, GRP-78
cellular response to topologically incorrect protein	ORP-150,GRP-94, HDGF, GRP-78

continued on next page...

Molecular Function	Proteins Involved
purine ribonucleoside binding	Tubulin β-4A chain, TCP-1- α, GRP-94, Actin-related protein 3, ORP-150, eRF3a, hnRNP U, Hsp60, PPlase FKBP4, TRIP-5, TRIP-13
purine ribonucleotide binding	Tubulin β-4A chain, TCP-1- α, GRP-94, Actin-related protein 3, ORP-150, eRF3a, hnRNP U, Hsp60, PPlase FKBP4, TRIP-5, TRIP-13
nucleotide binding	Tubulin β-4A chain, TCP-1- α, GRP-94, HDGF, GRP-78, Actin-related protein 3, ORP-150, eRF3a, Hsp60, hnRNP U, PPlase FKBP4, TRIP-5, TRIP-13, TMABADH
purine ribonucleoside triphosphate binding	Tubulin β-4A chain, TCP-1- α, GRP-94, GRP-78, Actin-related protein 3, ORP-150, eRF3a, hnRNP U, Hsp60, PPlase FKBP4, TRIP-5, TRIP-13
ribonucleoside binding	Tubulin β-4A chain, TCP-1- α, GRP-94, Actin-related protein 3, ORP-150, eRF3a, hnRNP U, Hsp60, PPlase FKBP4, TRIP-5, TRIP-13
purine nucleotide binding	Tubulin β-4A chain, TCP-1- α, GRP-94, Actin-related protein 3, ORP-150, eRF3a, hnRNP U, Hsp60, PPlase FKBP4, TRIP-5, TRIP-13
nucleoside binding	Tubulin β-4A chain, TCP-1- α, GRP-94, Actin-related protein 3, ORP-150, eRF3a, hnRNP U, Hsp60, PPlase FKBP4, TRIP-5, TRIP-13
purine nucleoside binding	Tubulin β-4A chain, TCP-1- α, GRP-94, Actin-related protein 3, ORP-150, eRF3a, hnRNP U, Hsp60, PPlase FKBP4, TRIP-5, TRIP-13
ribonucleotide binding	Tubulin β-4A chain, TCP-1- α, GRP-94, Actin-related protein 3, ORP-150, eRF3a, hnRNP U, Hsp60, PPlase FKBP4, TRIP-5, TRIP-13

Cellular Component	Proteins Involved
cytoplasmic part	PMI, GRP-94, GRP-78, Actin-related protein 3, ORP-150, Vimentin, ERp44, Glutaredoxin-3, TRIP-5, C1qBP, ERp46, Tubulin β-4A chain, Nucleobindin-1, TCP-1- α, Sequestosome-1, Serpin B6, CI-23kD, Hsp60, hnRNP U, Perilipin-3, PPlase FKBP4, PDCD4 , EF-1-δ, TMABADH
cytosol	Tubulin β-4A chain, PMI, TCP-1- α, GRP-94, Sequestosome-1, GRP-78, Vimentin, Serpin B6, Hsp60, PPlase FKBP4, TRIP-5, PDCD4 , EF-1-δ, TMABADH
endoplasmic reticulum lumen	ORP-150, ERp44, GRP-94, ERp46
cytoplasm	PMI, GRP-94, HDGF, GRP-78, Actin-related protein 3, ORP-150, Vimentin, ERp44, TRIP-5, Glutaredoxin-3, C1qBP, ERp46, Tubulin β-4A chain, Nucleobindin-1, TCP-1- α, Sequestosome-1, Serpin B6, CI-23kD, Hsp60, hnRNP U, Perilipin-3, PPlase FKBP4, PDCD4 , EF-1-δ, TMABADH
organelle part	GRP-94, HDGF, GRP-78, Actin-related protein 3, ORP-150, Vimentin, ERp44, Glutaredoxin-3, TRIP-5, C1qBP, ERp46, Tubulin β-4A chain, TCP-1- α, Sequestosome-1, CI-23kD, Serpin B6, Hsp60, hnRNP U, Perilipin-3, PPlase FKBP4, PDCD4
endoplasmic reticulum-Golgi intermediate compartment	Nucleobindin-1, ERp44, GRP-78
intracellular	PMI, GRP-94, HDGF, GRP-78, Actin-related protein 3, ORP-150, Vimentin, ERp44, TRIP-5, Glutaredoxin-3, C1qBP, ERp46, Tubulin β-4A chain, Nucleobindin-1, TCP-1- α, Sequestosome-1, eRF3a, Serpin B6, CI-23kD, Hsp60, hnRNP U, Perilipin-3, PPlase FKBP4,TRIP-13, PDCD4 , EF-1-δ, TMABADH
intracellular organelle part	GRP-94, HDGF, GRP-78, Actin-related protein 3, ORP-150, Vimentin, ERp44, TRIP-5, C1qBP, ERp46, Tubulin β-4A chain, TCP-1- α, Sequestosome-1, CI-23kD, Serpin B6, Hsp60, Perilipin-3, hnRNP U, PPlase FKBP4, PDCD4
protein complex	Tubulin β-4A chain, TCP-1- α, HDGF, GRP-94, Actin-related protein 3, Serpin B6, Vimentin, CI-23kD, Hsp60, hnRNP U, PPlase FKBP4, TRIP-5, EF-1-δ
intracellular organelle lumen	TCP-1- α, GRP-94, Sequestosome-1, HDGF, GRP-78, ORP-150, ERp44, Hsp60, hnRNP U, PPlase FKBP4, C1qBP, PDCD4 , ERp46

...continued.

As a second pathway analysis tool, KEGG pathway analysis identified protein processing in endoplasmic reticulum (including 4 genes) as significantly over-represented in the data (Table 8). Other pathways represented in the data set (though not significantly represented) were metabolism-related.

Table 8 KEGG pathway analysis

Pathway Name	Proteins Involved	Statistics
Protein processing in endoplasmic reticulum	ORP-150, GRP-94, GRP-78, ERp46	adjP=0.0001
Metabolic pathways	CI-23kD, PMI, TMABADH	adjP=0.2029

KEGG pathway analysis tool also provided a graphical overview of the proteins of interest in the cellular pathways identified during analysis. Figure 22 (see next page) shows the identified proteins in a map visualizing the targeted processes involved in protein processing in the ER.

Pathway Commons analysis identified 10 different pathways in the data set with a high overlap of proteins between them (Table 9). The lowest p value was obtained for the connection of the analysed data set to the unfolded protein response (UPR). In addition, Pathway Commons analysis showed similar overlap of shared protein functions in the pathways identified in the GO enrichment analysis. Again, the pathway with the highest statistical significance was (Table 9).

Table 9 Pathway Commons pathway analysis

Pathway Name	Proteins Involved	Statistics
Unfolded Protein Response	ORP-150, GRP-94, HDGF, GRP-78	adjP=9.02e-05
Activation of Chaperones by IRE1 α	ORP-150, HDGF, GRP-78	adjP=0.0009
Activation of Chaperones by ATF6- α	GRP-94, GRP-78	adjP=0.0012
Diabetes pathways	ORP-150, GRP-94, HDGF, GRP-78	adjP=0.0027
Metabolism of proteins	Tubulin β-4A chain, PMI, TCP-1- α, EF-1-δ	adjP=0.0044
Protein folding	Tubulin β-4A chain, TCP-1- α	adjP=0.0064
Signaling events mediated by focal adhesion kinase	GRP-94, Hsp60, PPIase FKBP4, Actin-related protein 3, PDCD4 , ERp46	adjP=0.0105
Arf6 downstream pathway	GRP-94, Hsp60, PPIase FKBP4, Actin-related protein 3, PDCD4 , ERp46	adjP=0.0105
mTOR signaling pathway	GRP-94, Hsp60, PPIase FKBP4, Actin-related protein 3, PDCD4 , ERp46	adjP=0.0105
Plasma membrane estrogen receptor signaling	GRP-94, Hsp60, PPIase FKBP4, Actin-related protein 3, PDCD4 , ERp46	adjP=0.0105

Considering these results, all three approaches strongly support an involvement of CAIX in the ER located protein processing and the UPR. This putative link was analysed in more detail.

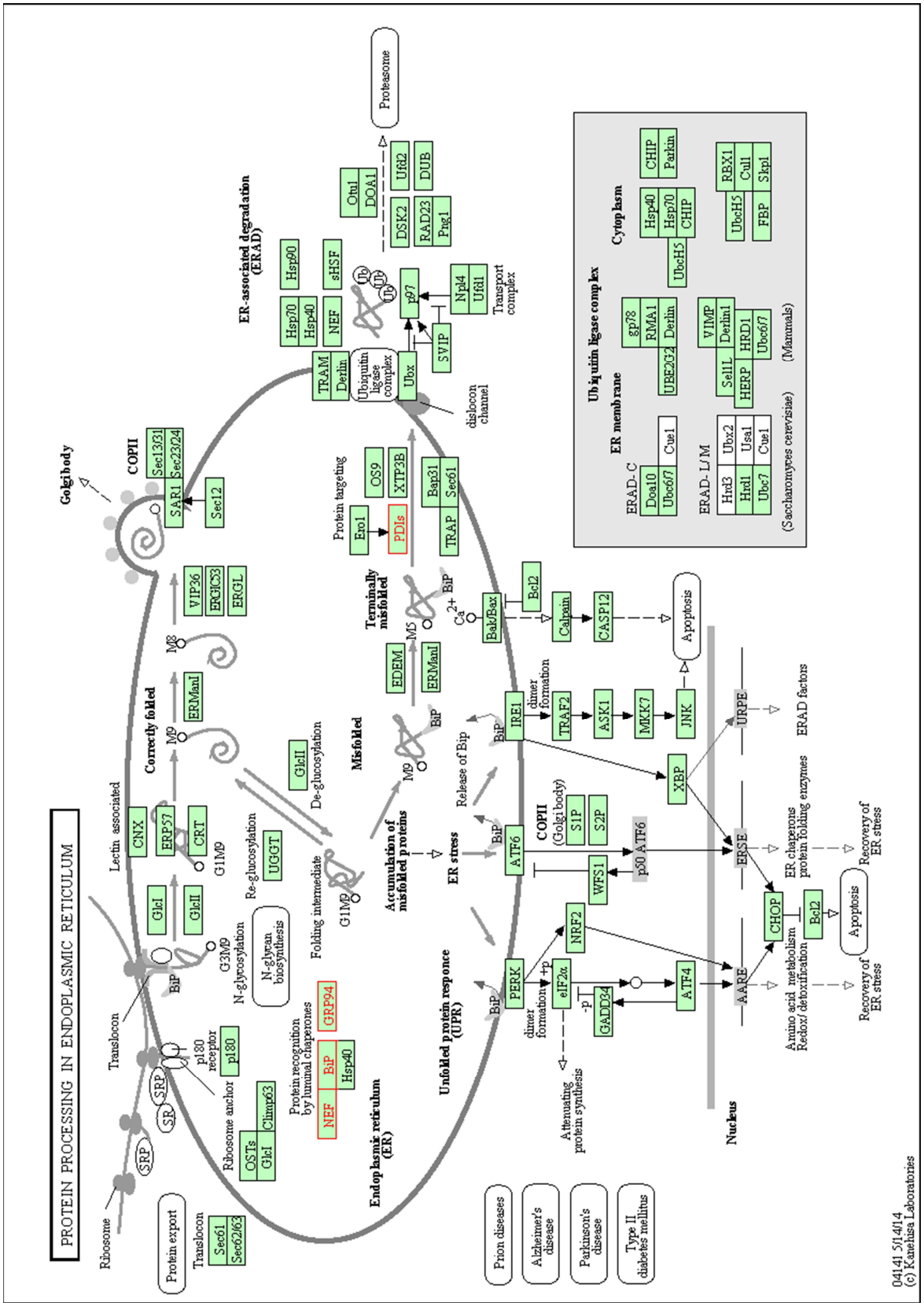

Figure 22 Results of KEGG pathway analysis - Protein processing in the endoplasmic reticulum
KEGG pathway analysis was performed using Webgestalt Software. Clusters containing genes of interest are displayed in red. NEF = ORP-150 and nucleotide exchange factor SIL1 (not included in list of proteins), GRP94 = GRP-94, BiP = GRP-78, PDIs = various proteins including ERp46.

5.5 The Role of CAIX in the UPR

Pathway analysis identified the unfolded protein response (UPR) as the most important protein pathway over-represented in the data set of proteins regulated in CAIX depleted cells (Table 7, Table 8, Figure 22 and Table 9). To investigate the involvement of CAIX in the UPR an experimental approach suitable to induce UPR in HeLa cells was designed.

UPR is known to be induced by chemical compounds such as thapsigargin or tunicamycin (Rzymski et al., 2012) or under prolonged severe hypoxic conditions (Fels and Koumenis, 2006). Since the setup chosen for the 2DE study was based on hypoxic stimulation of the cells, severe hypoxia was chosen as stimulus to induce UPR.

To create severe hypoxic conditions, the oxygen levels were decreased to 0.1% and the duration of the incubation was prolonged to 48 h. In line with the previous experimental plan, a step of 8 h of reoxygenation was included. Figure 23 displays the experimental procedure.

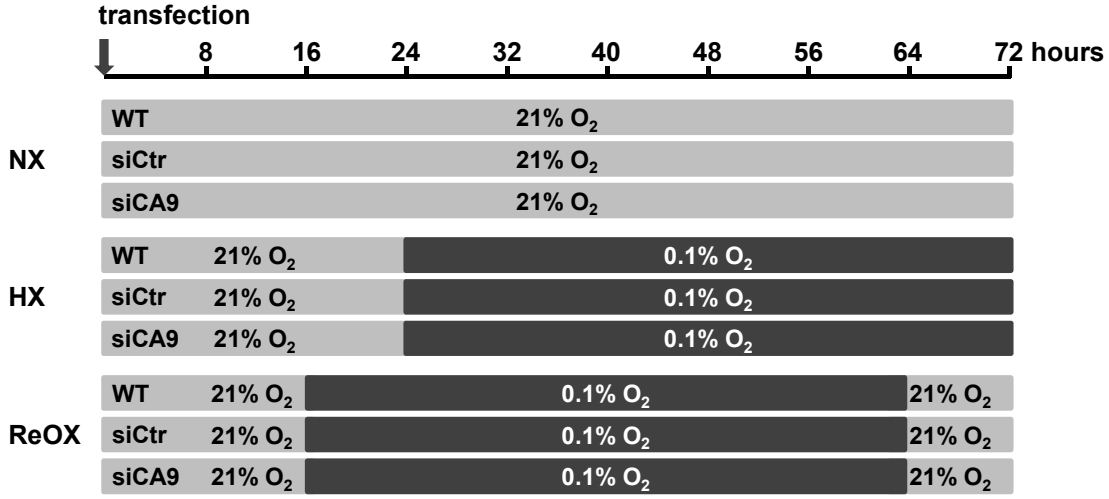

Figure 23 Experimental setup of the hypoxic treatment applied for induction of UPR in HeLa cells
Displayed is the experimental outline. Cells were treated using siRNA against *CA9* (siCA9) or control (siCtr) or left untransfected (WT) followed by treatment with either 72 h of normoxia (NX), 24 h of normoxia followed by 48 h of hypoxia (0.1% oxygen; HX) or 16 h of normoxia followed by 48 h hypoxia (0.1% oxygen) and 8 h of normoxia (21% oxygen; ReOX).

During UPR, high levels of chaperones accumulating in the ER activate a signaling cascade that leads to translation in order to rescue the cell that has to cope with a very high number of unfolded proteins giving the mechanism its name (Cao and Kaufman, 2012). cAMP-dependent transcription factor ATF-4 (ATF4), cAMP-dependent transcription factor ATF-6α (ATF6) and serine/threonine-protein kinase/endoribonuclease IRE1 (IRE1) are the major molecular players representing three

different pathways of the UPR of which ATF4 is known to be induced by severe hypoxia (Rzymski et al., 2010).

To confirm that the selected parameters can induce UPR, the level of the marker protein ATF4 was determined (Figure 24). Successful hypoxic induction was controlled by WB analysis of HIF-1α (WT: z=52.07, N=3, p<0.001 vs. NX; siCtr: z=13.36, N=3, p<0.001 vs. NX; siCA9: z=6.921, N=3, p<0.001 vs. NX). In addition, the reduction of CAIX was confirmed by WB analysis when comparing siCA9 samples to WT and siCtr cells under hypoxia (z=-8.159, N=3, p<0.001 vs. WT; z=-6.453, N=3, p<0.001vs. siCtr) and reoxygenation (z=-11.776, N=3, p<0.001 vs. WT; z=-11.492, N=3, p<0.001 vs. siCtr). Under severe hypoxic conditions, siCA9 significantly reduced HIF-1α levels (z=-8.909, N=3, p<0.001 vs. WT; z=-8.471, N=3, p<0.001 vs. siCtr).

Indeed, the levels of ATF4 increased upon stimulation with severe hypoxia (0.1% oxygen) for 48 h as compared to normoxia (WT: z=8.674, N=3, p<0.001 vs. NX; siCtr: z=3.909. N=3, p<0.001 vs. NX). Although the difference in ATF4 protein levels between untransfected WT and siCtr treated cells was significantly different (z=-8.438, N=3, p<0.001), the difference to siCA9 for both control conditions (z=-16.498, N=3, p<0.001 vs. WT; z=-8.060, N=3, p<0.001 vs. siCtr) clearly showed that siCA9 abolished ATF4 induction under severe hypoxic conditions as shown in Figure 24. Reoxygenation reduced this effect indicating that the induction is reversible.

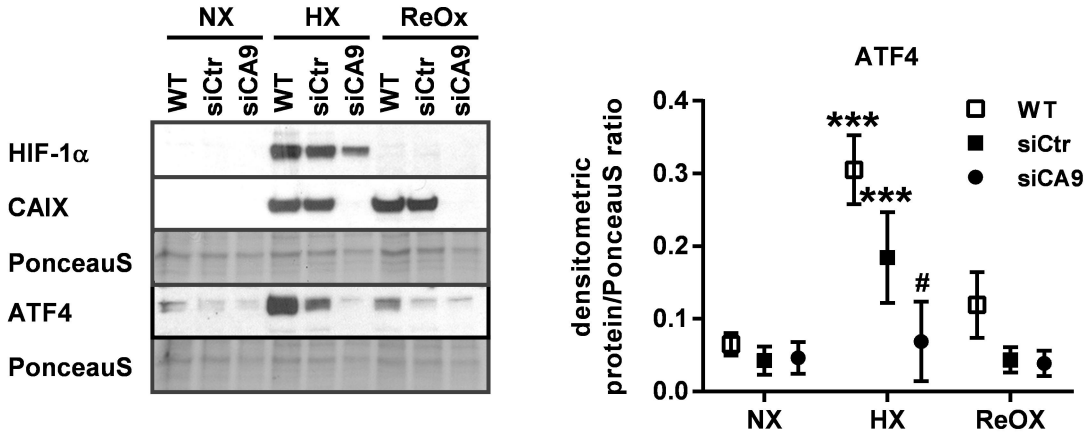

Figure 24 Silencing of *CA9* diminshes ATF4 induction under severe hypoxia in HeLa cells
HeLa cells were reversely transfected with siRNA against *CA9* (siCA9) or control siRNA (siCtr) or left untransfected (WT). Cells were subjected to 48 h of severe hypoxia (0.1% oxygen; HX), hypoxia followed by reoxygenation (21% oxygen, 8 h; ReOX) or normoxia (NX) as displayed in Figure 23. WB analysis for HIF-1α, CAIX and ATF4 as indicator for UPR was performed using specific antibodies. PonceauS staining served as loading control. Graph shows densiomentric analysis (ImageJ) of ATF4 protein levels normalised to PonceauS (n=3, mean±SEM, ***p<0.001 vs. NX, #p<0.001 vs. WT/siCtr).

Eukaryotic translation initiation factor 2α (eIF2α) is located upstream of ATF4 in the signaling cascade and increased levels of p-eIF2α lead to selective translation of ATF4 (Wang and Kaufman, 2014). Therefore, p-eIF2α levels were determined as further marker for the UPR.

In line with siCA9 abolishing ATF4 induction under severe hypoxia, protein levels of p-eIF2α were reduced when cells were depleted of CAIX under hypoxia (Figure 25). For siCtr cells the ratio between p-eIF2α and eIF2α increased in abundance during hypoxia ($z=5.176$, $N=3$, $p<0.001$ vs. NX) and decreased when *CA9* was silenced ($z=-3.594$, $N=3$, $p<0.001$ vs. WT; $z=-3.386$, $N=3$, $p=0.002$ vs. siCtr). Under reoxygenation this difference was preserved for WT cells showing a significant decrease of p-eIF2α levels as compared to eIF2α in CAIX depleted cells ($z=-4.852$, $N=3$, $p<0.001$ vs. WT; $z=-1.687$, $N=3$, $p=0.210$ vs. siCtr). Thus, siCA9 decreased eIF2α phosphorylation and subsequent induction of ATF4 under severe hypoxia.

While severe hypoxia induces UPR via ATF4 upregulation, silencing of *CA9* prevents UPR onset via lack of phosphorylation of eIF2α and absence of the upregulation of the ATF4 transcription factor.

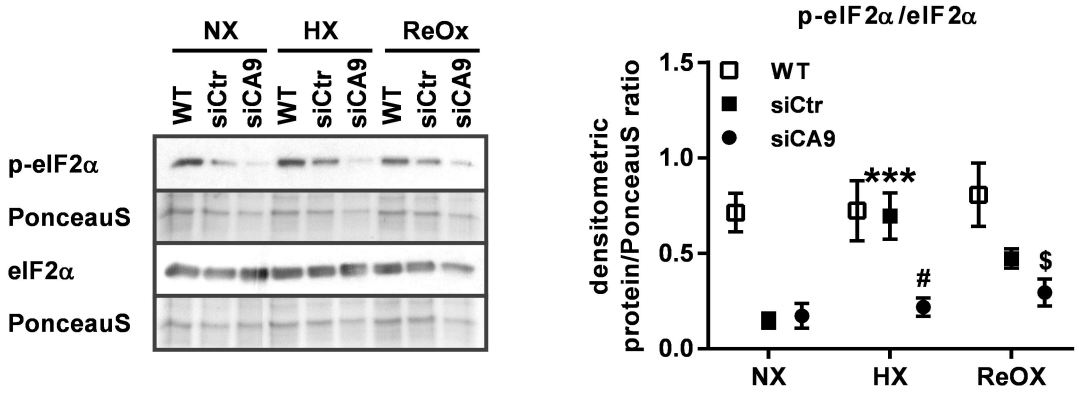

Figure 25 Silencing of *CA9* inhibits phosphorylation of eIF2α
HeLa cells were reversely transfected with siRNA against *CA9* (siCA9) or control siRNA (siCtr) or left untransfected (WT). Cells were subjected to 48 h of severe hypoxia (0.1% oxygen; HX), hypoxia followed by reoxygenation (21% oxygen, 8 h; ReOX) or normoxia (NX) as displayed in Figure 23. Levels of eIF2α and p-eIF2α were determined by WB analysis using specific antibodies. PonceauS staining served as loading control. Graph shows ratio between phosphorylated and unphosphorylated eIF2α after densitometric analysis (ImageJ) of protein levels normalised to PonceauS (n=3, mean±SEM, ***$p<0.001$ vs. NX, #$p<0.001$ vs. WT and $p<0.01$ vs. siCtr, \$$p<0.001$ vs. WT).

Chaperones are required under severe hypoxic conditions in order to cope with the accumulation of unfolded proteins in the ER. Indeed, the levels of ER resident chaperones such as GRP-78 (spots #18, #19, #20) and GRP-94 (spot #13) showed significant changes in their abundance in response to hypoxia in the proteomics analysis. WB analysis of cells exposed to severe hypoxia showed that

levels of GRP-94 were slightly decreased under hypoxia in untransfected cells (z=-1.947, N=3, p=0.052 vs. NX) or when cells were treated with siCtr (z=-1.671, N=3, p=0.095 vs. NX). Under reoxygenation, siCA9 treated cells showed reduced expression levels as compared to control cells (z=-2.671, N=3, p=0.021 vs. WT; z=-3.767, N=3, p<0.001 vs. siCtr; Figure 26 A and B).

In the case of the chaperone GRP-78, protein levels showed an increase in siCA9 cells under normoxia (z=5.111, N=3, p<0.001 vs. WT; z=4.531, N=3, p<0.001 vs. siCtr). The downregulation of GRP-78 levels in WT cells under hypoxia was significant (z=-4.314, N=3, p<0.001 vs. NX; Figure 26 A and C).

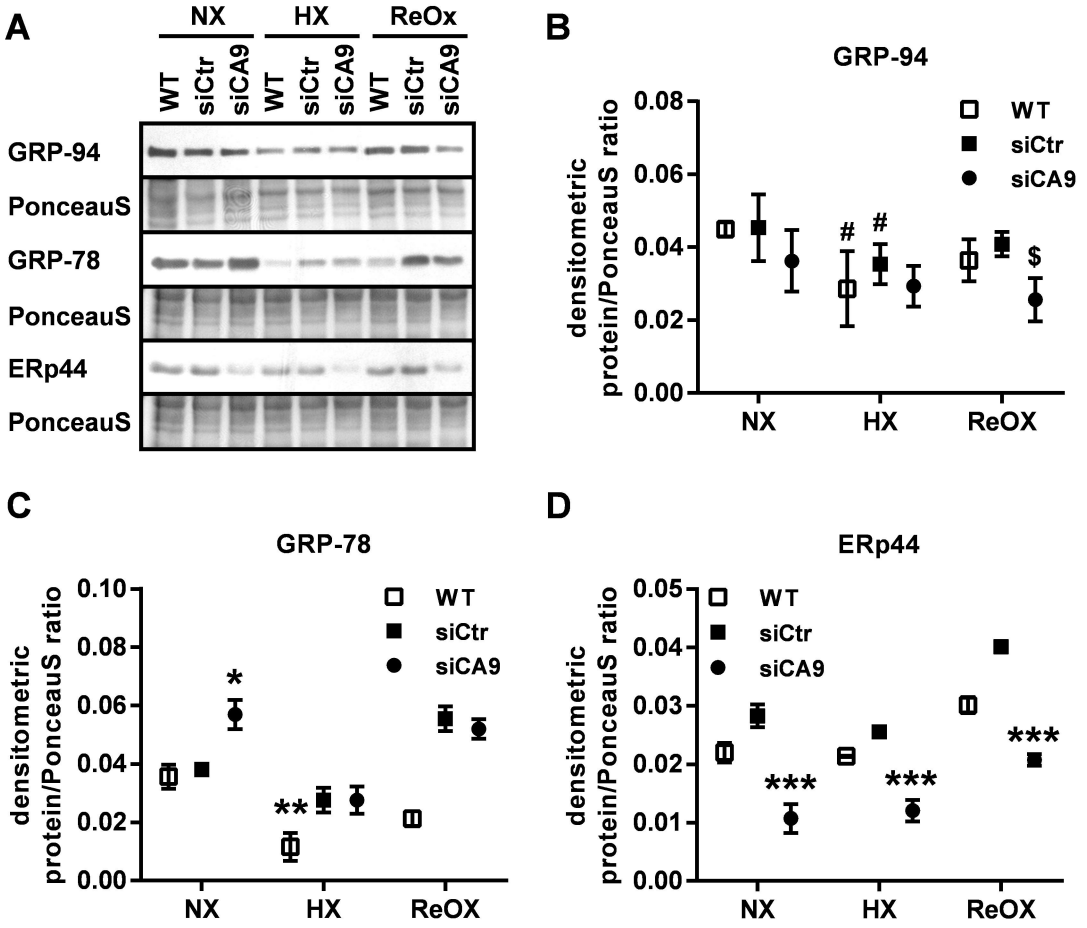

Figure 26 Severe hypoxia decreases levels of ER-located Chaperones GRP-94 and GRP-78 and silencing of *CA9* diminishes ERp44 levels
HeLa cells were reversely transfected with siRNA against *CA9* (siCA9) or control siRNA (siCtr) or left untransfected (WT). Cells were subjected to 48 h of severe hypoxia (0.1% oxygen; HX), hypoxia followed by reoxygenation (21% oxygen, 8 h; ReOX) or normoxia (NX) as displayed in Figure 23. (A) Levels of GRP-94, GRP-78 and ERp44 were determined by WB analysis using specific antibodies. PonceauS staining served as loading control. Graphs show densitometric analyses (ImageJ) of protein levels of GRP-94 (B), GRP-78 (C) and ERp44 (D) as ratio to PonceauS (n=3, mean±SEM, #p<0.1 vs. NX, $p<0.05 vs. WT and p<0.001 vs. siCtr, *p<0.001 vs. WT/siCtr, **p<0.001 vs. NX, ***p<0.001 vs. WT/siCtr).

Protein levels of ERp44 – another keyplayer in the ER – were decreased when cells were depleted of CAIX under normoxia (z=-5.184, N=3, p<0.001 vs. WT; z=-8.059, N=3, p<0.001 vs. siCtr), hypoxia (z=-5.613, N=3, p<0.001 vs. WT; z=-8.140, N=3, p<0.001 vs. siCtr) or reoxygenation (z=-6.496, N=3, p<0.001 vs. WT; z=-13.442, N=3, p<0.001 vs. siCtr; Figure 26 A, D).

Other proteins located in the ER that are involved in protein folding such as ERp72 and ERp57 were also regulated in response to CAIX (Figure 27). Basal ERp72 levels were significantly reduced under hypoxia (z=-2.342, N=3, p=0.036 vs. NX) and reoxygenation (z=-3.412, N=3, p=0.001 vs. NX). Furthermore, CAIX depleted cells showed decreased levels of ERp72 under hypoxia (z=-6.784, N=3, p<0.001 vs. WT; z=-5.052, N=3, p<0.001 vs. siCtr) as well as under reoxygenation (z=-4.741, N=3, p=<0.001 vs. WT; z=-5.296, N=3, p<0.001 vs. siCtr; Figure 27 B).

ERp57 showed the same trend under hypoxia with reduced protein levels when cells were depleted of CAIX (z=-3.535, N=3, p=0.001 vs. WT; z=-3.368, N=3, p=0.002 vs. siCtr), but not under reoxygenation (z=-1.637, N=3, p=0.230 vs. WT; z=-1.993, N=3, p=0.114 vs. siCtr; Figure 27 C).

The levels of PDI which is another key player involved in the protein folding machinery in the ER (Kleizen and Braakman, 2004), were relatively constant over all conditions, i.e. in relation to reduced CAIX levels during hypoxia (z=-1.111, N=3, p=0.507 vs. WT; z=-1.169, N=3, p=0.472 vs. siCtr) and reoxygenation (z=-1.631, N=3, p=0.232 vs. WT; z=-0.519, N=3, p=0.862 vs. siCtr; Figure 27 D).

In addition to the influence of CAIX on markers of the unfolded protein response there is a clear influence of CAIX on the levels of proteins involved in protein folding such as GRP-78, ERp44, ERp57 and ERp72.

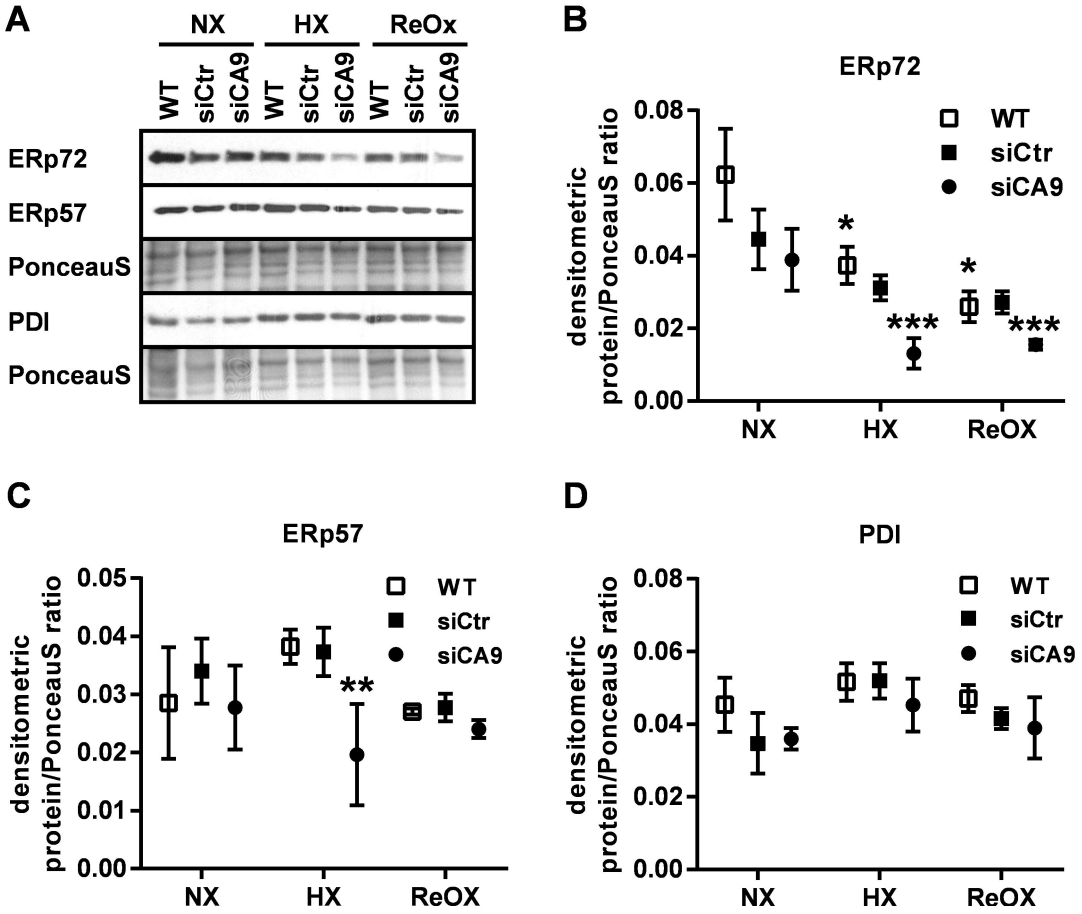

Figure 27 CAIX regulates ER-resident proteins ERp57 and ERp72 under severe hypoxia, but not PDI
HeLa cells were reversely transfected with siRNA against *CA9* (siCA9) or control siRNA (siCtr) or left untransfected (WT). Cells were subjected to 48 h of severe hypoxia (0.1% oxygen; HX), hypoxia followed by reoxygenation (21% oxygen, 8 h; ReOX) or normoxia (NX) as displayed in Figure 23. (A) Levels of ERp44, ERp57 and ERp72 were determined by WB analysis using specific antibodies. PonceauS staining served as loading control. Graphs show densitometric analyses of protein levels of ERp72 (B), ERp57 (C) and PDI (D) as ratio to PonceauS using ImageJ (n=3, mean±SEM, *p<0.05 vs. NX, **p<0.01 vs. WT/siCtr, ***p<0.001 vs. WT/siCtr).

5.6 The Role of CAIX in the Cap-Dependent Translation

In addition to the chaperones identified in the proteomics analysis, proteins involved in translational processes such as eukaryotic peptide chain release factor GTP-binding subunit ERF3A (eRF3a) and elongation factor 1 δ (EF-1-δ) were identified to be differentially regulated (Table 5).

Translational control in cancer cells is mediated by the Akt/mTOR/4E-BP pathway and involves eukaryotic initiation factors such as eIF4E and eIF4G (Silvera et al., 2010). Phosphorylation of mTOR was significantly decreased in CAIX depleted cells during hypoxia (z=-3.058, N=3, p=0.006 vs. WT; z=-2.165, N=3, p=0.0773 vs. siCtr) and reoxygenation (z=-3.038, N=3, p=0.007

vs. WT; z=-3.617, N=3, p<0.001 vs. siCtr) although hypoxia or reoxygenation did not affect p-mTOR levels (Figure 28).

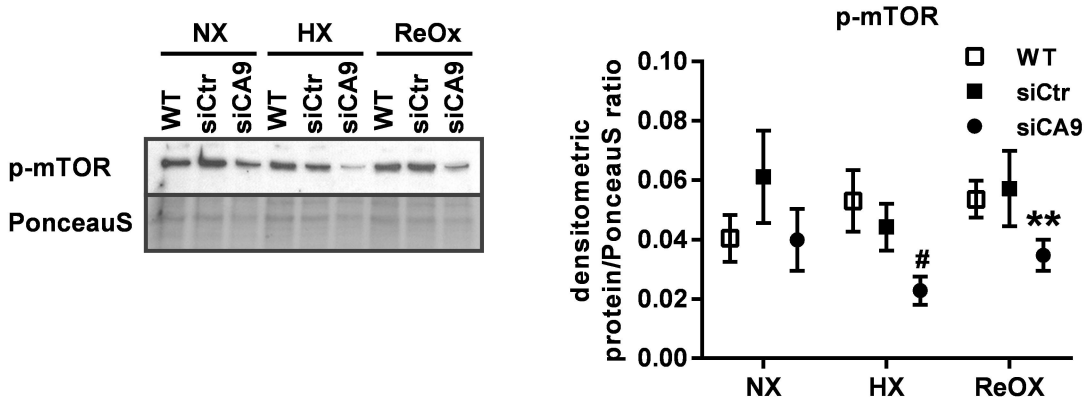

Figure 28 Silencing of *CA9* leads to a decrease in p-mTOR
HeLa cells were reversely transfected with siRNA against *CA9* (siCA9) or control siRNA (siCtr) or left untransfected (WT). Cells were subjected to 48 h of severe hypoxia (0.1% oxygen; HX), hypoxia followed by reoxygenation (21% oxygen, 8 h; ReOX) or normoxia (NX) as displayed in Figure 23. Levels of p-mTOR were determined by WB analysis using specific antibody. PonceauS staining served as loading control. Graph shows densitometric analysis of protein levels as ratio to PonceauS using ImageJ (n=3, mean±SEM, #p<0.01 vs. WT and p<0.1 vs. siCtr, **p<0.01 vs. WT/siCtr).

In addition, the levels of p-Akt in relation to Akt (p-Akt/Akt) were increased for siCtr cells during hypoxia (z=4.601, N=3, p<0.001 vs. NX) and reoxygenation (z=6.374, N=3, p<0.001 vs. NX), but not for WT cells during hypoxia (z=1.411, N=3, p=0.269 vs. NX) and reoxygenation (z=1.348, N=3, p=0.300 vs. NX), respectively (Figure 29).

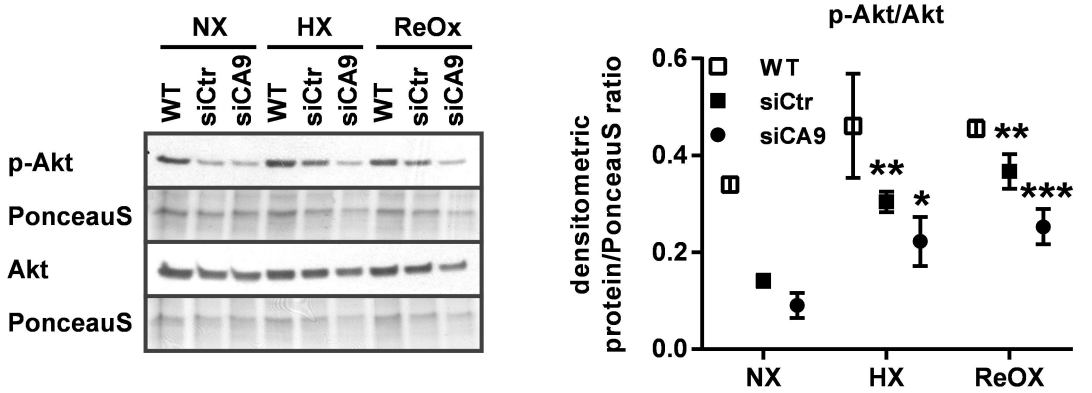

Figure 29 Silencing of *CA9* leads to a decrease in Akt
HeLa cells were reversely transfected with siRNA against *CA9* (siCA9) or control siRNA (siCtr) or left untransfected (WT). Cells were subjected to 48 h of severe hypoxia (0.1% oxygen; HX), hypoxia followed by reoxygenation (21% oxygen, 8 h; ReOX) or normoxia (NX) as displayed in Figure 23. (Levels of p-Akt/Akt were determined by WB analysis using specific antibodies. PonceauS staining served as loading control. Graphs show densitometric analyses of protein levels as ratio to PonceauS using ImageJ (n=3, mean±SEM, *p<0.05 vs. WT, **p<0.001 vs. NX, ***p<0.001 vs. WT/siCtr).

Under hypoxia, levels of p-Akt/Akt were decreased in response to siCA9 compared to WT samples (z=-2.425, N=3, p=0.029 vs. WT), but not in comparison to siCtr (z=-0.831, N=3, p=0.616 vs. siCtr). Under reoxygenation, the levels of p-Akt/Akt were significantly reduced in CAIX depleted cells (z=-7.320, N=3, p<0.001 vs. WT; z=-4.119, N=3, p<0.001 vs. siCtr; Figure 29).

In order to test for further downstream effects in the Akt/mTOR/4E-BP pathway, the levels of additional marker proteins were determined (Figure 30). Phosphorylated MAP kinase-interacting serine/threonine-protein kinase 1 (Mnk1) is a protein that is responsible for the phosphorylation of eukaryotic translation initiation factor 4E (eIF4E). Basal levels of p-Mnk1/Mnk1 only showed a trend to increase under hypoxia for WT cells (z=2.024, N=3, p=0.0784 vs. NX) and a hypoxic induction for siCtr cells (z=2.543, N=3, p=0.011). p-Mnk1 levels significantly decreased in comparison to its unphosphorylated form under hypoxia when *CA9* was silenced (z=-2.546, N=3, p=0.021 vs. WT; z=-2.140, N=3, p=0.060 vs. siCtr). Under reoxygenating conditions, the difference in p-Mnk1/Mnk1 was significant when comparing siCA9 to siCtr (z=-4.045, N=3, p<0.001 vs. siCtr), but this effect could not be validated against WT (z=-1.496, N=3, p=0.293 vs. WT; Figure 30).

In contrast, the protein levels of phosphorylated form of eukaryotic translation initiation factor 4E (p-eIF4E, Figure 30 B) remained unchanged. However, levels of the phosphorylated form of eukaryotic translation initiation factor 4 γ (p-eIF4G, Figure 30 C) displayed a behaviour similar to p-Mnk1. p-eIF4G is another component of the eIF4F complex that consists of the subunits eIF4A, eIF4E and eIF4G (Silvera et al., 2010). Similar patters of regulations to those of p-Mnk1 were detected for the active, i.e. phosphorylated form of eIF4G (Figure 30 C). Under hypoxia, siCA9 decreased the p-eIF4G/eIF4G levels as compared to WT (z=-2.292. N=3, p=0.060 vs. WT; z=-0.973, N=3, p=0.594 vs. siCtr). Under reoxygenating conditions the decrease was significant compared to both WT and siCtr (z=-3.481, N=3, p=0.001 vs. WT; z=-3.309, N=3, p=0.003 vs. siCtr; Figure 30).

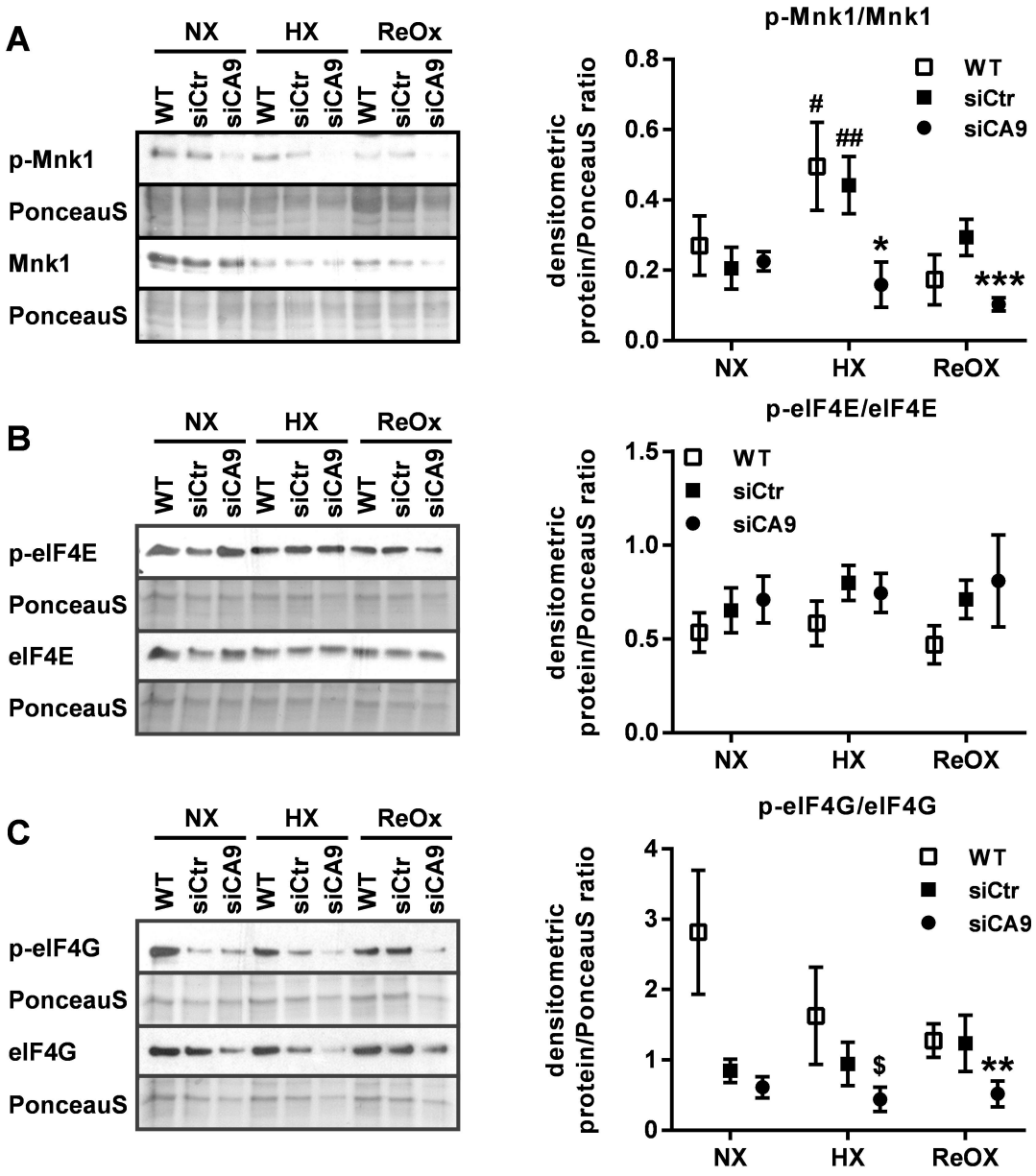

Figure 30 Silencing of *CA9* decreases levels of p-Mnk1 and p-eIF4G but not of p-eIF4E during severe hypoxic conditions in HeLa cells
HeLa cells were reversely transfected with siRNA against *CA9* (siCA9) or control siRNA (siCtr) or left untransfected (WT). Cells were subjected to 48 h of severe hypoxia (0.1% oxygen; HX), hypoxia followed by reoxygenation (21% oxygen, 8 h; ReOX) or normoxia (NX) as displayed in Figure 23. Levels of p-Mnk1/ Mnk1 (A), p-eIF4E/eIF4E (B) and p-eIF4G/eIF4G (C) were determined using specific antibodies. PonceauS staining served as loading control. Graph shows densitometric analyses presenting ratios between phosphorylated and unphosphorylated protein forms, both normalised to PonceauS using ImageJ (n=3, mean±SEM, #p<0.1 vs. NX, ##p<0.05 vs. NX, *p<0.05 vs. WT and p<0.1 vs. siCtr, **p<0.01 vs. WT/siCtr, ***p<0.001 vs. siCtr, $p<0.1 vs. WT).

EIF4E inhibitory binding proteins (4E-BPs) are phosphorylated by Mnks and mTORCs (mTOR complex proteins), and regulate the function of eIF4E (Silvera et al., 2010; Sonenberg and Hinnebusch, 2009). In addition to the finding that p-Mnk1 and p-eIF4G levels were both decreased

in their abundance in siCA9 cells, 4E-BP1 (eIF4E inhibitory binding protein 1) was also decreased in these cells (Figure 31). Basal levels of 4E-BP1 were increased partially during hypoxic treatment (WT: z=4.20, N=3, p<0.001 vs. NX; siCtr: z=1.907, N=3, p=0.057 vs. NX) and during reoxygenation (WT: z=4.07, N=3, p<0.001 vs. NX; siCtr: z=2.343, N=3, p=0.036 vs. NX).

Further analysis of protein levels of 4E-BP1 clearly showed significantly reduced protein levels when *CA9* was silenced both under hypoxic (z=-4.605, N=3, p<0.001 vs. WT; z=-3.561, N=3, p<0.001 vs. siCtr) and reoxygenation conditions (z=-2.831, N=3, p=0.009 vs. WT; z=-2.718, N=3, p=0.013 vs. siCtr). Thus, silencing of *CA9* decreased the phosphorylation of Akt and mTOR as well as the active phosphorylated forms of eIF4G and Mnk1 as well as the levels of 4E-BP1. These results collectively indicate a role of CAIX in cap-dependent translation.

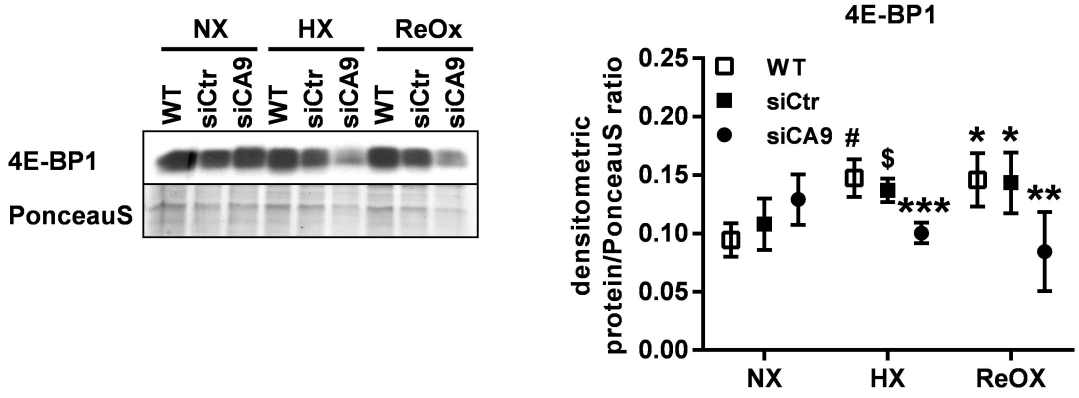

Figure 31 Silencing of *CA9* leads to decreased levels of 4E-BP1 during severe hypoxic conditions in HeLa cells
HeLa cells were reversely transfected with siRNA against *CA9* (siCA9) or control siRNA (siCtr) or left untransfected (WT). Cells were subjected to 48 h of severe hypoxia (0.1% oxygen; HX), hypoxia followed by reoxygenation (21% oxygen, 8 h; ReOX) or normoxia (NX) as displayed in Figure 23. Levels of 4E-BP1 were determined by WB analysis using a specific antibody. PonceauS staining served as loading control. Graph shows densitometric analyses (ImageJ) presenting ratios between phosphorylated and unphosphorylated protein forms, both normalised to PonceauS (n=3, mean±SEM, #p<0.001 vs. NX, $p<0.1 vs. NX, ***p<0.001 vs. WT/siCtr, *p<0.05 vs. NX, **p<0.05 vs. WT/siCtr).

5.7 The Role of CAIX in the Regulation of Apoptosis

The proteomics profiling of CAIX depleted cells identified proteins that are related to apoptosis, namely programmed cell death protein 4 (PDCD4) and mitochondrial complement component 1 Q subcomponent-binding protein (C1qBP). In addition, disturbances in the UPR can lead to cell death. This led to the hypothesis that CAIX is connected to programmed cell death.

In order to visualize and quantify the effect of CAIX on cell survival, trypan blue size exclusion assay was performed as described in 4.2.1.3 showing a higher number of dead cells under siCA9 condition (Figure 32 A). Under normoxia, the amount of dead cells only showed a decreasing tendency for siCA9 cells in comparison to control cells (z=-1.898, N=3, p=0.104 vs. WT; z=-1.716, N=3, p=0.153 vs. siCtr). Under hypoxia (z=-12.100, N=3, p<0.001 vs. WT; z=-9.087, N=3, p<0.001 vs. siCtr) and under reoxygenation (z=-3.956, N=3, p<0.001 vs. WT; z=-2.260, N=3, p=0.044 vs. siCtr), CAIX depleted cells showed a significantly reduced number of viable cells.

In addition, calcein staining was performed to investigate cell viability, and propidium iodide (PI) staining to identify necrotic cells (4.2.1.3). Under basal conditions, the calcein signal was significantly decreased under hypoxia (WT: z=-9.203, N=3, p<0.001 vs. NX; siCtr: z=-4.483, N=3, p<0.001 vs. NX) and reoxygenation (WT: z=-10.947, N=3, p<0.001 vs. NX; siCtr: z=-8.501, N=3, p<0.001 vs. NX) in comparison to normoxia (Figure 32 B).

In line with the the trypan blue based size exclusion assay, the calcein staining showed a clear decrease in viability under normoxia when cells were depleted of CAIX (z=-7.592, N=3, p<0.001 vs. WT; z=-2.098, N=3, p=0.067 vs. siCtr). The same was true under hypoxia (z=-7.010, N=3, p<0.001 vs. WT; vs. z=-3.455, N=3, p=0.001 siCtr), whereas under reoxygenation the decrease was only significant in relation to WT cells (z=-8.265, N=3, p<0.001 vs. WT; z=-1.200, N=3, p=0.38 vs. siCtr; Figure 32 B).

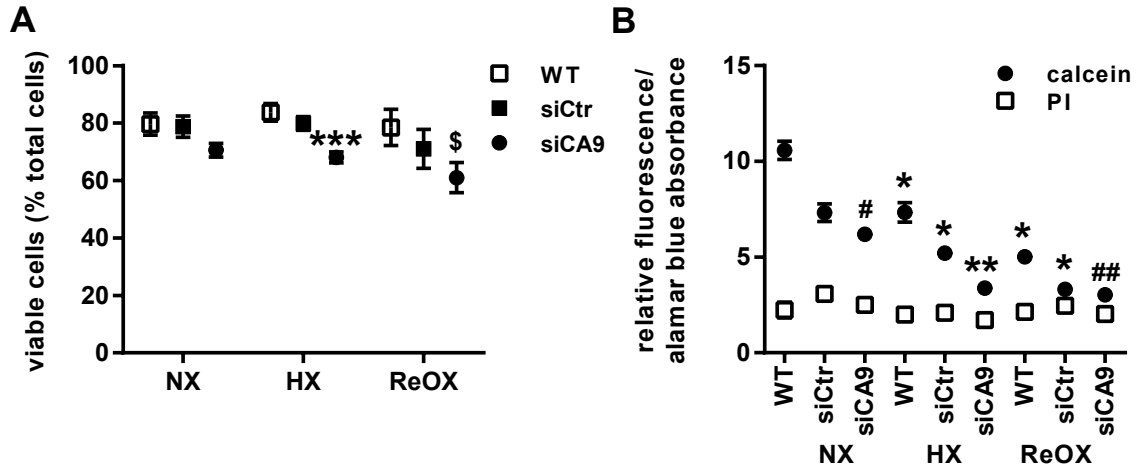

Figure 32 Silencing of *CA9* leads to impaired cell vitality but not to necrosis
HeLa cells were reversely transfected with siRNA against *CA9* (siCA9) or control siRNA (siCtr) or left untransfected (WT). Cells were subjected to 48 h of severe hypoxia (0.1% oxygen; HX), hypoxia followed by reoxygenation (21% oxygen, 8 h; ReOX) or normoxia (NX) as displayed in Figure 23. (A) Size exclusion assay using trypan blue, (B) calcein and propidium iodine staining normalized to alamar blue absorbance (n=3, mean±SEM, ***p<0.001 vs. WT/siCtr , $p<0.05 vs. WT/siCtr, *p<0.001 vs. NX, **p<0.001 vs. WT/siCtr, #p<0.001 vs. WT and p<0.1 vs. siCtr, ##p<0.01 vs. WT).

No statistically significant increase in necrotic cells could be detected using the PI staining (Figure 32 B). These findings strongly suggest that cells with reduced CAIX levels undergo programmed cell death and not necrosis.

To validate this hypothesis, WB analysis for apoptotic effector caspases 3 and 7 and activator caspase 8 was performed as shown in Figure 33. For cleaved caspase 3, higher levels of protein could be detected under normoxic conditions when *CA9* was silenced ($z=3.923$, $N=3$, $p<0.001$ vs. WT; $z=3.855$, $N=3$, $p<0.001$ vs. siCtr). Under hypoxia, the increase in cleaved caspase 3 was only marginally significant for siCA9 cells in comparison to siCtr cells ($z=2.279$, $N=3$, $p=0.0588$ vs. siCtr; Figure 33 A and B).

In addition, CAIX depletion resulted in the cleavage of caspase 7 independent of oxygen availability resulting in increased protein levels under normoxia ($z=6.970$, $N=3$, $p<0.001$ vs. WT; $z=6.564$, $N=3$, $p<0.001$ vs. siCtr), hypoxia ($z=3.904$, $N=3$, $p<0.001$ vs. WT; $z=3.673$, $N=3$, $p<0.001$ vs. siCtr) and also reoxygenation ($z=3.304$, $N=3$, $p=0.003$ vs. WT; $z=3.162$, $N=3$, $p=0.004$ vs. siCtr) in these cells (Figure 33 A and C).

Similarly, when cells were depleted of CAIX the levels of cleaved caspase 8 were significiantly increased during normoxia ($z=11.862$, $N=3$, $p<0.001$ vs. WT; $z=11.251$, $N=3$, $p<0.001$ vs. siCtr), hypoxia ($z=5.391$, $N=3$, $p<0.001$ vs. WT; $z=5.087$, $N=3$, $p<0.001$ vs. siCtr) and reoxygenation ($z=9.012$, $N=3$, $p<0.001$ vs. WT; $z=8.649$, $N=3$, $p<0.001$ vs. siCtr; Figure 33 A and D).

To determine whether the caspase cleavage resulted in functionally active caspases, the expression of their main target poly [ADP-ribose] polymerase 1 (PARP-1) was tested as shown in Figure 33. Cleavage of PARP-1 took place in the absence of CAIX independent of the oxygen status of the cells since significantly different values for the cleaved PARP-1 levels were detected under normoxic ($z=4.220$, $N=3$, $p<0.001$ vs. WT; $z=3.997$, $N=3$, $p<0.001$ vs. siCtr), hypoxic ($z=7.868$, $N=3$, $p<0.001$ vs. WT; $z=7.636$, $N=3$, $p<0.001$ vs. siCtr) and reoxygenating conditions ($z=9.198$, $N=3$, $p<0.001$ vs. WT; $z=9.398$, $N=3$, $p<0.001$ vs. siCtr; Figure 33 A and E).

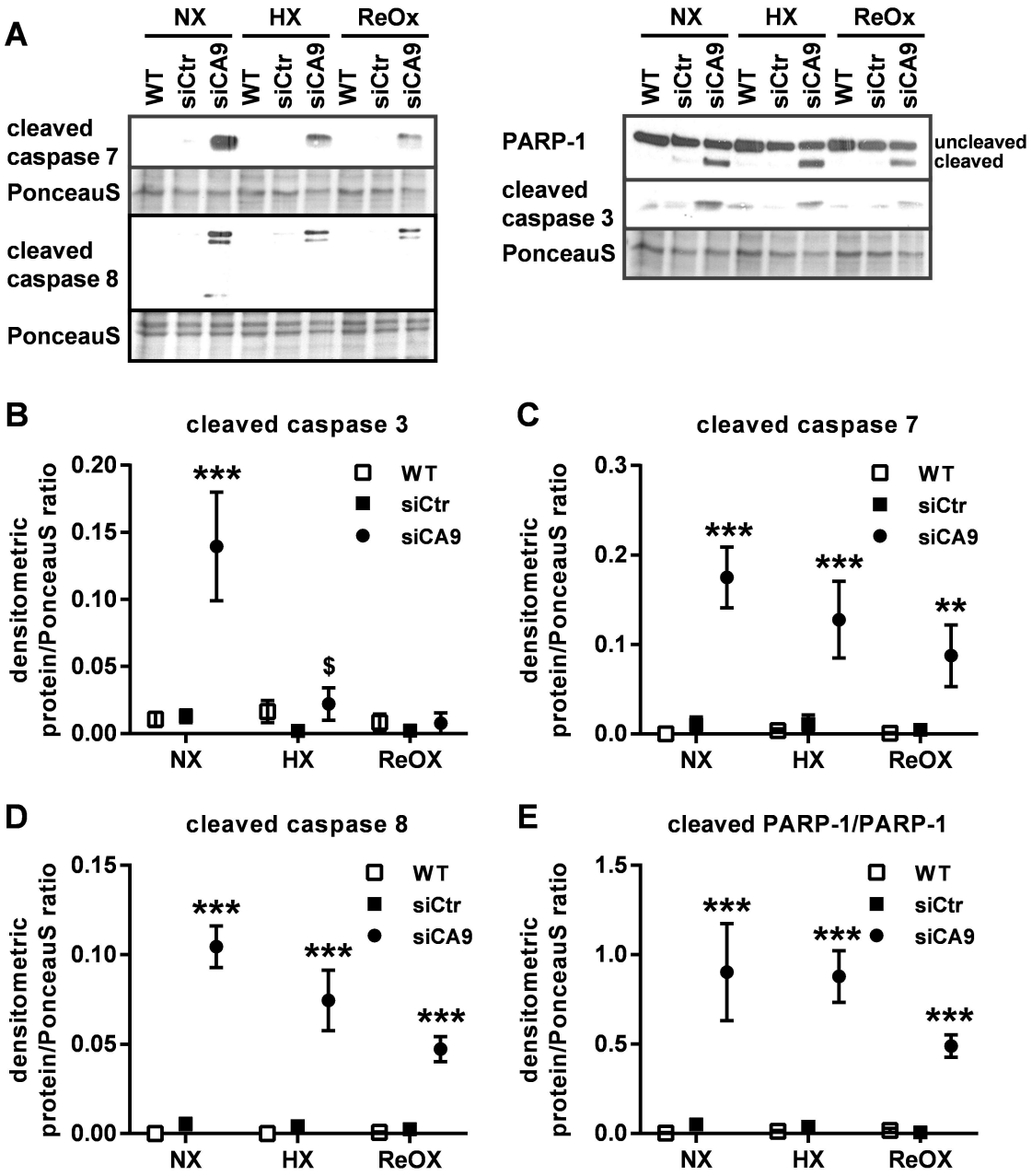

Figure 33 Silencing of *CA9* leads to activation of caspases 3, 7 and 8 and cleavage of PARP-1
HeLa cells were reversely transfected with siRNA against *CA9* (siCA9) or control siRNA (siCtr) or left untransfected (WT). Cells were subjected to 48 h of severe hypoxia (0.1% oxygen; HX), hypoxia followed by reoxygenation (21% oxygen, 8 h; ReOX) or normoxia (NX) as displayed in Figure 23. (A) Levels of cleaved caspases 3,7 and 8 and cleaved and uncleaved PARP-1 were determined by WB analysis using specific antibodies. PonceauS staining served as loading control. (B-E) Graphs show densitometric analyses (ImageJ) of protein levels as ratio to PonceauS (n=3, mean±SEM, **p<0.01 vs. WT/siCtr ,***p<0.001 vs. WT/siCtr, $p<0.1 vs. siCtr).

To further proof the activation of caspases, a caspase 3/7 activity assay was performed as described in 4.2.1.4. Generally, a decrease in caspase 3/7 activity was observed during hypoxia (WT: z=-11.53, N=3, p<0.001 vs. NX; siCtr: z=-9.138, N=3, p<0.001 vs. NX) as well as under

reoxygenation (WT: z=-11.13, N=3, p<0.001 vs. NX; siCtr: z=-12.161, N=3, p<0.001 vs. NX) in comparison to normoxia (Figure 34).

Under normoxic conditions, caspase 3/7 activity was significantly increased under siCA9 conditions in comparison to siCtr (z=3.990, N=3. p<0.001 vs. siCtr), but this change could not be validated against untransfected cells (z=1.902, N=3, p=0.103 vs. WT). Nevertheless, the difference in caspase 3/7 activity in CAIX depleted cells was significant under hypoxic (z=5.894, N=3, p<0.001 vs. WT, z=6.314. N=3, p<0.001 vs. siCtr) and under reoxygenating conditions (z=3.811, N=3, p<0.001 vs. WT, z=6.364, N=3, p<0.001 vs. siCtr). These results indicate an increase in apoptosis in CAIX depleted cells (Figure 34).

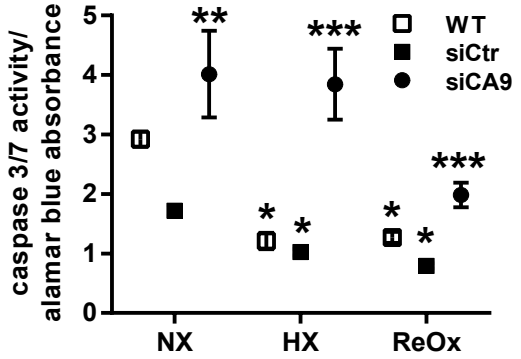

Figure 34 Silencing of *CA9* leads to caspase 3/7 activity
HeLa cells were reversely transfected with siRNA against *CA9* (siCA9) or control siRNA (siCtr) or left untransfected (WT). Cells were subjected to 48 h of severe hypoxia (0.1% oxygen; HX), hypoxia followed by reoxygenation (21% oxygen, 8 h; ReOX) or normoxia (NX) as displayed in Figure 23. Caspase 3/7 activity was determined and normalized to alamar blue absorbance (n=3, mean±SEM, *p<0.001 vs. NX, **p<0.001 vs. siCtr, ***p<0.001 vs. siCtr/WT).

These findings support a role of CAIX in cell survival in general and in the regulation of apoptosis in particular. It remained however unclear how CAIX can have an impact although not being expressed under normoxic conditions. Analysis of long-time exposures during WB analysis showed that CAIX levels are present also during normoxia, just at a very low level compared to the overexpression of CAIX during hypoxia (z=7.037, N=3, p<0.001 vs. NX) and reoxygenation (z=6.370, N=3, p<0.001 vs. NX), so that they only can be detected at an appropriate WB exposure (Figure 35).

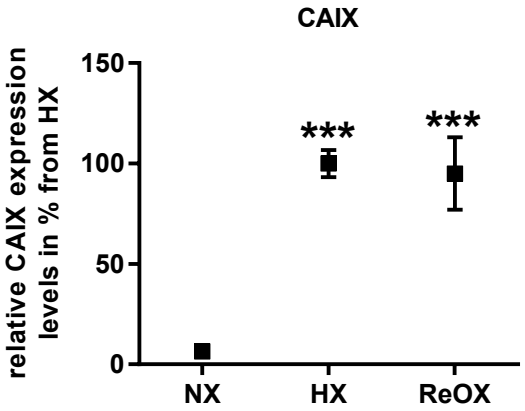

Figure 35 Levels of CAIX under different oxygen conditions
HeLa cells were subjected to 48 h of severe hypoxia (0.1% oxygen; HX), hypoxia followed by reoxygenation (21% oxygen, 8 h; ReOX) or normoxia (NX) as displayed in Figure 23. Levels of CAIX were determined by WB analysis using a specific antibody. PonceauS staining served as loading control. Densitometric analysis (ImageJ) of protein levels were determined. Graph shows relative CAIX expression levels normalised to HX (n=3, mean±SEM, ***p<0.001 vs. NX).

Still, the missing link between CAIX and onset of apoptosis remained unclear. A potential link between CAIX levels and apoptosis was found among the regulated proteins identified in the proteomics analysis: calpastatin, an inhibitor of calpain known to be involved in the regulation of apoptosis (Storr et al., 2011), was identified as differentially regulated in cells with reduced CAIX levels (Table 5).

Calpastatin levels were elevated in untransfected WT cells under hypoxia (WT: z=6.741, N=3, p<0.001 vs. NX; siCtr: z=0.739, N=3, p=0.740 vs. NX) as well as under reoxygenation (WT: z=4.731, N=3, p<0.001 vs. NX; siCtr: z=-1.195, N=3, p=0.456 vs. NX; Figure 36). In addition, calpastatin protein levels were indeed decreased in the absence of CAIX as shown by WB analysis (Figure 36). Under normoxia, calpastatin was downregulated in CAIX depleted cells in comparison to control transfected cells (z=4.088, N=3, p<0.001 vs. siCtr). This effect could not be validated against untransfected cells (z=-0.397, N=3, p=0.917 vs. WT). Nevertheless, the decrease in calpastatin abundance when *CA9* was silenced under hypoxia (z=-18.955, N=3, p<0.001 vs. WT; z=-12.683, N=3, p<0.001 vs. siCtr) as well as under reoxygenation (z=-12.353, N=3, p<0.001 vs.WT; z=-8.914, N=3, p<0.001 vs. siCtr) was significant.

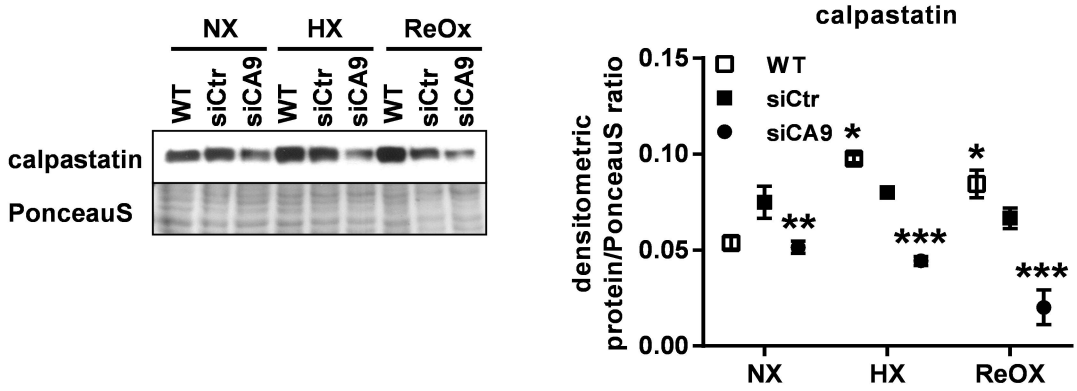

Figure 36 Calpastatin levels are regulated under siCA9 in HeLa cells under different oxygen conditions
HeLa cells were reversely transfected with siRNA against *CA9* (siCA9) or control siRNA (siCtr) or left untransfected (WT). Cells were subjected to 48 h of severe hypoxia (0.1% oxygen; HX), hypoxia followed by reoxygenation (21% oxygen, 8 h; ReOX) or normoxia (NX) as displayed in Figure 23**.** Levels of calpastatin were determined by WB analysis using specific antibodies. PonceauS staining served as loading control. Graph shows densitometric analysis (ImageJ) of protein levels of calpastatin as ratio to PonceauS (n=3, mean±SEM, *p<0.001 vs. NX, **p<0.001 vs. siCtr, ***p<0.001 vs. siCtr/WT).

In addition to the above findings, the proteomics screen showed that calpastatin is decreased upon CAIX depletion. This might increase calpain activity which might in turn be responsible for increased levels of cleaved caspase 3,7 and 8 and increased caspase 3/7 activity resulting in apoptosis in CAIX depleted cells.

6 Discussion

Carbonic anhydrase IX (CAIX) has been associated with poor prognosis and low survival rate of tumor patients for various types of tumors. However, the biochemical pathways controlled by CAIX in cancer cells have not been fully elucidated so far. The aim of this study was therefore to identify the downstream players of CAIX in the cervical carcinoma cell line HeLa and thus to gain more insight into the cellular pathways affected following CAIX depletion in tumor cells.

To this end, CAIX expression was induced under hypoxia and a reoxygenation step was added to additionally investigate the effect of reoxygenation following hypoxic incubation. RNAi technology was used to silence *CA9* and 2DE based proteomics in combination with MS served to identify proteins being differentially regulated in CAIX depleted cells.

6.1 Expression and Regulation of CAIX in HeLa Cells

It has been previously shown that CAIX is not only regulated under hypoxia (Wykoff et al., 2000) but also by cell density (Chrastina, 2003). In line with the scientific literature, both effects were reproduced in this study thus validating the experimental setup. In addition, previous reports (Ilie et al., 2013) could be confirmed that CAIX is not only upregulated by hypoxia, but also remains stable during reoxygenation (Figure 6 and Figure 7). The results were similar under an oxygen concentration of 1% as well as under the severe hypoxic conditions (0.1% oxygen) chosen for the induction of the UPR response (Figure 24).

CAXII has been described to compensate for missing CAIX function in cells depleted of CAIX (Chiche et al., 2009), but CAXII is not expressed in HeLa cells (Wykoff et al., 2000). In line with this report, *CA12* expression could not be detected in the chosen cells thus excluding the influence of CAXII (Figure 5A).

6.2 Proteomic Profiling of CAIX in HeLa Cells and under Different Oxygen Conditions

2DE based proteomics was employed as screening technique in order to characterise the intracellular effects of *CA9* silencing by identifying differential protein expression. Over all, 2,331 spots could be reproducibly quantified from the 2DE gels.

Prinicipal component analysis (PCA) is known as a valuable tool for revealing relevant patterns hidden in protein expression data (Chen et al., 2008; Lancashire et al., 2005). In this study, the PCA showed already on the level of 2DE gels that hypoxic samples cluster away form those treated with normoxia and reoxygenation (Figure 10). In addition, samples treated with reoxygenation showed more similarity to those treated with normoxia thus indicating that effects of hypoxia were reversible following reoxygenation.

From the 2,331 identified spots, differential display 2DE analysis revealed a total of 47 spots differing in abundance and 25 spots that showed differential phosphorylation (see 5.3.4 and 5.3.7) in CAIX depleted cells. 2DE spots dysregulated under different oxygen levels were also selected for further analysis (Figure 11, Figure 12 and Figure 13). Subsequent MS analysis of the 2DE spots which displayed statistically significant differences in abundance, revealed 25 proteins whos abundance depended on CAIX levels (Table 5). In addition, five protein species were identified showing differential phosphorylation in response to CAIX levels (Table 6). These results clearly indicated that CAIX depletion does not only result in changes in protein abundance, but also has an impact on protein phosphorylation which can potentially alter the activity of the targeted proteins (Cohen, 2000).

For all 2DE spots for which MS analysis has identified multiple components, spectral counting was used to identify the regulated proteins. When spectral counting analysis was not conclusive, WB analysis was employed to validate the results. In two cases, the WB analysis validated the spectral counting results, while for three of the 2DE spots, the WB validation was not conclusive. When comparing gel-based 2DE analysis and WB analysis, different patterns of regulation can sometimes be observed because the two methods use different approaches to measure protein abundance. In WB analysis, the whole protein contained on the cells is detected and split in bands according to the molecular weight of the isoforms. On a 2DE gel, however, isoforms carrying different post translational modifications may be characterised by different pI values in addition to the molecular weight, hence be separated during the IEF and thus spread over a various number of spots. At the same time, different molecular species with similar MW and pI can overlap and migrate together in a single 2DE spot and contribute to the abundance of the spot.

This has two major consequences that need to be considered when interpreting 2DE and WB analysis: 1. One protein (represented by one band in WB analysis) does not necessarily correspond to one 2DE spot, but can be divided between an unknown number of spots. 2. One 2DE spot may contain more than one protein, in which case its regulation represents the cumulative effect of the regulation of all its components.

In addition to the dysregulated proteins, five of the proteins differentially phosphorylated upon CAIX depletion or upon CAIX depletion and under hypoxia could be identified. The MS analysis could validate the results based on phosphoprotein-specific staining through the identification of the phosphorylated peptides.

6.3 Profiling of Regulated Protein Functions

Over the years, knowledge-based driven pathway analysis has become a standard tool for analysis of omics data (Khatri et al., 2012). In this study, an over-representation analysis was performed with WebGestalt software (Wang et al., 2013; Zhang et al., 2005) using the analysis tools GO enrichment analysis, KEGG pathway analysis and Pathway Commons analysis (see 5.4).

GO enrichment analysis clusters protein functions and links them to biological processes, molecular functions and cellular components (Table 7). The biological processes identified were mainly connected to protein folding, incorrect protein folding and the unfolded protein response. The clusters of molecular functions were linked to (ribo)nucleotide and (ribo)nucleoside binding. Most of the identified proteins are typically located in the cytosol or the ER, but a protein localized in the inner mitochondrial membrane could also be identified (Table 5 and Table 7), which confirms that the protein extraction and separation procedures were adequate for investigating both the soluble and the organelle and membrane bound proteome.

Interestingly, a closer look at the results of GO enrichment analysis revealed that most proteins overlap between the identified clusters (Table 10). In case of the biological processes, GRP-78, GRP-94, HDGF and ORP-150 were shared between 80% of the clusters (straight line) and the another 20% (dotted line) share four proteins (Table 10). Most of the clusters indicated an impact of CAIX reduction on biological processes related to protein folding and the unfolding protein response (UPR), strongly supporting an involvement of CAIX in ER stress and UPR.

Table 10 Analysis of GO enrichment analysis I

Biological Process	GRP-94	GRP-78	ORP-150	HDGF	ERp44	Hsp60	FKBP4	TCP-1	Tubulin	Actin rp 3	CI-23kD
response to topologically incorrect protein	●	●	●	●	●	●					
response to unfolded protein	●	●	●	●	●	●					
protein folding	●	●			●	●	●	●	●		
positive regulation of nuclease activity	●	●	●	●							
activation of signaling protein activity involved in UPR	●	●	●	●							
regulation of nuclease activity	●	●	●	●							
cellular protein complex assembly						●	●	●	●	●	●
cellular response to unfolded protein	●	●	●	●							
endoplasmic reticulum unfolded protein response	●	●	●	●							
cellular response to topologically incorrect protein	●	●	●	●							

The proteins were ordered alphabethically for better readability. Abbreviations (different to those in Table 5): Actin-rp3 = Actin-related protein 3, FKBP4 = PPlase FKBP4, TCP-1 = TCP-1-α, Tubulin = Tubulin β-4A chain.

The same was observed in the case of the molecular functions being affected by CAIX depletion. Here, 86% of proteins were shared among all clusters (indicated by box), only two functions contained two additional protein functions (Table 11). All proteins identified were involved in or required binding of (ribo)nucleotides or (ribo)nucleosides pointing to a role of CAIX in DNA and RNA synthesis.

Table 11 Analysis of GO enrichment analysis II

Molecular Function	Actin rp 3	eRF3a	FKBP4	GRP-78	GRP-94	hnRNP U	Hsp60	ORP-150	TCP-1	TRIP-5	TRIP-13	Tubulin	HDGF	TMABADH
purine ribonucleoside binding	●	●	●	●	●	●	●	●	●	●	●	●		
purine ribonucleotide binding	●	●	●	●	●	●	●	●	●	●	●	●		
nucleotide binding	●	●	●	●	●	●	●	●	●	●	●	●	●	●
purine ribonucleoside triphosphate binding	●	●	●	●	●	●	●	●	●	●	●	●		
ribonucleoside binding	●	●	●	●	●	●	●	●	●	●	●	●		
purine nucleotide binding	●	●	●	●	●	●	●	●	●	●	●	●		
nucleoside binding	●	●	●	●	●	●	●	●	●	●	●	●		
nucleoside phosphate binding	●	●	●	●	●	●	●	●	●	●	●	●	●	●
purine nucleoside binding	●	●	●	●	●	●	●	●	●	●	●	●		
ribonucleotide binding	●	●	●	●	●	●	●	●	●	●	●	●		

The proteins were ordered alphabethically for better readability. Actin-rp3 = Actin-related protein 3, FKBP4 = PPlase FKBP4, TCP-1 = TCP-1- α, Tubulin = Tubulin β-4A chain.

In line with these findings pointing to a clear role of CAIX in ER stress and UPR, KEGG pathway analysis (Table 8) mapped key proteins found in the 2DE study in the endoplasmic reticulum, namely GRP-78, GRP-94, HDGF and ORP-150. These were the same proteins that clustered together in the GO enrichment analysis. None of the other pathways identified through KEGG pathway analysis were significantly represented in the data set, further suggesting that the principal role of CAIX in the present experimental setup is related to cellular processes residing in the ER.

Furthermore, Pathway Commons analysis could identify 10 different affected pathways of which the UPR showed the lowest p-value (Table 9). Summarising, three different pathway analysis tools pointed to an involvement of CAIX in ER stress and the unfolded protein response.

Independent of the identified pathways or cellular processes that were found to be affected by CAIX, it was found that some spots are only regulated by CAIX whereas others are regulated by CAIX and hypoxia and/or reoxygenation (Figure 14 and Table 5). This suggests that CAIX expression can trigger intracellular effects independent of the oxygenation state of the cell. In order to elucidate the effects of CAIX depletion, the oxygen state needs to be taken into account.

6.4 The Role of CAIX in the UPR

The proteomics experiments suggested a manifold involvement of CAIX in protein folding and the unfolded protein response (UPR). ER stress causing the synthesis of two chaperones, GRP-78 and GRP-94, can be initiated by the accumulation of misfolded proteins in the ER (Kozutsumi et al., 1988). The cellular response to this accumulation is the unfolded protein response (UPR).

The UPR is involved in a large variety of diseases such as diabetes, infectious and inflammatory diseases, neurodegenerative disorders and cancer (Wang and Kaufman, 2012). The cause of the UPR is ER stress. The ER is the site of protein synthesis including subsequent processes such as folding, modification and quality control. In addition, an internal control system ensures that only fully functional proteins are released (Ellgaard and Helenius, 2003). Protein folding is mediated by molecular chaperones (Fink, 1999). ER homeostasis and its function are susceptible to disturbance through various factors such as changes in Ca^{++} levels (Booth and Koch, 1989), protein overload, hypoxia (Koumenis and Wouters, 2006) or even anoxia (Rzymski and Harris, 2007). The role of UPR induced by severe hypoxia and protein folding in the ER and their role in cancer development including therapeutic strategies has been summarised recently (Wang and Kaufman, 2014).

6.4.1 Chaperones, ER Resident Proteins and CAIX

Molecular chaperones assisting protein folding in the ER mainly derive from six different chaperone families: Hsp70s, Hsp40s, Hsp90, peptidyl-prolyl isomerases, calnexin and calreticulin and thiol-disulphide oxidoreductases (Ellgaard and Helenius, 2003). In addition, Hsp70 family member GRP-78 acts as an inhibitor of the ER stress sensors IRE1, ATF6, PERK (PRKR-like endoplasmic reticulum kinase), binds to misfolded proteins and plays an important role in the onset of the UPR (Gardner et al., 2013; Kimata and Kohno, 2011).

Four chaperones belonging to three of these families – Hsp70s, Hsp90s and peptidyl-prolyl isomerases (Table 5) – have been identified in this study including GRP-78, ORP-150, GRP-94 and PPlase FKBP4 supporting the role of CAIX in the UPR and in maintaining the ER homeostasis. In addition, CAIX itself has been suggested to posses chaperone-like function (Wang et al., 2008).

GRP-78 is a member of the Hsp70 family. Alternative names are endoplasmic reticulum lumenal Ca^{++}-binding protein grp78, heat shock 70 kDa protein 5 or immunoglobulin heavy chain-binding protein (BiP). Its function as a molecular chaperone is well established (Haas and Wabl, 1983; Munro and Pelham, 1986). In addition, GRP-78 has been associated with tumor progression (Dong et al., 2008; Li and Lee, 2006) and ER stress tolerance induced resistance to cisplatin in lung cancer cells (Lin et al., 2011). GRP-78 is upregulated under hypoxia and posseses anti-apoptotic potential (Koong et al., 1994; Reddy et al., 2003). In the present study, GRP-78 was identified in three different spots showing different regulation patterns depending on CAIX depletion and hypoxia (Table 5). The protein's presence in different spots may derive from different post translational modifications in the protein. Independent from this, the study shows a clear impact of CAIX levels both independent of and combined with hypoxia on GRP-78 protein levels.

The second member of the Hsp70 family in the ER is GRP-170. It is also referred to as ORP-150 (hypoxia up-regulated protein 1, the latter will be used further). ORP-150 has been shown to be upregulated in cancer cells following treatment with hypoxia (Cechowska-Pasko et al., 2006) and its induction is considered a marker for ER stress and UPR (Wang et al., 2015). Similarly to GRP-94 and GRP-78, ORP-150 has been shown to play a role in breast (Stojadinovic et al., 2007), bladder (Asahi et al., 2002) and prostate cancer (Miyagi et al., 2002). The significance of ORP-150 for diabetes, cardiovascular and neurodegerative diseases have been summarised (Kusaczuk and Cechowska-Pasko, 2013). A potential role for ORP-150 in cancer therapy has been suggested recently (Wang et al., 2015). In the present study, it was found that ORP-150 levels decreased

when cells were depleted of CAIX and when cells were exposed to hypoxia. This regulation stands in contrast to the established regulation of ORP-150 (Cechowska-Pasko et al., 2006). However, ORP-150 was found in three spots which can explain the unexpectedly found regulation.

GRP-94 – or endoplasmin – is the only member of the Hsp90 family located in the ER (Ellgaard and Helenius, 2003). GRP-94 functions with ATP consumption (Frey et al., 2007) and it is also known as one of the major Ca^{++} binding proteins in the ER (Macer and Koch, 1988). Besides its chaperone function in the ER, GRP-94 has also been suggested to play a role in the degradation of misfolded proteins (Christianson et al., 2008). Further, physiological roles of GRP-94 include mesoderm-induction and muscle development (Wanderling et al., 2007). GRP-94 has been associated with a decrease in radiosensitivity in cervical cancer cells (Kubota et al., 2005). Together with GRP-78, GRP-94 has been shown to play a role in other cancers such as colorectal (Takahashi et al., 2011) and lung cancer (Wang et al., 2005) and both their expression has been associated with aggressive behaviour and poor prognosis in gastric carcinoma (Zheng et al., 2008).

In the present study, GRP-94 was found in two spots of which one is likely a degradation product of the protein based on its position on the gel and its regulation pattern (see 5.3.6 and Figure 16). The spot corresponding to the native protein size showed decreased volume when cells were depleted of CAIX and an increase in spot volume under hypoxia. In contrast to this, WB validation showed a general downregulation of global GRP-94 levels in contrast to the regulation of one spot under hypoxia (Figure 18). In a 2DE study on endothelial cells, GRP-94 has been found to be upregulated following treatment with hypoxia and was identified as a target protein of HIF-1α (Paris et al., 2005). Differences from the present study may derive from the different cell types. Paris and co-authors showed (Paris et al., 2005) that the kinetics of the upregulation is not linear, but the increase in GRP-94 is clearly dependant on the incubation time. Considerring these, the regulation could be specific for the cell type or the cell density. Since HIF-1α is also present both after 24 h of 1% and 48 h of 0.1% hypoxia presented in this study, it is possible that the chosen time points present local maxima of HIF-1α expression and GRP-94 levels are subsequently upregulated at later time points in response to HIF-1α.

The fourth protein identified as regulated by CAIX, hypoxia as well as reoxygenation in this area of function is peptidyl-prolyl cis-trans isomerise FKBP4 (PPlase FKBP4). Peptiyl prolyl *cis/trans* isomerases are small proteins that co-chaperone with Hsp90 and modulate its function (Guy et al., 2015; Schiene-Fischer, 2014). FKBP4 has recently been identified as a potential prediction marker for therapeutic outcome in breast cancer (Yang et al., 2012). Another member of the same family

(FKBP38) is involved in the stabilisation of HIF-1α during hypoxia (Barth et al., 2007). A recent study with short-term stimulations (2 h) of dimethyloxalylglycine (DMOG) showed a down-regulation of FKBP4, clearly linking the HIF-1 pathway to FKBP4 regulation (Harrell et al., 2015). In the present study, PPlase FKBP4 was found to be upregulated in siCA9 cells, under hypoxia and partly during reoxygenation. Differences to the regulation found with DMOG incubation may derive from the differences in incubation times and the narrow identification of the protein in spots than rather the entire PPlase FKBP4 in the cell.

With GRP-78 and GRP-94, key players of the UPR were identified in the proteomics experiment. In addition, the levels of the ER located chaperones ORP-150 and PPlase FKBP4 were altered. Further proteins playing a role in protein folding in the ER identified in the 2DE experiment were T-complex protein 1 subunit α (TCP-1-α), heat shock protein 60 kD (Hsp60) and the ER resident proteins ERp44 and ERp46.

TCP-1-α and Hsp60 are chaperonins that assist chaperones in their folding function (Cappello et al., 2008; Kubota et al., 1995). The connection between TCP-1-α and hypoxia or the UPR is unclear, however prolyl hydroxylase 3 – one of the enzymes involved in degradation of HIF-1 – is a substrate of the TCP-1 ring complex chaperonin which contains TCP-1-α (Masson et al., 2004). Hsp60 is part of the mitochondrial stress response machinery that responds to the accumulation of unfolded proteins in the mitochondria similar to the UPR in the ER (Zhao et al., 2002). The cytosolic portion of Hsp60 was shown to relocate to the plasma membrane in response to hypoxia and reoxygenation in rat cardiac myoctes. At the same time, Hsp60 disassociates from its complex with the apoptosis regulator BAX (BCL2-associated X protein) and cells undergo apoptosis (Gupta and Knowlton, 2002). In the present study, both TCP-1-α and Hsp60 were found to be upregulated under hypoxia as well as when cells were depleted of CAIX. The upregulation under hypoxia could be a sign for compensation of chaperonin function under hypoxic stress conditions.

In the proteomics experiment, ERp44 was found to decrease in abundance in the response to CAIX depletion and hypoxia (Table 5) pointing to a novel connection of Ca^{++} levels and CAIX. ERp44 is an ER resident protein of the PDI family and has been shown to be involved in the maintenance of the Ca^{++} homeostasis in the ER. ERp44 regulates the Ca^{++} efflux by inhibiting inositol triphosphate receptor ($InsP_3R$) – a channel able to release Ca^{++} – in order to maintain the Ca^{++} levels in the ER where, among other proteins, various Ca^{++} sensitive chaperones such as GRP-78, GRP-94 or ORP-150 are localised (Anelli et al., 2002; Gorlach et al., 2006). It is known that ERp44 function is

regulated by pH (Vavassori et al., 2013), but the regulation of ERp44 protein levels by an pH regulating enzyme and by hypoxia is novel.

Another ER resident protein that has been identified in the proteomics experiment is thioredoxin reductase 1 or ERp46. It is known since long that thioredoxin reductase levels are increased in response to hypoxia in tumor cells leading to increased levels of thioredoxin which are believed to stimulate the tumor growth (Berggren et al., 1996). More recent data show that silencing of ERp46 impairs tumor growth in renal carcinoma suggesting ERp46 as a new therapeutic target protein (Duivenvoorden et al., 2014). The protein displayed complex regulation in dependence of CAIX, being upregulated when cells were depleted of CAIX under normoxia and downregulated in siCA9 cells under hypoxia. The regulation in relation to CAIX levels therefore depended on the oxygenation status of the cells. The regulation of ERp46 by CAIX and the oxygen levels in the cell is novel and can give new insight into the role of ERp46 regulation in the tumor.

Other proteins localised in the ER have been assessed by means of WB analysis, namely ERp72, and ERp57 and PDI (Figure 27). ERp72 is a thiol-protein disulphide oxidoreductase located in the ER. It is known since long that ERp72 is upregulated due to ischemia or changes in the Ca^{++} level in the brain (Paschen et al., 1998). ERp72 expression in the lung adenocarcinoma has been linked to chemotherapy resistance hence the clinical relevance of the protein (Tufo et al., 2014). In the present study, ERp72 was shown to be responding to CAIX levels under hypoxia as well as under reoxygenation leading to a decrease in ERp72 levels. Furthermore, hypoxia and reoxygenation both led to decreased ERp72 levels indicating that ERp72 is controlled both by the oxygen level and the pH.

ERp57 is an ER resident protein that is responsible for disulfide bond formation in glycoproteins (High et al., 2000; Jessop et al., 2007), for the assembly of major histocompatibility complex class I (Zhang et al., 2006) and plays a role in the onset of renal fibrosis (Dihazi et al., 2013). Furthermore, like GRP-78, ORP-150 and GRP94, ERp57 is an Ca^{++} sensitive chaperone. The protein's interaction with calreticulin in the ER is also Ca^{++} sensitive. ERp57 is responsible for disulfide bind formation in sarcoplasmic/endoplasmic reticulum calcium ATPase (SERCA) and regulates the activity of the Ca^{++} pump (Bedard et al., 2005; Gorlach et al., 2006; Li and Camacho, 2004; Michalak et al., 2002). That means that the Ca^{++} sensitive ERp57 also controls the Ca^{++} levels in the ER. Levels of ERp57 are decreased in the reduction of CAIX under hypoxia. Since this regulation is specific to cells under hypoxia, this suggests that the pH regulating function of CAIX might lead to the decrease in ERp57 levels which then can lead to an increase of the cytosolic Ca^{++} levels.

Both proteins, ERp72 and ERp57 belong to the same PDI family and their enzymatic finction depends on the pH (Alanen et al., 2006). The present study links for the first time the expression of these enzymes to the expression of a pH regulating enzyme, namely CAIX. Since CAIX depletion only has an effect on ERp72 and ERp57 under hypoxia, this leads to the conclusion that the pH regulating activity of CAIX causes this effect suggesting that not only the enzymatic activity of ERp72 and ERp57 are controlled by pH (Alanen et al., 2006), but also their expression level. Generally, ERp72 and ERp57 contribute to the decrease of expression of chaperones when cells cells are depleted of CAIX, thus further increasing the stress in the ER.

The above discussed results suggest that members of Hsp70 and Hsp90 families in the ER and also some of the ER resident proteins are regulated following CAIX depletion. Interestingly, all these proteins were downregulated following hypoxia or severe hypoxia. ER resident chaperones have been reported to be upregulated during UPR induced by severe hypoxia (Koumenis and Wouters, 2006) indicating an increased need of protein folding machinery under oxygen deprivated conditions. These partly unexpected results can derive from the fact that after 48h of severe hypoxia the onset of the UPR has already taken place and levels of chaperones are different in the later stage of the UPR. Furthermore, studies on UPR in Hela cells are often performed under reduced levels of glucose in order to facilitate the induction of stress and it cannot be excluded that the difference in glucose availiability influences protein expression levels as it does for example in the case of CAIX (Kaluz et al., 2002).

6.4.2 The Role of CAIX in the UPR

UPR is a reaction of the cells to the accumulation of misfolded proteins in the ER which prevents cell death (Cao and Kaufman, 2012). In mammalian cells, the UPR is translated via three pathways including IRE-1, PERK or ATF6 (Cao and Kaufman, 2012; Wang and Kaufman, 2014). Figure 37 gives an overview of the key players and downstream events. Misfolded proteins in the ER require the function of chaperones. Upon release of GRP-78 from the ER stress sensors PERK, IRE1 or ATF6, the onset of UPR is mediated via phosphorylation (in case of PERK and IRE1) or cleavage (in case of ATF6). Downstream signalling leads to a general translational block (translated by phosphorylation of eIF2α) and translation of specific proteins that are needed to compensate against protein misfolding taking place in the ER (mediated by ATF4, ATF6 and IRE1). The phosphorylation of eIF2α and its downstream events have been shown to be crucial steps in cell survival upon hypoxia (Koritzinsky et al., 2007).

In the present study, depletion of CAIX led to decrease of p-eIF2α levels and an abolishment of ATF4 induction (Figure 24 and Figure 25). Furthermore, chaperones, chaperonins and ER resident proteins such as GRP-78, ORP-150, GRP-94, PPlase FKBP4, TCP-1-α, Hsp60, ERp44, ERp46, ERp72 and ERp57 have been shown to be affected by the changes in hypoxia, but more often by CAIX depletion leading to a lack of chaperones that would be required to compensate the accumulation of misfolded proteins due to severe hypoxia.

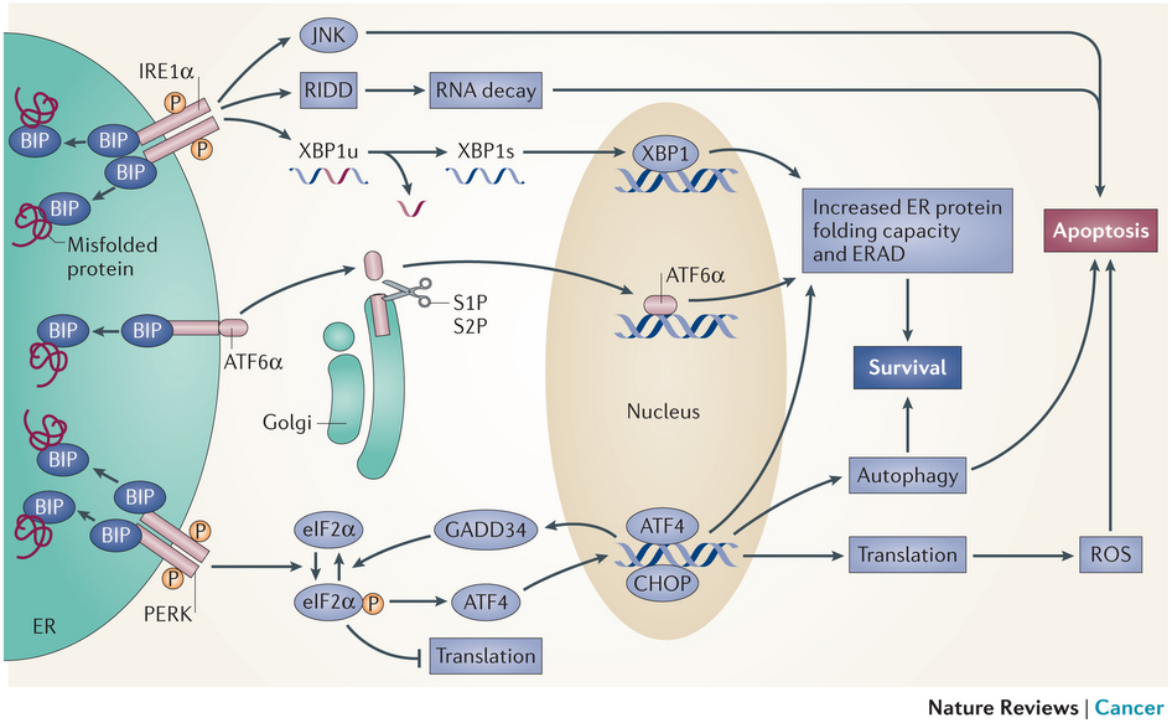

Figure 37 Overview of the Unfolded Protein Response (UPR)
UPR is activated via BiP (immunoglobulin heavy-chain binding protein) when unfolded and misfolded proteins accumulate in the ER lumen in response to ER stress. Possible ways of UPR onset can be via phosphorylation of eIF2α (eukaryotic translation initiation factor 2α) by PERK (PRKR-like ER kinase), XBP1 (inositol-requiring protein 1α (IRE1α)–X-box binding protein 1) or ATF6α (activating transcription factor 6α). The results of the UPR are increased activity of protein folding, transport and ER-associated protein degradation (ERAD) while proteins synthesis is reduced. When this is not enough to prevent protein misfolding cells undergo apoptosis. CHOP = C/EBP homologous protein; GADD34 = growth arrest and DNA damage-inducible protein 34; JNK = JUN N-terminal kinase; P = phosphorylation; RIDD = regulated IRE1-dependent decay; XBP1s = transcriptionally active XBP1; XBP1u = unspliced XBP1. Reprinted with permission from Macmillan Publishers Ltd: Nature Reviews Cancer (Wang and Kaufman, 2014), copyright 2014, licence #3595410908819.

It was shown for UPR-impaired cells that the depletion of CAIX expression and function results in reduced survival rate (van den Beucken et al., 2009b). CAIX itself has been identified as a target of UPR with decreased hypoxia-dependent induction of CAIX in ATF4 depleted cells (Rzymski et al., 2010; van den Beucken et al., 2009a). Taking this into account, the present results point to a feedback loop in the regulation, between CAIX and ATF4. Reconstitution of ATF4 in CAIX depleted cells could give further insight in the regulation between CAIX and ATF4.

The present study shows that CAIX plays a role in severe hypoxia induced UPR. CAIX expression acts on the ATF4 branch of UPR. Phosphorylation of eIF-2α was significantly reduced in CAIX depleted cells (Figure 25) supporting the hypothesis of CAIX being necessary for functional onset of the UPR response. Generally, high levels of p-eIF2α in WT cells under basal conditions are a known feature of HeLa cells (A. Petry, unpublished data). Still, the downregulation of p-eIF2α under hypoxia is a clear evidence for an effect of CAIX depletion on UPR. ATF4 transcription factor was found to be upregulated during severe hypoxia, but downregulated upon CAIX depletion (Figure 24) resulting in an abolishment of ATF4 induction when *CA9* was silenced. These results indicate that the presence of CAIX is required to switch on the UPR whereas the depletion of CAIX in the cells leads to an abolishment of the UPR, thus preventing the cells from reacting to the accumulation of misfolded proteins under severe hypoxia by initiating the rescue mechanism of UPR (Figure 38).

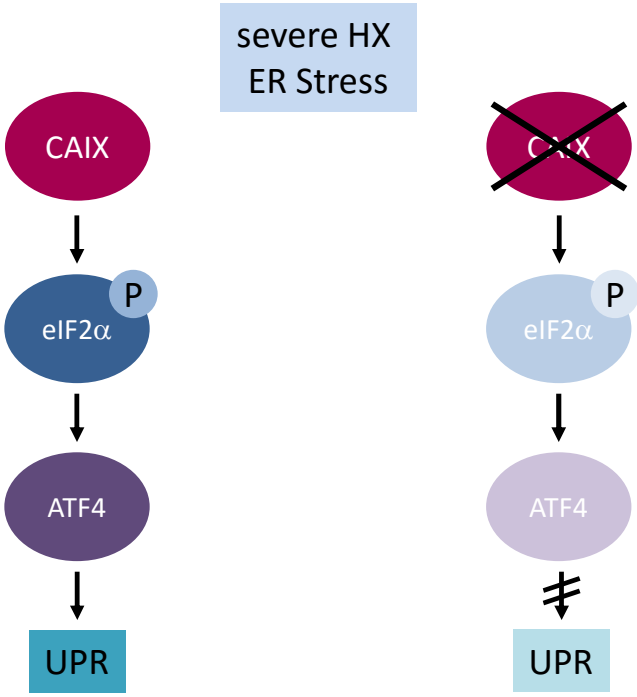

Figure 38 Mechanism of UPR abolishment when cells are depleted of CAIX
In the presence of CAIX, UPR is initiated via p-eIF2α and ATF4 under severe hypoxia (left), depletion of CAIX results in an abolishment of UPR induction (right).

Furthermore, CAIX was not only shown to have a major influence on the UPR key players ATF4 and p-eIF2α, but its expression level was shown to affect the expression of a prominent number of chaperones, chaperonins and ER resident proteins that are involved in protein folding and maintaining the protein folding machinery active. Among those were proteins that are regulated by

hypoxia and play a role in the UPR induced under severe hypoxia, but also other proteins that did not show any regulation by hypoxia, but responded solely to CAIX depletion.
These data suggest that CAIX depletion under severe hypoxic conditions did not only affect hypoxia-induced proteins, but also proteins that were not classically linked to UPR such as ER resident proteins or chaperonins, whose decreased levels contribute to ER stress and decrease the cells' capacity to cope with severe hypoxic conditions. Taking these results together, the presented results show the significant influence of CAIX on ER located processes and ER stress in general and the UPR in particular.

6.5 The Role of CAIX in the Cap-Dependent Translation

The successful onset of UPR requires selective translation in order to provide the cell with the required proteins (Wouters et al., 2005) to an extent that has been compared to the importance of transcription under hypoxic conditions (van den Beucken et al., 2011). This promotes cell survival and facilitates tumor growth under extreme conditions.

The eukaryotic translation initiation factor complex eIF4F as the cap-binding initiation complex is the best studied complexes in cancer (Silvera et al., 2010; Sonenberg and Hinnebusch, 2009). eIF4E inhibitory binding proteins (4E-BPs) regulate the functions of eIF4E. MAP kinase-interacting serine/threonine-protein kinases 1 and 2 (Mnk1 and Mnk2) are two kinases associated to eIF4G which phosphorylate eIF4E and thus regulate its function, since the binding to 4E-BP can only take place when eIF4E is dephosphorylated (Figure 39). This process is referred to as cap-dependent translation (Figure 39).

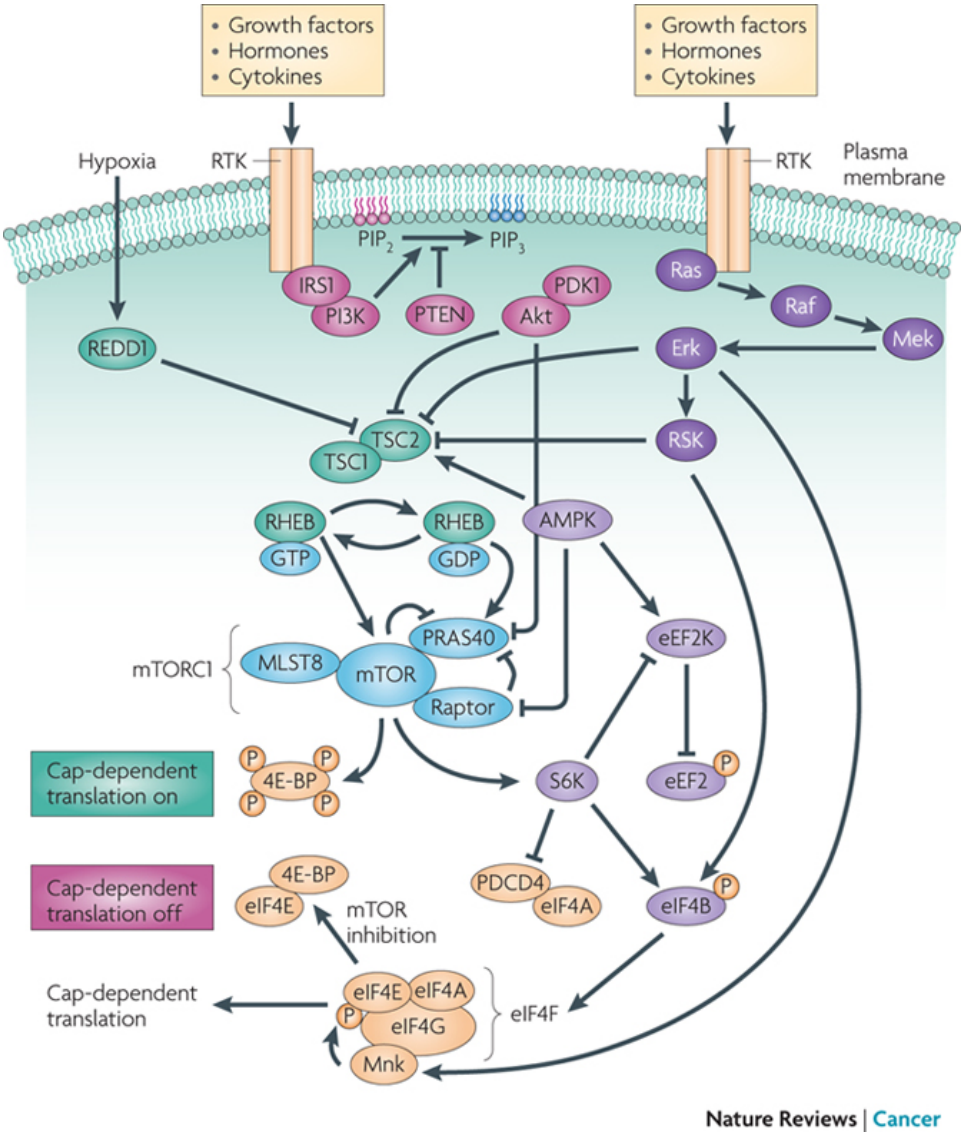

Figure 39 Cap-dependent translation in cancer cells

Ras GTPases and PI3K are activated via RTKs (receptor tyrosine kinases) after stimulation by mitogenic factors such as growth factors, cytokines or hormones. Upon Ras activation, the Raf–Mek–Erk kinase pathway signalling is initiated, activation of PI3K leads to signaling via Akt pathway. PTEN, a phosphatase depleted or inactivated in many cancers, inhibits Akt activation by PI3K. Erk influences the mRNA binding activity of the eIF4F complex via RSK and phosphorylation of eIF4B. In addition, Mnk1 and Mnk2 (MAP kinase-interacting serine/threonine-protein kinases 1 and 2) are activated and can phosphorylate eIF4E on Ser209. Akt inhibits mTORC1 inhibitor PRAS40, thus leading to activation of mTOR and mTOR itself is inhibited by hypoxia. By phosphorylation of 4E-BPs (eIF4E inhibitory binding proteins), the cap-dependent protein synthesis is maintained via mTOR since 4E-BPs cannot disconnect from the eIF4E in the eIF4F complex. In addition, active mTOR leads to activation of S6Ks (ribosomal S6 kinases) leading to phosphorylation of eIF4B. p-eIF4B blocks its inactivation of eIF4A by associating with both eIF4A and PDCD4. The cap binding complex eIF4F is formed and cap-dependent translation is initiated. Translational elongation is enhanced by eEF2 which is phosphorylated by its kinase eEF2K. Inhibition of mTOR leads to withdrawal of eIF4E and eIF4A, eIF4B and eEF2 become inactive. IRS1 = insulin receptor substrate 1; PDK1 = 3-phosphoinositide-dependent protein kinase 1; PIP2 = phosphatidylinositol-4,5-bisphosphate; PIP3 = phosphatidylinositol-3,4,5-trisphosphate; PRAS40 = AKT1S1, proline-rich AKT1 substrate 1; PTEN = Phosphatidylinositol 3,4,5-trisphosphate 3-phosphatase and dual-specificity protein phosphatase PTEN; RSK = ribosomal s6 kinase. Reprinted with permission from Macmillan Publishers Ltd: Nature Reviews Cancer (Silvera et al., 2010), copyright 2010, licence #3595410824747.

Mnk1 is a serine/threonine-protein kinase which is involved in cap-dependent translation. Mnk1 binds to a docking site at the eIF4G protein and phosphorylates eIF4E in the eIF4F complex (Pyronnet et al., 1999). Together with Mnk2, Mnk1 plays a pivotal role in tumor development as shown in a mouse model and therefore has been suggested as therapeutic target (Ueda et al., 2010) whereas the knockout does not affect cell growth during development (Ueda et al., 2004). This study revealed that the phosphorylation status of Mnk1 was increased under severe hypoxia in comparison to normoxic conditions (Figure 30). However, silencing of CA9 led to decreased levels of p-Mnk1 when cells are exposed to hypoxia and decreased levels of p-Mnk1 had no consequence on the phosphorylation levels of its target eIF4E (Figure 30).

Besides Mnk1 other components of the eIF4F complex are the helicase eIF4A, the cap binding protein eIF4E and the scaffold protein eIF4G (Holcik and Sonenberg, 2005; Silvera et al., 2010). In CAIX depleted cells, the levels p-eIF4E remained unchanged in relation to eIF4E. However, p-eIF4G, eIF4G and their ratio were reduced upon CAIX depletion (Figure 30) pointing to reduced capactiy of the eIF4F complex.

Furthermore, the expression of 4E-BP1 which is known to modulate changes in mRNA translation under normoxia as well as under hypoxia (Magagnin et al., 2008) was altered in cells with different CAIX levels (Figure 31). 4E-BP1 has been identified as key player in the dependence of the tumor on Akt signaling and has been suggested as therapeutic target protein due to this important role (She et al., 2010). In a mouse model for diabetes, 4E-BP1 was identified as a target of ATF4 during tapsigargin and tunicamycin induced ER stress (Yamaguchi et al., 2008). Phosphorylation of 4E-BP1 (Figure 39) determines its acitivity, with active 4E-BP1 protein when being hyperphosphorylated (Silvera et al., 2010). In breast cancer, the Akt/mTOR/4E-BP pathway is active during development and progression and has been associated with poor prognosis and therapy outcome (Zhou et al., 2004).

In the present study, 4E-BP levels showed a general increase during hypoxia and reoxygenation and a reduction when cells were depleted of CAIX under these conditions (Figure 31). Although the levels of the phosphorylated isoform could not be determined, the results suggest that silencing of *CA9* led to decreased acitivity of 4E-BP1 due to reduced availability of the protein. Since the levels of p-Akt and p-mTOR were also affected by *CA9* silencing, it can be speculated that the decrease in p-mTOR and p-Akt in CAIX depleted cells under hypoxia may have also influenced the activity of the 4E-BP1. In combination with generally reduced levels of 4E-BP1, this might have led to impaired cap-dependent translation.

Since both CAIX and 4E-BP1 are target proteins of ATF4 (Rzymski et al., 2010; Yamaguchi et al., 2008) and ATF4 itself is a target protein of CAIX, the decrease of 4E-BP1 can be explained by the downregulation of ATF4 when cells are depleted of CAIX. Moreover, a feedback loop via ATF4 can be suggested which is maintaining the downregualtion of both CAIX and 4E-BP1. In addition, 4E-BP1 was found to be regulated in dependence of CAIX levels. In contrast to the increase of p-Mnk1/Mnk1 under severe hypoxia, p-Mnk1/Mnk1 decreased siCA9 samples. Collectively, these results provide clear indications of a decrease in cap-dependent translation when cells depleted of CAIX undergo hypoxia-induced ER stress. The results suggest a novel link between CAIX, hypoxia and cap-dependent translation.

These conclusions are supported by the regulation of programmed cell death protein 4 (PDCD4) which has previously been found to play a role in breast cancer (Frankel et al., 2008). It was shown that PDCD4 can interact with eIF4A and act like a homologue to eIF4G (Goke et al., 2002). In line, PDCD4 was found to be differentially regulated (Table 5) and differentially phosphorylated (Table 6) in the present 2DE study. Both PDCD4 and eIF4G levels were reduced in CAIX depleted cells, such that a compensatory effect can be excluded in case PDCD4 acts as a homologue to eIF4G. In a different study PDCD4 has been shown to interact with eIF4G in fibroblasts suggesting that PDCD4 regulates translation via eIF4G (Kang et al., 2002). Furthermore, phosphorylation and activation of PDCD4 are closely linked to Akt (Lankat-Buttgereit and Goke, 2009) and Akt itself has been shown to be regulated following CAIX depletion in this study (Figure 29). Since p-PDCD4 was identified in a spot together with sequestosome-1, no definitive conclusion could be reached over how p-PDCD4 is affected by CAIX depletion. Nevertheless it remains noteworthy that PCDC4 levels are controlled following CAIX depletion and the function of PDCD4 and p-PDCD4 are likely to be affected both following CAIX depletion as well as via Akt, linking for the first time CAIX to the tumor surpressor PDCD4. This novel link calls for further investigation.

It has been previously proposed that PDCD4 is upregulated when programmed cell death takes place and the protein is assumed to inhibit translation (Lankat-Buttgereit and Goke, 2009). Interestingly, although PDCD4 was identified to be downregulated in the absence of CAIX (Table 5), CAIX depleted cells underwent apoptosis (see 5.7). Hence, the present study suggests a novel link between PDCD4, eIF4G and CAIX.

The degradation of tumor suppressor PDCD4 was suggested to increase protein synthesis and promote cell growth (Dorrello et al., 2006) hence the decrease of PDCD4 following CAIX depletion revealed by the differential display proteomic experiment was unexpected. It remains unclear how and to what degree PDCD4 phosphorylation is affected by CAIX levels. The link

between CAIX and PDCD4 is however of high interest and may provide further insight in tumor cell biology. While the link between PDCD4 and CAIX is novel, PDCD4 has been liked to CAII before (Lankat-Buttgereit et al., 2004) through its role in the regulation of tumor growth. This suggests a connection between pH regulation, tumor growth and programmed cell death and for the first time indicates a link between these events and CAIX.

PDCD4 was identified as one of the two components in a differentially phosphorylated spot in CAIX depleted cells giving potential indication that CAIX regulates not only the abundance of PDCD4, but also its function. Phosphorylation of PDCD4 by Akt enables the translocation of p-PDCD4 to the nucleus and inhibition of PDCD4 by Akt leads to an increase in transcription (Palamarchuk et al., 2005). Validating the change in phosphorylation of the two proteins contained in the differentially phosphorylated spot – PDCD4 and sequestosome-1 – could give further insight here.

Given that the regulation of the cap-dependent translation is under the control of the Akt/mTOR/4E-BP pathway (Silvera et al., 2010), the role of CAIX can be twofold: on the one hand, it is possible that depletion of CAIX leads to alterations in pH control. This could disturb the proton gradient across the plasma membrane leading to the phosphorylation of Akt and subsequent alteration of translation. On the other hand, the intracellular domain of CAIX could itself posses signalling activity which could then act on downstream targets in the cytosol. This would represent a novel function and activity of CAIX in this context and should be further investigated.

Overexpression of CAIX was shown to induce p-mTOR, p-4E-BP1 (while 4E-BP1 levels stay stable) and even an increase in HIF-1α (Kim et al., 2012). These findings are in line with the results from the present study, i.e. cells depleted of CAIX express reduced levels of p-mTOR. Furthermore the results suggest that p-4E-BP1 is reduced in CAIX depleted cells leading to a reduction of cap-dependent translation. Generally, Akt/mTOR signaling plays a pivotal role in cancer progression and is involved in invasion and metastasis in cancer such as hepatocellular carcinoma or leukemia (Chen et al., 2009a; Hay, 2005; Martelli et al., 2010). mTOR itself is known to be a potent regulator of translation and inhibition of mTOR leads to a reduction of cap-dependent translation (Mamane et al., 2006).

An overview of the presented hypotheses is given in Figure 40. Under hypoxia and in the presence of CAIX, levels of 4E-BP1 and p-Mnk1 are increased, supporting an increase in cap-dependent translation under ER stress conditions. Following CAIX depletion under hypoxia, levels of p-Akt

are decreased leading to an inhibition of mTOR. Further downstream this leads to a decrease in the levels of 4E-BP1, p-Mnk1 and p-eIF4G thus preventing the assembly of the cap complex resulting in decreased cap-dependent translation.

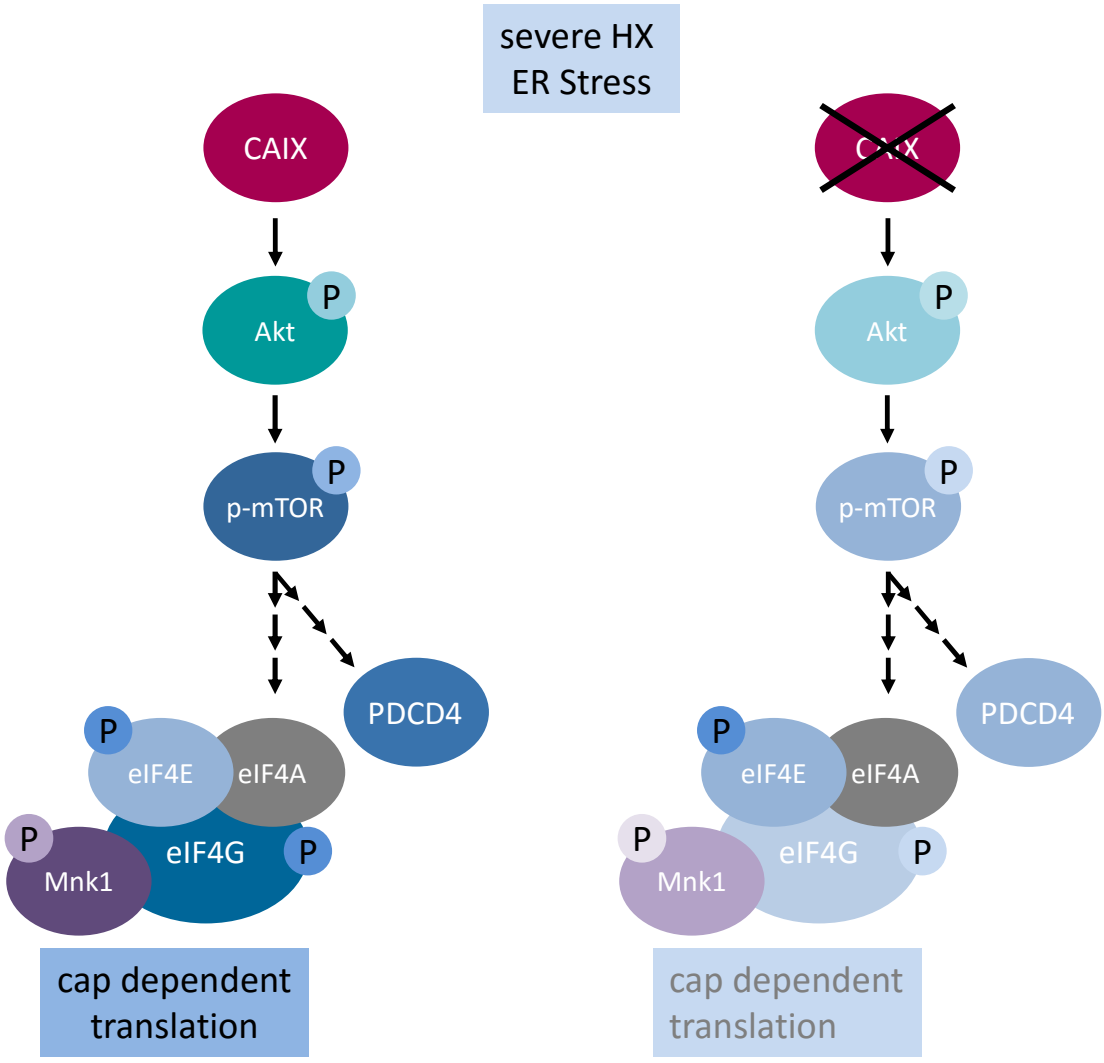

Figure 40 Overview of the role of CAIX in UPR and cap-dependent translation
Displayed is the possible role of CAIX under severe hypoxia conditions. In the presence of CAIX (left) Akt and mTOR signaling support the link to cap-dependent translation whereas under siCA9 conditions (right) reduced levels of p-Akt and p-mTOR lead to impaired signaling function. In line with the hypothesis is the regulation of PDCD4 revealed in the 2DE experiment.

The eukaryotic peptide chain release factor GTP-binding subunit ERF3A (eRF3a) is a GTPase which is a major factor responsible for the termination of the eukaryotic translation. The protein regulates the stability of eukaryotic peptide chain release factor subunit 1 (eRF1) which recognizes the stop codons during translation (Chauvin et al., 2005). The levels of eRF3a were increased both upon CAIX depletion and under hypoxia and partly decreased during reoxygenation independent of each other (Table 5) which indicates an increase in the termination of translation. Given that the

switch of Akt pathway in the absence of CAIX leads to a downregulation of cap-dependent translation, this could also mean that cap-independent translation is increased. An increase in cap-independent translation would then explain the increased levels of eRF3a when cells are depleted of CAIX and under hypoxic conditions.

Elongation factor 1 δ (EF-1-δ) is involved in the elongation process during mRNA translation. Kinectin has been suggested to serve as the membrane anchor that holds EF-1-δ in its position in the ER (Ong et al., 2003). qPCR results revealed that EF-1-δ is significantely upregulated in oesophagial carcinoma patients and showed a correlation with metastasis and decreased survival rate (Ogawa et al., 2004). In the present study, EF-1-δ levels were found to increase in abundance in response to hypoxia and CAIX depletion (Table 5). Furthermore, EF-1-δ was differentially phosphorylated in response to *CA9* silencing and under hypoxia showing increased phosphorylation following CAIX depletion or under hypoxia, respectively (Table 6). Together with the impact of the silencing of *CA9* on the levels of eRF3a, the data support the hypothesis that CAIX in general has impact on the regulation of translation while depletion of CAIX leads to reduced translation. Since EF-1-δ expression correlates with metastasis and reduced survival and CAIX depletion leads to an impaired response to cell stress, the data suggest that the decrease in CAIX is connected to diminished cell survival.

6.6 The Role of CAIX in the Regulation of Apoptosis

In CAIX depleted cells, the number of viable cells was significantly reduced under hypoxia and reoxygenation (Figure 32 A). Furthermore, calcein staining showed decreased viability in CAIX depleted cells independent of the oxygen status of the cell (Figure 32 B). PI staining was used to distinguish apoptotic from necrotic cells (Sawai and Domae, 2011) and provided no evidence for necrosis (Figure 32) suggesting that cells undergo apoptosis independent of the oxygen state.

It has been known since long that caspases execute apoptotic function (Budihardjo et al., 1999) and among these, caspase 3 and 7 play a key role (Lakhani et al., 2006; Slee et al., 2001). To consolidate these findings and elucidate the pathways involved, the expression patterns of caspases 3, 7 and 8 were tested. The hypothesis that cells undergo apoptosis in the absence of CAIX was supported by the finding that cleaved effector caspases 3 and 7 and activator caspase 8 were upregulated in the absence of CAIX (Figure 33). Furthermore, cleavage of PARP-1 was used as marker for caspase activity since PARP-1 is a known caspase substrate and cleaved PARP-1

accumulates during apoptosis (Soldani and Scovassi, 2002). Indeed, PARP cleavage could be found in the absence of CAIX when cleaved caspases were present. This finding could be confirmed by measurements of caspase activity that showed caspase 3/7 activity in addition to caspase 3/7 cleavage in cells depleted of CAIX and under different states of oxygenation (Figure 34) confirming that caspases 3/7 were not only cleaved, but also active.

It was shown before that inhibition of CAIX using inhibitors results in the induction of apoptosis and reduced proliferation in cancer cells (Cianchi et al., 2010), although not all CAIX inhibitors show this function (Meijer et al., 2014). In agreement with this report it could be shown in this study that silencing of CAIX leaded as well to apoptosis. Therefore, silencing of *CA9* using RNAi can be suggested to serve as a control experiment to validate inhibitor function. Still, it remained unclear how the absence of CAIX could be translated into apoptosis. A possible missing link between CAIX levels and apoptosis emerged from the results of the 2DE based proteomic approach. Both calpastatin and ERp44 displayed differential expression in control and CAIX depleted HeLa cells, respectively, with lower abundance in the latter (Table 5 and Figure 17).

Calpastatin is known to be upregulated by hypoxia (Blomgren et al., 1999). Although calpastatin was found to be downregulated in response to hypoxia and also reoxygenation in the 2DE experiment (Table 5), calpastatin levels were increased in response to severe hypoxia as well as when cells were depleted of CAIX (Figure 36). Calpastatin is an inhibitor of the Ca^{++} sensitive protease calpain (Hanna et al., 2008) which promotes apoptosis in cancer upon extrinsic and intrinsic stimulation e.g. changes in the Ca^{++} equilibrium in the cell (Storr et al., 2011). Also in other cell types, calpain has been shown to be sensitive to regulation by Ca^{++} and to induce apoptosis (Neumar et al., 2003; Ray et al., 2000). In a mouse model for melanoma it could be shown that the calpain/calpastatin system has a high impact on tumor growth and plays an pivotal role in tumor metastasis (Raimbourg et al., 2013).

Depending on the stimulus, calpain can lead either towards survival or apoptosis and have different influence on different caspases, but in cancer cells calpain has been connected to apoptosis as reviewed previously (Storr et al., 2011). Calpain cleaves caspase 7 leading to an active form of caspase 7 which is more potent than the form that results from caspase 3 cleavage (Gafni et al., 2009).

Although no link has been so far established between calpastatin and CAIX, studies on post-mortem muscle revealed a complex connection between pH, ionic strength, calpastatin and calpain (Carlin et al., 2006; Kendall et al., 1993; Maddock et al., 2005). Since calpastatin levels were

affected independent of the oxygen state and CAIX has a role in pH regulation only under hypoxic conditions, it remains unclear whether the pH is a key regulator of calpastatin in this case. However, further investigation of the calpain activity may provide more insight into the novel CAIX-calpastatin-calpain triangle and confirm whether caspases are activated via calpain activation in the absence of CAIX, when calpastin levels are reduced. In addition, calpain inhibition in CAIX depleted cells should rescue the effect by counteracting the missing inhibition of calpastin in the absence of CAIX.

In addition to the regulation of calpastatin following CAIX depletion, the 2DE experiment showed that ERp44 was differentially expressed following CAIX depletion leading to decreased ERp44 levels in siCA9 cells (Table 5). ERp44 is an ER resident protein that regulates the Ca^{++} efflux by inhibition of $InsP_3R$ (see 6.4) and thus is responsible to keep Ca^{++} in the ER. The link between ER stress and apoptosis has been established (Kim et al., 2010). In addition, a knockdown of ERp44 led to an increase of caspase 3 levels and activation of apoptosis in HeLa cells (Chang et al., 2015) supporting the suggested link between decreased ERp44 levels and the execution of apoptosis supported by the present study. ERp44 is responsible for the regulation of Ca^{++} levels in the ER and in CAIX depleted cells this should therefore lead to an increase in cytosolic Ca^{++} levels due to impaired efflux control of Ca^{++} from the ER. As a proof of principle-experiment, addition of EGTA, EDTA or BAPTA could be used to "rescue" the cells in the absence of CAIX.

Thus, in the presence of CAIX, basal levels of ERp44 and calpastatin are maintained under hypoxia in order to grant cell survival. When cells are depleted of CAIX, ERp44 levels decrease resulting in an efflux of Ca^{++} from the ER. Activation of calpain following CAIX depletion is thus supported firstly by increased Ca^{++} levels in the cytosol and secondly, by a decrease of its inhibitor calpastatin. This would directly lead to the onset of apoptosis and the lowered number of surviving cells observed (Figure 41). Furthermore, reduced levels of ERp57 under hypoxia following CAIX depletion contribute to the increase in Ca^{++} levels in the cytosol further strenghenting the relation between reduced CAIX levels and Ca^{++} flux from the ER.

In breast cancer, a link between Ca^{++}, calpain and cell death has been established showing that increased intracellular Ca^{++} levels lead to activation of calpain and programmed cell death. Inhibition of calpain with different specific inhibitors could reduce DNA fragmentation and inhibit apoptosis (Mathiasen and Jaattela, 2002). Thus it is hypothesised from the present study that Ca^{++} release form the ER – due to reduced levels of ERp44 independent of the oxygen status and of ERp57 under hypoxia – together with decreased levels of calpastatin lead to an increase in calpain

activity which further initiates caspase cleavage and activity, thus leading to apoptosis. Determination of Ca^{++} levels (with fluorescent probes, e.g.), calpain activity and inhibition of calpain may be required to confirm this hypothesis. Furthermore, binding of free Ca^{++} with EGTA, EDTA or BAPTA can serve to rescue the effect of ERp44 reduction (and reduction of ERp57 under hypoxia) by binding free Ca^{++} and restoring the equilibrium towards cell survival in CAIX depleted cells.

Figure 41 summarises the identified and hypothesised connection between CAIX and apoptosis.

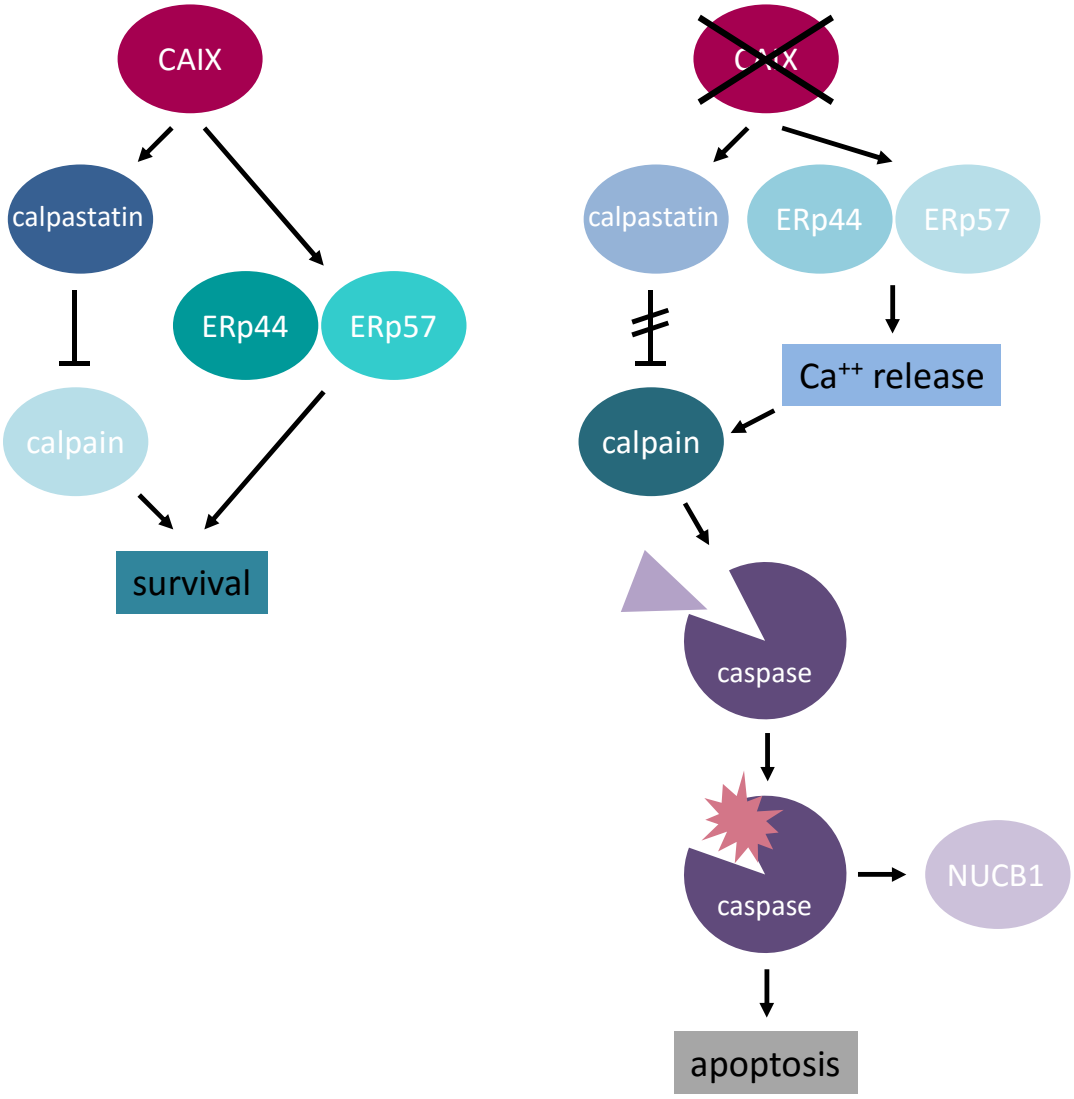

Figure 41 Suggested role of CAIX in apoptosis
In the presence of CAIX (left), basal levels of ERp44 and calpastatin maintain cellular stability and survival. In the absence of CAIX (right), Ca^{++} is released from the ER upon changes in ERp44 levels. Increase in Ca^{++} and decreased levels of calpain inhibitor calpastatin both lead to activation of caspases via calpain and apoptosis. NUCB1 = nucleobindin-1

A similar pathway connecting ER stress, calcium, calpain and apoptosis has been hypothethised for neuronal cell death during ischemia (Rami, 2003). In support of this hypothesis is also the finding that nucleobindin-1 is differentially expressed following *CA9* silencing (Table 5). Nucleobindin-1 is a Ca^{++} sensitive protein that is cleaved by caspases during apoptosis (Valencia et al., 2008). Caspase acitivity as shown in the absence of CAIX would therefore lead to decreased nucleobindin-1 levels due to its cleavage. Indeed, nucleobindin-1 levels were found to be decreased in CAIX depleted cells. These data further support the finding that absence of CAIX leads to caspase activity.

It is known that the inhibition of CAIX expression diminishes tumor growth and metastasis (Lou et al., 2011). Although the link between CAIX and tumor survival is well-established, it was unclear whether CAIX is involved in migration and invasion (Robertson et al., 2004). Together with CAXII, CAIX has been identified as a key player in tumor survival in an acidic environment by alkalising the pH_i (Chiche et al., 2009). The present study highlights the role of CAIX in survival. Furthermore, the present data suggest that *in vitro* CAIX has an impact on survival independent of its pH regulating activity since CAIX depleted cells showed impaired survival also under normoxic conditions. To further exclude that the pH plays a role in this context, determination of the pH_i could give more insight on the role of CAIX in dependence on the oxygen state of the cell.

6.7 Further Identified Protein Functions

A large number of further protein functions were identified as differentially expressed or differentially phosphorylated in CAIX depleted cells showing that CAIX has a defining impact upon cellular metabolism. Further classification of proteins was undertaken to outline the influence of CAIX on different areas of cellular functions.

6.7.1 Proteins Linked to Transcription, Cell Division and DNA Control

Heterogeneous nuclear ribonucleoprotein U (hnRNP U) was found to increase in abundance upon *CA9* silencing and also during hypoxia, but to decrease during reoxygenation (Table 5). hnRNP U is involved in transcription where it is believed to regulate the early transcription of RNA polymerase II together with actin (Kukalev et al., 2005). It has been shown to specifically regulate gene transcription by regulation of mRNA stability (Yugami et al., 2007). hnRNP U belongs to a

family of proteins that are involved in DNA damage response (DDR) upon radiation (Haley et al., 2009). Furthermore, hnRNP U is a novel target of the DNA dependent protein kinase (DNA-PK) which is activated when DNA double-strand breaks occur and is involved in the DDR (Britton et al., 2009). Since hnRNP U is upregulated in absence of CAIX this suggests that DDR might play a role under this condition. Furthermore, hnRNP U upregulation leads to splicing of pro-apoptotic caspase 9 (Vu et al., 2013). Since hnRNP U is upregulated when cells are depleted of CAIX, this supports the present hypothesis that depletion of CAIX leads to apoptopsis.

A motor protein that has been found to be regulated by CAIX levels is the motor protein tubulin β-4A chain that was both identified to be up and down regulated in response to CAIX depletion (Table 5). Tubulin isoforms build the cellular microtubule system that enables the cell to successfully carry out important tasks such as cell transport and cell division (Nogales, 2000). Mutations in tubulin β-4A chain can lead to neurodegenerative disorders (Blumkin et al., 2014; Lohmann and Klein, 2014). Tubulin isoforms have been suggested to serve as potential targets for cancer therapy (Ravanbakhsh et al., 2013). In this study, two isoforms of the tubulin β-4A chain appeared to be regulated in opposite directions, one being up- and one being downregulated following CAIX depletion. The two spots have different isoelectric points suggesting that CAIX depletion leads to a post translational modification of tubulin β-4A which results in a shift of the protein's pI towards a more basic value. It has been previously discussed that post translational modifications of tubulins can regulate their function in the cell (Sirajuddin et al., 2014). The present data suggest that the tubulin activity is thus modulated via post translational modification following CAIX depletion. In addition, it has been shown that CAIX plays a role in migration (Robertson et al., 2004) which is also a point where CAIX potentially has an impact on cellular fiber structures.

Actin-related protein 3 is involved in chromatin remodeling together with actin (Olave et al., 2002). Actin-related protein 3 was identified to be upregualted in the absence of CAIX and downregulated under hypoxia (Table 5). The regulation under CAIX depleted conditions was in line with the regulation of hnRNP U which by itself can interact with actin as well. Taken together, these findings suggest a potential novel role of CAIX in the regulation of transcription.

Kinesin-like protein KIF11 (alternative names are TR-interacting protein 5 or TRIP-5) is a member of the motorprotein family of kinesins which are macromolecule transporters involved in meiosis and mitosis. They have also been suggested to be potential targets for cancer therapy (Yu and Feng, 2010). KIF family member KIF11 has been found to be present in two spots together with

hnRNP U which showed increased spot volumes in absence of CAIX (Table 5). The data therefore support a relation between CAIX and meiosis and mitosis.

Another protein involved in meiosis and DNA repair is pachytene checkpoint protein homolog 2 (TRIP-13). Results from a mouse model suggest that this protein is required for the completion of meiosis. Mice depleted of TRIP-13 show loss of oocytes and spermatocytes around their birth suggesting that uncorrected DNA damages can lead to pachytene checkpoint response in mammals (Li and Schimenti, 2007). Proteomics profiling of hypoxia-exposed kidney fibroblasts identified proteins connected to meiosis (Shakib et al., 2005). In the present study, TRIP-13 was upregulated in CAIX depleted cells and under hypoxia as well as upon reoxygenation (Table 5). These data suggest that in the absence of CAIX TRIP-13 is upregulated to ensure DNA control mechanisms. In line with the differential epression of hnRNP U, the regulation of TRIP-13 supports a potential and novel role of CAIX in DDR.

6.7.2 Proteins Linked to Metabolism and Redox Regulation

Glutaredoxin-3 is a member of the glutaredoxin family (Holmgren et al., 2005; Lillig et al., 2008). In vertebrates, glutaredoxin-3 is involved in the regulation of iron levels and hemoglobin maturation (Haunhorst et al., 2013). Generally, the thioredoxion-glutaredoxin system controls the redox potential. Glutaredoxins are small proteins with cystein residues that sense, modulate and stabilize the redox status of the cell, use glutathione as a cofactor and can facilitate and regulate protein folding (Berndt et al., 2008). In the present study, levels of glutaredoxin-3 showed clear upregulation under hypoxia and when cells were depleted of CAIX protein. Hypoxia causes ER stress and during ER stress, elevated ROS levels in the ER can be observed to be controlled by ATF4 as recently summarized (Chakravarthi et al., 2006). Downregulation of ATF4 under severe hypoxia in the absence of CAIX therefore enhanced oxidative stress and thus the upregulation of glutaredoxin-3 can be explained as a compensatory effect. This regulation goes in line with an upregulation of chaperones that is postulated under hypoxia and UPR and implicate a compensatory and rescuing effect to maintain correct folded proteins when CAIX levels are reduced. Taken together, the regulation of glutaredoxin-3 and thioredoxin reductase 1 (ERp46, see 6.4.1) imply a role of CAIX in the regulation of the redox state of the cell or point to a possibly compensatory effect following CAIX depletion.

NADH dehydrogenase [ubiquinone] iron-sulfur protein 8 (CI-23kD, alternative name TYKY) is a subunit of the respiratory chain NADH dehydrogenase (Complex I) located in the mitochondrial membrane. The protein takes part in the electron transfer and proton pumping function of complex I which is the largest multiprotein complex in the cellular oxidative phosphorylation system. Patients with a mutation in the corresponding gene suffer from Leigh syndrome (Marina et al., 2013; Procaccio and Wallace, 2004). Complex I intermediate-associated protein 30, mitochondrial (NUFDAF1) mainly catalyzes the assembly and stability of CI-23kD (Vogel et al., 2005). In the present study, levels of CI-23kD were decreased when cells were depleted of CAIX. This is a novel potential connection between CAIX and the electron transfer in the respiratory chain.

4-trimethylaminobutyraldehyde dehydrogenase (TMABADH) is a member of the aldehyde dehydrogenase (ALDH) superfamily of enzymes that catalyze the detoxification of aldehydes (Jackson et al., 2011). Other members of the ALDH family have been associated with bladder cancer (Su et al., 2010), squamous cell carcinoma of head and neck (Chen et al., 2009b; Visus et al., 2007), but were also connected to cognitive ability (Plomin et al., 2004). In the case of TMABADH, a variation in the gene has been identifed as a potential risk factor for renal cancer (Henrion et al., 2015) and it has been patented as a marker protein for early stage liver cancer (Park et al., 2015). TMABADH was downregulated upon hypoxia and reoxygenation and upregulated following CAIX depletion. These result establish a novel link between CAIX and TMABADH or are a sign for a potential compensatory effect of the cell following CAIX depletion.

Mannose-6-phosphate isomerase (PMI) is a cytosolic enzyme that catalyzes the reversible conversion from fructose-6-phosphate to mannose-6-phosphate which is a process required in the nucleotide-sugar biosynthesis. PMI exhibited complex regulation in response to CAIX meaning that levels of PMI were downregulated in reoxygenated cells in comparison to hypoxic cells only in CAIX depleted cells, but not in control cells. These data suggest that the regulation of PMI depends not only on the oxygenation status, but also on the CAIX levels at the same time and not independent from each other. Deficiency in PMI leads to type Ib congenital disorder of glycosylation that can be handled with mannose supplementation (Niehues et al., 1998). Proteomic studies revealed that PMI is downregulated in gastric cancer (Kuramitsu and Nakamura, 2006; Nishigaki et al., 2005) and at the same time a downregulation of CA isoforms I and II could be shown. This finding is supported by the present study since PMI was found to be downregulated in dependance of CAIX indicating a connection between PMI and regulation of pH.

6.7.3 Other Protein Functions

Hepatoma-derived growth factor (HDGF) is a progonostic marker for pancreatic carcinoma (Uyama et al., 2006), hepatocellular carcinoma (Yamamoto et al., 2006), gastric carcinoma (Yamamoto et al., 2006) and lung cancer (Ren et al., 2004). HDGF has been shown to induce VEGF and to play a role in angiogenesis (Okuda et al., 2003). HDGF was identified in a spot together with endoplasmin. The spot volume increased under hypoxia and when cells were depleted of CAIX, but since it contains two different proteins, no conclusion could be drawn regarding the distinct regulation of HDGF under the investigated conditions.

Complement component 1Q subcomponent-binding protein (C1qBP) is a mitochondrial protein which is also known under the name p32. C1qBP is an ERK substrate and is translocated to the nucleus (Majumdar et al., 2002). C1qBP is overexpressed in cancer tissue and since its expression has been linked to the tumor stage it has been suggested to serve as a therapeutic marker in breast cancer (Zhang et al., 2013). Furthermore, C1qBP is upregulated in cancer cells and promotes cell proliferation, migration and was held responsible for protection against cell death in tumor cells (McGee et al., 2011). In the present study, C1qBP decreased in abundance upon treatment with hypoxia or when cells have been depleted of CAIX indicating that both the decrease in C1qBP and CAIX lead to cell death and with CAIX being upstream of C1qBP.

Serpin B6 belongs to a big family of protease inhibitors. In *Anopheles*, serpin B6 facilitates the immune response against *Plasmodium* (Abraham et al., 2005). Serpin B6 is an inhibitor of the serine protease cathepsin G that is located in lysosomes and inhibits cathepsin G leaking into the cytosol (Gettins, 2002; Law et al., 2006). In lung cancer, the inhibition of cathepsin B leads to prevention against caspase-independent apoptosis (Broker et al., 2004). Furthermore, cathepsin B secretion correlates with hypoxia (Cuvier et al., 1997). Serpin B6 was found to increase in abundance following CAIX depletion and in response to hypoxia. In the present model this could mean that serpin B6 is upregulated in response to an increase in cathepsin B. This could happen either as compensation or as protection against caspase-independent cell death which is favored by cathepsin B. This effect is even more pronounced in absence of CAIX. Investigation of cathepsin B levels could give further insight on the novel connection between CAIX and cathepsin B.

6.7.4 Differentially Phosphorylated Protein Functions

A number of five proteins were shown to be differentially phosphorylated in CAIX depleted cells: sequestosome-1, PDCD4, vimentin, perilipin 3 and EF-1-δ of which two, namely PDCD4 and EF-1-δ, have already been discussed above (see 6.5). A limitation in the investigation of phosphorylated proteins was the low sample size of phosphorstained gels. Nevertheless, the analysis of those gels gave interesting indication regarding differentially phosphorylated protein functions.

Sequestosome-1 (alternative name: p62) is a cytosolic protein involved in ubiquitin-mediated protein degradation inside the cell. It has various functions that include scaffolding, cargo movement and binding to polyubiquitin to persue its role in proteasomal degradation and autophagy (Seibenhener et al., 2004; Seibenhener et al., 2007; Wooten et al., 2008). The protein posseses multiple phosphorylation sites and its activity is regulated by its phosphorylation state (Matsumoto et al., 2011). Because aggregated proteins play a pivotal role in neurodegenerative diseases, the role of sequestosome-1 has been investigated with regard to Alzheimer's disease (Wooten et al., 2006). Mutations in sequestosome-1 result in a bone disorder named Paget's disease which involves bone deformation, pathological fractures and deafness (Hocking et al., 2002). In the present study sequestosome-1 was identified together with PDCD4 in a spot which showed increased phosphorylation following CAIX depletion. The link between CAIX and sequestosome-1 gives an interesting and novel indication for a potential role of CAIX in regulation of protein degradation.

Vimentin was found to be differentially phosphorylated in CAIX depleted cells and also in response to hypoxia. Vimentin is a marker protein for epithelial-to-mesenchymal-transition (EMT) which is a key event in cancer development towards metastasis. Being a mesenchymal marker, vimentin itself is upregulated during EMT (Kokkinos et al., 2007). Vimentin is required for EMT function and is needed to induce the downstream target Axl which itself regulates the migration (Vuoriluoto et al., 2011). Due to its role in EMT and cancer metastasis and progression, vimentin has been discussed as potential molecular target for therapy (Satelli and Li, 2011). Xenograft studies revealed vimentin as novel anti-cancer target for therapeutic strategies (Lahat et al., 2010).

The regulation of vimentin activity is mediated via phosphorylation of the protein (Ivaska et al., 2007). Phosphorylation and reorganisation of vimentin can be carried out by p21-activated kinase (PAK) and results in a loss of filament forming capacity (Goto et al., 2002; Li et al., 2006). In

prostate cancer vimentin overexpression contributes to invasion and metastasis via Src (proto-oncogene tyrosine-protein kinase Src) while downregulation of vimentin led to reduced invasiveness (Wei et al., 2008). Vimentin could also be found in less than 10 % of the patients with invasive breast cancer (Korsching et al., 2005). *In vitro* experiments with breast cancer cell lines revealed that the invasiveness correlates with the expression of vimentin being under the control of β-catenin (Gilles et al., 2003).

Phosphorylation of vimentin by Cdk1 (Cyclin-dependent kinase 1) has been shown to play a role during mitosis (Yamaguchi et al., 2005). Vimentin has been shown to be differentially phosphorylated in the present data set with higher levels of phosphorylation fellowing CAIX depletion. The data strongly suggest a relation between CAIX, HX and vimentin function and connect two molecular target proteins in cancer.

Perilipin-3 is a member of the PAT family (the name derives from three contained proteins perilipin, adipose differentiation-related protein [ADRP], tail-interacting protein of 47 kDa [TIP47], but TIP47 is also used as synonym for perilipin-3). In macrophages it is regulated under the control of toll-like receptor 9 and involved in the accummulation of lipid droplets that lead to the formation of foam cells which play a pivotal role in artheriosclerosis (Fan et al., 2013; Gu et al., 2010). The formation of lipid droplets involves mitochondria, peroxisomes and the ER (Brasaemle and Wolins, 2012). Silencing of *perilipin-3* leads to an abolishment of lipid droplet formation in neutrophils (Nose et al., 2013). Cancer cells show an altered metabolism that leads to changes in the glucose and lipid metabolism and a turn towards the lipogenic pathway has been shown to be associated with poor outome in hepatocellular carcinoma (Yamashita et al., 2009). Perilipin-3 has been shown to be expressed in several tumors that also show lipid droplets formation, both facts being suggested to be important in therapeutic strategies (Straub et al., 2010).

Nothing is known about phosphorylation of perilipin-3, but perilipin-1A is phosphorylated during the initiation of lipolysis and it has been suggested to regulate its function (McDonough et al., 2013). Phosphorylation of perilipin-3 was increased following CAIX depletion and also when cells were exposed to hypoxia. The connection between perilipin-3 and CAIX gives new perspectives for further investigations. Since the ER is involved in droplet formation, this might be the potential link between CAIX and perilipin-3. Furthermore, since perilipin-3 is a cargo protein for mannose-6-phosphate receptor (Orsel et al., 2000) and since PMI was found to be regulated following CAIX depletion this might be an interesting new link as well.

Taken together, all identified proteins support a strong impact of CAIX on a variety of cellular processes. In addition, they give new indications for further research on the role of CAIX in the cellular metabolism.

6.8 Possible Mechanisms of Regulation by CAIX

The present study showed that the depletion of CAIX is accompanied by the dysregulation of various protein functions in the cell. At functional level, a major involvement of CAIX on the UPR response, cap-dependent translation and apoptosis was revealed. These results cleary indicate a pivotal role of CAIX in cellular survival and health not only under reduced oxygen conditions, but also under normoxic and reoxygenating circumstances.

It remained however unclear how these downstream effects are mediated. Two different scenarios appear possible: since CAIX is responsible for the maintenance of the pH gradient across the plasma membrane it could be hypothesised that a disturbance in the machinery driving this gradient can initiate signaling cascades in the cytosol leading in turn to the observed changes in the proteomic profile of the cells.

Secondly, CAIX could have additional as yet undescribed functions promoting cell survival, translated by its intracellular domain. Since CAIX depletion affects p-Akt, the intracellular domain of the CAIX protein could trigger intracellular signaling. It has been shown that the intracellular domain has putative phosphorylation sites (threonine443, serine448 and tyrosine449) of which tyrosine449 has been shown to be phosphorylated. When CAIX is phosphorylated, induction with epidermal-growth factor leads to Akt signaling (Dorai et al., 2005), which has been shown to be affected in the present study.

The data presented here support a novel role of CAIX in signaling and cell survival that emphasizes the important role of CAIX in the tumor cell and sets the ground for future research with promising visions on future therapeutic strategies.

6.9 Concluding Remarks

To investigate the role of the tumor marker protein CAIX in HeLa cells, a 2DE differential display proteomic approach in combination with MS was employed. In this study, 25 differentially regulated protein functions were identified following the depletion of CAIX. Furthermore, five protein function were found to be differentially phosphorylated in CAIX depleted cells. Pathway analysis pointed to a role of CAIX in ER stress and the UPR.

Additional experiments demonstrated an involvement of CAIX in ER stress, the UPR and in cap-dependent translation. The functional studies also supported a role of CAIX in apoptosis. Evidence for further involvement of CAIX in translation, DNA control, metabolism and redox regulation could be retrieved from the proteomic results.

The effects of CAIX depletion on ER stress, UPR and cap-dependent translation were linked to severe hypoxia pointing to a role of the pH regulation of CAIX in these events. In contrast to this, the role of CAIX in apoptosis could be shown to be independent of the oxygenation state of the cell. For these results, the signaling function of CAIX was held responsible for the phenotype.

CAIX was thus identified as a prerequisite for the onset of UPR in response to ER stress. Furthermore, the present study suggests for the first time a link between CAIX, calpastatin and calpain in the regulation of apoptosis whereby CAIX expression was found to protect against apoptosis. Finally, this study revealed several new functional connections of CAIX suggesting a complex regulatory network, parts of which function under different oxygenation states. The results strengthen the influence and importance of CAIX in the cell and provide several new perspectives for future research.

Future analysis of the cytosolic concentrations of Ca^{++}, of calpain activity as well as rescue experiments with Ca^{++} chelators and calpain inhibitors would be required to further validate the suggested links and pathways and strengthen the influential role of CAIX in cancer. In addition, CAIX mutants containing only the catalytic site or the intracellular tail, respectively, should be created in order to analyse in detail the different functions of the CAIX protein. Thereby, a clear distinction between pH regulation and signalling function could be achieved. These, as well as other further research directions suggested by the results presented here, have great potential to further our understanding of the biology of cancer cells and to develop novel therapeutic approaches.

7 References

Abraham EG, Pinto SB, Ghosh A, Vanlandingham DL, Budd A, Higgs S, Kafatos FC, Jacobs-Lorena M, Michel K, 2005. An immune-responsive serpin, SRPN6, mediates mosquito defense against malaria parasites. Proc Natl Acad Sci U S A 102:16327-16332.

Aharonovitz O, Zaun HC, Balla T, York JD, Orlowski J, Grinstein S, 2000. Intracellular pH regulation by Na(+)/H(+) exchange requires phosphatidylinositol 4,5-bisphosphate. J Cell Biol 150:213-224.

Ahlskog JK, Dumelin CE, Trussel S, Marlind J, Neri D, 2009a. In vivo targeting of tumor-associated carbonic anhydrases using acetazolamide derivatives. Bioorg Med Chem Lett 19:4851-4856.

Ahlskog JK, Schliemann C, Marlind J, Qureshi U, Ammar A, Pedley RB, Neri D, 2009b. Human monoclonal antibodies targeting carbonic anhydrase IX for the molecular imaging of hypoxic regions in solid tumours. Br J Cancer 101:645-657.

Airley RE, Loncaster J, Raleigh JA, Harris AL, Davidson SE, Hunter RD, West CM, Stratford IJ, 2003. GLUT-1 and CAIX as intrinsic markers of hypoxia in carcinoma of the cervix: relationship to pimonidazole binding. Int J Cancer 104:85-91.

Alanen HI, Salo KE, Pirneskoski A, Ruddock LW, 2006. pH dependence of the peptide thiol-disulfide oxidase activity of six members of the human protein disulfide isomerase family. Antioxid Redox Signal 8:283-291.

Alterio V, Hilvo M, Di Fiore A, Supuran CT, Pan P, Parkkila S, Scaloni A, Pastorek J, Pastorekova S, Pedone C, Scozzafava A, Monti SM, De Simone G, 2009. Crystal structure of the catalytic domain of the tumor-associated human carbonic anhydrase IX. Proc Natl Acad Sci U S A 106:16233-16238.

Anelli T, Alessio M, Mezghrani A, Simmen T, Talamo F, Bachi A, Sitia R, 2002. ERp44, a novel endoplasmic reticulum folding assistant of the thioredoxin family. EMBO J 21:835-844.

Asahi H, Koshida K, Hori O, Ogawa S, Namiki M, 2002. Immunohistochemical detection of the 150-kDa oxygen-regulated protein in bladder cancer. BJU Int 90:462-466.

Bairoch A, Apweiler R, 2000. The SWISS-PROT protein sequence database and is supplemend TrEMBL in 2000. Nucleic Acids Res 28:45-48.

Barathova M, Takacova M, Holotnakova T, Gibadulinova A, Ohradanova A, Zatovicova M, Hulikova A, Kopacek J, Parkkila S, Supuran CT, Pastorekova S, Pastorek J, 2008. Alternative splicing variant of the hypoxia marker carbonic anhydrase IX expressed independently of hypoxia and tumour phenotype. Br J Cancer 98:129-136.

Barth S, Nesper J, Hasgall PA, Wirthner R, Nytko KJ, Edlich F, Katschinski DM, Stiehl DP, Wenger RH, Camenisch G, 2007. The peptidyl prolyl cis/trans isomerase FKBP38 determines hypoxia-inducible transcription factor prolyl-4-hydroxylase PHD2 protein stability. Mol Cell Biol 27:3758-3768.

Bateman A, Birney E, Cerruti L, Durbin R, Etwiller L, Eddy SR, Griffiths-Jones S, Howe KL, Marshall M, Sonnhammer EL, 2002. The Pfam protein families database. Nucleic Acids Res 30:276-280.

Bates D, Maechler M, Bolker BM, Walker S, 2014. lme4: Linear mixed-effects models using Eigen and S4. ArXiv e-print submitteed to Journal of Statistical Software, http://arxivorg/abs/14065823.

Bedard K, Szabo E, Michalak M, Opas M, 2005. Cellular functions of endoplasmic reticulum chaperones calreticulin, calnexin, and ERp57. Int Rev Cytol 245:91-121.

Benjamini Y, Hochberg Y, 1995. Controlling the false discovery rate: a practical and powerful approach to multiple testing. Journal of the Royal Statistical Society Series B 57:289-300.

Berggren M, Gallegos A, Gasdaska JR, Gasdaska PY, Warneke J, Powis G, 1996. Thioredoxin and thioredoxin reductase gene expression in human tumors and cell lines, and the effects of serum stimulation and hypoxia. Anticancer Res 16:3459-3466.

Berman HM, Westbrook J, Feng Z, Gilliland G, Bhat TN, Weissig H, Shindyalov IN, Bourne PE, 2000. The Protein Data Bank. Nucleic Acids Res 28:235-242.

Berndt C, Lillig CH, Holmgren A, 2008. Thioredoxins and glutaredoxins as facilitators of protein folding. Biochim Biophys Acta 1783:641-650.

Blomgren K, Hallin U, Andersson AL, Puka-Sundvall M, Bahr BA, McRae A, Saido TC, Kawashima S, Hagberg H, 1999. Calpastatin is up-regulated in response to hypoxia and is a suicide substrate to calpain after neonatal cerebral hypoxia-ischemia. J Biol Chem 274:14046-14052.

Blumkin L, Halevy A, Ben-Ami-Raichman D, Dahari D, Haviv A, Sarit C, Lev D, van der Knaap MS, Lerman-Sagie T, Leshinsky-Silver E, 2014. Expansion of the spectrum of TUBB4A-related disorders: a new phenotype associated with a novel mutation in the TUBB4A gene. Neurogenetics 15:107-113.

Booth C, Koch GL, 1989. Perturbation of cellular calcium induces secretion of luminal ER proteins. Cell 59:729-737.

Brasaemle DL, Wolins NE, 2012. Packaging of fat: an evolving model of lipid droplet assembly and expansion. J Biol Chem 287:2273-2279.

Breton S, 2001. The cellular physiology of carbonic anhydrases. JOP 2:159-164.

Bretz F, Hothorn T, Westfall P, 2010. Multiple Comparisons using R. CRC Press, Boca Raton.

Britton S, Froment C, Frit P, Monsarrat B, Salles B, Calsou P, 2009. Cell nonhomologous end joining capacity controls SAF-A phosphorylation by DNA-PK in response to DNA double-strand breaks inducers. Cell Cycle 8:3717-3722.

Broker LE, Huisman C, Span SW, Rodriguez JA, Kruyt FA, Giaccone G, 2004. Cathepsin B mediates caspase-independent cell death induced by microtubule stabilizing agents in non-small cell lung cancer cells. Cancer Res 64:27-30.

Brown PD, Davies SL, Speake T, Millar ID, 2004. Molecular mechanisms of cerebrospinal fluid production. Neuroscience 129:957-970.

Budihardjo I, Oliver H, Lutter M, Luo X, Wang X, 1999. Biochemical pathways of caspase activation during apoptosis. Annu Rev Cell Dev Biol 15:269-290.

Buller F, Steiner M, Frey K, Mircsof D, Scheuermann J, Kalisch M, Buhlmann P, Supuran CT, Neri D, 2011. Selection of Carbonic Anhydrase IX Inhibitors from One Million DNA-Encoded Compounds. ACS Chem Biol 6:336-344.

Cao SS, Kaufman RJ, 2012. Unfolded protein response. Curr Biol 22:R622-626.

Cappello F, Conway de Macario E, Marasa L, Zummo G, Macario AJ, 2008. Hsp60 expression, new locations, functions and perspectives for cancer diagnosis and therapy. Cancer Biol Ther 7:801-809.

Cardone RA, Casavola V, Reshkin SJ, 2005. The role of disturbed pH dynamics and the Na+/H+ exchanger in metastasis. Nat Rev Cancer 5:786-795.

Carlin KR, Huff-Lonergan E, Rowe LJ, Lonergan SM, 2006. Effect of oxidation, pH, and ionic strength on calpastatin inhibition of mu- and m-calpain. J Anim Sci 84:925-937.

Casey JR, Grinstein S, Orlowski J, 2010. Sensors and regulators of intracellular pH. Nat Rev Mol Cell Biol 11:50-61.

Cechowska-Pasko M, Bankowski E, Chene P, 2006. The effect of hypoxia on the expression of 150 kDa oxygen-regulated protein (ORP 150) in HeLa cells. Cell Physiol Biochem 17:89-96.

Chakravarthi S, Jessop CE, Bulleid NJ, 2006. The role of glutathione in disulphide bond formation and endoplasmic-reticulum-generated oxidative stress. EMBO Rep 7:271-275.

Chang Y, Wu Y, Liu W, Ji G, 2015. Knockdown of ERp44 leads to apoptosis via activation of ER stress in HeLa cells. Biochem Biophys Res Commun 463:606-611.

Chauvin C, Salhi S, Le Goff C, Viranaicken W, Diop D, Jean-Jean O, 2005. Involvement of human release factors eRF3a and eRF3b in translation termination and regulation of the termination complex formation. Mol Cell Biol 25:5801-5811.

Chegwidden WR, Carter ND, 2000. Introduction to the carbonic anhydrases. EXS:14-28.

Chen JS, Wang Q, Fu XH, Huang XH, Chen XL, Cao LQ, Chen LZ, Tan HX, Li W, Bi J, Zhang LJ, 2009a. Involvement of PI3K/PTEN/AKT/mTOR pathway in invasion and metastasis in hepatocellular carcinoma: Association with MMP-9. Hepatol Res 39:177-186.

Chen P, Lu Y, Harrington PB, 2008. Biomarker profiling and reproducibility study of MALDI-MS measurements of Escherichia coli by analysis of variance-principal component analysis. Anal Chem 80:1474-1481.

Chen YC, Chen YW, Hsu HS, Tseng LM, Huang PI, Lu KH, Chen DT, Tai LK, Yung MC, Chang SC, Ku HH, Chiou SH, Lo WL, 2009b. Aldehyde dehydrogenase 1 is a putative marker for cancer stem cells in head and neck squamous cancer. Biochem Biophys Res Commun 385:307-313.

Chia SK, Wykoff CC, Watson PH, Han C, Leek RD, Pastorek J, Gatter KC, Ratcliffe P, Harris AL, 2001. Prognostic significance of a novel hypoxia-regulated marker, carbonic anhydrase IX, in invasive breast carcinoma. J Clin Oncol 19:3660-3668.

Chiche J, Ilc K, Laferriere J, Trottier E, Dayan F, Mazure NM, Brahimi-Horn MC, Pouyssegur J, 2009. Hypoxia-inducible carbonic anhydrase IX and XII promote tumor cell growth by counteracting acidosis through the regulation of the intracellular pH. Cancer Res 69:358-368.

Cho M, Uemura H, Kim SC, Kawada Y, Yoshida K, Hirao Y, Konishi N, Saga S, Yoshikawa K, 2001. Hypomethylation of the MN/CA9 promoter and upregulated MN/CA9 expression in human renal cell carcinoma. Br J Cancer 85:563-567.

Chrastina A, 2003. High cell density-mediated pericellular hypoxia is a crucial factor inducing expression of the intrinsic hypoxia marker CA IX in vitro in HeLa cells. Neoplasma 50:251-256.

Chrastina A, Zavada J, Parkkila S, Kaluz S, Kaluzova M, Rajcani J, Pastorek J, Pastorekova S, 2003. Biodistribution and pharmacokinetics of 125I-labeled monoclonal antibody M75 specific for carbonic anhydrase IX, an intrinsic marker of hypoxia, in nude mice xenografted with human colorectal carcinoma. Int J Cancer 105:873-881.

Christianson JC, Shaler TA, Tyler RE, Kopito RR, 2008. OS-9 and GRP94 deliver mutant alpha1-antitrypsin to the Hrd1-SEL1L ubiquitin ligase complex for ERAD. Nat Cell Biol 10:272-282.

Cianchi F, Vinci MC, Supuran CT, Peruzzi B, De Giuli P, Fasolis G, Perigli G, Pastorekova S, Papucci L, Pini A, Masini E, Puccetti L, 2010. Selective inhibition of carbonic anhydrase IX decreases cell proliferation and induces ceramide-mediated apoptosis in human cancer cells. J Pharmacol Exp Ther 334:710-719.

Cohen P, 2000. The regulation of protein function by multisite phosphorylation--a 25 year update. Trends Biochem Sci 25:596-601.

Cuvier C, Jang A, Hill RP, 1997. Exposure to hypoxia, glucose starvation and acidosis: effect on invasive capacity of murine tumor cells and correlation with cathepsin (L + B) secretion. Clin Exp Metastasis 15:19-25.

Dayan F, Roux D, Brahimi-Horn MC, Pouyssegur J, Mazure NM, 2006. The oxygen sensor factor-inhibiting hypoxia-inducible factor-1 controls expression of distinct genes through the bifunctional transcriptional character of hypoxia-inducible factor-1alpha. Cancer Res 66:3688-3698.

Deitmer JW, Becker HM, 2013. Transport metabolons with carbonic anhydrases. Front Physiol 4:291.

Dihazi H, Dihazi GH, Bibi A, Eltoweissy M, Mueller CA, Asif AR, Rubel D, Vasko R, Mueller GA, 2013. Secretion of ERP57 is important for extracellular matrix accumulation and progression of renal fibrosis, and is an early sign of disease onset. J Cell Sci 126:3649-3663.

Ditte P, Dequiedt F, Svastova E, Hulikova A, Ohradanova-Repic A, Zatovicova M, Csaderova L, Kopacek J, Supuran CT, Pastorekova S, Pastorek J, 2011. Phosphorylation of carbonic

anhydrase IX controls its ability to mediate extracellular acidification in hypoxic tumors. Cancer Res 71:7558-7567.

Ditte Z, Ditte P, Labudova M, Simko V, Iuliano F, Zatovicova M, Csaderova L, Pastorekova S, Pastorek J, 2014. Carnosine inhibits carbonic anhydrase IX-mediated extracellular acidosis and suppresses growth of HeLa tumor xenografts. BMC Cancer 14:358.

Dong D, Ni M, Li J, Xiong S, Ye W, Virrey JJ, Mao C, Ye R, Wang M, Pen L, Dubeau L, Groshen S, Hofman FM, Lee AS, 2008. Critical role of the stress chaperone GRP78/BiP in tumor proliferation, survival, and tumor angiogenesis in transgene-induced mammary tumor development. Cancer Res 68:498-505.

Dorai T, Sawczuk IS, Pastorek J, Wiernik PH, Dutcher JP, 2005. The role of carbonic anhydrase IX overexpression in kidney cancer. Eur J Cancer 41:2935-2947.

Dorrello NV, Peschiaroli A, Guardavaccaro D, Colburn NH, Sherman NE, Pagano M, 2006. S6K1- and betaTRCP-mediated degradation of PDCD4 promotes protein translation and cell growth. Science 314:467-471.

Dubois L, Lieuwes NG, Maresca A, Thiry A, Supuran CT, Scozzafava A, Wouters BG, Lambin P, 2009. Imaging of CA IX with fluorescent labelled sulfonamides distinguishes hypoxic and (re)-oxygenated cells in a xenograft tumour model. Radiother Oncol 92:423-428.

Dubois L, Peeters S, Lieuwes NG, Geusens N, Thiry A, Wigfield S, Carta F, McIntyre A, Scozzafava A, Dogne JM, Supuran CT, Harris AL, Masereel B, Lambin P, 2011. Specific inhibition of carbonic anhydrase IX activity enhances the in vivo therapeutic effect of tumor irradiation. Radiother Oncol 99:424-431.

Duivenvoorden WC, Paschos A, Hopmans SN, Austin RC, Pinthus JH, 2014. Endoplasmic reticulum protein ERp46 in renal cell carcinoma. PLoS One 9:e90389.

Ellgaard L, Helenius A, 2003. Quality control in the endoplasmic reticulum. Nat Rev Mol Cell Biol 4:181-191.

Fan B, Gu JQ, Yan R, Zhang H, Feng J, Ikuyama S, 2013. High glucose, insulin and free fatty acid concentrations synergistically enhance perilipin 3 expression and lipid accumulation in macrophages. Metabolism 62:1168-1179.

Fels DR, Koumenis C, 2006. The PERK/eIF2alpha/ATF4 module of the UPR in hypoxia resistance and tumor growth. Cancer Biol Ther 5:723-728.

Fiaschi T, Giannoni E, Taddei ML, Cirri P, Marini A, Pintus G, Nativi C, Richichi B, Scozzafava A, Carta F, Torre E, Supuran CT, Chiarugi P, 2012. Carbonic anhydrase IX from cancer-associated fibroblasts drives epithelial-mesenchymal transition in prostate carcinoma cells. Cell Cycle 12:1791-1801.

Fink AL, 1999. Chaperone-mediated protein folding. Physiol Rev 79:425-449.

Fleming RE, Parkkila S, Parkkila AK, Rajaniemi H, Waheed A, Sly WS, 1995. Carbonic anhydrase IV expression in rat and human gastrointestinal tract regional, cellular, and subcellular localization. J Clin Invest 96:2907-2913.

Fox J, 2006. effects: Effect displays for linear and generalized linear models. P package version 21-0.

Frankel LB, Christoffersen NR, Jacobsen A, Lindow M, Krogh A, Lund AH, 2008. Programmed cell death 4 (PDCD4) is an important functional target of the microRNA miR-21 in breast cancer cells. J Biol Chem 283:1026-1033.

Frey S, Leskovar A, Reinstein J, Buchner J, 2007. The ATPase cycle of the endoplasmic chaperone Grp94. J Biol Chem 282:35612-35620.

Gafni J, Cong X, Chen SF, Gibson BW, Ellerby LM, 2009. Calpain-1 cleaves and activates caspase-7. J Biol Chem 284:25441-25449.

Gardner BM, Pincus D, Gotthardt K, Gallagher CM, Walter P, 2013. Endoplasmic reticulum stress sensing in the unfolded protein response. Cold Spring Harb Perspect Biol 5:a013169.

Gatenby RA, Gillies RJ, 2004. Why do cancers have high aerobic glycolysis? Nat Rev Cancer 4:891-899.

Gettins PG, 2002. Serpin structure, mechanism, and function. Chem Rev 102:4751-4804.

Giatromanolaki A, Koukourakis MI, Sivridis E, Pastorek J, Wykoff CC, Gatter KC, Harris AL, 2001. Expression of hypoxia-inducible carbonic anhydrase-9 relates to angiogenic pathways and independently to poor outcome in non-small cell lung cancer. Cancer Res 61:7992-7998.

Gilles C, Polette M, Mestdagt M, Nawrocki-Raby B, Ruggeri P, Birembaut P, Foidart JM, 2003. Transactivation of vimentin by beta-catenin in human breast cancer cells. Cancer Res 63:2658-2664.

Gilmour KM, 2010. Perspectives on carbonic anhydrase. Comp Biochem Physiol A Mol Integr Physiol 157:193-197.

Goke A, Goke R, Knolle A, Trusheim H, Schmidt H, Wilmen A, Carmody R, Goke B, Chen YH, 2002. DUG is a novel homologue of translation initiation factor 4G that binds eIF4A. Biochem Biophys Res Commun 297:78-82.

Gorlach A, Diebold I, Schini-Kerth VB, Berchner-Pfannschmidt U, Roth U, Brandes RP, Kietzmann T, Busse R, 2001. Thrombin activates the hypoxia-inducible factor-1 signaling pathway in vascular smooth muscle cells: Role of the p22(phox)-containing NADPH oxidase. Circ Res 89:47-54.

Gorlach A, Kietzmann T, 2007. Superoxide and derived reactive oxygen species in the regulation of hypoxia-inducible factors. Methods Enzymol 435:421-446.

Gorlach A, Klappa P, Kietzmann T, 2006. The endoplasmic reticulum: folding, calcium homeostasis, signaling, and redox control. Antioxid Redox Signal 8:1391-1418.

Goto H, Tanabe K, Manser E, Lim L, Yasui Y, Inagaki M, 2002. Phosphorylation and reorganization of vimentin by p21-activated kinase (PAK). Genes Cells 7:91-97.

Grabmaier K, MC AdW, Verhaegh GW, Schalken JA, Oosterwijk E, 2004. Strict regulation of CAIX(G250/MN) by HIF-1alpha in clear cell renal cell carcinoma. Oncogene 23:5624-5631.

Gu JQ, Wang DF, Yan XG, Zhong WL, Zhang J, Fan B, Ikuyama S, 2010. A Toll-like receptor 9-mediated pathway stimulates perilipin 3 (TIP47) expression and induces lipid accumulation in macrophages. Am J Physiol Endocrinol Metab 299:E593-600.

Gupta S, Knowlton AA, 2002. Cytosolic heat shock protein 60, hypoxia, and apoptosis. Circulation 106:2727-2733.

Gupta SC, Singh R, Pochampally R, Watabe K, Mo YY, 2014. Acidosis promotes invasiveness of breast cancer cells through ROS-AKT-NF-kappaB pathway. Oncotarget 5:12070-12082.

Guy NC, Garcia YA, Sivils JC, Galigniana MD, Cox MB, 2015. Functions of the Hsp90-Binding FKBP Immunophilins. Subcell Biochem 78:35-68.

Haas IG, Wabl M, 1983. Immunoglobulin heavy chain binding protein. Nature 306:387-389.

Haley B, Paunesku T, Protic M, Woloschak GE, 2009. Response of heterogeneous ribonuclear proteins (hnRNP) to ionising radiation and their involvement in DNA damage repair. Int J Radiat Biol 85:643-655.

Hanna RA, Campbell RL, Davies PL, 2008. Calcium-bound structure of calpain and its mechanism of inhibition by calpastatin. Nature 456:409-412.

Harrell CS, Rowson SA, Neigh GN, 2015. Pharmacological stimulation of hypoxia inducible factor-1alpha facilitates the corticosterone response to a mild acute stressor. Neurosci Lett 600:75-79.

Haunhorst P, Hanschmann EM, Brautigam L, Stehling O, Hoffmann B, Muhlenhoff U, Lill R, Berndt C, Lillig CH, 2013. Crucial function of vertebrate glutaredoxin 3 (PICOT) in iron homeostasis and hemoglobin maturation. Mol Biol Cell 24:1895-1903.

Hay N, 2005. The Akt-mTOR tango and its relevance to cancer. Cancer Cell 8:179-183.

Helmlinger G, Sckell A, Dellian M, Forbes NS, Jain RK, 2002. Acid production in glycolysis-impaired tumors provides new insights into tumor metabolism. Clin Cancer Res 8:1284-1291.

Henrion MY, Purdue MP, Scelo G, Broderick P, Frampton M, Ritchie A, Meade A, Li P, McKay J, Johansson M, Lathrop M, Larkin J, Rothman N, Wang Z, Chow WH, Stevens VL, Diver WR, Albanes D, Virtamo J, Brennan P, Eisen T, Chanock S, Houlston RS, 2015. Common

variation at 1q24.1 (ALDH9A1) is a potential risk factor for renal cancer. PLoS One 10:e0122589.

High S, Lecomte FJ, Russell SJ, Abell BM, Oliver JD, 2000. Glycoprotein folding in the endoplasmic reticulum: a tale of three chaperones? FEBS Lett 476:38-41.

Hilvo M, Baranauskiene L, Salzano AM, Scaloni A, Matulis D, Innocenti A, Scozzafava A, Monti SM, Di Fiore A, De Simone G, Lindfors M, Janis J, Valjakka J, Pastorekova S, Pastorek J, Kulomaa MS, Nordlund HR, Supuran CT, Parkkila S, 2008. Biochemical characterization of CA IX, one of the most active carbonic anhydrase isozymes. J Biol Chem 283:27799-27809.

Hocking LJ, Lucas GJ, Daroszewska A, Mangion J, Olavesen M, Cundy T, Nicholson GC, Ward L, Bennett ST, Wuyts W, Van Hul W, Ralston SH, 2002. Domain-specific mutations in sequestosome 1 (SQSTM1) cause familial and sporadic Paget's disease. Hum Mol Genet 11:2735-2739.

Holcik M, Sonenberg N, 2005. Translational control in stress and apoptosis. Nat Rev Mol Cell Biol 6:318-327.

Holmgren A, Johansson C, Berndt C, Lonn ME, Hudemann C, Lillig CH, 2005. Thiol redox control via thioredoxin and glutaredoxin systems. Biochem Soc Trans 33:1375-1377.

Hothorn T, 2011. Multcomp. R package version 2011.

Hulikova A, Vaughan-Jones RD, Swietach P, 2011. Dual role of CO2/HCO3(-) buffer in the regulation of intracellular pH of three-dimensional tumor growths. J Biol Chem 286:13815-13826.

Ilie M, Hofman V, Zangari J, Chiche J, Mouroux J, Mazure NM, Pouyssegur J, Brest P, Hofman P, 2013. Response of CAIX and CAXII to in vitro re-oxygenation and clinical significance of the combined expression in NSCLC patients. Lung Cancer 82:16-23.

Innocenti A, Pastorekova S, Pastorek J, Scozzafava A, De Simone G, Supuran CT, 2009. The proteoglycan region of the tumor-associated carbonic anhydrase isoform IX acts as anintrinsic buffer optimizing CO2 hydration at acidic pH values characteristic of solid tumors. Bioorg Med Chem Lett 19:5825-5828.

Ivaska J, Pallari HM, Nevo J, Eriksson JE, 2007. Novel functions of vimentin in cell adhesion, migration, and signaling. Exp Cell Res 313:2050-2062.

Izumi H, Torigoe T, Ishiguchi H, Uramoto H, Yoshida Y, Tanabe M, Ise T, Murakami T, Yoshida T, Nomoto M, Kohno K, 2003. Cellular pH regulators: potentially promising molecular targets for cancer chemotherapy. Cancer Treat Rev 29:541-549.

Jackson B, Brocker C, Thompson DC, Black W, Vasiliou K, Nebert DW, Vasiliou V, 2011. Update on the aldehyde dehydrogenase gene (ALDH) superfamily. Hum Genomics 5:283-303.

Jessop CE, Chakravarthi S, Garbi N, Hammerling GJ, Lovell S, Bulleid NJ, 2007. ERp57 is essential for efficient folding of glycoproteins sharing common structural domains. EMBO J 26:28-40.

Kalluri R, Weinberg RA, 2009. The basics of epithelial-mesenchymal transition. J Clin Invest 119:1420-1428.

Kaluz S, Kaluzova M, Chrastina A, Olive PL, Pastorekova S, Pastorek J, Lerman MI, Stanbridge EJ, 2002. Lowered oxygen tension induces expression of the hypoxia marker MN/carbonic anhydrase IX in the absence of hypoxia-inducible factor 1 alpha stabilization: a role for phosphatidylinositol 3'-kinase. Cancer Res 62:4469-4477.

Kaluz S, Kaluzova M, Liao SY, Lerman M, Stanbridge EJ, 2009. Transcriptional control of the tumor- and hypoxia-marker carbonic anhydrase 9: A one transcription factor (HIF-1) show? Biochim Biophys Acta 1795:162-172.

Kaluz S, Kaluzova M, Stanbridge EJ, 2003. Expression of the hypoxia marker carbonic anhydrase IX is critically dependent on SP1 activity. Identification of a novel type of hypoxia-responsive enhancer. Cancer Res 63:917-922.

Kaluzova M, Kaluz S, Lerman MI, Stanbridge EJ, 2004. DNA damage is a prerequisite for p53-mediated proteasomal degradation of HIF-1alpha in hypoxic cells and downregulation of the hypoxia marker carbonic anhydrase IX. Mol Cell Biol 24:5757-5766.

Kang MJ, Ahn HS, Lee JY, Matsuhashi S, Park WY, 2002. Up-regulation of PDCD4 in senescent human diploid fibroblasts. Biochem Biophys Res Commun 293:617-621.

Kendall TL, Koohmaraie M, Arbona JR, Williams SE, Young LL, 1993. Effect of pH and ionic strength on bovine m-calpain and calpastatin activity. J Anim Sci 71:96-104.

Khatri P, Sirota M, Butte AJ, 2012. Ten years of pathway analysis: current approaches and outstanding challenges. PLoS Comput Biol 8:e1002375.

Kim BR, Shin HJ, Kim JY, Byun HJ, Lee JH, Sung YK, Rho SB, 2012. Dickkopf-1 (DKK-1) interrupts FAK/PI3K/mTOR pathway by interaction of carbonic anhydrase IX (CA9) in tumorigenesis. Cell Signal 24:1406-1413.

Kim JW, Dang CV, 2006. Cancer's molecular sweet tooth and the Warburg effect. Cancer Res 66:8927-8930.

Kim KW, Moretti L, Mitchell LR, Jung DK, Lu B, 2010. Endoplasmic reticulum stress mediates radiation-induced autophagy by perk-eIF2alpha in caspase-3/7-deficient cells. Oncogene 29:3241-3251.

Kimata Y, Kohno K, 2011. Endoplasmic reticulum stress-sensing mechanisms in yeast and mammalian cells. Curr Opin Cell Biol 23:135-142.

Kimura H, Braun RD, Ong ET, Hsu R, Secomb TW, Papahadjopoulos D, Hong K, Dewhirst MW, 1996. Fluctuations in red cell flux in tumor microvessels can lead to transient hypoxia and reoxygenation in tumor parenchyma. Cancer Res 56:5522-5528.

Kivela J, Parkkila S, Parkkila AK, Leinonen J, Rajaniemi H, 1999. Salivary carbonic anhydrase isoenzyme VI. J Physiol 520 Pt 2:315-320.

Kleizen B, Braakman I, 2004. Protein folding and quality control in the endoplasmic reticulum. Curr Opin Cell Biol 16:343-349.

Kokkinos MI, Wafai R, Wong MK, Newgreen DF, Thompson EW, Waltham M, 2007. Vimentin and epithelial-mesenchymal transition in human breast cancer--observations in vitro and in vivo. Cells Tissues Organs 185:191-203.

Koong AC, Chen EY, Lee AS, Brown JM, Giaccia AJ, 1994. Increased cytotoxicity of chronic hypoxic cells by molecular inhibition of GRP78 induction. Int J Radiat Oncol Biol Phys 28:661-666.

Koritzinsky M, Rouschop KM, van den Beucken T, Magagnin MG, Savelkouls K, Lambin P, Wouters BG, 2007. Phosphorylation of eIF2alpha is required for mRNA translation inhibition and survival during moderate hypoxia. Radiother Oncol 83:353-361.

Korsching E, Packeisen J, Liedtke C, Hungermann D, Wulfing P, van Diest PJ, Brandt B, Boecker W, Buerger H, 2005. The origin of vimentin expression in invasive breast cancer: epithelial-mesenchymal transition, myoepithelial histogenesis or histogenesis from progenitor cells with bilinear differentiation potential? J Pathol 206:451-457.

Koukourakis MI, Giatromanolaki A, Sivridis E, Simopoulos K, Pastorek J, Wykoff CC, Gatter KC, Harris AL, 2001. Hypoxia-regulated carbonic anhydrase-9 (CA9) relates to poor vascularization and resistance of squamous cell head and neck cancer to chemoradiotherapy. Clin Cancer Res 7:3399-3403.

Koumenis C, Wouters BG, 2006. "Translating" tumor hypoxia: unfolded protein response (UPR)-dependent and UPR-independent pathways. Mol Cancer Res 4:423-436.

Kozutsumi Y, Segal M, Normington K, Gething MJ, Sambrook J, 1988. The presence of malfolded proteins in the endoplasmic reticulum signals the induction of glucose-regulated proteins. Nature 332:462-464.

Kubota H, Hynes G, Willison K, 1995. The chaperonin containing t-complex polypeptide 1 (TCP-1). Multisubunit machinery assisting in protein folding and assembly in the eukaryotic cytosol. Eur J Biochem 230:3-16.

Kubota H, Suzuki T, Lu J, Takahashi S, Sugita K, Sekiya S, Suzuki N, 2005. Increased expression of GRP94 protein is associated with decreased sensitivity to X-rays in cervical cancer cell lines. Int J Radiat Biol 81:701-709.

Kukalev A, Nord Y, Palmberg C, Bergman T, Percipalle P, 2005. Actin and hnRNP U cooperate for productive transcription by RNA polymerase II. Nat Struct Mol Biol 12:238-244.

Kuramitsu Y, Nakamura K, 2006. Proteomic analysis of cancer tissues: shedding light on carcinogenesis and possible biomarkers. Proteomics 6:5650-5661.

Kusaczuk M, Cechowska-Pasko M, 2013. Molecular chaperone ORP150 in ER stress-related diseases. Curr Pharm Des 19:2807-2818.

Lahat G, Zhu QS, Huang KL, Wang S, Bolshakov S, Liu J, Torres K, Langley RR, Lazar AJ, Hung MC, Lev D, 2010. Vimentin is a novel anti-cancer therapeutic target; insights from in vitro and in vivo mice xenograft studies. PLoS One 5:e10105.

Lakhani SA, Masud A, Kuida K, Porter GA, Jr., Booth CJ, Mehal WZ, Inayat I, Flavell RA, 2006. Caspases 3 and 7: key mediators of mitochondrial events of apoptosis. Science 311:847-851.

Lamanda A, Cheaib Z, Turgut MD, Lussi A, 2007. Protein buffering in model systems and in whole human saliva. PLoS One 2:e263.

Lancashire L, Schmid O, Shah H, Ball G, 2005. Classification of bacterial species from proteomic data using combinatorial approaches incorporating artificial neural networks, cluster analysis and principal components analysis. Bioinformatics 21:2191-2199.

Lankat-Buttgereit B, Goke R, 2009. The tumour suppressor Pdcd4: recent advances in the elucidation of function and regulation. Biol Cell 101:309-317.

Lankat-Buttgereit B, Gregel C, Knolle A, Hasilik A, Arnold R, Goke R, 2004. Pdcd4 inhibits growth of tumor cells by suppression of carbonic anhydrase type II. Mol Cell Endocrinol 214:149-153.

Law RH, Zhang Q, McGowan S, Buckle AM, Silverman GA, Wong W, Rosado CJ, Langendorf CG, Pike RN, Bird PI, Whisstock JC, 2006. An overview of the serpin superfamily. Genome Biol 7:216.

Li J, Lee AS, 2006. Stress induction of GRP78/BiP and its role in cancer. Curr Mol Med 6:45-54.

Li J, Ning Y, Hedley W, Saunders B, Chen Y, Tindill N, Hannay T, Subramaniam S, 2002. The Molecule Pages database. Nature 420:716-717.

Li QF, Spinelli AM, Wang R, Anfinogenova Y, Singer HA, Tang DD, 2006. Critical role of vimentin phosphorylation at Ser-56 by p21-activated kinase in vimentin cytoskeleton signaling. J Biol Chem 281:34716-34724.

Li XC, Schimenti JC, 2007. Mouse pachytene checkpoint 2 (trip13) is required for completing meiotic recombination but not synapsis. PLoS Genet 3:e130.

Li Y, Camacho P, 2004. Ca2+-dependent redox modulation of SERCA 2b by ERp57. J Cell Biol 164:35-46.

Li Y, Wang H, Tu C, Shiverick KT, Silverman DN, Frost SC, 2011. Role of hypoxia and EGF on expression, activity, localization and phosphorylation of carbonic anhydrase IX in MDA-MB-231 breast cancer cells. Biochim Biophys Acta 1813:159-167.

Lillig CH, Berndt C, Holmgren A, 2008. Glutaredoxin systems. Biochim Biophys Acta 1780:1304-1317.

Lin Y, Wang Z, Liu L, Chen L, 2011. Akt is the downstream target of GRP78 in mediating cisplatin resistance in ER stress-tolerant human lung cancer cells. Lung Cancer 71:291-297.

Lohmann K, Klein C, 2014. The many faces of TUBB4A mutations. Neurogenetics 15:81-82.

Loncaster JA, Harris AL, Davidson SE, Logue JP, Hunter RD, Wycoff CC, Pastorek J, Ratcliffe PJ, Stratford IJ, West CM, 2001. Carbonic anhydrase (CA IX) expression, a potential new intrinsic marker of hypoxia: correlations with tumor oxygen measurements and prognosis in locally advanced carcinoma of the cervix. Cancer Res 61:6394-6399.

Lou Y, McDonald PC, Oloumi A, Chia S, Ostlund C, Ahmadi A, Kyle A, Auf dem Keller U, Leung S, Huntsman D, Clarke B, Sutherland BW, Waterhouse D, Bally M, Roskelley C, Overall CM, Minchinton A, Pacchiano F, Carta F, Scozzafava A, Touisni N, Winum JY, Supuran CT, Dedhar S, 2011. Targeting tumor hypoxia: suppression of breast tumor growth and metastasis by novel carbonic anhydrase IX inhibitors. Cancer Res 71:3364-3376.

Macer DR, Koch GL, 1988. Identification of a set of calcium-binding proteins in reticuloplasm, the luminal content of the endoplasmic reticulum. J Cell Sci 91 (Pt 1):61-70.

Maddock KR, Huff-Lonergan E, Rowe LJ, Lonergan SM, 2005. Effect of pH and ionic strength on mu- and m-calpain inhibition by calpastatin. J Anim Sci 83:1370-1376.

Magagnin MG, van den Beucken T, Sergeant K, Lambin P, Koritzinsky M, Devreese B, Wouters BG, 2008. The mTOR target 4E-BP1 contributes to differential protein expression during normoxia and hypoxia through changes in mRNA translation efficiency. Proteomics 8:1019-1028.

Majumdar M, Meenakshi J, Goswami SK, Datta K, 2002. Hyaluronan binding protein 1 (HABP1)/C1QBP/p32 is an endogenous substrate for MAP kinase and is translocated to the nucleus upon mitogenic stimulation. Biochem Biophys Res Commun 291:829-837.

Mamane Y, Petroulakis E, LeBacquer O, Sonenberg N, 2006. mTOR, translation initiation and cancer. Oncogene 25:6416-6422.

Maren TH, 1967. Carbonic anhydrase: chemistry, physiology, and inhibition. Physiol Rev 47:595-781.

Maresca A, Temperini C, Vu H, Pham NB, Poulsen SA, Scozzafava A, Quinn RJ, Supuran CT, 2009. Non-zinc mediated inhibition of carbonic anhydrases: coumarins are a new class of suicide inhibitors. J Am Chem Soc 131:3057-3062.

Marina AD, Schara U, Pyle A, Moller-Hartmann C, Holinski-Feder E, Abicht A, Czermin B, Lochmuller H, Griffin H, Santibanez-Koref M, Chinnery PF, Horvath R, 2013. NDUFS8-related Complex I Deficiency Extends Phenotype from "PEO Plus" to Leigh Syndrome. JIMD Rep 10:17-22.

Martelli AM, Evangelisti C, Chiarini F, McCubrey JA, 2010. The phosphatidylinositol 3-kinase/Akt/mTOR signaling network as a therapeutic target in acute myelogenous leukemia patients. Oncotarget 1:89-103.

Masson N, Appelhoff RJ, Tuckerman JR, Tian YM, Demol H, Puype M, Vandekerckhove J, Ratcliffe PJ, Pugh CW, 2004. The HIF prolyl hydroxylase PHD3 is a potential substrate of the TRiC chaperonin. FEBS Lett 570:166-170.

Mathiasen IS, Jaattela M, 2002. Triggering caspase-independent cell death to combat cancer. Trends Mol Med 8:212-220.

Matsumoto G, Wada K, Okuno M, Kurosawa M, Nukina N, 2011. Serine 403 phosphorylation of p62/SQSTM1 regulates selective autophagic clearance of ubiquitinated proteins. Mol Cell 44:279-289.

Matsumoto S, Yasui H, Mitchell JB, Krishna MC, 2010. Imaging cycling tumor hypoxia. Cancer Res 70:10019-10023.

Matsuyama S, Reed JC, 2000. Mitochondria-dependent apoptosis and cellular pH regulation. Cell Death Differ 7:1155-1165.

McDonough PM, Maciejewski-Lenoir D, Hartig SM, Hanna RA, Whittaker R, Heisel A, Nicoll JB, Buehrer BM, Christensen K, Mancini MG, Mancini MA, Edwards DP, Price JH, 2013. Differential phosphorylation of perilipin 1A at the initiation of lipolysis revealed by novel monoclonal antibodies and high content analysis. PLoS One 8:e55511.

McGee AM, Douglas DL, Liang Y, Hyder SM, Baines CP, 2011. The mitochondrial protein C1qbp promotes cell proliferation, migration and resistance to cell death. Cell Cycle 10:4119-4127.

McIntyre A, Patiar S, Wigfield S, Li JL, Ledaki I, Turley H, Leek R, Snell C, Gatter K, Sly WS, Vaughan-Jones RD, Swietach P, Harris AL, 2012. Carbonic anhydrase IX promotes tumor growth and necrosis in vivo and inhibition enhances anti-VEGF therapy. Clin Cancer Res 18:3100-3111.

McKenna R, Supuran CT, 2014. Carbonic anhydrase inhibitors drug design. Subcell Biochem 75:291-323.

Meijer TW, Bussink J, Zatovicova M, Span PN, Lok J, Supuran CT, Kaanders JH, 2014. Tumor microenvironmental changes induced by the sulfamate carbonic anhydrase IX inhibitor S4 in a laryngeal tumor model. PLoS One 9:e108068.

Mellergard P, Ouyang YB, Siesjo BK, 1994. The regulation of intracellular pH is strongly dependent on extracellular pH in cultured rat astrocytes and neurons. Acta Neurochir Suppl (Wien) 60:34-37.

Michalak M, Robert Parker JM, Opas M, 2002. Ca2+ signaling and calcium binding chaperones of the endoplasmic reticulum. Cell Calcium 32:269-278.

Miyagi T, Hori O, Koshida K, Egawa M, Kato H, Kitagawa Y, Ozawa K, Ogawa S, Namiki M, 2002. Antitumor effect of reduction of 150-kDa oxygen-regulated protein expression on human prostate cancer cells. Int J Urol 9:577-585.

Morgan PE, Pastorekova S, Stuart-Tilley AK, Alper SL, Casey JR, 2007. Interactions of transmembrane carbonic anhydrase, CAIX, with bicarbonate transporters. Am J Physiol Cell Physiol 293:C738-748.

Munro S, Pelham HR, 1986. An Hsp70-like protein in the ER: identity with the 78 kd glucose-regulated protein and immunoglobulin heavy chain binding protein. Cell 46:291-300.

Neri D, Supuran CT, 2011. Interfering with pH regulation in tumours as a therapeutic strategy. Nat Rev Drug Discov 10:767-777.

Neumar RW, Xu YA, Gada H, Guttmann RP, Siman R, 2003. Cross-talk between calpain and caspase proteolytic systems during neuronal apoptosis. J Biol Chem 278:14162-14167.

Niehues R, Hasilik M, Alton G, Korner C, Schiebe-Sukumar M, Koch HG, Zimmer KP, Wu R, Harms E, Reiter K, von Figura K, Freeze HH, Harms HK, Marquardt T, 1998. Carbohydrate-deficient glycoprotein syndrome type Ib. Phosphomannose isomerase deficiency and mannose therapy. J Clin Invest 101:1414-1420.

Nishigaki R, Osaki M, Hiratsuka M, Toda T, Murakami K, Jeang KT, Ito H, Inoue T, Oshimura M, 2005. Proteomic identification of differentially-expressed genes in human gastric carcinomas. Proteomics 5:3205-3213.

Nogales E, 2000. Structural insights into microtubule function. Annu Rev Biochem 69:277-302.

Nose F, Yamaguchi T, Kato R, Aiuchi T, Obama T, Hara S, Yamamoto M, Itabe H, 2013. Crucial role of perilipin-3 (TIP47) in formation of lipid droplets and PGE2 production in HL-60-derived neutrophils. PLoS One 8:e71542.

Obenauer JC, Cantley LC, Yaffe MB, 2003. Scansite 2.0: Proteome-wide prediction of cell signaling interactions using short sequence motifs. Nucleic Acids Res 31:3635-3641.

Ogawa K, Utsunomiya T, Mimori K, Tanaka Y, Tanaka F, Inoue H, Murayama S, Mori M, 2004. Clinical significance of elongation factor-1 delta mRNA expression in oesophageal carcinoma. Br J Cancer 91:282-286.

Okuda Y, Nakamura H, Yoshida K, Enomoto H, Uyama H, Hirotani T, Funamoto M, Ito H, Everett AD, Hada T, Kawase I, 2003. Hepatoma-derived growth factor induces tumorigenesis in vivo through both direct angiogenic activity and induction of vascular endothelial growth factor. Cancer Sci 94:1034-1041.

Olave IA, Reck-Peterson SL, Crabtree GR, 2002. Nuclear actin and actin-related proteins in chromatin remodeling. Annu Rev Biochem 71:755-781.

Olive PL, Aquino-Parsons C, MacPhail SH, Liao SY, Raleigh JA, Lerman MI, Stanbridge EJ, 2001. Carbonic anhydrase 9 as an endogenous marker for hypoxic cells in cervical cancer. Cancer Res 61:8924-8929.

Ong LL, Er CP, Ho A, Aung MT, Yu H, 2003. Kinectin anchors the translation elongation factor-1 delta to the endoplasmic reticulum. J Biol Chem 278:32115-32123.

Opavsky R, Pastorekova S, Zelnik V, Gibadulinova A, Stanbridge EJ, Zavada J, Kettmann R, Pastorek J, 1996. Human MN/CA9 gene, a novel member of the carbonic anhydrase family: structure and exon to protein domain relationships. Genomics 33:480-487.

Orlowski A, De Giusti VC, Morgan PE, Aiello EA, Alvarez BV, 2012. Binding of carbonic anhydrase IX to extracellular loop 4 of the NBCe1 Na+/HCO3- cotransporter enhances NBCe1-mediated HCO3- influx in the rat heart. Am J Physiol Cell Physiol 303:C69-80.

Orsel JG, Sincock PM, Krise JP, Pfeffer SR, 2000. Recognition of the 300-kDa mannose 6-phosphate receptor cytoplasmic domain by 47-kDa tail-interacting protein. Proc Natl Acad Sci U S A 97:9047-9051.

Pacchiano F, Carta F, McDonald PC, Lou Y, Vullo D, Scozzafava A, Dedhar S, Supuran CT, 2011. Ureido-substituted benzenesulfonamides potently inhibit carbonic anhydrase IX and show antimetastatic activity in a model of breast cancer metastasis. J Med Chem 54:1896-1902.

Palamarchuk A, Efanov A, Maximov V, Aqeilan RI, Croce CM, Pekarsky Y, 2005. Akt phosphorylates and regulates Pdcd4 tumor suppressor protein. Cancer Res 65:11282-11286.

Paris S, Denis H, Delaive E, Dieu M, Dumont V, Ninane N, Raes M, Michiels C, 2005. Up-regulation of 94-kDa glucose-regulated protein by hypoxia-inducible factor-1 in human endothelial cells in response to hypoxia. FEBS Lett 579:105-114.

Park JY, Hong SJ, Kim JM, Shim Y, 2015. Proteinic marker for early diagnosis of liver cancer. Google Patents.

Parks SK, Chiche J, Pouyssegur J, 2013. Disrupting proton dynamics and energy metabolism for cancer therapy. Nat Rev Cancer 13:611-623.

Paschen W, Gissel C, Linden T, Doutheil J, 1998. Erp72 expression activated by transient cerebral ischemia or disturbance of neuronal endoplasmic reticulum calcium stores. Metab Brain Dis 13:55-68.

Pastorek J, Pastorekova S, 2015. Hypoxia-induced carbonic anhydrase IX as a target for cancer therapy: from biology to clinical use. Semin Cancer Biol 31:52-64.

Pastorekova S, Parkkila S, Parkkila AK, Opavsky R, Zelnik V, Saarnio J, Pastorek J, 1997. Carbonic anhydrase IX, MN/CA IX: analysis of stomach complementary DNA sequence and expression in human and rat alimentary tracts. Gastroenterology 112:398-408.

Pastorekova S, Parkkila S, Pastorek J, Supuran CT, 2004. Carbonic anhydrases: current state of the art, therapeutic applications and future prospects. J Enzyme Inhib Med Chem 19:199-229.

Pastorekova S, Zavada J, 2004. Carbonic anhydrase IX (CA IX) as a potential target for cancer therapy. Cancer Therapy 2:245-262.

Pastorekova S, Zavadova Z, Kostal M, Babusikova O, Zavada J, 1992. A novel quasi-viral agent, MaTu, is a two-component system. Virology 187:620-626.

Perkins D, Pappin D, Creasy D, Cottrell J, 1999. Probability-based protein identification by searching sequence databases using mass spectrometry data. Electrophoresis 20:3551-3567.

Pfaffl MW, Horgan GW, Dempfle L, 2002. Relative expression software tool (REST) for group-wise comparison and statistical analysis of relative expression results in real-time PCR. Nucleic Acids Res 30:e36.

Plomin R, Turic DM, Hill L, Turic DE, Stephens M, Williams J, Owen MJ, O'Donovan MC, 2004. A functional polymorphism in the succinate-semialdehyde dehydrogenase (aldehyde dehydrogenase 5 family, member A1) gene is associated with cognitive ability. Mol Psychiatry 9:582-586.

Procaccio V, Wallace DC, 2004. Late-onset Leigh syndrome in a patient with mitochondrial complex I NDUFS8 mutations. Neurology 62:1899-1901.

Pyronnet S, Imataka H, Gingras AC, Fukunaga R, Hunter T, Sonenberg N, 1999. Human eukaryotic translation initiation factor 4G (eIF4G) recruits mnk1 to phosphorylate eIF4E. EMBO J 18:270-279.

R-Development-Core-Team, 2006. R: A language and environment for statistiacl computing. R Foundation for Statistical Computing, Vienna, Austria.

Radvak P, Repic M, Svastova E, Takacova M, Csaderova L, Strnad H, Pastorek J, Pastorekova S, Kopacek J, 2013. Suppression of carbonic anhydrase IX leads to aberrant focal adhesion and decreased invasion of tumor cells. Oncol Rep 29:1147-1153.

Raimbourg Q, Perez J, Vandermeersch S, Prignon A, Hanouna G, Haymann JP, Baud L, Letavernier E, 2013. The calpain/calpastatin system has opposing roles in growth and metastatic dissemination of melanoma. PLoS One 8:e60469.

Rami A, 2003. Ischemic neuronal death in the rat hippocampus: the calpain-calpastatin-caspase hypothesis. Neurobiol Dis 13:75-88.

Ravanbakhsh S, Gajewski M, Greiner R, Tuszynski JA, 2013. Determination of the optimal tubulin isotype target as a method for the development of individualized cancer chemotherapy. Theor Biol Med Model 10:29.

Ray SK, Fidan M, Nowak MW, Wilford GG, Hogan EL, Banik NL, 2000. Oxidative stress and Ca2+ influx upregulate calpain and induce apoptosis in PC12 cells. Brain Res 852:326-334.

Reddy RK, Mao C, Baumeister P, Austin RC, Kaufman RJ, Lee AS, 2003. Endoplasmic reticulum chaperone protein GRP78 protects cells from apoptosis induced by topoisomerase inhibitors: role of ATP binding site in suppression of caspase-7 activation. J Biol Chem 278:20915-20924.

Ren H, Tang X, Lee JJ, Feng L, Everett AD, Hong WK, Khuri FR, Mao L, 2004. Expression of hepatoma-derived growth factor is a strong prognostic predictor for patients with early-stage non-small-cell lung cancer. J Clin Oncol 22:3230-3237.

Riihonen R, Supuran CT, Parkkila S, Pastorekova S, Vaananen HK, Laitala-Leinonen T, 2007. Membrane-bound carbonic anhydrases in osteoclasts. Bone 40:1021-1031.

Robertson N, Potter C, Harris AL, 2004. Role of carbonic anhydrase IX in human tumor cell growth, survival, and invasion. Cancer Res 64:6160-6165.

Rohrmann K, Staehler M, Haseke N, Bachmann A, Stief CG, Siebels M, 2005. Immunotherapy in metastatic renal cell carcinoma. World J Urol 23:196-201.

Rzymski T, Harris AL, 2007. The unfolded protein response and integrated stress response to anoxia. Clin Cancer Res 13:2537-2540.

Rzymski T, Milani M, Pike L, Buffa F, Mellor HR, Winchester L, Pires I, Hammond E, Ragoussis I, Harris AL, 2010. Regulation of autophagy by ATF4 in response to severe hypoxia. Oncogene 29:4424-4435.

Rzymski T, Petry A, Kracun D, Riess F, Pike L, Harris AL, Gorlach A, 2012. The unfolded protein response controls induction and activation of ADAM17/TACE by severe hypoxia and ER stress. Oncogene 31:3621-3634.

Saarnio J, Parkkila S, Parkkila AK, Waheed A, Casey MC, Zhou XY, Pastorekova S, Pastorek J, Karttunen T, Haukipuro K, Kairaluoma MI, Sly WS, 1998. Immunohistochemistry of carbonic anhydrase isozyme IX (MN/CA IX) in human gut reveals polarized expression in the epithelial cells with the highest proliferative capacity. J Histochem Cytochem 46:497-504.

Satelli A, Li S, 2011. Vimentin in cancer and its potential as a molecular target for cancer therapy. Cell Mol Life Sci 68:3033-3046.

Sawai H, Domae N, 2011. Discrimination between primary necrosis and apoptosis by necrostatin-1 in Annexin V-positive/propidium iodide-negative cells. Biochem Biophys Res Commun 411:569-573.

Schiene-Fischer C, 2014. Multidomain peptidyl prolyl cis/trans Isomerases. Biochim Biophys Acta.

Schneider CA, Rasband WS, Eliceiri KW, 2012. NIH Image to ImageJ: 25 years of image analysis. Nat Methods 9:671-675.

Sedlakova O, Svastova E, Takacova M, Kopacek J, Pastorek J, Pastorekova S, 2014. Carbonic anhydrase IX, a hypoxia-induced catalytic component of the pH regulating machinery in tumors. Front Physiol 4:400.

Seibenhener ML, Babu JR, Geetha T, Wong HC, Krishna NR, Wooten MW, 2004. Sequestosome 1/p62 is a polyubiquitin chain binding protein involved in ubiquitin proteasome degradation. Mol Cell Biol 24:8055-8068.

Seibenhener ML, Geetha T, Wooten MW, 2007. Sequestosome 1/p62--more than just a scaffold. FEBS Lett 581:175-179.

Semenza GL, 2001. HIF-1 and mechanisms of hypoxia sensing. Curr Opin Cell Biol 13:167-171.

Shakib K, Norman JT, Fine LG, Brown LR, Godovac-Zimmermann J, 2005. Proteomics profiling of nuclear proteins for kidney fibroblasts suggests hypoxia, meiosis, and cancer may meet in the nucleus. Proteomics 5:2819-2838.

She QB, Halilovic E, Ye Q, Zhen W, Shirasawa S, Sasazuki T, Solit DB, Rosen N, 2010. 4E-BP1 is a key effector of the oncogenic activation of the AKT and ERK signaling pathways that integrates their function in tumors. Cancer Cell 18:39-51.

Shevchenko A, Valcu CM, Junqueira M, 2009. Tools for exploring the proteomosphere. J Proteomics 72:137-144.

Siebels M, Rohrmann K, Oberneder R, Stahler M, Haseke N, Beck J, Hofmann R, Kindler M, Kloepfer P, Stief C, 2010. A clinical phase I/II trial with the monoclonal antibody cG250 (RENCAREX(R)) and interferon-alpha-2a in metastatic renal cell carcinoma patients. World J Urol 29:121-126.

Silvera D, Formenti SC, Schneider RJ, 2010. Translational control in cancer. Nat Rev Cancer 10:254-266.

Sirajuddin M, Rice LM, Vale RD, 2014. Regulation of microtubule motors by tubulin isotypes and post-translational modifications. Nat Cell Biol 16:335-344.

Slee EA, Adrain C, Martin SJ, 2001. Executioner caspase-3, -6, and -7 perform distinct, non-redundant roles during the demolition phase of apoptosis. J Biol Chem 276:7320-7326.

Soldani C, Scovassi AI, 2002. Poly(ADP-ribose) polymerase-1 cleavage during apoptosis: an update. Apoptosis 7:321-328.

Sonenberg N, Hinnebusch AG, 2009. Regulation of translation initiation in eukaryotes: mechanisms and biological targets. Cell 136:731-745.

Span PN, Bussink J, Manders P, Beex LV, Sweep CG, 2003. Carbonic anhydrase-9 expression levels and prognosis in human breast cancer: association with treatment outcome. Br J Cancer 89:271-276.

Stojadinovic A, Hooke JA, Shriver CD, Nissan A, Kovatich AJ, Kao TC, Ponniah S, Peoples GE, Moroni M, 2007. HYOU1/Orp150 expression in breast cancer. Med Sci Monit 13:BR231-239.

Storr SJ, Carragher NO, Frame MC, Parr T, Martin SG, 2011. The calpain system and cancer. Nat Rev Cancer 11:364-374.

Straub BK, Herpel E, Singer S, Zimbelmann R, Breuhahn K, Macher-Goeppinger S, Warth A, Lehmann-Koch J, Longerich T, Heid H, Schirmacher P, 2010. Lipid droplet-associated PAT-proteins show frequent and differential expression in neoplastic steatogenesis. Mod Pathol 23:480-492.

Su Y, Qiu Q, Zhang X, Jiang Z, Leng Q, Liu Z, Stass SA, Jiang F, 2010. Aldehyde dehydrogenase 1 A1-positive cell population is enriched in tumor-initiating cells and associated with progression of bladder cancer. Cancer Epidemiol Biomarkers Prev 19:327-337.

Supuran CT, 2008. Carbonic anhydrases: novel therapeutic applications for inhibitors and activators. Nat Rev Drug Discov 7:168-181.

Svastova E, Hulikova A, Rafajova M, Zat'ovicova M, Gibadulinova A, Casini A, Cecchi A, Scozzafava A, Supuran CT, Pastorek J, Pastorekova S, 2004. Hypoxia activates the capacity of tumor-associated carbonic anhydrase IX to acidify extracellular pH. FEBS Lett 577:439-445.

Svastova E, Pastorekova S, 2013. Carbonic anhydrase IX: a hypoxia-controlled "catalyst" of cell migration. Cell Adh Migr 7:226-231.

Svastova E, Zilka N, Zat'ovicova M, Gibadulinova A, Ciampor F, Pastorek J, Pastorekova S, 2003. Carbonic anhydrase IX reduces E-cadherin-mediated adhesion of MDCK cells via interaction with beta-catenin. Exp Cell Res 290:332-345.

Swietach P, Hulikova A, Vaughan-Jones RD, Harris AL, 2010. New insights into the physiological role of carbonic anhydrase IX in tumour pH regulation. Oncogene 29:6509-6521.

Swietach P, Patiar S, Supuran CT, Harris AL, Vaughan-Jones RD, 2009. The role of carbonic anhydrase 9 in regulating extracellular and intracellular ph in three-dimensional tumor cell growths. J Biol Chem 284:20299-20310.

Takahashi H, Wang JP, Zheng HC, Masuda S, Takano Y, 2011. Overexpression of GRP78 and GRP94 is involved in colorectal carcinogenesis. Histol Histopathol 26:663-671.

Tufo G, Jones AW, Wang Z, Hamelin J, Tajeddine N, Esposti DD, Martel C, Boursier C, Gallerne C, Migdal C, Lemaire C, Szabadkai G, Lemoine A, Kroemer G, Brenner C, 2014. The protein disulfide isomerases PDIA4 and PDIA6 mediate resistance to cisplatin-induced cell death in lung adenocarcinoma. Cell Death Differ 21:685-695.

Ueda T, Sasaki M, Elia AJ, Chio, II, Hamada K, Fukunaga R, Mak TW, 2010. Combined deficiency for MAP kinase-interacting kinase 1 and 2 (Mnk1 and Mnk2) delays tumor development. Proc Natl Acad Sci U S A 107:13984-13990.

Ueda T, Watanabe-Fukunaga R, Fukuyama H, Nagata S, Fukunaga R, 2004. Mnk2 and Mnk1 are essential for constitutive and inducible phosphorylation of eukaryotic initiation factor 4E but not for cell growth or development. Mol Cell Biol 24:6539-6549.

Uniprot-Consortium, 2014. Activities at the Universal Protein Resource (UniProt). Nucleic Acids Res 42:D191-D198.

Uyama H, Tomita Y, Nakamura H, Nakamori S, Zhang B, Hoshida Y, Enomoto H, Okuda Y, Sakon M, Aozasa K, Kawase I, Hayashi N, Monden M, 2006. Hepatoma-derived growth factor is a novel prognostic factor for patients with pancreatic cancer. Clin Cancer Res 12:6043-6048.

Valcu CM, Reger K, Ebner J, Gorlach A, 2012. Accounting for biological variation in differential display two-dimensional electrophoresis experiments. J Proteomics 75:3585-3591.

Valencia CA, Cotten SW, Duan J, Liu R, 2008. Modulation of nucleobindin-1 and nucleobindin-2 by caspases. FEBS Lett 582:286-290.

van den Beucken T, Koritzinsky M, Niessen H, Dubois L, Savelkouls K, Mujcic H, Jutten B, Kopacek J, Pastorekova S, van der Kogel AJ, Lambin P, Voncken W, Rouschop KM, Wouters BG, 2009a. Hypoxia-induced expression of carbonic anhydrase 9 is dependent on the unfolded protein response. J Biol Chem 284:24204-24212.

van den Beucken T, Magagnin MG, Jutten B, Seigneuric R, Lambin P, Koritzinsky M, Wouters BG, 2011. Translational control is a major contributor to hypoxia induced gene expression. Radiother Oncol 99:379-384.

van den Beucken T, Ramaekers CH, Rouschop K, Koritzinsky M, Wouters BG, 2009b. Deficient carbonic anhydrase 9 expression in UPR-impaired cells is associated with reduced survival in an acidic microenvironment. Radiother Oncol 92:437-442.

Vander Heiden MG, Cantley LC, Thompson CB, 2009. Understanding the Warburg effect: the metabolic requirements of cell proliferation. Science 324:1029-1033.

Vaupel P, Mayer A, 2007. Hypoxia in cancer: significance and impact on clinical outcome. Cancer Metastasis Rev 26:225-239.

Vavassori S, Cortini M, Masui S, Sannino S, Anelli T, Caserta IR, Fagioli C, Mossuto MF, Fornili A, van Anken E, Degano M, Inaba K, Sitia R, 2013. A pH-regulated quality control cycle for surveillance of secretory protein assembly. Mol Cell 50:783-792.

Visus C, Ito D, Amoscato A, Maciejewska-Franczak M, Abdelsalem A, Dhir R, Shin DM, Donnenberg VS, Whiteside TL, DeLeo AB, 2007. Identification of human aldehyde dehydrogenase 1 family member A1 as a novel CD8+ T-cell-defined tumor antigen in squamous cell carcinoma of the head and neck. Cancer Res 67:10538-10545.

Vogel RO, Janssen RJ, Ugalde C, Grovenstein M, Huijbens RJ, Visch HJ, van den Heuvel LP, Willems PH, Zeviani M, Smeitink JA, Nijtmans LG, 2005. Human mitochondrial complex I assembly is mediated by NDUFAF1. FEBS J 272:5317-5326.

Vu NT, Park MA, Shultz JC, Goehe RW, Hoeferlin LA, Shultz MD, Smith SA, Lynch KW, Chalfant CE, 2013. hnRNP U enhances caspase-9 splicing and is modulated by AKT-dependent phosphorylation of hnRNP L. J Biol Chem 288:8575-8584.

Vuoriluoto K, Haugen H, Kiviluoto S, Mpindi JP, Nevo J, Gjerdrum C, Tiron C, Lorens JB, Ivaska J, 2011. Vimentin regulates EMT induction by Slug and oncogenic H-Ras and migration by governing Axl expression in breast cancer. Oncogene 30:1436-1448.

Wanderling S, Simen BB, Ostrovsky O, Ahmed NT, Vogen SM, Gidalevitz T, Argon Y, 2007. GRP94 is essential for mesoderm induction and muscle development because it regulates insulin-like growth factor secretion. Mol Biol Cell 18:3764-3775.

Wang H, Pezeshki AM, Yu X, Guo C, Subjeck JR, Wang XY, 2015. The Endoplasmic Reticulum Chaperone GRP170: From Immunobiology to Cancer Therapeutics. Front Oncol 4:377.

Wang J, Duncan D, Shi Z, Zhang B, 2013. WEB-based GEne SeT AnaLysis Toolkit (WebGestalt): update 2013. Nucleic Acids Res 41:W77-83.

Wang M, Kaufman RJ, 2014. The impact of the endoplasmic reticulum protein-folding environment on cancer development. Nat Rev Cancer 14:581-597.

Wang Q, He Z, Zhang J, Wang Y, Wang T, Tong S, Wang L, Wang S, Chen Y, 2005. Overexpression of endoplasmic reticulum molecular chaperone GRP94 and GRP78 in human lung cancer tissues and its significance. Cancer Detect Prev 29:544-551.

Wang S, Kaufman RJ, 2012. The impact of the unfolded protein response on human disease. J Cell Biol 197:857-867.

Wang Y, Wang XY, Subjeck JR, Kim HL, 2008. Carbonic anhydrase IX has chaperone-like functions and is an immunoadjuvant. Mol Cancer Ther 7:3867-3877.

Wei J, Xu G, Wu M, Zhang Y, Li Q, Liu P, Zhu T, Song A, Zhao L, Han Z, Chen G, Wang S, Meng L, Zhou J, Lu Y, Ma D, 2008. Overexpression of vimentin contributes to prostate cancer invasion and metastasis via src regulation. Anticancer Res 28:327-334.

Wickham H, 2009. ggplot2: elegant graphics for data analysis. Springer New York.

Wooten MW, Geetha T, Babu JR, Seibenhener ML, Peng J, Cox N, Diaz-Meco MT, Moscat J, 2008. Essential role of sequestosome 1/p62 in regulating accumulation of Lys63-ubiquitinated proteins. J Biol Chem 283:6783-6789.

Wooten MW, Hu X, Babu JR, Seibenhener ML, Geetha T, Paine MG, Wooten MC, 2006. Signaling, polyubiquitination, trafficking, and inclusions: sequestosome 1/p62's role in neurodegenerative disease. J Biomed Biotechnol 2006:62079.

Wouters BG, van den Beucken T, Magagnin MG, Koritzinsky M, Fels D, Koumenis C, 2005. Control of the hypoxic response through regulation of mRNA translation. Semin Cell Dev Biol 16:487-501.

Wykoff CC, Beasley NJ, Watson PH, Turner KJ, Pastorek J, Sibtain A, Wilson GD, Turley H, Talks KL, Maxwell PH, Pugh CW, Ratcliffe PJ, Harris AL, 2000. Hypoxia-inducible expression of tumor-associated carbonic anhydrases. Cancer Res 60:7075-7083.

Yamaguchi S, Ishihara H, Yamada T, Tamura A, Usui M, Tominaga R, Munakata Y, Satake C, Katagiri H, Tashiro F, Aburatani H, Tsukiyama-Kohara K, Miyazaki J, Sonenberg N, Oka Y, 2008. ATF4-mediated induction of 4E-BP1 contributes to pancreatic beta cell survival under endoplasmic reticulum stress. Cell Metab 7:269-276.

Yamaguchi T, Goto H, Yokoyama T, Sillje H, Hanisch A, Uldschmid A, Takai Y, Oguri T, Nigg EA, Inagaki M, 2005. Phosphorylation by Cdk1 induces Plk1-mediated vimentin phosphorylation during mitosis. J Cell Biol 171:431-436.

Yamamoto S, Tomita Y, Hoshida Y, Takiguchi S, Fujiwara Y, Yasuda T, Doki Y, Yoshida K, Aozasa K, Nakamura H, Monden M, 2006. Expression of hepatoma-derived growth factor is correlated with lymph node metastasis and prognosis of gastric carcinoma. Clin Cancer Res 12:117-122.

Yamashita T, Honda M, Takatori H, Nishino R, Minato H, Takamura H, Ohta T, Kaneko S, 2009. Activation of lipogenic pathway correlates with cell proliferation and poor prognosis in hepatocellular carcinoma. J Hepatol 50:100-110.

Yang J, Weinberg RA, 2008. Epithelial-mesenchymal transition: at the crossroads of development and tumor metastasis. Dev Cell 14:818-829.

Yang WS, Moon HG, Kim HS, Choi EJ, Yu MH, Noh DY, Lee C, 2012. Proteomic approach reveals FKBP4 and S100A9 as potential prediction markers of therapeutic response to neoadjuvant chemotherapy in patients with breast cancer. J Proteome Res 11:1078-1088.

Yu Y, Feng YM, 2010. The role of kinesin family proteins in tumorigenesis and progression: potential biomarkers and molecular targets for cancer therapy. Cancer 116:5150-5160.

Yugami M, Kabe Y, Yamaguchi Y, Wada T, Handa H, 2007. hnRNP-U enhances the expression of specific genes by stabilizing mRNA. FEBS Lett 581:1-7.

Zatovicova M, Sedlakova O, Svastova E, Ohradanova A, Ciampor F, Arribas J, Pastorek J, Pastorekova S, 2005. Ectodomain shedding of the hypoxia-induced carbonic anhydrase IX is a metalloprotease-dependent process regulated by TACE/ADAM17. Br J Cancer 93:1267-1276.

Zavada J, Zavadova Z, Pastorekova S, Ciampor F, Pastorek J, Zelnik V, 1993. Expression of MaTu-MN protein in human tumor cultures and in clinical specimens. Int J Cancer 54:268-274.

Zhang B, Kirov S, Snoddy J, 2005. WebGestalt: an integrated system for exploring gene sets in various biological contexts. Nucleic Acids Res 33:W741-748.

Zhang X, Zhang F, Guo L, Wang Y, Zhang P, Wang R, Zhang N, Chen R, 2013. Interactome analysis reveals that C1QBP (complement component 1, q subcomponent binding protein) is associated with cancer cell chemotaxis and metastasis. Mol Cell Proteomics 12:3199-3209.

Zhang Y, Baig E, Williams DB, 2006. Functions of ERp57 in the folding and assembly of major histocompatibility complex class I molecules. J Biol Chem 281:14622-14631.

Zhao Q, Wang J, Levichkin IV, Stasinopoulos S, Ryan MT, Hoogenraad NJ, 2002. A mitochondrial specific stress response in mammalian cells. EMBO J 21:4411-4419.

Zheng HC, Takahashi H, Li XH, Hara T, Masuda S, Guan YF, Takano Y, 2008. Overexpression of GRP78 and GRP94 are markers for aggressive behavior and poor prognosis in gastric carcinomas. Hum Pathol 39:1042-1049.

Zhou X, Tan M, Stone Hawthorne V, Klos KS, Lan KH, Yang Y, Yang W, Smith TL, Shi D, Yu D, 2004. Activation of the Akt/mammalian target of rapamycin/4E-BP1 pathway by ErbB2 overexpression predicts tumor progression in breast cancers. Clin Cancer Res 10:6779-6788.

8 Appendix

8.1 Lists of Tables and Figures

8.1.1 Tables

8.1.2 Figures

8.2 Publications

Manuscripts

Chalupsy K, Kračun D, Kanchev I, **Bertram K**, Görlach A. Folic acid promotes recycling of tetrahydrobiopterin and protects against hypoxia-induced pulmonary vascular remodeling by recoupling endothelial nitric oxide synthase.
Antioxidant & Redox Signaling. doi:10.1089/ars.2015.6329

Görlach A, **Bertram K**, Hudecova S, Krizanova O. Calcium and ROS: a mutual interplay.
Redox Biol. 6:260-271

Bertram K*, Valcu CM*, Weitnauer M, Linne U, Görlach A, 2015. NOX1 supports the metabolic remodeling of HepG2 cells.
PLoS One 10:e0122002
*authors contributed equally

Edin NJ, Sandvik JA, Vollan HS, **Reger K**, Görlach A, Pettersen EO, 2013. The role of nitric oxide radicals in removal of hyper-radiosensitivity by priming irradiation.
J Radiat Res. 54:1015-28

Valcu CM, **Reger K**, Ebner J, Görlach A, 2012. Accounting for biological variation in differential display two-dimensional electrophoresis experiments.
J Proteomics. 75:3585-91

Qbadou S, Becker T, Bionda T**, Reger K**, Ruprecht M, Soll J, Schleiff E, 2007. Toc64 – a preprotein-receptor at the outer membrane with bipartite function.
J Mol Biol. 367:1330-1346

Oreb M, **Reger K**, Schleiff E, 2006. Chloroplast protein import: reverse genetic approaches. Current Genomics. 7:235-244

Bertram K, Valcu CM, Gührs KH, Görlach A. Differential protein display of CAIX-depleted HeLa cells reveals impact of CAIX on UPR and apoptosis.
manuscript prepared

Bertram K, Valcu CM, Zhang Z, Gührs KH, Görlach A. Differential protein expression in p22phox deficient mice.
in preparation

Abstracts and Posters

Bertram K, Valcu CM, Weitnauer M, Linne U, Görlach A, 2015. NOX1 supports the metabolic remodeling of HepG2 cells.
Poster presented at the 1st International Munich ROS Meeting, April 2015, Munich, Germany

Kračun D, Chalupsky K, Kanchev I, **Bertram K**, Petry A, Görlach A, 2015. Folic acid promotes recycling of tetrahydrobiopterin and protects against hypoxia-induced pulmonary vascular remodeling by recoupling endothelial nitric oxide synthase.
Poster presented at the 1st International Munich ROS Meeting, April 2015, Munich, Germany

Kračun D, Kanchev I, Rieß F, **Bertram K**, Petry A, Görlach A, 2015. Low dose dexamethasone induces vascular proliferation and remodeling via NADPH oxidases and HIF1.
Poster at the 1st International Munich ROS Meeting, April 2015, Munich, Germany

Kračun D, Chalupsky K, Kanchev I, **Reger K**, Hess J, Görlach A, 2011. Folic acid prevents uncoupling of NO synthase and pulmonary vascular remodeling under hypoxia. J Vascular Research 48:85-85

Reger K, Chalupsky K, Kračun D, Görlach A, 2009. TGF beta 1 increases superoxide production by uncoupling nitric oxide synthase in hepatoma cells. J Vascular Research 46:47-47
Poster presented at the Annual Meeting of the Society of Microcirculation and Vascular Biology, October 2009, Bern, Switzerland

Kračun D, Chalupsky K, Buchstaller A, Quillet R, **Reger K**, Görlach A, 2009. Dexamethasone upregulates HIF-1α via superoxide derived from NOX2 and NOX4 in vascular cells. J Vascular Research 46:46-46
Poster presented at the Annual Meeting of the Society of Microcirculation and Vascular Biology, October 2009, Bern, Switzerland

Weitnauer M, Becht S, **Reger K**, Chalupsky K, Görlach A, 2008. Detection of free radicals by electron spin resonance in hypoxic models.
Poster at Euroxy Course "Tumor hypoxia: from biology to therapy", November 2008, Monsummano Terme, Italy

8.3 Acknowledgements

I wish to express my gratitude to my supervisor Prof. Dr. med. Agnes Görlach for giving me the opportunity and privilege to persue my PhD in her laboratory. I thank her for the continuous support of my PhD study with her patience, motivation, enthusiasm and immense knowledge. Her guidance and constant support helped me in all the time of research and have been a constant inspiration to me.

My sincere thanks go to Prof. Dr. rer. nat. Gabriele Multhoff for accepting me as a PhD student and for her external supervision that made it possible to persue my PhD studies at the TUM.

I am very grateful to my mentor Dr. rer. nat. Andreas Petry for his support, motivation and advice. Our discussions were a constant source of motivation and inspiration in our daily lab life.

My very special thanks go to Dr. rer. nat. Cristina-Maria Vâlcu. Her supervision and training provided me with the knowledge and skills to persue this study. Her unconditioned support and friendship made me grow both as a scientist and a person.

I thank Dr. rer. nat. Mihai Vâlcu from the Max Planck Institute for Ornithology for advice on the statistical analysis of 2DE data and Dr. Karl-Heinz Gührs from the Friedrich Schiller University Jena for MS analysis.

I thank Prof. Silva Pastorekova, PhD., for kindly providing the CAIX antibody.

I thank all my fellow lab mates that I was able to meet and work with during my time at the Experimental und Molecular Pediatric Cardiology. Among those, my special thanks go to Johanna Brandl, Karel Chalupsky, Ivan Kanchev, Damir Kračun, Florian Rieß, Michael Weitnauer and Zuwen Zhang.

My special thanks go to Andrea, Madeleine and Barbara.

I want to express my gratitude to my mother for always supporting and being there for me.

My final thanks go to Horst for always supporting me unconditionally and E. – who always reminds me of what really matters in life. Without your unconditioned love this would not have been possible!

8.4 Supporting Information

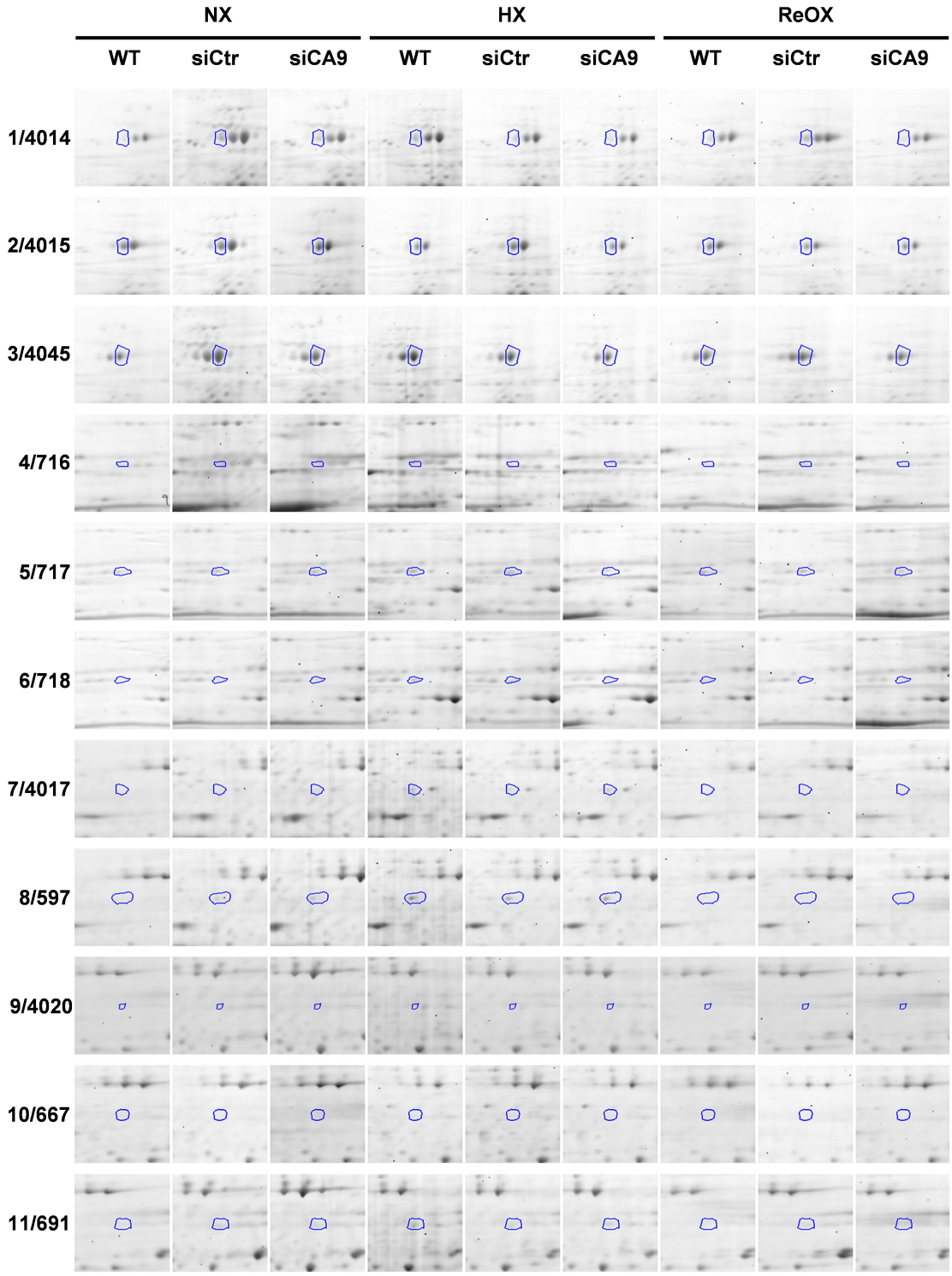

continued on next page...

Supporting Figure 1 2DE spots differentially regulated in HeLa cells
Cells were incubated at 21% oxygen for 24 h (normoxia, NX), 1% oxygen for 24 h (hypoxia; HX) or 1% oxygen for 24 h followed by 21% oxygen for 8 h (reoxygenation; ReOX). In addition, cells were transfected using control siRNA (siCtr), siRNA specific against *CA9* (siCA9) or left untransfected (WT). For each spot and each condition the regulation is shown using one representative repeat out of three. Spots were circled by SameSpots software. Spot IDs are indicated according to numbering during MS analysis (left) and image analysis (right).

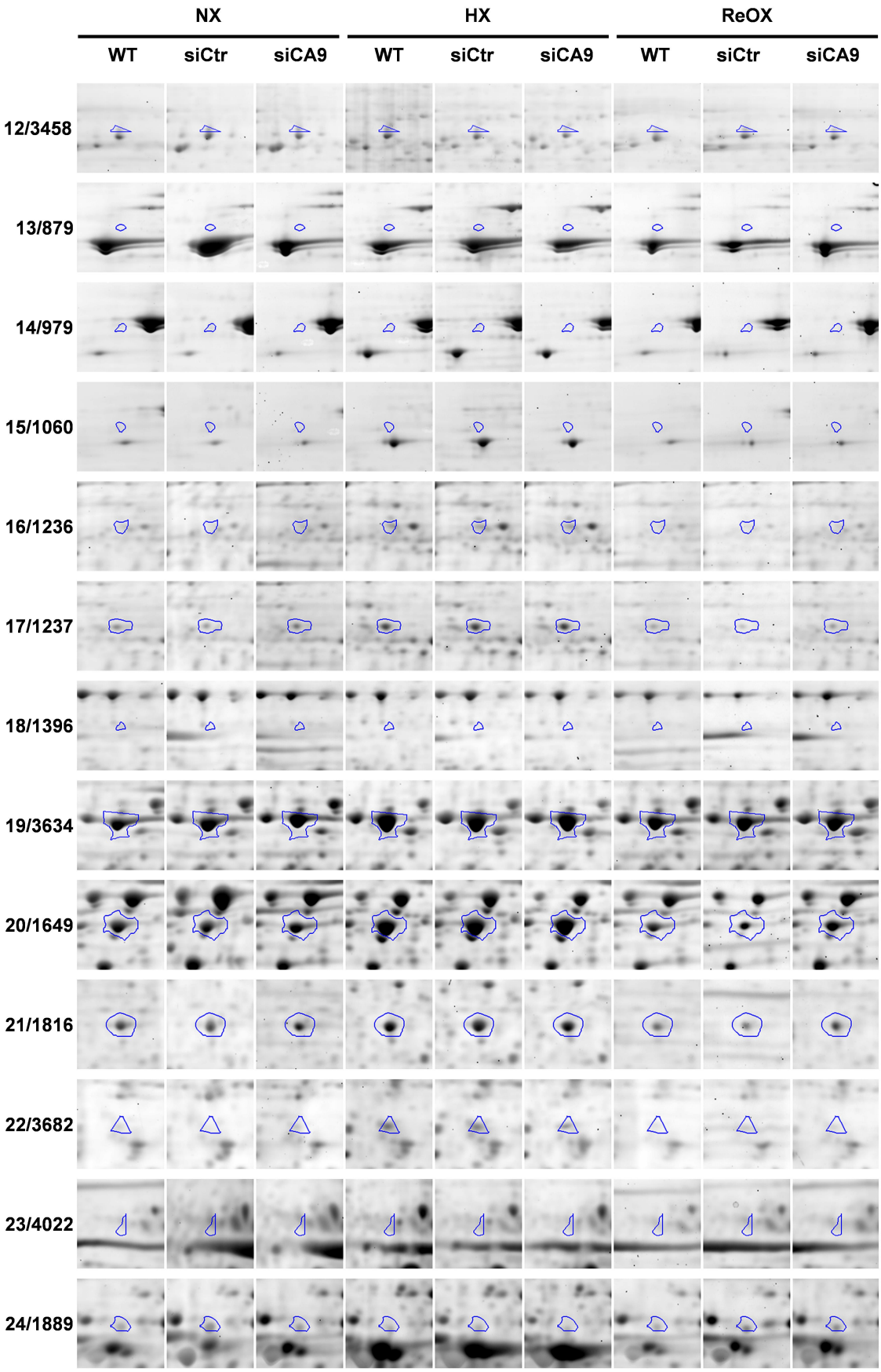

continued on next page...

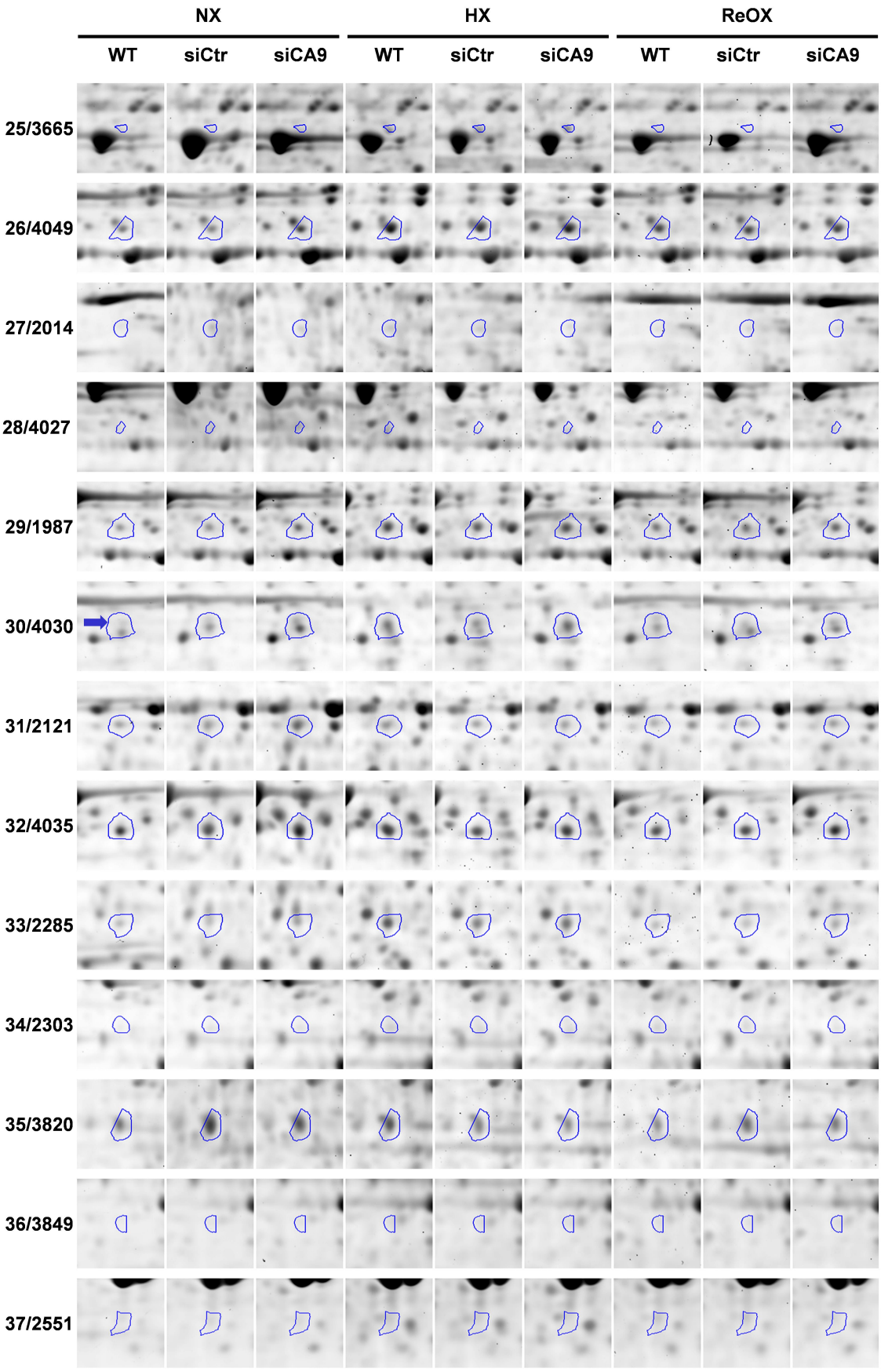

continued on next page...

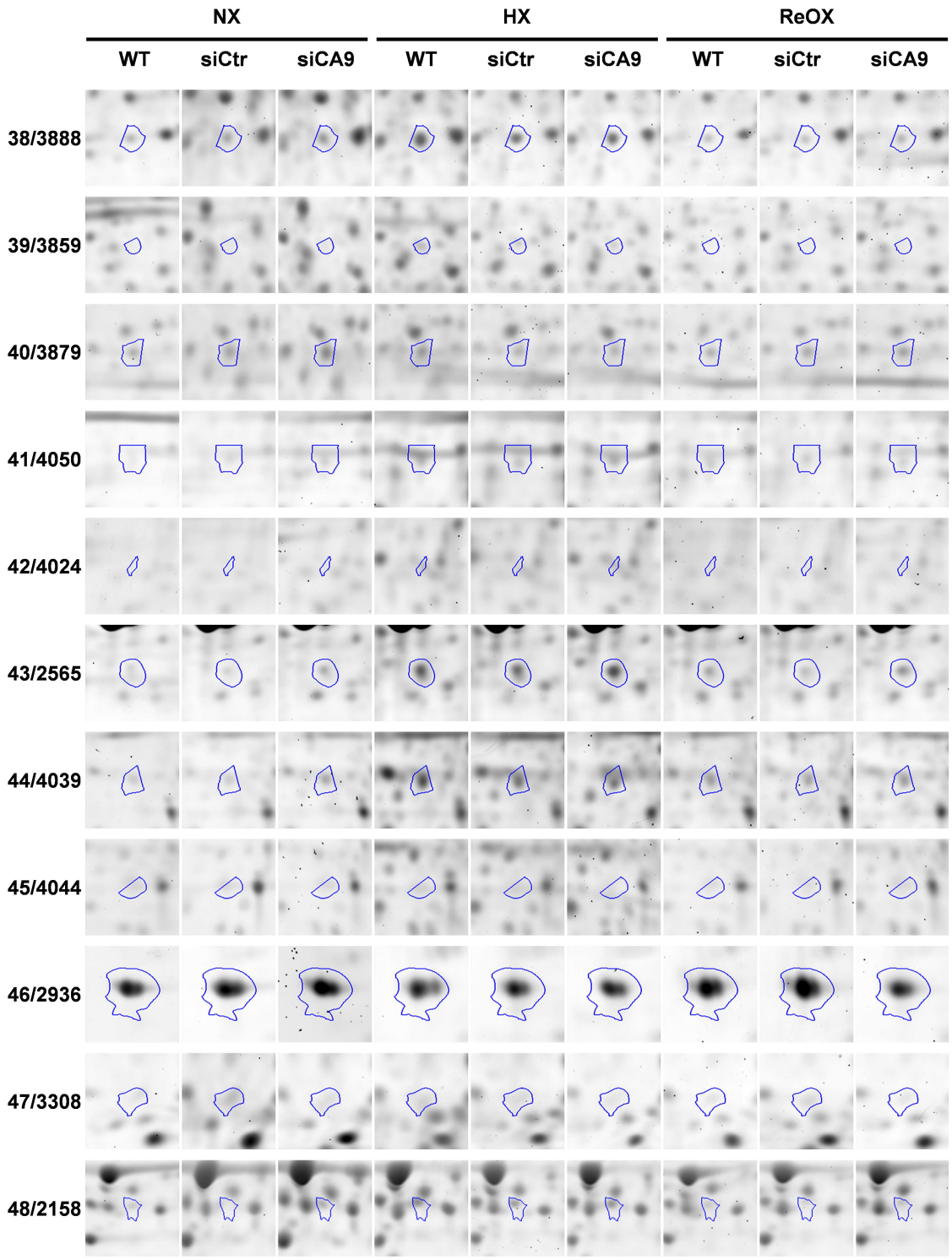
NX
HX
ReOX
WT
siCtr
siCA9
WT
siCtr
siCA9
WT
siCtr
siCA9
38/3888
39/3859
40/3879
41/4050
42/4024
43/2565
44/4039
45/4044
46/2936
47/3308
48/2158

...continued.

Supporting Table 1 P-values of statistical analysis of spots
Spot IDs are given both according to MS analysis and SameSpots number (SS). Spots are sorted by the statistical models (cell3, cell5, cell9).

model	Spot ID MS	Spot ID SS	siCtr vs. WT	siCA9 vs. siCtr
cell3	4	716	0.63008	0.02685
cell3	6	718	0.15675	0.01217
cell3	9	4020	0.07926	0.01384
cell3	10	667	0.10722	0.01554
cell3	11	691	0.08607	0.01206
cell3	14	979	0.04316	0.00246
cell3	23	4022	0.34583	0.00555
cell3	28	4027	0.16372	0.02745
cell3	47	3308	0.02370	0.00233

model	Spot ID MS	Spot ID SS	siCtr vs. WT	siCA9 vs. siCtr	HX vs. NX	ReOX vs. NX
cell5	2	4015	0.37748	0.01471	0.00159	0.20120
cell5	3	4045	0.41222	0.00535	0.00224	0.14057
cell5	5	717	0.19721	0.00550	0.00246	0.02168
cell5	7	4017	0.06630	0.00017	0.00004	0.27659
cell5	8	597	0.11964	0.00031	0.00001	0.00334
cell5	12	3458	0.44379	0.00409	0.00069	0.12132
cell5	13	879	0.07719	0.01645	0.00253	0.88911
cell5	15	1060	0.05701	0.03516	0.00005	0.59057
cell5	16	1236	0.98836	0.03516	0.00002	0.09370
cell5	17	1237	0.02952	0.00494	0.00000	0.79581
cell5	18	1396	0.08052	0.01174	0.00018	0.30411
cell5	19	3634	0.66472	0.04987	0.17834	0.55648
cell5	20	1649	0.07975	0.02698	0.00019	0.80850
cell5	21	1816	0.09487	0.03992	0.00008	0.29515
cell5	24	1889	0.23924	0.01385	0.00000	0.99963
cell5	25	3665	0.07065	0.01912	0.00000	0.61714
cell5	26	4049	0.04520	0.02820	0.00000	0.02530
cell5	27	2014	0.17361	0.03728	0.97667	0.12506
cell5	29	1987	0.24858	0.01479	0.00000	0.96680
cell5	30	4030	1.00000	0.13512	1.00000	0.73672
cell5	31	2121	0.62502	0.02855	0.00321	0.01248
cell5	32	4035	0.25622	0.02163	0.00337	0.92884
cell5	33	2285	0.10664	0.00544	0.00000	0.06237
cell5	34	2303	0.07915	0.00970	0.12581	0.15223
cell5	35	3820	0.01763	0.00013	0.00065	0.90355
cell5	36	3849	0.64087	0.03472	0.01202	0.23431
cell5	37	2551	0.88435	0.00190	0.10094	0.53563
cell5	38	3888	0.05262	0.02082	0.00000	0.98589
cell5	40	3879	0.08974	0.04223	0.01010	0.74685
cell5	41	4050	0.12472	0.05186	0.00001	0.80155
cell5	42	4024	0.07073	0.17453	0.00000	0.23678
cell5	43	2565	0.30037	0.01217	0.00000	0.94556
cell5	44	4039	0.39731	0.02071	0.00000	0.49964
cell5	45	4044	0.06109	0.01147	0.00803	0.99495
cell5	46	2936	0.29555	0.00816	0.00002	0.87525
cell5	48	2158	0.06080	0.01884	0.00003	0.11353

model	Spot ID MS	Spot ID SS	HX:WT	ReOX:WT	HX:siCA9	ReOX:siCA9
cell9	1	4014	0.65367	0.27316	1.00000	0.96812
cell9	22	3682	0.57009	0.73817	0.02510	0.09672
cell9	39	3859	0.99988	0.17343	0.93548	0.03515

$p>0.1$ not significant, $0.1 \geq p > 0.05$ marginally significant, $p<0.05$ significant.

Supporting Table 2 Mascot search results I

		MASCOT search against NCBI					
Spot	**Best homolog**	***Species***	**uniprot accession**	**MW on DE gel (kDa)**	**pI on 2DE gel**	**Expected MW (Da)**	**Expected pI**
1	Hypoxia up-regulated protein 1	*Homo sapiens*	Q9Y4L1	148,974	5.08	111,335	5.16
2	Hypoxia up-regulated protein 1	*Homo sapiens*	Q9Y4L1	148,974	5.12	111,335	5.16
3	Hypoxia up-regulated protein 1	*Homo sapiens*	Q9Y4L1	148,974	5.14	111,335	5.16
4	Calpastatin	*Homo sapiens*	P20810	124,872	4.93	76,573	4.98
5	Calpastatin	*Homo sapiens*	P20810	124,872	4.98	76,573	4.98
6	Calpastatin	*Homo sapiens*	P20810	124,872	5.02	76,573	4.98
7	Heterogeneous nuclear ribonucleoprotein U	*Homo sapiens*	Q00839	132,821	5.58	90,584	5.76
7	Kinesin-like protein KIF11	*Homo sapiens*	P52732	132,821	5.58	119,159	5,47
8	Heterogeneous nuclear ribonucleoprotein U	*Homo sapiens*	Q00839	133,077	5.62	90,584	5.76
10	Heterogeneous nuclear ribonucleoprotein U	*Homo sapiens*	Q00839	128,974	5.67	90,584	5.76
10	Kinesin-like protein KIF11	*Homo sapiens*	P52732	128,974	5.67	119,159	5,47
11	Heterogeneous nuclear ribonucleoprotein U	*Homo sapiens*	Q00839	128,205	5.75	90,584	5.76
13	Endoplasmin	*Homo sapiens*	P14625	114,054	4.73	92,469	4.76
16	Eukaryotic pept. chain release fact. GTP-bind. subunit ERF3A	*Homo sapiens*	P15170	94,390	5.29	55,756	5.45
17	Eukaryotic pept. chain release fact. GTP-bind. subunit ERF3A	*Homo sapiens*	P15170	94,390	5.33	55,756	5.45
18	78 kDa glucose-regulated protein	*Homo sapiens*	P11021	87,561	5.8	72,333	5.07
19	78 kDa glucose-regulated protein	*Homo sapiens*	P11021	76,341	5.36	72,333	5.07
20	78 kDa glucose-regulated protein	*Homo sapiens*	P11021	74,878	5.5	72,333	5.07
21	T-complex protein 1 subunit α	*Homo sapiens*	P17987	66,636	6.01	60,344	5.8
22	Thioredoxin reductase 1, cytoplasmic	*Homo sapiens*	Q16881	61,776	6.18	70,906	7.16
23	Programmed cell death protein 4	*Homo sapiens*	Q53EL6	63,925	4.83	51,735	5.07
24	Nucleobindin-1	*Homo sapiens*	Q02818	62,523	5.07	53,879	5.15
25	60 kDa heat shock protein, mitochondrial	*Homo sapiens*	P10809	64,486	5.31	61,055	5.7
26	Peptidyl-prolyl cis-trans isomerase FKBP4	*Homo sapiens*	Q02790	58,276	5.45	51,805	5.35
27	Tubulin β-4A chain	*Homo sapiens*	P04350	57,241	4.7	49,586	4.78
28	Tubulin β-4A chain	*Homo sapiens*	P04350	56,690	5.32	49,586	4.78
29	Peptidyl-prolyl cis-trans isomerase FKBP4	*Homo sapiens*	Q02790	58,621	5.37	51,805	5.35
30	4-trimethylaminobutyraldehyde dehydrogenase	*Homo sapiens*	P49189	52,190	5.76	53,802	5.69
31	4-trimethylaminobutyraldehyde dehydrogenase	*Homo sapiens*	P49189	52,966	5.95	53,802	5.69
32	Actin-related protein 3	*Homo sapiens*	P61158	49,762	5.73	47,371	5.61
33	Pachytene checkpoint protein 2 homolog	*Homo sapiens*	Q15645	45,556	5.97	48,551	5.73
35	Endoplasmic reticulum resident protein 44	*Homo sapiens*	Q9BS26	42,698	4.99	46,971	5.09
38	Glutaredoxin-3	*Homo sapiens*	O76003	29,324	5.41	37,432	5.31
39	Mannose-6-phosphate isomerase	*Homo sapiens*	P34949	36,168	5.66	46,656	5.62
41	Elongation factor 1-delta	*Homo sapiens*	P29692	26,162	5.68	31,122	4.9
43	Serpin B6	*Homo sapiens*	P35237	29,973	5.27	42,622	5.18
44	Endoplasmin	*Homo sapiens*	P14625	28,703	4.63	92,469	4.76
44	Hepatoma-derived growth factor	*Homo sapiens*	P51858	28,703	4.63	26,788	4.7
46	Complement comp. 1 Q subcomponent-binding protein, mitoch.	*Homo sapiens*	Q07021	22,379	4.24	31,362	4.74
47	NADH dehydrogenase [ubiquinone] iron-sulfur protein 8, mitoch.	*Homo sapiens*	O00217	14,579	5.12	23,705	6
101	Sequestosome-1	*Homo sapiens*	Q13501	n.d.	4.81	47,687	5.1
101	Programmed cell death protein 4	*Homo sapiens*	Q53EL6	n.d.	4.81	51,735	5.07
104	Vimentin	*Homo sapiens*	P08670	n.d.	4.82	53,652	5.06
105	Vimentin	*Homo sapiens*	P08670	n.d.	4.89	53,652	5.06
112	Perilipin-3	*Homo sapiens*	O60664	42,394	5.15	47,075	5.3
115	Elongation factor 1-δ	*Homo sapiens*	P29692	33,614	4.77	31,122	4.9

Supporting Table 3 Mascot search results II

Biological sample name (spot ID_gel ID)	Protein name/ Accession Number/ Molecular weight (Da)	Protein identification probability (%)	Exclusive unique peptide count	Exclusive unique spectrum count	Total spectrum count	Percentage of total spectra (%)	Percentage sequence coverage (%)	Previous amino acid	Peptide sequence	Next amino acid	Total TIC
01_87	Hypoxia up-regulated	100.0	12	15	22	1.42	15.8	K	AEAGPEGVAPAPEGEK	K	1082.62
	protein 1	100.0	12	15	22	1.42	15.8	R	DAVVYPILVEFTR	E	15328.5
	OS=Homo sapiens	100.0	12	15	22	1.42	15.8	K	EAGMQPQLQIR	G	10784.7
	GN=HYOU1 PE=1	100.0	12	15	22	1.42	15.8	R	FFGDSAASMAIK	N	13450.0
	SV=1	100.0	12	15	22	1.42	15.8	R	LAGLFNEQR	K	47571.6
	HYOU1_HUMAN	100.0	12	15	22	1.42	15.8	K	LGNTISSLFGGGTTPDAK	E	3680.73
	111336.8	100.0	12	15	22	1.42	15.8	K	LPATEKPVLLSK	D	3313.38
		100.0	12	15	22	1.42	15.8	R	RKTPVIVTLK	E	8149.75
		100.0	12	15	22	1.42	15.8	R	SLAEDFAEQPIK	D	4182.63
		100.0	12	15	22	1.42	15.8	R	TLGGLEMELR	L	31479.5
		100.0	12	15	22	1.42	15.8	K	VAIVKPGVPMEIVLNK	E	12456.2
		100.0	12	15	22	1.42	15.8	K	VLQLINDNTATALSYGVFR	R	1107.76
02_87	Hypoxia up-regulated	100.0	18	22	120	6.11	38.2	K	AANSLEAFIFETQDK	L	5650.20
	protein 1	100.0	18	22	120	6.11	38.2	K	AEAGPEGVAPAPEGEK	K	14547.1
	OS=Homo sapiens	100.0	18	22	120	6.11	38.2	K	DAVITVPVFFNQAER	R	5499.91
	GN=HYOU1 PE=1	100.0	18	22	120	6.11	38.2	R	DAVVYPILVEFTR	E	26725.7
	SV=1	100.0	18	22	120	6.11	38.2	K	EAGMQPQLQIR	G	85546.2
	HYOU1_HUMAN	100.0	18	22	120	6.11	38.2	R	EVQYLLNK	A	31749.3
	111336.8	100.0	18	22	120	6.11	38.2	R	FFGDSAASMAIK	N	67732.0
		100.0	18	22	120	6.11	38.2	R	FFGDSAASMAIKNPK	A	2843.37
		100.0	18	22	120	6.11	38.2	R	FPEHELTFDPQR	Q	70575.2
		100.0	18	22	120	6.11	38.2	R	KTPVIVTLKENER	F	21205.6
		100.0	18	22	120	6.11	38.2	R	LAGLFNEQR	K	252581
		100.0	18	22	120	6.11	38.2	R	LAGLFNEQRK	G	5672.16
		100.0	18	22	120	6.11	38.2	K	LCQGLFFR	V	43537.2
		100.0	18	22	120	6.11	38.2	K	LGNTISSLFGGGTTPDAK	E	26574.7
		100.0	18	22	120	6.11	38.2	R	LIPEMDQIFTEVEMTTLEK	V	13635.7
		100.0	18	22	120	6.11	38.2	K	LPATEKPVLLSK	D	165299
		100.0	18	22	120	6.11	38.2	K	LPATEKPVLLSKDIEAK	M	7800.34
		100.0	18	22	120	6.11	38.2	K	LQDLTLRDLEK	Q	8960.78
		100.0	18	22	120	6.11	38.2	K	LQDLTLRDLEKQER	E	10564.4
		100.0	18	22	120	6.11	38.2	K	LSAASTWLEDEGVGATTVMLK	E	6428.98
		100.0	18	22	120	6.11	38.2	K	MMALDREVQYLLNK	A	30014.1
		100.0	18	22	120	6.11	38.2	K	NINADEAAAMGAVYQAAALSK	A	50853.9
		100.0	18	22	120	6.11	38.2	K	QADNPHVALYQAR	F	60442.1
		100.0	18	22	120	6.11	38.2	R	RKTPVIVTLK	E	28008.2
		100.0	18	22	120	6.11	38.2	R	SLAEDFAEQPIK	D	8188.61
		100.0	18	22	120	6.11	38.2	K	TKEAGMQPQLQIR	G	18105.3
		100.0	18	22	120	6.11	38.2	R	TLGGLEMELR	L	278494
		100.0	18	22	120	6.11	38.2	K	TPVIVTLK	E	138363
		100.0	18	22	120	6.11	38.2	K	TPVIVTLKENER	F	15211.5
		100.0	18	22	120	6.11	38.2	K	TVLSANADHMAQIEGLMDDVDFK	A	1821.19
		100.0	18	22	120	6.11	38.2	K	TVLSANADHMAQIEGLMDDVDFKAK	V	12870.1
		100.0	18	22	120	6.11	38.2	K	VAIVKPGVPMEIVLNK	E	85808.8
		100.0	18	22	120	6.11	38.2	K	VAIVKPGVPMEIVLNKESR	R	12964.7
		100.0	18	22	120	6.11	38.2	R	VEFEELCADLFER	V	5883.95
		100.0	18	22	120	6.11	38.2	K	VLQLINDNTATALSYGVFR	R	17867.8
		100.0	18	22	120	6.11	38.2	K	VLQLINDNTATALSYGVFRR	K	2586.87
		100.0	18	22	120	6.11	38.2	R	VQEVLLK	A	233856
		100.0	18	22	120	6.11	38.2	R	YFQHLLGK	Q	62762.5
02_85	Hypoxia up-regulated	100.0	3	3	4	0.307	2.60	R	LAGLFNEQR	K	21789.4
	protein 1	100.0	3	3	4	0.307	2.60	R	TLGGLEMELR	L	10250.4
	1OS=Homo sapiens	100.0	3	3	4	0.307	2.60	R	VQEVLLK	A	15625.2
	GN=HYOU1 PE=1 SV=1	100.0	7	7	9	0.484	6.31	R	AVLQAAR	M	31162.5
	HYOU1_HUMAN	100.0	7	7	9	0.484	6.31	K	EAGMQPQLQIR	G	8687.39
	111336.8	100.0	7	7	9	0.484	6.31	R	LAGLFNEQR	K	55857.2
		100.0	7	7	9	0.484	6.31	K	LPATEKPVLLSK	D	5128.93
		100.0	7	7	9	0.484	6.31	R	MGPYPQR	K	19696.1
		100.0	7	7	9	0.484	6.31	R	TLGGLEMELR	L	22174.4
		100.0	7	7	9	0.484	6.31	R	VQEVLLK	A	50672.7
03_85	Hypoxia up-regulated	100.0	13	14	19	1.36	14.7	K	AEAGPEGVAPAPEGEK	K	2576.21
	protein 1	100.0	13	14	19	1.36	14.7	R	DAVVYPILVEFTR	E	6294.81
	OS=Homo sapiens	100.0	13	14	19	1.36	14.7	K	EAGMQPQLQIR	G	7091.33

	GN=HYOU1 PE=1 SV=1	100.0	13	14	19	1.36	14.7	R	FFGDSAASMAIK	N	6841.11
	HYOU1_HUMAN	100.0	13	14	19	1.36	14.7	R	FFGDSAASMAIKNPK	A	2315.59
	111336.8	100.0	13	14	19	1.36	14.7	R	LAGLFNEQR	K	41067.8
		100.0	13	14	19	1.36	14.7	K	LGNTISSLFGGGTTPDAK	E	7444.61
		100.0	13	14	19	1.36	14.7	K	LPATEKPVLLSK	D	3289.90
		100.0	13	14	19	1.36	14.7	K	LQDLTLR	D	15193.3
		100.0	13	14	19	1.36	14.7	K	QADNPHVALYQAR	F	1945.04
		100.0	13	14	19	1.36	14.7	R	TLGGLEMELR	L	39945.4
		100.0	13	14	19	1.36	14.7	K	VAIVKPGVPMEIVLNK	E	11016.9
		100.0	13	14	19	1.36	14.7	R	VQEVLLK	A	76208.7
03_87	Hypoxia up-regulated	100.0	31	45	103	5.49	32.6	K	AANSLEAFIFETQDK	L	4500.51
	protein 1	100.0	31	45	103	5.49	32.6	K	AEAGPEGVAPAPEGEK	K	12790.1
	OS=Homo sapiens	100.0	31	45	103	5.49	32.6	K	DAVITVPVFFNQAER	R	2236.92
	GN=HYOU1 PE=1 SV=1	100.0	31	45	103	5.49	32.6	R	DAVVYPILVEFTR	E	8674.78
	HYOU1_HUMAN	100.0	31	45	103	5.49	32.6	K	EAGMQPQLQIR	G	110314
	111336.8	100.0	31	45	103	5.49	32.6	R	EVQYLLNK	A	36628.9
		100.0	31	45	103	5.49	32.6	R	FFGDSAASMAIK	N	59173.6
		100.0	31	45	103	5.49	32.6	R	FFGDSAASMAIKNPK	A	90298.5
		100.0	31	45	103	5.49	32.6	R	FPEHELTFDPQR	Q	33838.9
		100.0	31	45	103	5.49	32.6	R	KTPVIVTLK	E	8687.94
		100.0	31	45	103	5.49	32.6	R	KTPVIVTLKENER	F	23749.4
		100.0	31	45	103	5.49	32.6	R	LAGLFNEQR	K	282495
		100.0	31	45	103	5.49	32.6	R	LAGLFNEQRK	G	17367.6
		100.0	31	45	103	5.49	32.6	K	LCQGLFFR	V	44912.7
		100.0	31	45	103	5.49	32.6	K	LGNTISSLFGGGTTPDAK	E	17911.5
		100.0	31	45	103	5.49	32.6	R	LIPEMDQIFTEVEMTTLEK	V	1929.88
		100.0	31	45	103	5.49	32.6	K	LPATEKPVLLSK	D	110611
		100.0	31	45	103	5.49	32.6	K	LQDLTLR	D	55571.2
		100.0	31	45	103	5.49	32.6	K	LQDLTLRDLEK	Q	5499.73
		100.0	31	45	103	5.49	32.6	K	LYQPEYQEVSTEEQREEISGK	L	4491.32
		100.0	31	45	103	5.49	32.6	K	NINADEAAAMGAVYQAAALSK	A	19564.8
		100.0	31	45	103	5.49	32.6	K	QADNPHVALYQAR	F	83955.1
		100.0	31	45	103	5.49	32.6	R	RKTPVIVTLK	E	39123.3
		100.0	31	45	103	5.49	32.6	R	SLAEDFAEQPIK	D	11221.6
		100.0	31	45	103	5.49	32.6	K	TKEAGMQPQLQIR	G	31737.9
		100.0	31	45	103	5.49	32.6	R	TLGGLEMELR	L	274167
		100.0	31	45	103	5.49	32.6	K	TPVIVTLK	E	82728.3
		100.0	31	45	103	5.49	32.6	K	TPVIVTLKENER	F	19545.2
		100.0	31	45	103	5.49	32.6	K	VAIVKPGVPMEIVLNK	E	83485.0
		100.0	31	45	103	5.49	32.6	K	VLQLINDNTATALSYGVFR	R	14971.8
		100.0	31	45	103	5.49	32.6	R	VQEVLLK	A	291861
		100.0	31	45	103	5.49	32.6	R	YFQHLLGK	Q	30668.6
04_81	Calpastatin	100.0	6	7	14	0.960	14.5	K	AAAPAPVSEAVCR	T	18217.4
	OS=Homo sapiens	100.0	6	7	14	0.960	14.5	K	CGEDDETIPSEYR	L	4064.49
	GN=CAST PE=1 SV=4	100.0	6	7	14	0.960	14.5	K	LAAAISEVVSQTPASTTQAGAPPR	D	5443.27
	ICAL_HUMAN	100.0	6	7	14	0.960	14.5	R	QAEPELDLR	S	61202.7
	76575.3	100.0	6	7	14	0.960	14.5	K	TKPQDMISAGGESVAGITAISGKPGDK	K	23564.6
		100.0	6	7	14	0.960	14.5	R	TSMCSIQSAPPEPATLK	G	2317.19
05_81	Calpastatin	100.0	5	6	10	0.740	10.7	K	AAAPAPVSEAVCR	T	16065.1
	OS=Homo sapiens	100.0	5	6	10	0.740	10.7	K	CGEDDETIPSEYR	L	7210.26
	GN=CAST PE=1 SV=4	100.0	5	6	10	0.740	10.7	K	LAAAISEVVSQTPASTTQAGAPPR	D	3023.16
	ICAL_HUMAN	100.0	5	6	10	0.740	10.7	R	QAEPELDLR	S	70935.4
	76575.3	100.0	5	6	10	0.740	10.7	R	TSMCSIQSAPPEPATLK	G	1529.63
05_82	Calpastatin	100.0	8	10	17	1.00	19.6	K	AAAPAPVSEAVCR	T	29033.2
	OS=Homo sapiens	100.0	8	10	17	1.00	19.6	K	CGEDDETIPSEYR	L	4477.09
	GN=CAST PE=1 SV=4	100.0	8	10	17	1.00	19.6	R	HLLDDNGQDKPVKPPTK	K	6989.31
	ICAL_HUMAN	100.0	8	10	17	1.00	19.6	K	LAAAISEVVSQTPASTTQAGAPPR	D	2846.82
	76575.3	100.0	8	10	17	1.00	19.6	R	QAEPELDLR	S	93029.4
		100.0	8	10	17	1.00	19.6	K	TEKEESTEVLKAQSAGTVR	S	11977.4
		100.0	8	10	17	1.00	19.6	K	TKPQDMISAGGESVAGITAISGKPGDK	K	14397.8
		100.0	8	10	17	1.00	19.6	R	TSMCSIQSAPPEPATLK	G	4101.67
06_81	Calpastatin	100.0	2	2	3	0.228	3.11	K	AAAPAPVSEAVCR	T	8071.36
	OS=Homo sapiens	100.0	2	2	3	0.228	3.11	R	QAEPELDLR	S	26651.3
	GN=CAST PE=1 SV=4	100.0	4	5	8	0.358	5.37	K	AAAPAPVSEAVCR	T	12548.2
	ICAL_HUMAN	100.0	4	5	8	0.358	5.37	K	LSVVHEK	K	10907.3
	76575.3	100.0	4	5	8	0.358	5.37	R	QAEPELDLR	S	65084.8
		100.0	4	5	8	0.358	5.37	R	SIKEVDEAK	A	7722.78
06_83	Calpastatin	100.0	5	5	7	0.481	12.7	K	AAAPAPVSEAVCR	T	8457.92
	OS=Homo sapiens	100.0	5	5	7	0.481	12.7	K	GTVPDDAVEALADSLGK	K	984.774
	GN=CAST PE=1 SV=4	100.0	5	5	7	0.481	12.7	K	LAAAISEVVSQTPASTTQAGAPPR	D	14116.8
	ICAL_HUMAN	100.0	5	5	7	0.481	12.7	R	QAEPELDLR	S	19290.0
	76575.3	100.0	5	5	7	0.481	12.7	K	TKPQDMISAGGESVAGITAISGKPGDK	K	6819.16
		100.0	3	3	4	0.197	6.50	K	AAAPAPVSEAVCR	T	3794.01
		100.0	3	3	4	0.197	6.50	K	LAAAISEVVSQTPASTTQAGAPPR	D	2209.71

		100.0	3	3	4	0.197	6.50	R	QAEPELDLR	S	24023.5
07_81	Heterogeneous nuclear	100.0	11	13	33	1.94	14.8	K	AVVVCPKDEDYK	Q	2973.67
	ribonucleoprotein U	100.0	11	13	33	1.94	14.8	K	DCEVVMMIGLPGAGK	T	2004.39
	OS=Homo sapiens	100.0	11	13	33	1.94	14.8	K	DIDIHEVR	I	16141.7
	GN=HNRNPU PE=1	100.0	11	13	33	1.94	14.8	K	DLPEHAVLK	M	14021.0
	SV=6	100.0	11	13	33	1.94	14.8	K	FIEIAAR	K	307604
	HNRPU_HUMAN	100.0	11	13	33	1.94	14.8	K	LNTLLQR	A	86636.2
	87918.5	100.0	11	13	33	1.94	14.8	K	MCLFAGFQR	K	16935.6
		100.0	11	13	33	1.94	14.8	R	NFILDQTNVSAAAQR	R	57880.7
		100.0	11	13	33	1.94	14.8	K	NGQDLGVAFK	I	79431.4
		100.0	11	13	33	1.94	14.8	K	SSGPTSLFAVTVAPPGAR	Q	51883.4
		100.0	11	13	33	1.94	14.8	K	YNILGTNTIMDK	M	36915.5
		100.0	11	13	33	1.94	14.8	K	AVVVCPKDEDYK	Q	2973.67
		100.0	11	13	33	1.94	14.8	K	DCEVVMMIGLPGAGK	T	2004.39
		100.0	11	13	33	1.94	14.8	K	DIDIHEVR	I	16141.7
		100.0	11	13	33	1.94	14.8	K	DLPEHAVLK	M	14021.0
		100.0	11	13	33	1.94	14.8	K	FIEIAAR	K	307604
		100.0	11	13	33	1.94	14.8	K	LNTLLQR	A	86636.2
		100.0	11	13	33	1.94	14.8	K	MCLFAGFQR	K	16935.6
		100.0	11	13	33	1.94	14.8	R	NFILDQTNVSAAAQR	R	57880.7
		100.0	11	13	33	1.94	14.8	K	NGQDLGVAFK	I	79431.4
		100.0	11	13	33	1.94	14.8	K	SSGPTSLFAVTVAPPGAR	Q	51883.4
		100.0	11	13	33	1.94	14.8	K	YNILGTNTIMDK	M	36915.5
07_82	Heterogeneous nuclear	100.0	3	3	5	0.488	4.85	K	FIEIAAR	K	4145.34
	ribonucleoprotein U	100.0	3	3	5	0.488	4.85	R	NFILDQTNVSAAAQR	R	1927.90
	OS=Homo sapiens	100.0	3	3	5	0.488	4.85	K	SSGPTSLFAVTVAPPGAR	Q	1623.11
	GN=HNRNPU PE=1	100.0	3	3	5	0.488	4.85	K	FIEIAAR	K	4145.34
	SV=6	100.0	3	3	5	0.488	4.85	R	NFILDQTNVSAAAQR	R	1927.90
	HNRPU_HUMAN	100.0	3	3	5	0.488	4.85	K	SSGPTSLFAVTVAPPGAR	Q	1623.11
	87918.5										
07_82	Kinesin-like protein KIF11	100.0	5	6	12	1.17	5.30	R	EAGNINQSLLTLGR	V	3001.37
	OS=Homo sapiens	100.0	5	6	12	1.17	5.30	K	IGAVEEELNR	V	5276.16
	GN=KIF11 PE=1 SV=2	100.0	5	6	12	1.17	5.30	K	LTDNGTEFSVK	V	2167.62
	KIF11_HUMAN	100.0	5	6	12	1.17	5.30	R	TTAATLMNAYSSR	S	14286.2
	119161.9	100.0	5	6	12	1.17	5.30	R	VITALVER	T	6855.18
08_81	Heterogeneous nuclear	100.0	13	15	33	1.79	20.1	K	AVVVCPKDEDYK	Q	1471.03
	ribonucleoprotein U	100.0	13	15	33	1.79	20.1	K	AVVVCPKDEDYKQR	T	6395.01
	OS=Homo sapiens	100.0	13	15	33	1.79	20.1	K	DCEVVMMIGLPGAGK	T	2186.91
	GN=HNRNPU PE=1	100.0	13	15	33	1.79	20.1	K	FIEIAAR	K	345384
	SV=6	100.0	13	15	33	1.79	20.1	R	GYFEYIEENK	Y	14482.3
	HNRPU_HUMAN	100.0	13	15	33	1.79	20.1	K	KAEVEGKDLPEHAVLK	M	10256.8
	87918.5	100.0	13	15	33	1.79	20.1	K	KDCEVVMMIGLPGAGK	T	19424.9
		100.0	13	15	33	1.79	20.1	K	LNTLLQR	A	73340.2
		100.0	13	15	33	1.79	20.1	R	LQAALDDEEAGGRPAMEPGNGS-LDLGGDSAGR	S	1806.05
		100.0	13	15	33	1.79	20.1	K	MCLFAGFQR	K	48209.1
		100.0	13	15	33	1.79	20.1	R	NFILDQTNVSAAAQR	R	67937.9
		100.0	13	15	33	1.79	20.1	K	NGQDLGVAFK	I	66414.7
		100.0	13	15	33	1.79	20.1	K	SSGPTSLFAVTVAPPGAR	Q	91970.4
		100.0	13	15	33	1.79	20.1	K	YNILGTNTIMDK	M	40380.1
08_83	Heterogeneous nuclear	100.0	4	4	7	0.669	5.70	K	FIEIAAR	K	19215.5
	ribonucleoprotein U	100.0	4	4	7	0.669	5.70	K	LNTLLQR	A	12902.1
	OS=Homo sapiens	100.0	4	4	7	0.669	5.70	R	NFILDQTNVSAAAQR	R	11531.5
	GN=HNRNPU PE=1	100.0	4	4	7	0.669	5.70	K	SSGPTSLFAVTVAPPGAR	Q	2696.56
	SV=6	100.0	4	4	7	0.669	5.70	K	FIEIAAR	K	19215.5
	HNRPU_HUMAN	100.0	4	4	7	0.669	5.70	K	LNTLLQR	A	12902.1
	87918.5	100.0	4	4	7	0.669	5.70	R	NFILDQTNVSAAAQR	R	11531.5
		100.0	4	4	7	0.669	5.70	K	SSGPTSLFAVTVAPPGAR	Q	2696.56
		100.0	2	2	8	0.444	3.27	R	NFILDQTNVSAAAQR	R	16819.7
		100.0	2	2	8	0.444	3.27	K	YNILGTNTIMDK	M	5766.88
		100.0	2	2	8	0.444	3.27	R	NFILDQTNVSAAAQR	R	16819.7
		100.0	2	2	8	0.444	3.27	K	YNILGTNTIMDK	M	5766.88
10_86	Heterogeneous nuclear	100.0	3	3	11	0.830	5.45	R	NFILDQTNVSAAAQR	R	14835.9
	ribonucleoprotein U	100.0	3	3	11	0.830	5.45	K	SSGPTSLFAVTVAPPGAR	Q	9478.37
	OS=Homo sapiens	100.0	3	3	11	0.830	5.45	K	YNILGTNTIMDK	M	6051.90
	GN=HNRNPU PE=1	100.0	3	3	11	0.830	5.45	R	NFILDQTNVSAAAQR	R	14835.9
	SV=6	100.0	3	3	11	0.830	5.45	K	SSGPTSLFAVTVAPPGAR	Q	9478.37
	HNRPU_HUMAN	100.0	3	3	11	0.830	5.45	K	YNILGTNTIMDK	M	6051.90
	87918.5										
10_86	Kinesin-like protein KIF11	100.0	4	5	9	0.679	3.98	K	IGAVEEELNR	V	3099.83
	OS=Homo sapiens	100.0	4	5	9	0.679	3.98	R	ILQDSLGGR	T	8390.10
	GN=KIF11 PE=1 SV=2	100.0	4	5	9	0.679	3.98	K	SYLYPSTLVR	T	7518.57
	KIF11_HUMAN	100.0	4	5	9	0.679	3.98	R	TTAATLMNAYSSR	S	12608.6
	119161.9										

11_81	Heterogeneous nuclear	100.0	6	8	15	1.13	9.45	K	FIEIAAR	K	10542.9
	ribonucleoprotein U	100.0	6	8	15	1.13	9.45	K	LNTLLQR	A	28321.2
	OS=Homo sapiens	100.0	6	8	15	1.13	9.45	K	MCLFAGFQR	K	36870.1
	GN=HNRNPU PE=1	100.0	6	8	15	1.13	9.45	R	NFILDQTNVSAAAQR	R	45101.0
	SV=6	100.0	6	8	15	1.13	9.45	K	NGQDLGVAFK	I	33075.7
	HNRPU_HUMAN	100.0	6	8	15	1.13	9.45	K	SSGPTSLFAVTVAPPGAR	Q	40896.8
	87918.5	100.0	6	8	15	1.13	9.45	K	YNILGTNTIMDK	M	3952.21
11_83	Heterogeneous nuclear	100.0	8	8	20	1.39	10.4	K	DIDIHEVR	I	10499.7
	ribonucleoprotein U	100.0	8	8	20	1.39	10.4	K	FIEIAAR	K	38019.8
	OS=Homo sapiens	100.0	8	8	20	1.39	10.4	K	LNTLLQR	A	29055.2
	GN=HNRNPU PE=1	100.0	8	8	20	1.39	10.4	K	MCLFAGFQR	K	21180.9
	SV=6	100.0	8	8	20	1.39	10.4	R	NFILDQTNVSAAAQR	R	21291.8
	HNRPU_HUMAN	100.0	8	8	20	1.39	10.4	K	NGQDLGVAFK	I	9074.96
	87918.5	100.0	8	8	20	1.39	10.4	K	SSGPTSLFAVTVAPPGAR	Q	18612.3
		100.0	8	8	20	1.39	10.4	K	YNILGTNTIMDK	M	7907.28
		100.0	8	8	20	1.39	10.4	K	DIDIHEVR	I	10499.7
		100.0	8	8	20	1.39	10.4	K	FIEIAAR	K	38019.8
		100.0	8	8	20	1.39	10.4	K	LNTLLQR	A	29055.2
		100.0	8	8	20	1.39	10.4	K	MCLFAGFQR	K	21180.9
		100.0	8	8	20	1.39	10.4	R	NFILDQTNVSAAAQR	R	21291.8
		100.0	8	8	20	1.39	10.4	K	NGQDLGVAFK	I	9074.96
		100.0	8	8	20	1.39	10.4	K	SSGPTSLFAVTVAPPGAR	Q	18612.3
		100.0	8	8	20	1.39	10.4	K	YNILGTNTIMDK	M	7907.28
13_82	Endoplasmin	100.0	10	10	21	1.75	15.3	K	DISTNYYASQK	K	6718.78
	OS=Homo sapiens	100.0	10	10	21	1.75	15.3	R	ELISNASDALDK	I	5193.88
	GN=HSP90B1 PE=1	100.0	10	10	21	1.75	15.3	R	ELISNASDALDKIR	L	7490.28
	SV=1	100.0	10	10	21	1.75	15.3	K	FAFQAEVNR	M	61152.3
	ENPL_HUMAN	100.0	10	10	21	1.75	15.3	R	GLFDEYGSK	K	16613.6
	92583.9	100.0	10	10	21	1.75	15.3	K	GVVDSDDLPLNVSR	E	16198.1
		100.0	10	10	21	1.75	15.3	K	IYFMAGSSR	K	16391.6
		100.0	10	10	21	1.75	15.3	K	LIINSLYK	N	28351.8
		100.0	10	10	21	1.75	15.3	R	LISLTDENALSGNEELTVK	I	2577.26
		100.0	10	10	21	1.75	15.3	R	LSLNIDPDAK	V	13381.3
		100.0	10	10	21	1.75	15.3	R	SGYLLPDTK	A	32128.2
		100.0	10	10	21	1.75	15.3	K	SILFVPTSAPR	G	60201.6
		100.0	10	10	21	1.75	15.3	K	DISTNYYASQK	K	6718.78
		100.0	10	10	21	1.75	15.3	R	ELISNASDALDK	I	5193.88
		100.0	10	10	21	1.75	15.3	R	ELISNASDALDKIR	L	7490.28
		100.0	10	10	21	1.75	15.3	K	FAFQAEVNR	M	61152.3
		100.0	10	10	21	1.75	15.3	R	GLFDEYGSK	K	16613.6
		100.0	10	10	21	1.75	15.3	K	GVVDSDDLPLNVSR	E	16198.1
		100.0	10	10	21	1.75	15.3	K	IYFMAGSSR	K	16391.6
		100.0	10	10	21	1.75	15.3	K	LIINSLYK	N	28351.8
		100.0	10	10	21	1.75	15.3	R	LISLTDENALSGNEELTVK	I	2577.26
		100.0	10	10	21	1.75	15.3	R	LSLNIDPDAK	V	13381.3
		100.0	10	10	21	1.75	15.3	R	SGYLLPDTK	A	32128.2
		100.0	10	10	21	1.75	15.3	K	SILFVPTSAPR	G	60201.6
		100.0	10	10	21	1.75	15.3	K	DISTNYYASQK	K	6718.78
		100.0	10	10	21	1.75	15.3	R	ELISNASDALDK	I	5193.88
		100.0	10	10	21	1.75	15.3	R	ELISNASDALDKIR	L	7490.28
		100.0	10	10	21	1.75	15.3	K	FAFQAEVNR	M	61152.3
		100.0	10	10	21	1.75	15.3	R	GLFDEYGSK	K	16613.6
		100.0	10	10	21	1.75	15.3	K	GVVDSDDLPLNVSR	E	16198.1
		100.0	10	10	21	1.75	15.3	K	IYFMAGSSR	K	16391.6
		100.0	10	10	21	1.75	15.3	K	LIINSLYK	N	28351.8
		100.0	10	10	21	1.75	15.3	R	LISLTDENALSGNEELTVK	I	2577.26
		100.0	10	10	21	1.75	15.3	R	LSLNIDPDAK	V	13381.3
		100.0	10	10	21	1.75	15.3	R	SGYLLPDTK	A	32128.2
		100.0	10	10	21	1.75	15.3	K	SILFVPTSAPR	G	60201.6
13_83	Endoplasmin	100.0	11	11	23	1.97	17.1	K	DISTNYYASQK	K	3105.32
	OS=Homo sapiens	100.0	11	11	23	1.97	17.1	K	EAESSPFVER	L	12233.1
	GN=HSP90B1 PE=1	100.0	11	11	23	1.97	17.1	R	ELISNASDALDK	I	22457.0
	SV=1	100.0	11	11	23	1.97	17.1	K	FAFQAEVNR	M	53157.1
	ENPL_HUMAN	100.0	11	11	23	1.97	17.1	R	GLFDEYGSK	K	44445.2
	92583.9	100.0	11	11	23	1.97	17.1	K	GVVDSDDLPLNVSR	E	15379.0
		100.0	11	11	23	1.97	17.1	K	IYFMAGSSR	K	25367.4
		100.0	11	11	23	1.97	17.1	K	LIINSLYK	N	49097.6
		100.0	11	11	23	1.97	17.1	R	LISLTDENALSGNEELTVK	I	2913.54
		100.0	11	11	23	1.97	17.1	R	LSLNIDPDAK	V	28159.0
		100.0	11	11	23	1.97	17.1	K	SILFVPTSAPR	G	50426.0
		100.0	11	11	23	1.97	17.1	K	YSQFINFPIYVWSSK	T	5766.47
		100.0	11	11	23	1.97	17.1	K	DISTNYYASQK	K	3105.32
		100.0	11	11	23	1.97	17.1	K	EAESSPFVER	L	12233.1
		100.0	11	11	23	1.97	17.1	R	ELISNASDALDK	I	22457.0

		100.0	11	11	23	1.97	17.1	K	FAFQAEVNR	M	53157.1
		100.0	11	11	23	1.97	17.1	R	GLFDEYGSK	K	44445.2
		100.0	11	11	23	1.97	17.1	K	GVVDSDDLPLNVSR	E	15379.0
		100.0	11	11	23	1.97	17.1	K	IYFMAGSSR	K	25367.4
		100.0	11	11	23	1.97	17.1	K	LIINSLYK	N	49097.6
		100.0	11	11	23	1.97	17.1	R	LISLTDENALSGNEELTVK	I	2913.54
		100.0	11	11	23	1.97	17.1	R	LSLNIDPDAK	V	28159.0
		100.0	11	11	23	1.97	17.1	K	SILFVPTSAPR	G	50426.0
		100.0	11	11	23	1.97	17.1	K	YSQFINFPIYVWSSK	T	5766.47
		100.0	11	11	23	1.97	17.1	K	DISTNYYASQK	K	3105.32
		100.0	11	11	23	1.97	17.1	K	EAESSPFVER	L	12233.1
		100.0	11	11	23	1.97	17.1	R	ELISNASDALDK	I	22457.0
		100.0	11	11	23	1.97	17.1	K	FAFQAEVNR	M	53157.1
		100.0	11	11	23	1.97	17.1	R	GLFDEYGSK	K	44445.2
		100.0	11	11	23	1.97	17.1	K	GVVDSDDLPLNVSR	E	15379.0
		100.0	11	11	23	1.97	17.1	K	IYFMAGSSR	K	25367.4
		100.0	11	11	23	1.97	17.1	K	LIINSLYK	N	49097.6
		100.0	11	11	23	1.97	17.1	R	LISLTDENALSGNEELTVK	I	2913.54
		100.0	11	11	23	1.97	17.1	R	LSLNIDPDAK	V	28159.0
		100.0	11	11	23	1.97	17.1	K	SILFVPTSAPR	G	50426.0
		100.0	11	11	23	1.97	17.1	K	YSQFINFPIYVWSSK	T	5766.47
16_85	Eukaryotic peptide chain release factor GTP-binding subunit ERF3A OS=Homo sapiens GN=GSPT1 PE=1 SV=1 ERF3A_HUMAN 55756.7	100.0	1	1	4	0.194	5.81	R	FVKQDQVCIAR	L	3401.47
		100.0	1	1	4	0.194	5.81	K	LESGSICK	G	15694.7
		100.0	1	1	4	0.194	5.81	K	SVVAPPGAPK	K	53255.9
17_83	Eukaryotic peptide chain release factor GTP-binding subunit ERF3A OS=Homo sapiens GN=GSPT1 PE=1 SV=1 ERF3A_HUMAN 55756.7	100.0	5	6	8	0.538	12.8	R	FVKQDQVCIAR	L	12859.6
		100.0	5	6	8	0.538	12.8	K	HLIVLINK	M	11622.9
		100.0	5	6	8	0.538	12.8	K	SFVPNMIGGASQADLAVLVISAR	K	1959.87
		100.0	5	6	8	0.538	12.8	K	SVVAPPGAPK	K	13727.6
		100.0	5	6	8	0.538	12.8	R	TFDAQIVIIEHK	S	8094.16
17_85	Eukaryotic peptide chain release factor GTP-binding subunit ERF3A OS=Homo sapiens GN=GSPT1 PE=1 SV=1 ERF3A_HUMAN 55756.7	100.0	1	1	6	0.346	6.21	R	FVKQDQVCIAR	L	5774.45
		100.0	1	1	6	0.346	6.21	K	GQQLVMMPNK	H	8116.37
		100.0	1	1	6	0.346	6.21	K	SVVAPPGAPK	K	106037
18_81	78 kDa glucose-regulated protein OS=Homo sapiens GN=HSPA5 PE=1 SV=2 GRP78_HUMAN 72334.7	100.0	13	14	42	3.07	29.7	K	DAGTIAGLNVMR	I	31252.1
		100.0	13	14	42	3.07	29.7	K	ELEEIVQPIISK	L	9278.14
		100.0	13	14	42	3.07	29.7	K	FEELNMDLFR	S	4559.14
		100.0	13	14	42	3.07	29.7	R	IINEPTAAAIAYGLDKR	E	18854.4
		100.0	13	14	42	3.07	29.7	R	ITPSYVAFTPEGER	L	21989.0
		100.0	13	14	42	3.07	29.7	R	LTPEEIER	M	22142.2
		100.0	13	14	42	3.07	29.7	K	LYGSAGPPPTGEEDTAEKDEL	-	2912.46
		100.0	13	14	42	3.07	29.7	R	NELESYAYSLK	N	10367.5
		100.0	13	14	42	3.07	29.7	K	NQLTSNPENTVFDAK	R	5916.97
		100.0	13	14	42	3.07	29.7	K	SDIDEIVLVGGSTR	I	3107.99
		100.0	13	14	42	3.07	29.7	K	SQIFSTASDNQPTVTIK	V	13635.8
		100.0	13	14	42	3.07	29.7	K	TFAPEEISAMVLTK	M	23901.6
		100.0	13	14	42	3.07	29.7	R	TWNDPSVQQDIK	F	7502.17
		100.0	13	14	42	3.07	29.7	K	VTHAVVTVPAYFNDAQR	Q	13682.0
18_82	78 kDa glucose-regulated protein OS=Homo sapiens GN=HSPA5 PE=1 SV=2 GRP78_HUMAN 72334.7	100.0	11	12	34	2.30	23.4	K	DAGTIAGLNVMR	I	31747.6
		100.0	11	12	34	2.30	23.4	K	ELEEIVQPIISK	L	13225.0
		100.0	11	12	34	2.30	23.4	R	ITPSYVAFTPEGER	L	12236.2
		100.0	11	12	34	2.30	23.4	R	LTPEEIER	M	17882.8
		100.0	11	12	34	2.30	23.4	K	LYGSAGPPPTGEEDTAEKDEL	-	625.841
		100.0	11	12	34	2.30	23.4	R	NELESYAYSLK	N	5390.78
		100.0	11	12	34	2.30	23.4	K	NQLTSNPENTVFDAK	R	5491.05
		100.0	11	12	34	2.30	23.4	K	SQIFSTASDNQPTVTIK	V	9759.83
		100.0	11	12	34	2.30	23.4	K	TFAPEEISAMVLTK	M	27664.9
		100.0	11	12	34	2.30	23.4	R	TWNDPSVQQDIK	F	5513.85
		100.0	11	12	34	2.30	23.4	K	VTHAVVTVPAYFNDAQR	Q	13301.6
19_83	Cluster of 78 kDa glucose-regulated protein OS=Homo sapiens GN=HSPA5 PE=1 SV=2	100.0	8	12	160	4.80	47.1	R	ARFEELNADLFR	G	57705.2
		100.0	8	12	160	4.80	47.1	K	DAGTIAGLNVLR	I	1071240
		100.0	8	12	160	4.80	47.1	K	ELEKVCNPIITK	L	3573.53
		100.0	8	12	160	4.80	47.1	R	FDDAVVQSDMK	H	36424.1

GRP78_HUMAN	100.0	8	12	160	4.80	47.1	R	FEELNADLFR	G	105587
70899.8	100.0	8	12	160	4.80	47.1	R	FEELNADLFRGTLDPVEK	A	6120.61
	100.0	8	12	160	4.80	47.1	R	GTLDPVEK	A	20824.7
	100.0	8	12	160	4.80	47.1	R	GTLDPVEKALR	D	18168.2
	100.0	8	12	160	4.80	47.1	R	IINEPTAAAIAYGLDK	K	84320.5
	100.0	8	12	160	4.80	47.1	R	IINEPTAAAIAYGLDKK	V	1236620
	100.0	8	12	160	4.80	47.1	R	LIGDAAKNQVAMNPTNTVFDAK	R	45340.3
	100.0	8	12	160	4.80	47.1	R	LIGDAAKNQVAMNPTNTVFDAKR	L	13404.3
	100.0	8	12	160	4.80	47.1	K	LLQDFFNGK	E	89352.0
	100.0	8	12	160	4.80	47.1	K	LYQSAGGMPGGMPGGFPGGGA-PPSGGASSGPTIEEVD	-	7948.91
	100.0	8	12	160	4.80	47.1	K	MKEIAEAYLGK	T	169529
	100.0	8	12	160	4.80	47.1	R	MVNHFIAEFK	R	189299
	100.0	8	12	160	4.80	47.1	R	MVNHFIAEFKR	K	31344.0
	100.0	8	12	160	4.80	47.1	K	NQVAMNPTNTVFDAK	R	181123
	100.0	8	12	160	4.80	47.1	K	NQVAMNPTNTVFDAKR	L	298085
	100.0	8	12	160	4.80	47.1	K	NSLESYAFNMK	A	484579
	100.0	8	12	160	4.80	47.1	R	QATKDAGTIAGLNVLR	I	224485
	100.0	8	12	160	4.80	47.1	K	QTQTFTTYSDNQPGVLIQVYEGER	A	3132.63
	100.0	8	12	160	4.80	47.1	R	RFDDAVVQSDMK	H	2014.24
	100.0	8	12	160	4.80	47.1	K	SFYPEEVSSMVLTK	M	142231
	100.0	8	12	160	4.80	47.1	K	SINPDEAVAYGAAVQAAILSGDK	S	16354.5
	100.0	8	12	160	4.80	47.1	K	SQIHDIVLVGGSTR	I	3492.94
	100.0	8	12	160	4.80	47.1	K	STAGDTHLGGEDFDNR	M	161268
	100.0	8	12	160	4.80	47.1	R	TTPSYVAFTDTER	L	818982
	100.0	8	12	160	4.80	47.1	K	TVTNAVVTVPAYFNDSQR	Q	320870
	100.0	8	12	160	4.80	47.1	K	VCNPIITK	L	858696
	100.0	8	12	160	4.80	47.1	R	ARFEELNADLFR	G	57705.2
	100.0	8	12	160	4.80	47.1	K	DAGTIAGLNVLR	I	1071240
	100.0	8	12	160	4.80	47.1	K	ELEKVCNPIITK	L	3573.53
	100.0	8	12	160	4.80	47.1	R	FDDAVVQSDMK	H	36424.1
	100.0	8	12	160	4.80	47.1	R	FEELNADLFR	G	105587
	100.0	8	12	160	4.80	47.1	R	FEELNADLFRGTLDPVEK	A	6120.61
	100.0	8	12	160	4.80	47.1	R	GTLDPVEK	A	20824.7
	100.0	8	12	160	4.80	47.1	R	GTLDPVEKALR	D	18168.2
	100.0	8	12	160	4.80	47.1	R	IINEPTAAAIAYGLDK	K	84320.5
	100.0	8	12	160	4.80	47.1	R	IINEPTAAAIAYGLDKK	V	1236620
	100.0	8	12	160	4.80	47.1	R	LIGDAAKNQVAMNPTNTVFDAK	R	45340.3
	100.0	8	12	160	4.80	47.1	R	LIGDAAKNQVAMNPTNTVFDAKR	L	13404.3
	100.0	8	12	160	4.80	47.1	K	LLQDFFNGK	E	89352.0
	100.0	8	12	160	4.80	47.1	K	LYQSAGGMPGGMPGGFPGGGA-PPSGGASSGPTIEEVD	-	7948.91
	100.0	8	12	160	4.80	47.1	K	MKEIAEAYLGK	T	169529
	100.0	8	12	160	4.80	47.1	R	MVNHFIAEFK	R	189299
	100.0	8	12	160	4.80	47.1	R	MVNHFIAEFKR	K	31344.0
	100.0	8	12	160	4.80	47.1	K	NQVAMNPTNTVFDAK	R	181123
	100.0	8	12	160	4.80	47.1	K	NQVAMNPTNTVFDAKR	L	298085
	100.0	8	12	160	4.80	47.1	K	NSLESYAFNMK	A	484579
	100.0	8	12	160	4.80	47.1	R	QATKDAGTIAGLNVLR	I	224485
	100.0	8	12	160	4.80	47.1	K	QTQTFTTYSDNQPGVLIQVYEGER	A	3132.63
	100.0	8	12	160	4.80	47.1	R	RFDDAVVQSDMK	H	2014.24
	100.0	8	12	160	4.80	47.1	K	SFYPEEVSSMVLTK	M	142231
	100.0	8	12	160	4.80	47.1	K	SINPDEAVAYGAAVQAAILSGDK	S	16354.5
	100.0	8	12	160	4.80	47.1	K	SQIHDIVLVGGSTR	I	3492.94
	100.0	8	12	160	4.80	47.1	K	STAGDTHLGGEDFDNR	M	161268
	100.0	8	12	160	4.80	47.1	R	TTPSYVAFTDTER	L	818982
	100.0	8	12	160	4.80	47.1	K	TVTNAVVTVPAYFNDSQR	Q	320870
	100.0	8	12	160	4.80	47.1	K	VCNPIITK	L	858696
	100.0	8	12	160	4.80	47.1	R	ARFEELNADLFR	G	57705.2
	100.0	8	12	160	4.80	47.1	K	DAGTIAGLNVLR	I	1071240
	100.0	8	12	160	4.80	47.1	K	ELEKVCNPIITK	L	3573.53
	100.0	8	12	160	4.80	47.1	R	FDDAVVQSDMK	H	36424.1
	100.0	8	12	160	4.80	47.1	R	FEELNADLFR	G	105587
	100.0	8	12	160	4.80	47.1	R	FEELNADLFRGTLDPVEK	A	6120.61
	100.0	8	12	160	4.80	47.1	R	GTLDPVEK	A	20824.7
	100.0	8	12	160	4.80	47.1	R	GTLDPVEKALR	D	18168.2
	100.0	8	12	160	4.80	47.1	R	IINEPTAAAIAYGLDK	K	84320.5
	100.0	8	12	160	4.80	47.1	R	IINEPTAAAIAYGLDKK	V	1236620
	100.0	8	12	160	4.80	47.1	R	LIGDAAKNQVAMNPTNTVFDAK	R	45340.3
	100.0	8	12	160	4.80	47.1	R	LIGDAAKNQVAMNPTNTVFDAKR	L	13404.3
	100.0	8	12	160	4.80	47.1	K	LLQDFFNGK	E	89352.0
	100.0	8	12	160	4.80	47.1	K	LYQSAGGMPGGMPGGFPGGGA-PPSGGASSGPTIEEVD	-	7948.91
	100.0	8	12	160	4.80	47.1	K	MKEIAEAYLGK	T	169529
	100.0	8	12	160	4.80	47.1	R	MVNHFIAEFK	R	189299

100.0	8	12	160	4.80	47.1	R	MVNHFIAEFKR	K	31344.0
100.0	8	12	160	4.80	47.1	K	NQVAMNPTNTVFDAK	R	181123
100.0	8	12	160	4.80	47.1	K	NQVAMNPTNTVFDAKR	L	298085
100.0	8	12	160	4.80	47.1	K	NSLESYAFNMK	A	484579
100.0	8	12	160	4.80	47.1	R	QATKDAGTIAGLNVLR	I	224485
100.0	8	12	160	4.80	47.1	K	QTQTFTTYSDNQPGVLIQVYEGER	A	3132.63
100.0	8	12	160	4.80	47.1	R	RFDDAVVQSDMK	H	2014.24
100.0	8	12	160	4.80	47.1	K	SFYPEEVSSMVLTK	M	142231
100.0	8	12	160	4.80	47.1	K	SINPDEAVAYGAAVQAAILSGDK	S	16354.5
100.0	8	12	160	4.80	47.1	K	SQIHDIVLVGGSTR	I	3492.94
100.0	8	12	160	4.80	47.1	K	STAGDTHLGGEDFDNR	M	161268
100.0	8	12	160	4.80	47.1	R	TTPSYVAFTDTER	L	818982
100.0	8	12	160	4.80	47.1	K	TVTNAVVTVPAYFNDSQR	Q	320870
100.0	8	12	160	4.80	47.1	K	VCNPIITK	L	858696
100.0	8	12	160	4.80	47.1	R	ARFEELNADLFR	G	57705.2
100.0	8	12	160	4.80	47.1	K	DAGTIAGLNVLR	I	1071240
100.0	8	12	160	4.80	47.1	K	ELEKVCNPIITK	L	3573.53
100.0	8	12	160	4.80	47.1	R	FDDAVVQSDMK	H	36424.1
100.0	8	12	160	4.80	47.1	R	FEELNADLFR	G	105587
100.0	8	12	160	4.80	47.1	R	FEELNADLFRGTLDPVEK	A	6120.61
100.0	8	12	160	4.80	47.1	R	GTLDPVEK	A	20824.7
100.0	8	12	160	4.80	47.1	R	GTLDPVEKALR	D	18168.2
100.0	8	12	160	4.80	47.1	R	IINEPTAAAIAYGLDK	K	84320.5
100.0	8	12	160	4.80	47.1	R	IINEPTAAAIAYGLDKK	V	1236620
100.0	8	12	160	4.80	47.1	R	LIGDAAKNQVAMNPTNTVFDAK	R	45340.3
100.0	8	12	160	4.80	47.1	R	LIGDAAKNQVAMNPTNTVFDAKR	L	13404.3
100.0	8	12	160	4.80	47.1	K	LLQDFFNGK	E	89352.0
100.0	8	12	160	4.80	47.1	K	LYQSAGGMPGGMPGGFPGGGA-PPSGGASSGPTIEEVD	-	7948.91
100.0	8	12	160	4.80	47.1	K	MKEIAEAYLGK	T	169529
100.0	8	12	160	4.80	47.1	R	MVNHFIAEFK	R	189299
100.0	8	12	160	4.80	47.1	R	MVNHFIAEFKR	K	31344.0
100.0	8	12	160	4.80	47.1	K	NQVAMNPTNTVFDAK	R	181123
100.0	8	12	160	4.80	47.1	K	NQVAMNPTNTVFDAKR	L	298085
100.0	8	12	160	4.80	47.1	K	NSLESYAFNMK	A	484579
100.0	8	12	160	4.80	47.1	R	QATKDAGTIAGLNVLR	I	224485
100.0	8	12	160	4.80	47.1	K	QTQTFTTYSDNQPGVLIQVYEGER	A	3132.63
100.0	8	12	160	4.80	47.1	R	RFDDAVVQSDMK	H	2014.24
100.0	8	12	160	4.80	47.1	K	SFYPEEVSSMVLTK	M	142231
100.0	8	12	160	4.80	47.1	K	SINPDEAVAYGAAVQAAILSGDK	S	16354.5
100.0	8	12	160	4.80	47.1	K	SQIHDIVLVGGSTR	I	3492.94
100.0	8	12	160	4.80	47.1	K	STAGDTHLGGEDFDNR	M	161268
100.0	8	12	160	4.80	47.1	R	TTPSYVAFTDTER	L	818982
100.0	8	12	160	4.80	47.1	K	TVTNAVVTVPAYFNDSQR	Q	320870
100.0	8	12	160	4.80	47.1	K	VCNPIITK	L	858696
100.0	8	12	160	4.80	47.1	R	ARFEELNADLFR	G	57705.2
100.0	8	12	160	4.80	47.1	K	DAGTIAGLNVLR	I	1071240
100.0	8	12	160	4.80	47.1	K	ELEKVCNPIITK	L	3573.53
100.0	8	12	160	4.80	47.1	R	FDDAVVQSDMK	H	36424.1
100.0	8	12	160	4.80	47.1	R	FEELNADLFR	G	105587
100.0	8	12	160	4.80	47.1	R	FEELNADLFRGTLDPVEK	A	6120.61
100.0	8	12	160	4.80	47.1	R	GTLDPVEK	A	20824.7
100.0	8	12	160	4.80	47.1	R	GTLDPVEKALR	D	18168.2
100.0	8	12	160	4.80	47.1	R	IINEPTAAAIAYGLDK	K	84320.5
100.0	8	12	160	4.80	47.1	R	IINEPTAAAIAYGLDKK	V	1236620
100.0	8	12	160	4.80	47.1	R	LIGDAAKNQVAMNPTNTVFDAK	R	45340.3
100.0	8	12	160	4.80	47.1	R	LIGDAAKNQVAMNPTNTVFDAKR	L	13404.3
100.0	8	12	160	4.80	47.1	K	LLQDFFNGK	E	89352.0
100.0	8	12	160	4.80	47.1	K	LYQSAGGMPGGMPGGFPGGGA-PPSGGASSGPTIEEVD	-	7948.91
100.0	8	12	160	4.80	47.1	K	MKEIAEAYLGK	T	169529
100.0	8	12	160	4.80	47.1	R	MVNHFIAEFK	R	189299
100.0	8	12	160	4.80	47.1	R	MVNHFIAEFKR	K	31344.0
100.0	8	12	160	4.80	47.1	K	NQVAMNPTNTVFDAK	R	181123
100.0	8	12	160	4.80	47.1	K	NQVAMNPTNTVFDAKR	L	298085
100.0	8	12	160	4.80	47.1	K	NSLESYAFNMK	A	484579
100.0	8	12	160	4.80	47.1	R	QATKDAGTIAGLNVLR	I	224485
100.0	8	12	160	4.80	47.1	K	QTQTFTTYSDNQPGVLIQVYEGER	A	3132.63
100.0	8	12	160	4.80	47.1	R	RFDDAVVQSDMK	H	2014.24
100.0	8	12	160	4.80	47.1	K	SFYPEEVSSMVLTK	M	142231
100.0	8	12	160	4.80	47.1	K	SINPDEAVAYGAAVQAAILSGDK	S	16354.5
100.0	8	12	160	4.80	47.1	K	SQIHDIVLVGGSTR	I	3492.94
100.0	8	12	160	4.80	47.1	K	STAGDTHLGGEDFDNR	M	161268
100.0	8	12	160	4.80	47.1	R	TTPSYVAFTDTER	L	818982
100.0	8	12	160	4.80	47.1	K	TVTNAVVTVPAYFNDSQR	Q	320870

		100.0	8	12	160	4.80	47.1	K	VCNPIITK	L	858696
19_85	Cluster of 78 kDa	100.0	3	5	198	5.53	53.3	D	AGTIAGLNVLR	I	35954.6
	glucose-regulated protein	100.0	3	5	198	5.53	53.3	R	ARFEELNADLFR	G	178862
	OS=Homo sapiens	100.0	3	5	198	5.53	53.3	R	ARFEELNADLFRGTLDPVEK	A	20125.3
	GN=HSPA5 PE=1 SV=2	100.0	3	5	198	5.53	53.3	K	DAGTIAGLNVLR	I	1507150
	GRP78_HUMAN	100.0	3	5	198	5.53	53.3	R	DAKLDKSQIHDIVLVGGSTR	I	21885.1
	70899.8	100.0	3	5	198	5.53	53.3	K	EIAEAYLGK	T	56021.2
		100.0	3	5	198	5.53	53.3	K	ELEKVCNPIITK	L	16716.9
		100.0	3	5	198	5.53	53.3	R	FDDAVVQSDMK	H	25449.7
		100.0	3	5	198	5.53	53.3	R	FEELNADLFR	G	206924
		100.0	3	5	198	5.53	53.3	R	FEELNADLFRGTLDPVEK	A	33554.6
		100.0	3	5	198	5.53	53.3	K	GPAVGIDLGTTYSCVGVFQHGK	V	24050.9
		100.0	3	5	198	5.53	53.3	R	GTLDPVEK	A	21995.8
		100.0	3	5	198	5.53	53.3	R	GTLDPVEKALR	D	30712.5
		100.0	3	5	198	5.53	53.3	R	IINEPTAAAIAYGLDK	K	75894.6
		100.0	3	5	198	5.53	53.3	R	IINEPTAAAIAYGLDKK	V	34158.3
		100.0	3	5	198	5.53	53.3	K	IQKLLQDFFNGK	E	6110.08
		100.0	3	5	198	5.53	53.3	K	LDKSQIHDIVLVGGSTR	I	164671
		100.0	3	5	198	5.53	53.3	K	LLQDFFNGK	E	130246
		100.0	3	5	198	5.53	53.3	K	LYQSAGGMPGGMPGGFPGGG-APPSGGASSGPTIEEVD	-	12499.7
		100.0	3	5	198	5.53	53.3	K	MKEIAEAYLGK	T	211286
		100.0	3	5	198	5.53	53.3	R	MVNHFIAEFK	R	321290
		100.0	3	5	198	5.53	53.3	K	NQVAMNPTNTVFDAK	R	222606
		100.0	3	5	198	5.53	53.3	K	NQVAMNPTNTVFDAKR	L	378008
		100.0	3	5	198	5.53	53.3	K	NSLESYAFNMK	A	724779
		100.0	3	5	198	5.53	53.3	R	QATKDAGTIAGLNVLR	I	532863
		100.0	3	5	198	5.53	53.3	K	QTQTFTTYSDNQPGVLIQVYEGER	A	14099.3
		100.0	3	5	198	5.53	53.3	R	RFDDAVVQSDMK	H	7451.11
		100.0	3	5	198	5.53	53.3	K	SFYPEEVSSMVLTK	M	337807
		100.0	3	5	198	5.53	53.3	K	SINPDEAVAYGAAVQAAILSGDK	S	10752.5
		100.0	3	5	198	5.53	53.3	M	SKGPAVGIDLGTTYSCVGVFQHGK	V	28845.8
		100.0	3	5	198	5.53	53.3	K	SQIHDIVLVGGSTR	I	59176.1
		100.0	3	5	198	5.53	53.3	K	STAGDTHLGGEDFDNR	M	142279
		100.0	3	5	198	5.53	53.3	R	TTPSYVAFTDTER	L	1005850
		100.0	3	5	198	5.53	53.3	K	TVTNAVVTVPAYFNDSQR	Q	516618
		100.0	3	5	198	5.53	53.3	K	TVTNAVVTVPAYFNDSQRQATK	D	10127.4
		100.0	3	5	198	5.53	53.3	K	VCNPIITK	L	502970
		100.0	3	5	198	5.53	53.3	K	VEIIANDQGNRTTPSYVAFTDTER	L	16190.8
		100.0	3	5	198	5.53	53.3	K	VSSKNSLESYAFNMK	A	45713.6
		100.0	3	5	198	5.53	53.3	D	AGTIAGLNVLR	I	35954.6
		100.0	3	5	198	5.53	53.3	R	ARFEELNADLFR	G	178862
		100.0	3	5	198	5.53	53.3	R	ARFEELNADLFRGTLDPVEK	A	20125.3
		100.0	3	5	198	5.53	53.3	K	DAGTIAGLNVLR	I	1507150
		100.0	3	5	198	5.53	53.3	R	DAKLDKSQIHDIVLVGGSTR	I	21885.1
		100.0	3	5	198	5.53	53.3	K	EIAEAYLGK	T	56021.2
		100.0	3	5	198	5.53	53.3	K	ELEKVCNPIITK	L	16716.9
		100.0	3	5	198	5.53	53.3	R	FDDAVVQSDMK	H	25449.7
		100.0	3	5	198	5.53	53.3	R	FEELNADLFR	G	206924
		100.0	3	5	198	5.53	53.3	R	FEELNADLFRGTLDPVEK	A	33554.6
		100.0	3	5	198	5.53	53.3	K	GPAVGIDLGTTYSCVGVFQHGK	V	24050.9
		100.0	3	5	198	5.53	53.3	R	GTLDPVEK	A	21995.8
		100.0	3	5	198	5.53	53.3	R	GTLDPVEKALR	D	30712.5
		100.0	3	5	198	5.53	53.3	R	IINEPTAAAIAYGLDK	K	75894.6
		100.0	3	5	198	5.53	53.3	R	IINEPTAAAIAYGLDKK	V	34158.3
		100.0	3	5	198	5.53	53.3	K	IQKLLQDFFNGK	E	6110.08
		100.0	3	5	198	5.53	53.3	K	LDKSQIHDIVLVGGSTR	I	164671
		100.0	3	5	198	5.53	53.3	K	LLQDFFNGK	E	130246
		100.0	3	5	198	5.53	53.3	K	LYQSAGGMPGGMPGGFPGGGA-PPSGGASSGPTIEEVD	-	12499.7
		100.0	3	5	198	5.53	53.3	K	MKEIAEAYLGK	T	211286
		100.0	3	5	198	5.53	53.3	R	MVNHFIAEFK	R	321290
		100.0	3	5	198	5.53	53.3	K	NQVAMNPTNTVFDAK	R	222606
		100.0	3	5	198	5.53	53.3	K	NQVAMNPTNTVFDAKR	L	378008
		100.0	3	5	198	5.53	53.3	K	NSLESYAFNMK	A	724779
		100.0	3	5	198	5.53	53.3	R	QATKDAGTIAGLNVLR	I	532863
		100.0	3	5	198	5.53	53.3	K	QTQTFTTYSDNQPGVLIQVYEGER	A	14099.3
		100.0	3	5	198	5.53	53.3	R	RFDDAVVQSDMK	H	7451.11
		100.0	3	5	198	5.53	53.3	K	SFYPEEVSSMVLTK	M	337807
		100.0	3	5	198	5.53	53.3	K	SINPDEAVAYGAAVQAAILSGDK	S	10752.5
		100.0	3	5	198	5.53	53.3	M	SKGPAVGIDLGTTYSCVGVFQHGK	V	28845.8
		100.0	3	5	198	5.53	53.3	K	SQIHDIVLVGGSTR	I	59176.1
		100.0	3	5	198	5.53	53.3	K	STAGDTHLGGEDFDNR	M	142279
		100.0	3	5	198	5.53	53.3	R	TTPSYVAFTDTER	L	1005850
		100.0	3	5	198	5.53	53.3	K	TVTNAVVTVPAYFNDSQR	Q	516618

100.0	3	5	198	5.53	53.3	K	TVTNAVVTVPAYFNDSQRQATK	D	10127.4
100.0	3	5	198	5.53	53.3	K	VCNPIITK	L	502970
100.0	3	5	198	5.53	53.3	K	VEIIANDQGNRTTPSYVAFTDTER	L	16190.8
100.0	3	5	198	5.53	53.3	K	VSSKNSLESYAFNMK	A	45713.6
100.0	3	5	198	5.53	53.3	D	AGTIAGLNVLR	I	35954.6
100.0	3	5	198	5.53	53.3	R	ARFEELNADLFR	G	178862
100.0	3	5	198	5.53	53.3	R	ARFEELNADLFRGTLDPVEK	A	20125.3
100.0	3	5	198	5.53	53.3	K	DAGTIAGLNVLR	I	1507150
100.0	3	5	198	5.53	53.3	R	DAKLDKSQIHDIVLVGGSTR	I	21885.1
100.0	3	5	198	5.53	53.3	K	EIAEAYLGK	T	56021.2
100.0	3	5	198	5.53	53.3	K	ELEKVCNPIITK	L	16716.9
100.0	3	5	198	5.53	53.3	R	FDDAVVQSDMK	H	25449.7
100.0	3	5	198	5.53	53.3	R	FEELNADLFR	G	206924
100.0	3	5	198	5.53	53.3	R	FEELNADLFRGTLDPVEK	A	33554.6
100.0	3	5	198	5.53	53.3	K	GPAVGIDLGTTYSCVGVFQHGK	V	24050.9
100.0	3	5	198	5.53	53.3	R	GTLDPVEK	A	21995.8
100.0	3	5	198	5.53	53.3	R	GTLDPVEKALR	D	30712.5
100.0	3	5	198	5.53	53.3	R	IINEPTAAAIAYGLDK	K	75894.6
100.0	3	5	198	5.53	53.3	R	IINEPTAAAIAYGLDKK	V	34158.3
100.0	3	5	198	5.53	53.3	K	IQKLLQDFFNGK	E	6110.08
100.0	3	5	198	5.53	53.3	K	LDKSQIHDIVLVGGSTR	I	164671
100.0	3	5	198	5.53	53.3	K	LLQDFFNGK	E	130246
100.0	3	5	198	5.53	53.3	K	LYQSAGGMPGGMPGGFPGGGA-PPSGGASSGPTIEEVD	-	12499.7
100.0	3	5	198	5.53	53.3	K	MKEIAEAYLGK	T	211286
100.0	3	5	198	5.53	53.3	R	MVNHFIAEFK	R	321290
100.0	3	5	198	5.53	53.3	K	NQVAMNPTNTVFDAK	R	222606
100.0	3	5	198	5.53	53.3	K	NQVAMNPTNTVFDAKR	L	378008
100.0	3	5	198	5.53	53.3	K	NSLESYAFNMK	A	724779
100.0	3	5	198	5.53	53.3	R	QATKDAGTIAGLNVLR	I	532863
100.0	3	5	198	5.53	53.3	K	QTQTFTTYSDNQPGVLIQVYEGER	A	14099.3
100.0	3	5	198	5.53	53.3	R	RFDDAVVQSDMK	H	7451.11
100.0	3	5	198	5.53	53.3	K	SFYPEEVSSMVLTK	M	337807
100.0	3	5	198	5.53	53.3	K	SINPDEAVAYGAAVQAAILSGDK	S	10752.5
100.0	3	5	198	5.53	53.3	M	SKGPAVGIDLGTTYSCVGVFQHGK	V	28845.8
100.0	3	5	198	5.53	53.3	K	SQIHDIVLVGGSTR	I	59176.1
100.0	3	5	198	5.53	53.3	K	STAGDTHLGGEDFDNR	M	142279
100.0	3	5	198	5.53	53.3	R	TTPSYVAFTDTER	L	1005850
100.0	3	5	198	5.53	53.3	K	TVTNAVVTVPAYFNDSQR	Q	516618
100.0	3	5	198	5.53	53.3	K	TVTNAVVTVPAYFNDSQRQATK	D	10127.4
100.0	3	5	198	5.53	53.3	K	VCNPIITK	L	502970
100.0	3	5	198	5.53	53.3	K	VEIIANDQGNRTTPSYVAFTDTER	L	16190.8
100.0	3	5	198	5.53	53.3	K	VSSKNSLESYAFNMK	A	45713.6
100.0	3	5	198	5.53	53.3	D	AGTIAGLNVLR	I	35954.6
100.0	3	5	198	5.53	53.3	R	ARFEELNADLFR	G	178862
100.0	3	5	198	5.53	53.3	R	ARFEELNADLFRGTLDPVEK	A	20125.3
100.0	3	5	198	5.53	53.3	K	DAGTIAGLNVLR	I	1507150
100.0	3	5	198	5.53	53.3	R	DAKLDKSQIHDIVLVGGSTR	I	21885.1
100.0	3	5	198	5.53	53.3	K	EIAEAYLGK	T	56021.2
100.0	3	5	198	5.53	53.3	K	ELEKVCNPIITK	L	16716.9
100.0	3	5	198	5.53	53.3	R	FDDAVVQSDMK	H	25449.7
100.0	3	5	198	5.53	53.3	R	FEELNADLFR	G	206924
100.0	3	5	198	5.53	53.3	R	FEELNADLFRGTLDPVEK	A	33554.6
100.0	3	5	198	5.53	53.3	K	GPAVGIDLGTTYSCVGVFQHGK	V	24050.9
100.0	3	5	198	5.53	53.3	R	GTLDPVEK	A	21995.8
100.0	3	5	198	5.53	53.3	R	GTLDPVEKALR	D	30712.5
100.0	3	5	198	5.53	53.3	R	IINEPTAAAIAYGLDK	K	75894.6
100.0	3	5	198	5.53	53.3	R	IINEPTAAAIAYGLDKK	V	34158.3
100.0	3	5	198	5.53	53.3	K	IQKLLQDFFNGK	E	6110.08
100.0	3	5	198	5.53	53.3	K	LDKSQIHDIVLVGGSTR	I	164671
100.0	3	5	198	5.53	53.3	K	LLQDFFNGK	E	130246
100.0	3	5	198	5.53	53.3	K	LYQSAGGMPGGMPGGFPGGGA-PPSGGASSGPTIEEVD	-	12499.7
100.0	3	5	198	5.53	53.3	K	MKEIAEAYLGK	T	211286
100.0	3	5	198	5.53	53.3	R	MVNHFIAEFK	R	321290
100.0	3	5	198	5.53	53.3	K	NQVAMNPTNTVFDAK	R	222606
100.0	3	5	198	5.53	53.3	K	NQVAMNPTNTVFDAKR	L	378008
100.0	3	5	198	5.53	53.3	K	NSLESYAFNMK	A	724779
100.0	3	5	198	5.53	53.3	R	QATKDAGTIAGLNVLR	I	532863
100.0	3	5	198	5.53	53.3	K	QTQTFTTYSDNQPGVLIQVYEGER	A	14099.3
100.0	3	5	198	5.53	53.3	R	RFDDAVVQSDMK	H	7451.11
100.0	3	5	198	5.53	53.3	K	SFYPEEVSSMVLTK	M	337807
100.0	3	5	198	5.53	53.3	K	SINPDEAVAYGAAVQAAILSGDK	S	10752.5
100.0	3	5	198	5.53	53.3	M	SKGPAVGIDLGTTYSCVGVFQHGK	V	28845.8
100.0	3	5	198	5.53	53.3	K	SQIHDIVLVGGSTR	I	59176.1

		100.0	3	5	198	5.53	53.3	K	STAGDTHLGGEDFDNR	M	142279
		100.0	3	5	198	5.53	53.3	R	TTPSYVAFTDTER	L	1005850
		100.0	3	5	198	5.53	53.3	K	TVTNAVVTVPAYFNDSQR	Q	516618
		100.0	3	5	198	5.53	53.3	K	TVTNAVVTVPAYFNDSQRQATK	D	10127.4
		100.0	3	5	198	5.53	53.3	K	VCNPIITK	L	502970
		100.0	3	5	198	5.53	53.3	K	VEIIANDQGNRTTPSYVAFTDTER	L	16190.8
		100.0	3	5	198	5.53	53.3	K	VSSKNSLESYAFNMK	A	45713.6
		100.0	3	5	198	5.53	53.3	D	AGTIAGLNVLR	I	35954.6
		100.0	3	5	198	5.53	53.3	R	ARFEELNADLFR	G	178862
		100.0	3	5	198	5.53	53.3	R	ARFEELNADLFRGTLDPVEK	A	20125.3
		100.0	3	5	198	5.53	53.3	K	DAGTIAGLNVLR	I	1507150
		100.0	3	5	198	5.53	53.3	R	DAKLDKSQIHDIVLVGGSTR	I	21885.1
		100.0	3	5	198	5.53	53.3	K	EIAEAYLGK	T	56021.2
		100.0	3	5	198	5.53	53.3	K	ELEKVCNPIITK	L	16716.9
		100.0	3	5	198	5.53	53.3	R	FDDAVVQSDMK	H	25449.7
		100.0	3	5	198	5.53	53.3	R	FEELNADLFR	G	206924
		100.0	3	5	198	5.53	53.3	R	FEELNADLFRGTLDPVEK	A	33554.6
		100.0	3	5	198	5.53	53.3	K	GPAVGIDLGTTYSCVGVFQHGK	V	24050.9
		100.0	3	5	198	5.53	53.3	R	GTLDPVEK	A	21995.8
		100.0	3	5	198	5.53	53.3	R	GTLDPVEKALR	D	30712.5
		100.0	3	5	198	5.53	53.3	R	IINEPTAAAIAYGLDK	K	75894.6
		100.0	3	5	198	5.53	53.3	R	IINEPTAAAIAYGLDKK	V	34158.3
		100.0	3	5	198	5.53	53.3	K	IQKLLQDFFNGK	E	6110.08
		100.0	3	5	198	5.53	53.3	K	LDKSQIHDIVLVGGSTR	I	164671
		100.0	3	5	198	5.53	53.3	K	LLQDFFNGK	E	130246
		100.0	3	5	198	5.53	53.3	K	LYQSAGGMPGGMPGGFPGGGA-PPSGGASSGPTIEEVD	-	12499.7
		100.0	3	5	198	5.53	53.3	K	MKEIAEAYLGK	T	211286
		100.0	3	5	198	5.53	53.3	R	MVNHFIAEFK	R	321290
		100.0	3	5	198	5.53	53.3	K	NQVAMNPTNTVFDAK	R	222606
		100.0	3	5	198	5.53	53.3	K	NQVAMNPTNTVFDAKR	L	378008
		100.0	3	5	198	5.53	53.3	K	NSLESYAFNMK	A	724779
		100.0	3	5	198	5.53	53.3	R	QATKDAGTIAGLNVLR	I	532863
		100.0	3	5	198	5.53	53.3	K	QTQTFTTYSDNQPGVLIQVYEGER	A	14099.3
		100.0	3	5	198	5.53	53.3	R	RFDDAVVQSDMK	H	7451.11
		100.0	3	5	198	5.53	53.3	K	SFYPEEVSSMVLTK	M	337807
		100.0	3	5	198	5.53	53.3	K	SINPDEAVAYGAAVQAAILSGDK	S	10752.5
		100.0	3	5	198	5.53	53.3	M	SKGPAVGIDLGTTYSCVGVFQHGK	V	28845.8
		100.0	3	5	198	5.53	53.3	K	SQIHDIVLVGGSTR	I	59176.1
		100.0	3	5	198	5.53	53.3	K	STAGDTHLGGEDFDNR	M	142279
		100.0	3	5	198	5.53	53.3	R	TTPSYVAFTDTER	L	1005850
		100.0	3	5	198	5.53	53.3	K	TVTNAVVTVPAYFNDSQR	Q	516618
		100.0	3	5	198	5.53	53.3	K	TVTNAVVTVPAYFNDSQRQATK	D	10127.4
		100.0	3	5	198	5.53	53.3	K	VCNPIITK	L	502970
		100.0	3	5	198	5.53	53.3	K	VEIIANDQGNRTTPSYVAFTDTER	L	16190.8
		100.0	3	5	198	5.53	53.3	K	VSSKNSLESYAFNMK	A	45713.6
20_82	Cluster of 78 kDa	100.0	11	18	296	6.18	64.0	K	AAAIGIDLGTTYSCVGVFQHGK	V	73226.3
	glucose-regulated protein	100.0	11	18	296	6.18	64.0	K	AFYPEEISSMVLTK	M	1300990
	OS=Homo sapiens	100.0	11	18	296	6.18	64.0	R	AMTKDNNLLGR	F	16697.1
	GN=HSPA5 PE=1 SV=2	100.0	11	18	296	6.18	64.0	K	AQIHDLVLVGGSTR	I	403685
	GRP78_HUMAN	100.0	11	18	296	6.18	64.0	R	ARFEELCSDLFR	S	1405750
	70054.0	100.0	11	18	296	6.18	64.0	K	ATAGDTHLGGEDFDNR	L	4405.53
		100.0	11	18	296	6.18	64.0	K	DAGVIAGLNVLR	I	6101900
		100.0	11	18	296	6.18	64.0	R	DAKLDKAQIHDLVLVGGSTR	I	89073.5
		100.0	11	18	296	6.18	64.0	K	DNNLLGR	F	12394.4
		100.0	11	18	296	6.18	64.0	K	ELEQVCNPIISGLYQGAGGPGP-GGFGAQGPK	G	29834.0
		100.0	11	18	296	6.18	64.0	R	FEELCSDLFR	S	606598
		100.0	11	18	296	6.18	64.0	R	FELSGIPPAPR	G	35328.4
		100.0	11	18	296	6.18	64.0	K	FGDPVVQSDMK	H	401269
		100.0	11	18	296	6.18	64.0	K	FGDPVVQSDMKHWPFQVINDGDKPK	V	10822.4
		100.0	11	18	296	6.18	64.0	K	GGSGSGPTIEEVD	-	111697
		100.0	11	18	296	6.18	64.0	K	HWPFQVINDGDKPK	V	71497.1
		100.0	11	18	296	6.18	64.0	R	IINEPTAAAIAYGLDR	T	2552550
		100.0	11	18	296	6.18	64.0	R	IINEPTAAAIAYGLDRTGK	G	9880.85
		100.0	11	18	296	6.18	64.0	R	IINEPTAAAIAYGLDRTGKGER	N	48672.9
		100.0	11	18	296	6.18	64.0	R	IPKVQKLLQDFFNGR	D	9155.00
		100.0	11	18	296	6.18	64.0	R	KELEQVCNPIISGLYQGAGGPG-PGGFGAQGPK	G	23036.1
		100.0	11	18	296	6.18	64.0	R	KFGDPVVQSDMK	H	93715.1
		100.0	11	18	296	6.18	64.0	K	LDKAQIHDLVLVGGSTR	I	54808.1
		100.0	11	18	296	6.18	64.0	R	LIGDAAKNQVALNPQNTVFDAK	R	144320
		100.0	11	18	296	6.18	64.0	R	LIGDAAKNQVALNPQNTVFDAKR	L	74840.8
		100.0	11	18	296	6.18	64.0	K	LLQDFFNGR	D	2570610
		100.0	11	18	296	6.18	64.0	K	LLQDFFNGRDLNK	S	1463020

		100.0	11	18	296	6.18	64.0	R	LVNHFVEEFK	R	1361770
		100.0	11	18	296	6.18	64.0	R	LVNHFVEEFKR	K	552399
		100.0	11	18	296	6.18	64.0	K	MKEIAEAYLGYPVTNAVITVPAY-FNDSQR	Q	2940.77
		100.0	11	18	296	6.18	64.0	R	MVQEAEKYKAEDEVQR	E	85688.9
		100.0	11	18	296	6.18	64.0	K	NALESYAFNMK	S	5197760
		100.0	11	18	296	6.18	64.0	K	NQVALNPQNTVFDAK	R	1135000
		100.0	11	18	296	6.18	64.0	K	NQVALNPQNTVFDAKR	L	2777110
		100.0	11	18	296	6.18	64.0	R	NSTIPTK	Q	21347.2
		100.0	11	18	296	6.18	64.0	W	PFQVINDGDKPK	V	4281.03
		100.0	11	18	296	6.18	64.0	T	PSYVAFTDTER	L	14704.7
		100.0	11	18	296	6.18	64.0	R	QATKDAGVIAGLNVLR	I	834074
		100.0	11	18	296	6.18	64.0	L	QDFFNGRDLNK	S	38181.3
		100.0	11	18	296	6.18	64.0	K	QTQIFTTYSDNQPGVLIQVYEGER	A	11528.4
		100.0	11	18	296	6.18	64.0	K	SINPDEAVAYGAAVQAAILMGDK	S	41869.1
		100.0	11	18	296	6.18	64.0	R	STLEPVEK	A	75583.6
		100.0	11	18	296	6.18	64.0	R	TTPSYVAFTDTER	L	4374050
		100.0	11	18	296	6.18	64.0	K	VEIIANDQGNR	T	24257.8
		100.0	11	18	296	6.18	64.0	K	AAAIGIDLGTTYSCVGVFQHGK	V	73226.3
		100.0	11	18	296	6.18	64.0	K	AFYPEEISSMVLTK	M	1300990
		100.0	11	18	296	6.18	64.0	R	AMTKDNNLLGR	F	16697.1
		100.0	11	18	296	6.18	64.0	K	AQIHDLVLVGGSTR	I	403685
		100.0	11	18	296	6.18	64.0	R	ARFEELCSDLFR	S	1405750
		100.0	11	18	296	6.18	64.0	K	ATAGDTHLGGEDFDNR	L	4405.53
		100.0	11	18	296	6.18	64.0	K	DAGVIAGLNVLR	I	6101900
		100.0	11	18	296	6.18	64.0	R	DAKLDKAQIHDLVLVGGSTR	I	89073.5
		100.0	11	18	296	6.18	64.0	K	DNNLLGR	F	12394.4
		100.0	11	18	296	6.18	64.0	K	ELEQVCNPIISGLYQGAGGPGPGG-FGAQGPK	G	29834.0
		100.0	11	18	296	6.18	64.0	R	FEELCSDLFR	S	606598
		100.0	11	18	296	6.18	64.0	R	FELSGIPPAPR	G	35328.4
		100.0	11	18	296	6.18	64.0	K	FGDPVVQSDMK	H	401269
		100.0	11	18	296	6.18	64.0	K	FGDPVVQSDMKHWPFQVINDGDKPK	V	10822.4
		100.0	11	18	296	6.18	64.0	K	GGSGSGPTIEEVD	-	111697
		100.0	11	18	296	6.18	64.0	K	HWPFQVINDGDKPK	V	71497.1
		100.0	11	18	296	6.18	64.0	R	IINEPTAAAIAYGLDR	T	2552550
		100.0	11	18	296	6.18	64.0	R	IINEPTAAAIAYGLDRTGK	G	9880.85
		100.0	11	18	296	6.18	64.0	R	IINEPTAAAIAYGLDRTGKGER	N	48672.9
		100.0	11	18	296	6.18	64.0	R	IPKVQKLLQDFFNGR	D	9155.00
		100.0	11	18	296	6.18	64.0	R	KELEQVCNPIISGLYQGAGGPGP-GGFGAQGPK	G	23036.1
		100.0	11	18	296	6.18	64.0	R	KFGDPVVQSDMK	H	93715.1
		100.0	11	18	296	6.18	64.0	K	LDKAQIHDLVLVGGSTR	I	54808.1
		100.0	11	18	296	6.18	64.0	R	LIGDAAKNQVALNPQNTVFDAK	R	144320
		100.0	11	18	296	6.18	64.0	R	LIGDAAKNQVALNPQNTVFDAKR	L	74840.8
		100.0	11	18	296	6.18	64.0	K	LLQDFFNGR	D	2570610
		100.0	11	18	296	6.18	64.0	K	LLQDFFNGRDLNK	S	1463020
		100.0	11	18	296	6.18	64.0	R	LVNHFVEEFK	R	1361770
		100.0	11	18	296	6.18	64.0	R	LVNHFVEEFKR	K	552399
		100.0	11	18	296	6.18	64.0	K	MKEIAEAYLGYPVTNAVITVPAYFN-DSQR	Q	2940.77
		100.0	11	18	296	6.18	64.0	R	MVQEAEKYKAEDEVQR	E	85688.9
		100.0	11	18	296	6.18	64.0	K	NALESYAFNMK	S	5197760
		100.0	11	18	296	6.18	64.0	K	NQVALNPQNTVFDAK	R	1135000
		100.0	11	18	296	6.18	64.0	K	NQVALNPQNTVFDAKR	L	2777110
		100.0	11	18	296	6.18	64.0	R	NSTIPTK	Q	21347.2
		100.0	11	18	296	6.18	64.0	W	PFQVINDGDKPK	V	4281.03
		100.0	11	18	296	6.18	64.0	T	PSYVAFTDTER	L	14704.7
		100.0	11	18	296	6.18	64.0	R	QATKDAGVIAGLNVLR	I	834074
		100.0	11	18	296	6.18	64.0	L	QDFFNGRDLNK	S	38181.3
		100.0	11	18	296	6.18	64.0	K	QTQIFTTYSDNQPGVLIQVYEGER	A	11528.4
		100.0	11	18	296	6.18	64.0	K	SINPDEAVAYGAAVQAAILMGDK	S	41869.1
		100.0	11	18	296	6.18	64.0	R	STLEPVEK	A	75583.6
		100.0	11	18	296	6.18	64.0	R	TTPSYVAFTDTER	L	4374050
		100.0	11	18	296	6.18	64.0	K	VEIIANDQGNR	T	24257.8
20_87	Cluster of 78 kDa	100.0	3	4	116	4.34	43.4	K	AFYPEEISSMVLTK	M	137840
	glucose-regulated protein	100.0	3	4	116	4.34	43.4	D	AGVIAGLNVLR	I	16823.4
	OS=Homo sapiens	100.0	3	4	116	4.34	43.4	R	ARFEELCSDLFR	S	23997.9
	GN=HSPA5 PE=1 SV=2	100.0	3	4	116	4.34	43.4	K	ATAGDTHLGGEDFDNR	L	1614.22
	GRP78_HUMAN	100.0	3	4	116	4.34	43.4	K	DAGVIAGLNVLR	I	537854
	70054.0	100.0	3	4	116	4.34	43.4	K	ELEQVCNPIISGLYQGAGGPG-PGGFGAQGPK	G	3470.21
		100.0	3	4	116	4.34	43.4	R	FEELCSDLFR	S	46755.8
		100.0	3	4	116	4.34	43.4	K	FGDPVVQSDMK	H	37752.6
		100.0	3	4	116	4.34	43.4	K	GGSGSGPTIEEVD	-	51693.9
		100.0	3	4	116	4.34	43.4	R	IINEPTAAAIAYGLDR	T	230055

		100.0	3	4	116	4.34	43.4	K	LDKAQIHDLVLVGGSTR	I	27067.0
		100.0	3	4	116	4.34	43.4	R	LIGDAAKNQVALNPQNTVFDAK	R	31285.9
		100.0	3	4	116	4.34	43.4	R	LIGDAAKNQVALNPQNTVFDAKR	L	11235.7
		100.0	3	4	116	4.34	43.4	K	LLQDFFNGR	D	128180
		100.0	3	4	116	4.34	43.4	K	LLQDFFNGRDLNK	S	13125.2
		100.0	3	4	116	4.34	43.4	R	LVNHFVEEFK	R	18114.2
		100.0	3	4	116	4.34	43.4	R	MVQEAEKYKAEDEVQR	E	2745.08
		100.0	3	4	116	4.34	43.4	K	NALESYAFNMK	S	472404
		100.0	3	4	116	4.34	43.4	K	NQVALNPQNTVFDAK	R	98396.4
		100.0	3	4	116	4.34	43.4	K	NQVALNPQNTVFDAKR	L	161280
		100.0	3	4	116	4.34	43.4	R	QATKDAGVIAGLNVLR	I	169961
		100.0	3	4	116	4.34	43.4	K	SINPDEAVAYGAAVQAAILMGDK	S	7128.38
		100.0	3	4	116	4.34	43.4	R	STLEPVEK	A	9900.81
		100.0	3	4	116	4.34	43.4	R	TTPSYVAFTDTER	L	461338
		100.0	3	4	116	4.34	43.4	K	VEIIANDQGNR	T	12214.1
		100.0	3	4	116	4.34	43.4	R	VSAKNALESYAFNMK	S	52275.9
		100.0	3	4	116	4.34	43.4	K	AFYPEEISSMVLTK	M	137840
		100.0	3	4	116	4.34	43.4	D	AGVIAGLNVLR	I	16823.4
		100.0	3	4	116	4.34	43.4	R	ARFEELCSDLFR	S	23997.9
		100.0	3	4	116	4.34	43.4	K	ATAGDTHLGGEDFDNR	L	1614.22
		100.0	3	4	116	4.34	43.4	K	DAGVIAGLNVLR	I	537854
		100.0	3	4	116	4.34	43.4	K	ELEQVCNPIISGLYQGAGGPGP-GGFGAQGPK	G	3470.21
		100.0	3	4	116	4.34	43.4	R	FEELCSDLFR	S	46755.8
		100.0	3	4	116	4.34	43.4	K	FGDPVVQSDMK	H	37752.6
		100.0	3	4	116	4.34	43.4	K	GGSGSGPTIEEVD	-	51693.9
		100.0	3	4	116	4.34	43.4	R	IINEPTAAAIAYGLDR	T	230055
		100.0	3	4	116	4.34	43.4	K	LDKAQIHDLVLVGGSTR	I	27067.0
		100.0	3	4	116	4.34	43.4	R	LIGDAAKNQVALNPQNTVFDAK	R	31285.9
		100.0	3	4	116	4.34	43.4	R	LIGDAAKNQVALNPQNTVFDAKR	L	11235.7
		100.0	3	4	116	4.34	43.4	K	LLQDFFNGR	D	128180
		100.0	3	4	116	4.34	43.4	K	LLQDFFNGRDLNK	S	13125.2
		100.0	3	4	116	4.34	43.4	R	LVNHFVEEFK	R	18114.2
		100.0	3	4	116	4.34	43.4	R	MVQEAEKYKAEDEVQR	E	2745.08
		100.0	3	4	116	4.34	43.4	K	NALESYAFNMK	S	472404
		100.0	3	4	116	4.34	43.4	K	NQVALNPQNTVFDAK	R	98396.4
		100.0	3	4	116	4.34	43.4	K	NQVALNPQNTVFDAKR	L	161280
		100.0	3	4	116	4.34	43.4	R	QATKDAGVIAGLNVLR	I	169961
		100.0	3	4	116	4.34	43.4	K	SINPDEAVAYGAAVQAAILMGDK	S	7128.38
		100.0	3	4	116	4.34	43.4	R	STLEPVEK	A	9900.81
		100.0	3	4	116	4.34	43.4	R	TTPSYVAFTDTER	L	461338
		100.0	3	4	116	4.34	43.4	K	VEIIANDQGNR	T	12214.1
		100.0	3	4	116	4.34	43.4	R	VSAKNALESYAFNMK	S	52275.9
21_83	T-complex protein 1	100.0	11	14	82	4.43	47.5	K	ARTSASIILR	G	5831.80
	Subunit α	100.0	11	14	82	4.43	47.5	R	EQLAIAEFAR	S	274248
	OS=Homo sapiens	100.0	11	14	82	4.43	47.5	L	EVEHPAAK	V	17225.1
	GN=TCP1 PE=1 SV=1	100.0	11	14	82	4.43	47.5	K	FATEAAITILR	I	51159.0
	TCPA_HUMAN	100.0	11	14	82	4.43	47.5	R	GANDFMCDEMER	S	23002.5
	60345.2	100.0	11	14	82	4.43	47.5	K	IACLDFSLQK	T	132507
		100.0	11	14	82	4.43	47.5	R	ICDDELILIK	N	82390.6
		100.0	11	14	82	4.43	47.5	R	ICDDELILIKNTK	A	5771.81
		100.0	11	14	82	4.43	47.5	K	ILATGANVILTTGGIDDMCLK	Y	10973.4
		100.0	11	14	82	4.43	47.5	K	LGVQVVITDPEK	L	17312.1
		100.0	11	14	82	4.43	47.5	K	LLEVEHPAAK	V	30757.7
		100.0	11	14	82	4.43	47.5	-	MEGPLSVFGDR	S	61354.0
		100.0	11	14	82	4.43	47.5	-	MEGPLSVFGDRSTGETIR	S	4722.17
		100.0	11	14	82	4.43	47.5	K	MLVDDIGDVTITNDGATILK	L	5863.38
		100.0	11	14	82	4.43	47.5	K	QAGVFEPTIVK	V	86794.8
		100.0	11	14	82	4.43	47.5	R	SLHDALCVVK	R	9034.83
		100.0	11	14	82	4.43	47.5	R	SLHDALCVVKR	V	3402.80
		100.0	11	14	82	4.43	47.5	R	SLLVIPNTLAVNAAQDSTDLVAK	L	742.842
		100.0	11	14	82	4.43	47.5	R	SQNVMAAASIANIVK	S	45718.2
		100.0	11	14	82	4.43	47.5	K	SSLGPVGLDK	M	101862
		100.0	11	14	82	4.43	47.5	R	TSASIILR	G	307468
		100.0	11	14	82	4.43	47.5	K	VLCELADLQDK	E	4060.08
		100.0	11	14	82	4.43	47.5	K	YFVEAGAMAVR	R	73753.0
		100.0	11	14	82	4.43	47.5	R	YINENLIVNTDELGR	D	5466.54
		100.0	11	14	82	4.43	47.5	R	YPVNSVNILK	A	244785
21_85	T-complex protein 1	100.0	10	13	52	3.60	38.5	R	DNKQAGVFEPTIVK	V	18710.7
	Subunit α	100.0	10	13	52	3.60	38.5	R	EQLAIAEFAR	S	85093.4
	OS=Homo sapiens	100.0	10	13	52	3.60	38.5	K	FATEAAITILR	I	26668.5
	GN=TCP1 PE=1 SV=1	100.0	10	13	52	3.60	38.5	K	IACLDFSLQK	T	41558.4
	TCPA_HUMAN	100.0	10	13	52	3.60	38.5	R	ICDDELILIK	N	22570.7
	60345.2	100.0	10	13	52	3.60	38.5	R	ICDDELILIKNTK	A	2719.23
		100.0	10	13	52	3.60	38.5	K	IHPTSVISGYR	L	10356.0

		100.0	10	13	52	3.60	38.5	K	ILATGANVILTTGGIDDMCLK	Y	8387.48
		100.0	10	13	52	3.60	38.5	K	LLEVEHPAAK	V	44279.0
		100.0	10	13	52	3.60	38.5	-	MEGPLSVFGDR	S	40735.8
		100.0	10	13	52	3.60	38.5	K	QAGVFEPTIVK	V	55455.3
		100.0	10	13	52	3.60	38.5	R	SLLVIPNTLAVNAAQDSTDLVAK	L	1644.52
		100.0	10	13	52	3.60	38.5	R	SQNVMAAASIANIVK	S	45721.9
		100.0	10	13	52	3.60	38.5	K	SSLGPVGLDK	M	52250.2
		100.0	10	13	52	3.60	38.5	R	TSASIILR	G	242563
		100.0	10	13	52	3.60	38.5	K	VLCELADLQDK	E	4047.02
		100.0	10	13	52	3.60	38.5	K	YFVEAGAMAVR	R	32147.1
		100.0	10	13	52	3.60	38.5	R	YINENLIVNTDELGR	D	9611.70
		100.0	10	13	52	3.60	38.5	R	YPVNSVNILK	A	170822
22_82	Thioredoxin reductase 1. cytoplasmic OS=Homo sapiens GN=TXNRD1 PE=1 SV=3 TRXR1_HUMAN 54751.2	100.0	6	7	37	2.25	17.7	R	FLIATGERPR	Y	141872
		100.0	6	7	37	2.25	17.7	L	IATGERPR	Y	22149.9
		100.0	6	7	37	2.25	17.7	K	IGLETVGVK	I	37480.7
		100.0	6	7	37	2.25	17.7	K	IGLETVGVKINEK	T	6433.63
		100.0	6	7	37	2.25	17.7	R	KIGLETVGVK	I	18437.2
		100.0	6	7	37	2.25	17.7	R	KIGLETVGVKINEK	T	8667.64
		100.0	6	7	37	2.25	17.7	K	KLMHQAALLGQALQDSR	N	9843.88
		100.0	6	7	37	2.25	17.7	R	QFVPIKVEQIEAGTPGR	L	21017.5
		100.0	6	7	37	2.25	17.7	K	VELTPVAIQAGR	L	19988.5
		100.0	6	7	37	2.25	17.7	K	VMVLDFVTPTPLGTR	W	79277.6
		100.0	6	7	37	2.25	17.7	K	VVYENAYGQFIGPHR	I	33711.1
		100.0	6	7	37	2.25	17.7	R	WGLGGTCVNVGCIPK	K	9633.54
		100.0	6	7	37	2.25	17.7	R	FLIATGERPR	Y	141872
		100.0	6	7	37	2.25	17.7	L	IATGERPR	Y	22149.9
		100.0	6	7	37	2.25	17.7	K	IGLETVGVK	I	37480.7
		100.0	6	7	37	2.25	17.7	K	IGLETVGVKINEK	T	6433.63
		100.0	6	7	37	2.25	17.7	R	KIGLETVGVK	I	18437.2
		100.0	6	7	37	2.25	17.7	R	KIGLETVGVKINEK	T	8667.64
		100.0	6	7	37	2.25	17.7	K	KLMHQAALLGQALQDSR	N	9843.88
		100.0	6	7	37	2.25	17.7	R	QFVPIKVEQIEAGTPGR	L	21017.5
		100.0	6	7	37	2.25	17.7	K	VELTPVAIQAGR	L	19988.5
		100.0	6	7	37	2.25	17.7	K	VMVLDFVTPTPLGTR	W	79277.6
		100.0	6	7	37	2.25	17.7	K	VVYENAYGQFIGPHR	I	33711.1
		100.0	6	7	37	2.25	17.7	R	WGLGGTCVNVGCIPK	K	9633.54
23_87	Programmed cell death protein 4 OS=Homo sapiens GN=PDCD4 PE=1 SV=2 PDCD4_HUMAN 51736.4	100.0	3	3	7	0.363	6.40	R	APQLVGQFIAR	A	13371.1
		100.0	3	3	7	0.363	6.40	K	ATVLLSMSK	G	14120.9
		100.0	3	3	7	0.363	6.40	R	SGLTVPTSPK	G	7684.13
24_81	Nucleobindin-1 OS=Homo sapiens GN=NUCB1 PE=1 SV=4 NUCB1_HUMAN 53879.6	100.0	13	14	26	1.61	23.2	R	DLELLIQTATR	D	39938.0
		100.0	13	14	26	1.61	23.2	R	ELQQAVLHMEQR	K	30053.9
		100.0	13	14	26	1.61	23.2	R	FEEELAAR	E	27767.4
		100.0	13	14	26	1.61	23.2	K	LLERLPEVEVPQHL	-	33701.7
		100.0	13	14	26	1.61	23.2	R	LPEVEVPQHL	-	44601.3
		100.0	13	14	26	1.61	23.2	K	LQAANAEDIK	S	13180.7
		100.0	13	14	26	1.61	23.2	K	LQAANAEDIKSGKLSR	E	4684.68
		100.0	13	14	26	1.61	23.2	R	LSQETEALGR	S	25509.4
		100.0	13	14	26	1.61	23.2	R	LVTLEEFLASTQR	K	2844.57
		100.0	13	14	26	1.61	23.2	R	LVTLEEFLASTQRK	E	5945.60
		100.0	13	14	26	1.61	23.2	K	VNVPGSQAQLK	E	77525.1
		100.0	13	14	26	1.61	23.2	R	YLESLGEEQR	K	12234.8
		100.0	13	14	26	1.61	23.2	R	YLESLGEEQRK	E	2723.84
25_81	60 kDa heat shock protein, mitochondrial OS=Homo sapiens GN=HSPD1 PE=1 SV=2 CH60_HUMAN 61055.7	100.0	6	6	11	0.735	15.2	R	AAVEEGIVLGGGCALLR	C	4425.71
		100.0	6	6	11	0.735	15.2	R	GYISPYFINTSK	G	10376.7
		100.0	6	6	11	0.735	15.2	K	LSDGVAVLK	V	12780.4
		100.0	6	6	11	0.735	15.2	K	LVQDVANNTNEEAGDGTTTATVLAR	S	2446.33
		100.0	6	6	11	0.735	15.2	K	NAGVEGSLIVEK	I	12889.9
		100.0	6	6	11	0.735	15.2	R	TVIIEQSWGSPK	V	9987.33
25_85	60 kDa heat shock protein, mitochondrial OS=Homo sapiens GN=HSPD1 PE=1 SV=2 CH60_HUMAN 61055.7	100.0	10	11	21	1.31	23.6	R	AAVEEGIVLGGGCALLR	C	7324.86
		100.0	10	11	21	1.31	23.6	K	CEFQDAYVLLSEK	K	5346.47
		100.0	10	11	21	1.31	23.6	R	GYISPYFINTSK	G	23194.7
		100.0	10	11	21	1.31	23.6	K	LSDGVAVLK	V	43817.8
		100.0	10	11	21	1.31	23.6	K	LVQDVANNTNEEAGDGTTTATVLAR	S	3494.04
		100.0	10	11	21	1.31	23.6	K	NAGVEGSLIVEK	I	18251.1
		100.0	10	11	21	1.31	23.6	R	TLKIPAMTIAK	N	24016.0
		100.0	10	11	21	1.31	23.6	R	TVIIEQSWGSPK	V	47509.5
		100.0	10	11	21	1.31	23.6	K	VGEVIVTKDDAMLLK	G	2014.26
		100.0	10	11	21	1.31	23.6	K	VGLQVVAVK	A	18890.4
26_85	Peptidyl-prolyl cis-trans isomerase FKBP4 OS=Homo sapiens	100.0	14	16	37	2.19	32.9	K	ALELDSNNEKGLFR	R	4533.14
		100.0	14	16	37	2.19	32.9	K	ATESGAQSAPLPMEGVDISPK	Q	1502.80
		100.0	14	16	37	2.19	32.9	K	ATESGAQSAPLPMEGVDISPKQ-	V	1189.07

									DEGVLK		
	GN=FKBP4 PE=1 SV=3	100.0	14	16	37	2.19	32.9	K	AWDIAIATMK	V	37015.5
	FKBP4_HUMAN	100.0	14	16	37	2.19	32.9	R	FEIGEGENLDLPYGLER	A	5208.73
	51805.9	100.0	14	16	37	2.19	32.9	R	GEAHLAVNDFELAR	A	25045.0
		100.0	14	16	37	2.19	32.9	K	IVSWLEYESSFSNEEAQK	A	6808.15
		100.0	14	16	37	2.19	32.9	K	LQAFSAAIESCNK	A	42122.1
		100.0	14	16	37	2.19	32.9	K	LYANMFER	L	84020.5
		100.0	14	16	37	2.19	32.9	R	RGEAHLAVNDFELAR	A	43841.8
		100.0	14	16	37	2.19	32.9	K	TQLAVCQQR	I	4957.16
		100.0	14	16	37	2.19	32.9	K	VLQLYPNNK	A	128698
		100.0	14	16	37	2.19	32.9	K	YKQALLQYK	K	5523.48
		100.0	14	16	37	2.19	32.9	K	YKQALLQYKK	I	5927.89
26_87	Peptidyl-prolyl cis-trans	100.0	29	42	115	3.83	60.1	R	ADFQKVLQLYPNNK	A	58104.9
	isomerase FKBP4	100.0	29	42	115	3.83	60.1	K	ALELDSNNEK	G	8327.85
	OS=Homo sapiens	100.0	29	42	115	3.83	60.1	K	ALELDSNNEKGLFR	R	69175.1
	GN=FKBP4 PE=1 SV=3	100.0	29	42	115	3.83	60.1	K	ATESGAQSAPLPMEGVDISPK	Q	13670.0
	FKBP4_HUMAN	100.0	29	42	115	3.83	60.1	K	ATESGAQSAPLPMEGVDISPKQ-DEGVLK	V	4895.84
	51805.9	100.0	29	42	115	3.83	60.1	K	AWDIAIATMK	V	94308.3
		100.0	29	42	115	3.83	60.1	K	DKFSFDLGKGEVIK	A	41792.2
		100.0	29	42	115	3.83	60.1	R	EGTGTEMPMIGDR	V	30377.1
		100.0	29	42	115	3.83	60.1	R	EKKLYANMFER	L	17039.1
		100.0	29	42	115	3.83	60.1	R	FEIGEGENLDLPYGLER	A	25397.9
		100.0	29	42	115	3.83	60.1	K	FQIPPNAELK	Y	53297.8
		100.0	29	42	115	3.83	60.1	K	FSFDLGKGEVIK	A	6650.59
		100.0	29	42	115	3.83	60.1	R	GEAHLAVNDFELAR	A	55346.1
		100.0	29	42	115	3.83	60.1	K	GEHSIVYLKPSYAFGSVGK	E	46848.5
		100.0	29	42	115	3.83	60.1	K	IVSWLEYESSFSNEEAQK	A	15498.3
		100.0	29	42	115	3.83	60.1	R	LASHLNLAMCHLK	L	31738.2
		100.0	29	42	115	3.83	60.1	K	LQAFSAAIESCNK	A	213535
		100.0	29	42	115	3.83	60.1	K	LQAFSAAIESCNKALELDSNNEK	G	16647.9
		100.0	29	42	115	3.83	60.1	K	LYANMFER	L	313295
		100.0	29	42	115	3.83	60.1	R	MEKGEHSIVYLKPSYAFGSVGK	E	8932.73
		100.0	29	42	115	3.83	60.1	R	RGEAHLAVNDFELAR	A	140508
		100.0	29	42	115	3.83	60.1	M	TAEEMKATESGAQSAPLPMEGVDISPK	Q	6544.71
		100.0	29	42	115	3.83	60.1	M	TAEEMKATESGAQSAPLPMEGV-DISPKQDEGVLK	V	6697.19
		100.0	29	42	115	3.83	60.1	K	TQLAVCQQR	I	17239.9
		100.0	29	42	115	3.83	60.1	R	VFVHYTGWLLDGTK	F	29596.2
		100.0	29	42	115	3.83	60.1	K	VGEVCHITCKPEYAYGSAGSPPK	I	32315.7
		100.0	29	42	115	3.83	60.1	K	VLQLYPNNK	A	390113
		100.0	29	42	115	3.83	60.1	K	VLQLYPNNKAAK	T	65271.6
		100.0	29	42	115	3.83	60.1	K	YKQALLQYK	K	97700.1
27_85	Tubulin beta-1 chain	99.5	1	1	6	0.399	7.61	R	AVLLDLEPGTMDSVR	S	1558.06
	OS=Homo sapiens	99.5	1	1	6	0.399	7.61	K	LAVNMVPFPR	L	27293.0
	GN=TUBB1 PE=1 SV=1	99.5	1	1	6	0.399	7.61	R	YLTVAAVFR	G	32736.6
	TBB1_HUMAN										
	50447.9										
28_82	Tubulin beta-1 chain	99.9	1	1	26	0.790	15.4	R	AVLLDLEPGTMDSVR	S	1652.30
	OS=Homo sapiens	99.9	1	1	26	0.790	15.4	R	FPGQLNADLR	K	72457.3
	GN=TUBB1 PE=1 SV=1	99.9	1	1	26	0.790	15.4	R	ISEQFTAMFR	R	85718.4
	TBB1_HUMAN	99.9	1	1	26	0.790	15.4	R	KLAVNMVPFPR	L	4773.50
	50447.9	99.9	1	1	26	0.790	15.4	K	LAVNMVPFPR	L	111970
		99.9	1	1	26	0.790	15.4	R	LHFFMPGFAPLTSR	G	14112.7
		99.9	1	1	26	0.790	15.4	R	YLTVAAVFR	G	94843.0
28_85	Tubulin beta-1 chain	99.9	1	1	15	0.888	12.1	R	AVLLDLEPGTMDSVR	S	2177.05
	OS=Homo sapiens	99.9	1	1	15	0.888	12.1	R	FPGQLNADLR	K	46562.8
	GN=TUBB1 PE=1 SV=1	99.9	1	1	15	0.888	12.1	R	ISEQFTAMFR	R	42715.0
	TBB1_HUMAN	99.9	1	1	15	0.888	12.1	K	LAVNMVPFPR	L	80731.4
	50447.9	99.9	1	1	15	0.888	12.1	R	YLTVAAVFR	G	65381.4
29_85	Peptidyl-prolyl cis-trans	100.0	12	16	45	2.26	34.0	K	ATESGAQSAPLPMEGVDISPK	Q	2858.25
	isomerase FKBP4	100.0	12	16	45	2.26	34.0	K	AWDIAIATMK	V	60644.5
	OS=Homo sapiens	100.0	12	16	45	2.26	34.0	R	EGTGTEMPMIGDR	V	16423.7
	GN=FKBP4 PE=1 SV=3	100.0	12	16	45	2.26	34.0	R	FEIGEGENLDLPYGLER	A	15397.2
	FKBP4_HUMAN	100.0	12	16	45	2.26	34.0	R	GEAHLAVNDFELAR	A	8496.77
	51805.9	100.0	12	16	45	2.26	34.0	K	IVSWLEYESSFSNEEAQK	A	6738.11
		100.0	12	16	45	2.26	34.0	K	LQAFSAAIESCNK	A	66664.6
		100.0	12	16	45	2.26	34.0	K	LYANMFER	L	129040
		100.0	12	16	45	2.26	34.0	R	RGEAHLAVNDFELAR	A	21447.5
		100.0	12	16	45	2.26	34.0	K	VGEVCHITCKPEYAYGSAGSPPK	I	7741.10
		100.0	12	16	45	2.26	34.0	K	VLQLYPNNK	A	165610
		100.0	12	16	45	2.26	34.0	K	YKQALLQYK	K	4169.87
29_87	Peptidyl-prolyl cis-trans	100.0	25	34	98	3.48	57.5	K	ALELDSNNEK	G	7059.22
	isomerase FKBP4	100.0	25	34	98	3.48	57.5	K	ALELDSNNEKGLFR	R	3402.38
	OS=Homo sapiens	100.0	25	34	98	3.48	57.5	K	ATESGAQSAPLPMEGVDISPK	Q	25399.8

	GN=FKBP4 PE=1 SV=3	100.0	25	34	98	3.48	57.5	K	ATESGAQSAPLPMEGVDISPKQ-DEGVLK	V	10099.8
	FKBP4_HUMAN	100.0	25	34	98	3.48	57.5	K	AWDIAIATMK	V	117888
	51805.9	100.0	25	34	98	3.48	57.5	K	DKFSFDLGKGEVIK	A	24586.0
		100.0	25	34	98	3.48	57.5	R	EGTGTEMPMIGDR	V	62757.6
		100.0	25	34	98	3.48	57.5	R	FEIGEGENLDLPYGLER	A	26232.3
		100.0	25	34	98	3.48	57.5	K	FQIPPNAELK	Y	22823.6
		100.0	25	34	98	3.48	57.5	K	FSFDLGKGEVIK	A	10006.9
		100.0	25	34	98	3.48	57.5	R	GEAHLAVNDFELAR	A	41228.4
		100.0	25	34	98	3.48	57.5	K	GEDLTEEEDGGIIR	R	8982.94
		100.0	25	34	98	3.48	57.5	K	GEHSIVYLKPSYAFGSVGK	E	18818.6
		100.0	25	34	98	3.48	57.5	K	IVSWLEYESSFSNEEAQK	A	8385.15
		100.0	25	34	98	3.48	57.5	K	LQAFSAAIESCNK	A	185708
		100.0	25	34	98	3.48	57.5	K	LYANMFER	L	337808
		100.0	25	34	98	3.48	57.5	-	MTAEEMKATESGAQSAPLPMEGV-DISPK	Q	2430.82
		100.0	25	34	98	3.48	57.5	K	QALLQYK	K	138481
		100.0	25	34	98	3.48	57.5	R	RGEAHLAVNDFELAR	A	49956.9
		100.0	25	34	98	3.48	57.5	M	TAEEMKATESGAQSAPLPMEGVDISPK	Q	4072.25
		100.0	25	34	98	3.48	57.5	K	TQLAVCQQR	I	8882.59
		100.0	25	34	98	3.48	57.5	R	VFVHYTGWLLDGTK	F	23788.8
		100.0	25	34	98	3.48	57.5	K	VGEVCHITCKPEYAYGSAGSPPK	I	33625.7
		100.0	25	34	98	3.48	57.5	K	VLQLYPNNK	A	415247
		100.0	25	34	98	3.48	57.5	K	YKQALLQYK	K	31199.0
30_81	4-trimethylaminobutyr-	100.0	6	9	43	1.60	32.2	R	ANDTTFGLAAGVFTR	D	26389.7
	aldehyde dehydrogenase	100.0	6	9	43	1.60	32.2	K	EVNLAVQNAK	A	5123.67
	OS=Homo sapiens	100.0	6	9	43	1.60	32.2	K	GALMANFLTQGQVCCNGTR	V	5309.74
	GN=ALDH9A1 PE=1	100.0	6	9	43	1.60	32.2	K	GIKPVTLELGGK	S	38428.3
	SV=3	100.0	6	9	43	1.60	32.2	K	IGDPLLEDTR	M	47100.4
	AL9A1_HUMAN	100.0	6	9	43	1.60	32.2	-	MSTGTFVVSQPLNYR	G	22380.2
	53787.0	100.0	6	9	43	1.60	32.2	K	SPLIIFSDCDMNNAVK	G	15049.7
		100.0	6	9	43	1.60	32.2	M	STGTFVVSQPLNYR	G	6899.89
		100.0	6	9	43	1.60	32.2	K	TVCVEMGDVESAF	-	4720.93
		100.0	6	9	43	1.60	32.2	R	VIATFTCSGEK	E	25280.0
		100.0	6	9	43	1.60	32.2	R	VIATFTCSGEKEVNLAVQNAK	A	22442.4
		100.0	6	9	43	1.60	32.2	K	VLCGGDIYVPEDPK	L	13658.6
		100.0	6	9	43	1.60	32.2	K	VLCGGDIYVPEDPKLK	D	21948.9
		100.0	6	9	43	1.60	32.2	K	VSFTGSVPTGMK	I	78032.3
		100.0	6	9	43	1.60	32.2	R	VTIEYYSQLK	T	75516.7
		100.0	6	9	43	1.60	32.2	R	ANDTTFGLAAGVFTR	D	26389.7
		100.0	6	9	43	1.60	32.2	K	EVNLAVQNAK	A	5123.67
		100.0	6	9	43	1.60	32.2	K	GALMANFLTQGQVCCNGTR	V	5309.74
		100.0	6	9	43	1.60	32.2	K	GIKPVTLELGGK	S	38428.3
		100.0	6	9	43	1.60	32.2	K	IGDPLLEDTR	M	47100.4
		100.0	6	9	43	1.60	32.2	-	MSTGTFVVSQPLNYR	G	22380.2
		100.0	6	9	43	1.60	32.2	K	SPLIIFSDCDMNNAVK	G	15049.7
		100.0	6	9	43	1.60	32.2	M	STGTFVVSQPLNYR	G	6899.89
		100.0	6	9	43	1.60	32.2	K	TVCVEMGDVESAF	-	4720.93
		100.0	6	9	43	1.60	32.2	R	VIATFTCSGEK	E	25280.0
		100.0	6	9	43	1.60	32.2	R	VIATFTCSGEKEVNLAVQNAK	A	22442.4
		100.0	6	9	43	1.60	32.2	K	VLCGGDIYVPEDPK	L	13658.6
		100.0	6	9	43	1.60	32.2	K	VLCGGDIYVPEDPKLK	D	21948.9
		100.0	6	9	43	1.60	32.2	K	VSFTGSVPTGMK	I	78032.3
		100.0	6	9	43	1.60	32.2	R	VTIEYYSQLK	T	75516.7
30_87	4-trimethylaminobutyr-	100.0	8	10	78	2.87	41.5	R	ANDTTFGLAAGVFTR	D	57851.3
	aldehyde dehydrogenase	100.0	8	10	78	2.87	41.5	R	CRILLEAAR	I	10192.8
	OS=Homo sapiens	100.0	8	10	78	2.87	41.5	R	EDEIATMECINNGK	S	1809.31
	GN=ALDH9A1 PE=1	100.0	8	10	78	2.87	41.5	K	EVNLAVQNAK	A	38229.0
	SV=3	100.0	8	10	78	2.87	41.5	K	GALMANFLTQGQVCCNGTR	V	7336.15
	AL9A1_HUMAN	100.0	8	10	78	2.87	41.5	K	GIKPVTLELGGK	S	20015.5
	53802.0	100.0	8	10	78	2.87	41.5	K	IGDPLLEDTR	M	111875
		100.0	8	10	78	2.87	41.5	R	ILLEAAR	I	46159.7
		100.0	8	10	78	2.87	41.5	-	MSTGTFVVSQPLNYR	G	43327.3
		100.0	8	10	78	2.87	41.5	K	SPLIIFSDCDMNNAVK	G	30102.5
		100.0	8	10	78	2.87	41.5	M	STGTFVVSQPLNYR	G	28432.9
		100.0	8	10	78	2.87	41.5	M	STGTFVVSQPLNYRGGAR	V	6064.35
		100.0	8	10	78	2.87	41.5	K	TVCVEMGDVESAF	-	15042.1
		100.0	8	10	78	2.87	41.5	R	VEPADASGTEKAFEPATGR	V	11331.5
		100.0	8	10	78	2.87	41.5	R	VIATFTCSGEK	E	59817.3
		100.0	8	10	78	2.87	41.5	R	VIATFTCSGEKEVNLAVQNAK	A	2496.19
		100.0	8	10	78	2.87	41.5	K	VLCGGDIYVPEDPK	L	33371.9
		100.0	8	10	78	2.87	41.5	K	VLCGGDIYVPEDPKLK	D	53995.9
		100.0	8	10	78	2.87	41.5	K	VSFTGSVPTGMK	I	210979
		100.0	8	10	78	2.87	41.5	R	VTIEYYSQLK	T	91220.3
31_82	4-trimethylaminobutyr-	100.0	10	15	99	3.35	47.6	R	ANDTTFGLAAGVFTR	D	93714.8

	aldehyde dehydrogenase	100.0	10	15	99	3.35	47.6	R	CRILLEAAR	I	21580.8
	OS=Homo sapiens	100.0	10	15	99	3.35	47.6	K	DGYYMRPCVLTNCR	D	13528.5
	GN=ALDH9A1 PE=1	100.0	10	15	99	3.35	47.6	R	EDEIATMECINNGK	S	5463.63
	SV=3	100.0	10	15	99	3.35	47.6	K	EILDKFTEEVVK	Q	14659.1
	AL9A1_HUMAN	100.0	10	15	99	3.35	47.6	R	ENGRVTIEYYSQLK	T	11121.2
	53802.0	100.0	10	15	99	3.35	47.6	R	EREDEIATMECINNGK	S	8756.06
		100.0	10	15	99	3.35	47.6	K	EVNLAVQNAK	A	12149.3
		100.0	10	15	99	3.35	47.6	K	GALMANFLTQGQVCCNGTR	V	31780.2
		100.0	10	15	99	3.35	47.6	K	GIKPVTLELGGK	S	54539.7
		100.0	10	15	99	3.35	47.6	K	IGDPLLEDTR	M	151440
		100.0	10	15	99	3.35	47.6	R	IKIGDPLLEDTR	M	50616.4
		100.0	10	15	99	3.35	47.6	R	ILLEAAR	I	273407
		100.0	10	15	99	3.35	47.6	-	MSTGTFVVSQPLNYR	G	60154.7
		100.0	10	15	99	3.35	47.6	K	SPLIIFSDCDMNNAVK	G	38245.9
		100.0	10	15	99	3.35	47.6	M	STGTFVVSQPLNYR	G	18405.1
		100.0	10	15	99	3.35	47.6	K	TVCVEMGDVESAF	-	8081.73
		100.0	10	15	99	3.35	47.6	R	VEPADASGTEKAFEPATGR	V	13318.3
		100.0	10	15	99	3.35	47.6	R	VIATFTCSGEK	E	70873.2
		100.0	10	15	99	3.35	47.6	R	VIATFTCSGEKEVNLAVQNAK	A	55664.4
		100.0	10	15	99	3.35	47.6	K	VLCGGDIYVPEDPK	L	56270.7
		100.0	10	15	99	3.35	47.6	K	VLCGGDIYVPEDPKLK	D	67403.8
		100.0	10	15	99	3.35	47.6	K	VSFTGSVPTGMK	I	244077
		100.0	10	15	99	3.35	47.6	R	VTIEYYSQLK	T	190265
31_84	4-trimethylaminobutyr-	100.0	8	8	14	0.970	21.1	R	ANDTTFGLAAGVFTR	D	3595.85
	aldehyde dehydrogenase	100.0	8	8	14	0.970	21.1	K	IGDPLLEDTR	M	11450.2
	OS=Homo sapiens	100.0	8	8	14	0.970	21.1	R	ILLEAAR	I	11477.5
	GN=ALDH9A1 PE=1	100.0	8	8	14	0.970	21.1	-	MSTGTFVVSQPLNYR	G	4940.43
	SV=3	100.0	8	8	14	0.970	21.1	R	VIATFTCSGEKEVNLAVQNAK	A	2879.85
	AL9A1_HUMAN	100.0	8	8	14	0.970	21.1	K	VLCGGDIYVPEDPK	L	3831.08
	53787.0	100.0	8	8	14	0.970	21.1	K	VSFTGSVPTGMK	I	10895.7
		100.0	8	8	14	0.970	21.1	R	VTIEYYSQLK	T	12074.1
		100.0	8	8	14	0.970	21.1	R	ANDTTFGLAAGVFTR	D	3595.85
		100.0	8	8	14	0.970	21.1	K	IGDPLLEDTR	M	11450.2
		100.0	8	8	14	0.970	21.1	R	ILLEAAR	I	11477.5
		100.0	8	8	14	0.970	21.1	-	MSTGTFVVSQPLNYR	G	4940.43
		100.0	8	8	14	0.970	21.1	R	VIATFTCSGEKEVNLAVQNAK	A	2879.85
		100.0	8	8	14	0.970	21.1	K	VLCGGDIYVPEDPK	L	3831.08
		100.0	8	8	14	0.970	21.1	K	VSFTGSVPTGMK	I	10895.7
		100.0	8	8	14	0.970	21.1	R	VTIEYYSQLK	T	12074.1
32_82	Actin-related protein 3	100.0	21	28	199	6.88	68.4	R	AEPEDHYFLLTEPPLNTPENR	E	50140.8
	OS=Homo sapiens	100.0	21	28	199	6.88	68.4	M	AGRLPACVVDCGTGYTK	L	346417
	GN=ACTR3 PE=1 SV=3	100.0	21	28	199	6.88	68.4	R	DITYFIQQLLR	D	19190.1
	ARP3_HUMAN	100.0	21	28	199	6.88	68.4	R	DREVGIPPEQSLETAK	A	127114
	47371.9	100.0	21	28	199	6.88	68.4	K	DYEEIGPSICR	H	133501
		100.0	21	28	199	6.88	68.4	K	EFSIDVGYER	F	329956
		100.0	21	28	199	6.88	68.4	K	ERYSYVCPDLVK	E	3420.33
		100.0	21	28	199	6.88	68.4	R	EVGIPPEQSLETAK	A	72098.0
		100.0	21	28	199	6.88	68.4	R	FMEQVIFK	Y	452700
		100.0	21	28	199	6.88	68.4	R	FMEQVIFKYLR	A	12327.6
		100.0	21	28	199	6.88	68.4	K	GVDDLDFFIGDEAIEKPTYATK	W	63973.5
		100.0	21	28	199	6.88	68.4	R	HGIVEDWDLMER	F	26809.6
		100.0	21	28	199	6.88	68.4	R	HNPVFGVMS	-	256696
		100.0	21	28	199	6.88	68.4	K	KDYEEIGPSICR	H	29481.5
		100.0	21	28	199	6.88	68.4	K	KEFSIDVGYER	F	50963.8
		100.0	21	28	199	6.88	68.4	K	LGYAGNTEPQFIIPSCIAIK	E	24430.4
		100.0	21	28	199	6.88	68.4	K	LGYAGNTEPQFIIPSCIAIKESAK	V	87840.5
		100.0	21	28	199	6.88	68.4	R	LKLSEELSGGR	L	80608.5
		100.0	21	28	199	6.88	68.4	R	LPACVVDCGTGYTK	L	68922.6
		100.0	21	28	199	6.88	68.4	K	LSEELSGGR	L	4681.36
		100.0	21	28	199	6.88	68.4	K	NIVLSGGSTMFR	D	370274
		100.0	21	28	199	6.88	68.4	K	NIVLSGGSTMFRDFGR	R	107959
		100.0	21	28	199	6.88	68.4	K	QYTGINAISK	K	188646
		100.0	21	28	199	6.88	68.4	K	QYTGINAISKK	E	87517.0
		100.0	21	28	199	6.88	68.4	K	QYTGINAISKKEFSIDVGYER	F	1863.27
		100.0	21	28	199	6.88	68.4	R	RVMKGVDDLDFFIGDEAIEKPTYATK	W	4393.80
		100.0	21	28	199	6.88	68.4	R	TLTGTVIDSGDGVTHVIPVAEGYV-IGSCIK	H	11402.6
		100.0	21	28	199	6.88	68.4	R	VMKGVDDLDFFIGDEAIEKPTYATK	W	20021.7
		100.0	21	28	199	6.88	68.4	K	WIKQYTGINAISK	K	12753.0
		100.0	21	28	199	6.88	68.4	R	YAVWFGGSMLASTPEFYQVCHTK	K	15524.9
		100.0	21	28	199	6.88	68.4	K	YDTDGSKWIK	Q	6712.07
		100.0	21	28	199	6.88	68.4	K	YLRAEPEDHYFLLTEPPLNTPENR	E	26253.7
		100.0	21	28	199	6.88	68.4	R	YSYVCPDLVK	E	305823
		100.0	21	28	199	6.88	68.4	R	YSYVCPDLVKEFNK	Y	30402.2
		100.0	21	28	199	6.88	68.4	R	YSYVCPDLVKEFNKYDTDGSK	W	2884.25

		100.0	21	28	199	6.88	68.4	R	AEPEDHYFLLTEPPLNTPENR	E	50140.8
		100.0	21	28	199	6.88	68.4	M	AGRLPACVVDCGTGYTK	L	346417
		100.0	21	28	199	6.88	68.4	R	DITYFIQQLLR	D	19190.1
		100.0	21	28	199	6.88	68.4	R	DREVGIPPEQSLETAK	A	127114
		100.0	21	28	199	6.88	68.4	K	DYEEIGPSICR	H	133501
		100.0	21	28	199	6.88	68.4	K	EFSIDVGYER	F	329956
		100.0	21	28	199	6.88	68.4	K	ERYSYVCPDLVK	E	3420.33
		100.0	21	28	199	6.88	68.4	R	EVGIPPEQSLETAK	A	72098.0
		100.0	21	28	199	6.88	68.4	R	FMEQVIFK	Y	452700
		100.0	21	28	199	6.88	68.4	R	FMEQVIFKYLR	A	12327.6
		100.0	21	28	199	6.88	68.4	K	GVDDLDFFIGDEAIEKPTYATK	W	63973.5
		100.0	21	28	199	6.88	68.4	R	HGIVEDWDLMER	F	26809.6
		100.0	21	28	199	6.88	68.4	R	HNPVFGVMS	-	256696
		100.0	21	28	199	6.88	68.4	K	KDYEEIGPSICR	H	29481.5
		100.0	21	28	199	6.88	68.4	K	KEFSIDVGYER	F	50963.8
		100.0	21	28	199	6.88	68.4	K	LGYAGNTEPQFIIPSCIAIK	E	24430.4
		100.0	21	28	199	6.88	68.4	K	LGYAGNTEPQFIIPSCIAIKESAK	V	87840.5
		100.0	21	28	199	6.88	68.4	R	LKLSEELSGGR	L	80608.5
		100.0	21	28	199	6.88	68.4	R	LPACVVDCGTGYTK	L	68922.6
		100.0	21	28	199	6.88	68.4	K	LSEELSGGR	L	4681.36
		100.0	21	28	199	6.88	68.4	K	NIVLSGGSTMFR	D	370274
		100.0	21	28	199	6.88	68.4	K	NIVLSGGSTMFRDFGR	R	107959
		100.0	21	28	199	6.88	68.4	K	QYTGINAISK	K	188646
		100.0	21	28	199	6.88	68.4	K	QYTGINAISKK	E	87517.0
		100.0	21	28	199	6.88	68.4	K	QYTGINAISKKEFSIDVGYER	F	1863.27
		100.0	21	28	199	6.88	68.4	R	RVMKGVDDLDFFIGDEAIEKPTYATK	W	4393.80
		100.0	21	28	199	6.88	68.4	R	TLTGTVIDSGDGVTHVIPVAEGYV-IGSCIK	H	11402.6
		100.0	21	28	199	6.88	68.4	R	VMKGVDDLDFFIGDEAIEKPTYATK	W	20021.7
		100.0	21	28	199	6.88	68.4	K	WIKQYTGINAISK	K	12753.0
		100.0	21	28	199	6.88	68.4	R	YAVWFGGSMLASTPEFYQVCHTK	K	15524.9
		100.0	21	28	199	6.88	68.4	K	YDTDGSKWIK	Q	6712.07
		100.0	21	28	199	6.88	68.4	K	YLRAEPEDHYFLLTEPPLNTPENR	E	26253.7
		100.0	21	28	199	6.88	68.4	R	YSYVCPDLVK	E	305823
		100.0	21	28	199	6.88	68.4	R	YSYVCPDLVKEFNK	Y	30402.2
		100.0	21	28	199	6.88	68.4	R	YSYVCPDLVKEFNKYDTDGSK	W	2884.25
		100.0	21	28	199	6.88	68.4	R	AEPEDHYFLLTEPPLNTPENR	E	50140.8
		100.0	21	28	199	6.88	68.4	M	AGRLPACVVDCGTGYTK	L	346417
		100.0	21	28	199	6.88	68.4	R	DITYFIQQLLR	D	19190.1
		100.0	21	28	199	6.88	68.4	R	DREVGIPPEQSLETAK	A	127114
		100.0	21	28	199	6.88	68.4	K	DYEEIGPSICR	H	133501
		100.0	21	28	199	6.88	68.4	K	EFSIDVGYER	F	329956
		100.0	21	28	199	6.88	68.4	K	ERYSYVCPDLVK	E	3420.33
		100.0	21	28	199	6.88	68.4	R	EVGIPPEQSLETAK	A	72098.0
		100.0	21	28	199	6.88	68.4	R	FMEQVIFK	Y	452700
		100.0	21	28	199	6.88	68.4	R	FMEQVIFKYLR	A	12327.6
		100.0	21	28	199	6.88	68.4	K	GVDDLDFFIGDEAIEKPTYATK	W	63973.5
		100.0	21	28	199	6.88	68.4	R	HGIVEDWDLMER	F	26809.6
		100.0	21	28	199	6.88	68.4	R	HNPVFGVMS	-	256696
		100.0	21	28	199	6.88	68.4	K	KDYEEIGPSICR	H	29481.5
		100.0	21	28	199	6.88	68.4	K	KEFSIDVGYER	F	50963.8
		100.0	21	28	199	6.88	68.4	K	LGYAGNTEPQFIIPSCIAIK	E	24430.4
		100.0	21	28	199	6.88	68.4	K	LGYAGNTEPQFIIPSCIAIKESAK	V	87840.5
		100.0	21	28	199	6.88	68.4	R	LKLSEELSGGR	L	80608.5
		100.0	21	28	199	6.88	68.4	R	LPACVVDCGTGYTK	L	68922.6
		100.0	21	28	199	6.88	68.4	K	LSEELSGGR	L	4681.36
		100.0	21	28	199	6.88	68.4	K	NIVLSGGSTMFR	D	370274
		100.0	21	28	199	6.88	68.4	K	NIVLSGGSTMFRDFGR	R	107959
		100.0	21	28	199	6.88	68.4	K	QYTGINAISK	K	188646
		100.0	21	28	199	6.88	68.4	K	QYTGINAISKK	E	87517.0
		100.0	21	28	199	6.88	68.4	K	QYTGINAISKKEFSIDVGYER	F	1863.27
		100.0	21	28	199	6.88	68.4	R	RVMKGVDDLDFFIGDEAIEKPTYATK	W	4393.80
		100.0	21	28	199	6.88	68.4	R	TLTGTVIDSGDGVTHVIPVAEGYV-IGSCIK	H	11402.6
		100.0	21	28	199	6.88	68.4	R	VMKGVDDLDFFIGDEAIEKPTYATK	W	20021.7
		100.0	21	28	199	6.88	68.4	K	WIKQYTGINAISK	K	12753.0
		100.0	21	28	199	6.88	68.4	R	YAVWFGGSMLASTPEFYQVCHTK	K	15524.9
		100.0	21	28	199	6.88	68.4	K	YDTDGSKWIK	Q	6712.07
		100.0	21	28	199	6.88	68.4	K	YLRAEPEDHYFLLTEPPLNTPENR	E	26253.7
		100.0	21	28	199	6.88	68.4	R	YSYVCPDLVK	E	305823
		100.0	21	28	199	6.88	68.4	R	YSYVCPDLVKEFNK	Y	30402.2
		100.0	21	28	199	6.88	68.4	R	YSYVCPDLVKEFNKYDTDGSK	W	2884.25
32_86	Actin-related protein 3	100.0	19	27	203	5.91	72.2	R	AEPEDHYFLLTEPPLNTPENR	E	91431.4
	OS=Homo sapiens	100.0	19	27	203	5.91	72.2	M	AGRLPACVVDCGTGYTK	L	948357
	GN=ACTR3 PE=1 SV=3	100.0	19	27	203	5.91	72.2	R	DITYFIQQLLR	D	25847.1

ARP3_HUMAN	100.0	19	27	203	5.91	72.2	R	DREVGIPPEQSLETAK	A	193776
47371.9	100.0	19	27	203	5.91	72.2	K	DYEEIGPSICR	H	178928
	100.0	19	27	203	5.91	72.2	K	EFSIDVGYER	F	475781
	100.0	19	27	203	5.91	72.2	K	ERYSYVCPDLVK	E	25763.8
	100.0	19	27	203	5.91	72.2	R	EVGIPPEQSLETAK	A	103464
	100.0	19	27	203	5.91	72.2	R	FMEQVIFK	Y	624698
	100.0	19	27	203	5.91	72.2	K	GVDDLDFFIGDEAIEKPTYATK	W	121892
	100.0	19	27	203	5.91	72.2	R	HGIVEDWDLMER	F	87474.5
	100.0	19	27	203	5.91	72.2	R	HNPVFGVMS	-	413599
	100.0	19	27	203	5.91	72.2	K	KDYEEIGPSICR	H	28070.2
	100.0	19	27	203	5.91	72.2	K	KEFSIDVGYER	F	31449.2
	100.0	19	27	203	5.91	72.2	K	LGYAGNTEPQFIIPSCIAIK	E	30307.1
	100.0	19	27	203	5.91	72.2	K	LGYAGNTEPQFIIPSCIAIKESAK	V	66278.3
	100.0	19	27	203	5.91	72.2	R	LKLSEELSGGR	L	160237
	100.0	19	27	203	5.91	72.2	R	LKPKPIDVQVITHHMQR	Y	12941.7
	100.0	19	27	203	5.91	72.2	R	LPACVVDCGTGYTK	L	127211
	100.0	19	27	203	5.91	72.2	K	LSEELSGGR	L	14161.1
	100.0	19	27	203	5.91	72.2	K	NIVLSGGSTMFR	D	542435
	100.0	19	27	203	5.91	72.2	K	NIVLSGGSTMFRDFGR	R	127368
	100.0	19	27	203	5.91	72.2	K	QYTGINAISK	K	332480
	100.0	19	27	203	5.91	72.2	K	QYTGINAISKK	E	311926
	100.0	19	27	203	5.91	72.2	K	QYTGINAISKKEFSIDVGYER	F	3275.57
	100.0	19	27	203	5.91	72.2	R	TLTGTVIDSGDGVTHVIPVAEG-YVIGSCIK	H	35985.0
	100.0	19	27	203	5.91	72.2	R	VMKGVDDLDFFIGDEAIEKPTYATK	W	31850.4
	100.0	19	27	203	5.91	72.2	K	WIKQYTGINAISK	K	14322.1
	100.0	19	27	203	5.91	72.2	R	YAVWFGGSMLASTPEFYQVCHTK	K	40433.0
	100.0	19	27	203	5.91	72.2	K	YLRAEPEDHYFLLTEPPLNTPENR	E	32338.5
	100.0	19	27	203	5.91	72.2	R	YSYVCPDLVK	E	439349
	100.0	19	27	203	5.91	72.2	R	YSYVCPDLVKEFNK	Y	3104.24
	100.0	19	27	203	5.91	72.2	R	YSYVCPDLVKEFNKYDTDGSK	W	11256.8
	100.0	19	27	203	5.91	72.2	R	AEPEDHYFLLTEPPLNTPENR	E	91431.4
	100.0	19	27	203	5.91	72.2	M	AGRLPACVVDCGTGYTK	L	948357
	100.0	19	27	203	5.91	72.2	R	DITYFIQQLLR	D	25847.1
	100.0	19	27	203	5.91	72.2	R	DREVGIPPEQSLETAK	A	193776
	100.0	19	27	203	5.91	72.2	K	DYEEIGPSICR	H	178928
	100.0	19	27	203	5.91	72.2	K	EFSIDVGYER	F	475781
	100.0	19	27	203	5.91	72.2	K	ERYSYVCPDLVK	E	25763.8
	100.0	19	27	203	5.91	72.2	R	EVGIPPEQSLETAK	A	103464
	100.0	19	27	203	5.91	72.2	R	FMEQVIFK	Y	624698
	100.0	19	27	203	5.91	72.2	K	GVDDLDFFIGDEAIEKPTYATK	W	121892
	100.0	19	27	203	5.91	72.2	R	HGIVEDWDLMER	F	87474.5
	100.0	19	27	203	5.91	72.2	R	HNPVFGVMS	-	413599
	100.0	19	27	203	5.91	72.2	K	KDYEEIGPSICR	H	28070.2
	100.0	19	27	203	5.91	72.2	K	KEFSIDVGYER	F	31449.2
	100.0	19	27	203	5.91	72.2	K	LGYAGNTEPQFIIPSCIAIK	E	30307.1
	100.0	19	27	203	5.91	72.2	K	LGYAGNTEPQFIIPSCIAIKESAK	V	66278.3
	100.0	19	27	203	5.91	72.2	R	LKLSEELSGGR	L	160237
	100.0	19	27	203	5.91	72.2	R	LKPKPIDVQVITHHMQR	Y	12941.7
	100.0	19	27	203	5.91	72.2	R	LPACVVDCGTGYTK	L	127211
	100.0	19	27	203	5.91	72.2	K	LSEELSGGR	L	14161.1
	100.0	19	27	203	5.91	72.2	K	NIVLSGGSTMFR	D	542435
	100.0	19	27	203	5.91	72.2	K	NIVLSGGSTMFRDFGR	R	127368
	100.0	19	27	203	5.91	72.2	K	QYTGINAISK	K	332480
	100.0	19	27	203	5.91	72.2	K	QYTGINAISKK	E	311926
	100.0	19	27	203	5.91	72.2	K	QYTGINAISKKEFSIDVGYER	F	3275.57
	100.0	19	27	203	5.91	72.2	R	TLTGTVIDSGDGVTHVIPVAEGY-VIGSCIK	H	35985.0
	100.0	19	27	203	5.91	72.2	R	VMKGVDDLDFFIGDEAIEKPTYATK	W	31850.4
	100.0	19	27	203	5.91	72.2	K	WIKQYTGINAISK	K	14322.1
	100.0	19	27	203	5.91	72.2	R	YAVWFGGSMLASTPEFYQVCHTK	K	40433.0
	100.0	19	27	203	5.91	72.2	K	YLRAEPEDHYFLLTEPPLNTPENR	E	32338.5
	100.0	19	27	203	5.91	72.2	R	YSYVCPDLVK	E	439349
	100.0	19	27	203	5.91	72.2	R	YSYVCPDLVKEFNK	Y	3104.24
	100.0	19	27	203	5.91	72.2	R	YSYVCPDLVKEFNKYDTDGSK	W	11256.8
	100.0	19	27	203	5.91	72.2	R	AEPEDHYFLLTEPPLNTPENR	E	91431.4
	100.0	19	27	203	5.91	72.2	M	AGRLPACVVDCGTGYTK	L	948357
	100.0	19	27	203	5.91	72.2	R	DITYFIQQLLR	D	25847.1
	100.0	19	27	203	5.91	72.2	R	DREVGIPPEQSLETAK	A	193776
	100.0	19	27	203	5.91	72.2	K	DYEEIGPSICR	H	178928
	100.0	19	27	203	5.91	72.2	K	EFSIDVGYER	F	475781
	100.0	19	27	203	5.91	72.2	K	ERYSYVCPDLVK	E	25763.8
	100.0	19	27	203	5.91	72.2	R	EVGIPPEQSLETAK	A	103464
	100.0	19	27	203	5.91	72.2	R	FMEQVIFK	Y	624698
	100.0	19	27	203	5.91	72.2	K	GVDDLDFFIGDEAIEKPTYATK	W	121892

		100.0	19	27	203	5.91	72.2	R	HGIVEDWDLMER	F	87474.5
		100.0	19	27	203	5.91	72.2	R	HNPVFGVMS	-	413599
		100.0	19	27	203	5.91	72.2	K	KDYEEIGPSICR	H	28070.2
		100.0	19	27	203	5.91	72.2	K	KEFSIDVGYER	F	31449.2
		100.0	19	27	203	5.91	72.2	K	LGYAGNTEPQFIIPSCIAIK	E	30307.1
		100.0	19	27	203	5.91	72.2	K	LGYAGNTEPQFIIPSCIAIKESAK	V	66278.3
		100.0	19	27	203	5.91	72.2	R	LKLSEELSGGR	L	160237
		100.0	19	27	203	5.91	72.2	R	LKPKPIDVQVITHHMQR	Y	12941.7
		100.0	19	27	203	5.91	72.2	R	LPACVVDCGTGYTK	L	127211
		100.0	19	27	203	5.91	72.2	K	LSEELSGGR	L	14161.1
		100.0	19	27	203	5.91	72.2	K	NIVLSGGSTMFR	D	542435
		100.0	19	27	203	5.91	72.2	K	NIVLSGGSTMFRDFGR	R	127368
		100.0	19	27	203	5.91	72.2	K	QYTGINAISK	K	332480
		100.0	19	27	203	5.91	72.2	K	QYTGINAISKK	E	311926
		100.0	19	27	203	5.91	72.2	K	QYTGINAISKKEFSIDVGYER	F	3275.57
		100.0	19	27	203	5.91	72.2	R	TLTGTVIDSGDGVTHVIPVAEGYVI-GSCIK	H	35985.0
		100.0	19	27	203	5.91	72.2	R	VMKGVDDLDFFIGDEAIEKPTYATK	W	31850.4
		100.0	19	27	203	5.91	72.2	K	WIKQYTGINAISK	K	14322.1
		100.0	19	27	203	5.91	72.2	R	YAVWFGGSMLASTPEFYQVCHTK	K	40433.0
		100.0	19	27	203	5.91	72.2	K	YLRAEPEDHYFLLTEPPLNTPENR	E	32338.5
		100.0	19	27	203	5.91	72.2	R	YSYVCPDLVK	E	439349
		100.0	19	27	203	5.91	72.2	R	YSYVCPDLVKEFNK	Y	3104.24
		100.0	19	27	203	5.91	72.2	R	YSYVCPDLVKEFNKYDTDGSK	W	11256.8
33_82	Pachytene checkpoint	100.0	10	13	127	3.17	58.6	R	ADIKQYIGPPSAAAIFK	I	22919.2
	protein 2 homolog	100.0	10	13	127	3.17	58.6	R	AGTEPSDAIR	V	8233.92
	OS=Homo sapiens	100.0	10	13	127	3.17	58.6	K	ALAQKLTIR	L	28330.5
	GN=TRIP13 PE=1 SV=2	100.0	10	13	127	3.17	58.6	K	CQIIYPR	Q	553139
	PCH2_HUMAN	100.0	10	13	127	3.17	58.6	K	EDINLSVRK	L	9672.64
	48552.1	100.0	10	13	127	3.17	58.6	R	ELEMIGFIENNVSK	L	64030.0
		100.0	10	13	127	3.17	58.6	R	GSSTAKKEDINLSVR	K	2186.69
		100.0	10	13	127	3.17	58.6	R	HSNVVILTTSNITEK	I	78427.1
		100.0	10	13	127	3.17	58.6	K	IDVAFVDR	A	210889
		100.0	10	13	127	3.17	58.6	K	IDVAFVDRADIK	Q	86702.0
		100.0	10	13	127	3.17	58.6	K	IQDLIDDK	D	12727.5
		100.0	10	13	127	3.17	58.6	K	IYLSCLEELMK	C	93679.1
		100.0	10	13	127	3.17	58.6	R	KKLAAYI	-	10769.3
		100.0	10	13	127	3.17	58.6	K	LSLLLNDISR	K	462668
		100.0	10	13	127	3.17	58.6	K	LSLLLNDISRK	S	78873.5
		100.0	10	13	127	3.17	58.6	-	MDEAVGDLK	Q	101885
		100.0	10	13	127	3.17	58.6	K	NVNSNLITWNR	V	82288.0
		100.0	10	13	127	3.17	58.6	R	NVQSVSIIDTELK	V	153262
		100.0	10	13	127	3.17	58.6	R	NVQSVSIIDTELKVK	D	138788
		100.0	10	13	127	3.17	58.6	K	QALPCVAESPTVHVEVHQR	G	3985.34
		100.0	10	13	127	3.17	58.6	R	QQLLTLR	E	432935
		100.0	10	13	127	3.17	58.6	R	QQLLTLRELEMIGFIENNVSK	L	8379.52
		100.0	10	13	127	3.17	58.6	K	QYIGPPSAAAIFK	I	274235
		100.0	10	13	127	3.17	58.6	K	RHSNVVILTTSNITEK	I	6852.70
		100.0	10	13	127	3.17	58.6	K	SHLLDYVMTTLLFSDK	N	22001.9
		100.0	10	13	127	3.17	58.6	V	VLLHGPPGTGK	T	17757.8
		100.0	10	13	127	3.17	58.6	R	VVLLHGPPGTGK	T	639469
		100.0	10	13	127	3.17	58.6	R	VVNAVLTQIDQIK	R	33313.8
		100.0	10	13	127	3.17	58.6	R	VVNAVLTQIDQIKR	H	784561
		100.0	10	13	127	3.17	58.6	R	YGQLIEINSHSLFSK	W	64672.2
		100.0	10	13	127	3.17	58.6	R	YRYGQLIEINSHSLFSK	W	4738.36
33_87	Pachytene checkpoint	100.0	15	20	57	2.52	35.9	R	ELEMIGFIENNVSK	L	24187.3
	protein 2 homolog	100.0	15	20	57	2.52	35.9	R	HSNVVILTTSNITEK	I	29194.0
	OS=Homo sapiens	100.0	15	20	57	2.52	35.9	K	IDVAFVDR	A	63172.3
	GN=TRIP13 PE=1 SV=2	100.0	15	20	57	2.52	35.9	K	IQDLIDDK	D	9198.72
	PCH2_HUMAN	100.0	15	20	57	2.52	35.9	K	IYLSCLEELMK	C	29543.5
	48552.1	100.0	15	20	57	2.52	35.9	K	LSLLLNDISR	K	140965
		100.0	15	20	57	2.52	35.9	-	MDEAVGDLK	Q	24741.9
		100.0	15	20	57	2.52	35.9	K	NVNSNLITWNR	V	39722.8
		100.0	15	20	57	2.52	35.9	R	NVQSVSIIDTELK	V	59302.8
		100.0	15	20	57	2.52	35.9	R	NVQSVSIIDTELKVK	D	6871.68
		100.0	15	20	57	2.52	35.9	K	QYIGPPSAAAIFK	I	120240
		100.0	15	20	57	2.52	35.9	R	VVLLHGPPGTGK	T	307688
		100.0	15	20	57	2.52	35.9	R	VVNAVLTQIDQIK	R	11725.1
		100.0	15	20	57	2.52	35.9	R	VVNAVLTQIDQIKR	H	130655
		100.0	15	20	57	2.52	35.9	R	YGQLIEINSHSLFSK	W	1728.67
35_81	Endoplasmic reticulum	100.0	12	13	57	2.54	24.4	K	ALADYIR	Q	29141.6
	resident protein 44	100.0	12	13	57	2.54	24.4	K	ALADYIRQQK	S	8624.95
	OS=Homo sapiens	100.0	12	13	57	2.54	24.4	D	CPVIAIDSFR	H	6538.91
	GN=ERP44 PE=1 SV=1	100.0	12	13	57	2.54	24.4	R	DLAEITTLDR	S	264415
	46,972.5	100.0	12	13	57	2.54	24.4	K	DVLIPGK	L	24025.5

		100.0	12	13	57	2.54	24.4	K	EDTESLEIFQNEVAR	Q	9085.78
		100.0	12	13	57	2.54	24.4	K	EEFPNENQVVFAR	V	7253.88
		100.0	12	13	57	2.54	24.4	R	NIIGYFEQK	D	84446.7
		100.0	12	13	57	2.54	24.4	K	QFVFDLHSGK	L	36946.8
		100.0	12	13	57	2.54	24.4	K	SDPIQEIR	D	212462
		100.0	12	13	57	2.54	24.4	R	SVKALADYIR	Q	48962.5
		100.0	12	13	57	2.54	24.4	K	TPADCPVIAIDSFR	H	387755
35_85	Endoplasmic reticulum	100.0	11	14	44	2.28	27.7	K	ALADYIRQQK	S	8474.67
	resident protein 44	100.0	11	14	44	2.28	27.7	R	DLAEITTLDR	S	152086
	OS=Homo sapiens	100.0	11	14	44	2.28	27.7	K	EDTESLEIFQNEVAR	Q	6618.56
	GN=ERP44 PE=1 SV=1	100.0	11	14	44	2.28	27.7	K	EEFPNENQVVFAR	V	8166.43
	46,972.5	100.0	11	14	44	2.28	27.7	R	NIIGYFEQK	D	40052.1
		100.0	11	14	44	2.28	27.7	K	QFVFDLHSGK	L	27995.1
		100.0	11	14	44	2.28	27.7	R	QQKSDPIQEIR	D	7662.77
		100.0	11	14	44	2.28	27.7	K	SDPIQEIR	D	118515
		100.0	11	14	44	2.28	27.7	K	SDPIQEIRDLAEITTLDR	S	6878.37
		100.0	11	14	44	2.28	27.7	R	SVKALADYIR	Q	45690.5
		100.0	11	14	44	2.28	27.7	K	TPADCPVIAIDSFR	H	200116
38_82	Glutaredoxin-3	100.0	20	25	80	2.27	46.6	K	ASVMLFMK	G	623805
	OS=Homo sapiens	100.0	20	25	80	2.27	46.6	K	ASVMLFMKGNK	Q	19670.4
	GN=GLRX3 PE=1 SV=2	100.0	20	25	80	2.27	46.6	K	AYSNWPTYPQLYVK	G	35738.3
	GLRX3_HUMAN	100.0	20	25	80	2.27	46.6	K	ELEASEELDTICPK	A	22213.9
	37432.8	100.0	20	25	80	2.27	46.6	K	ELKENGELLPILR	G	3241.21
		100.0	20	25	80	2.27	46.6	K	ELPQVSFVK	L	460540
		100.0	20	25	80	2.27	46.6	K	ELPQVSFVKLEAEGVPEVSEK	Y	14195.8
		100.0	20	25	80	2.27	46.6	K	ENGELLPILR	G	67325.9
		100.0	20	25	80	2.27	46.6	K	ENGELLPILRGEN	-	18609.7
		100.0	20	25	80	2.27	46.6	K	GELVGGLDIVK	E	156124
		100.0	20	25	80	2.27	46.6	K	GELVGGLDIVKELK	E	2771.59
		100.0	20	25	80	2.27	46.6	K	HNIQFSSFDIFSDEEVR	Q	2394.49
		100.0	20	25	80	2.27	46.6	K	IDRLDGAHAPELTK	K	53740.9
		100.0	20	25	80	2.27	46.6	K	KLTHAAPCMLFMK	G	17404.0
		100.0	20	25	80	2.27	46.6	R	LDGAHAPELTK	K	93929.9
		100.0	20	25	80	2.27	46.6	K	LEAEGVPEVSEK	Y	60258.7
		100.0	20	25	80	2.27	46.6	K	LTHAAPCMLFMK	G	210912
		100.0	20	25	80	2.27	46.6	K	NSQKIDRLDGAHAPELTK	K	140449
		100.0	20	25	80	2.27	46.6	K	QMVEILHK	H	24487.2
		100.0	20	25	80	2.27	46.6	K	YEISSVPTFLFFK	N	4864.49
38_87	Glutaredoxin-3	100.0	6	6	39	1.15	35.8	K	ASVMLFMK	G	230541
	OS=Homo sapiens	100.0	6	6	39	1.15	35.8	K	AYSNWPTYPQLYVK	G	2387.93
	GN=GLRX3 PE=1 SV=2	100.0	6	6	39	1.15	35.8	K	ELEASEELDTICPK	A	6516.16
	GLRX3_HUMAN	100.0	6	6	39	1.15	35.8	K	ELKENGELLPILR	G	1407.78
	37432.8	100.0	6	6	39	1.15	35.8	K	ELPQVSFVK	L	145891
		100.0	6	6	39	1.15	35.8	K	ENGELLPILR	G	11127.6
		100.0	6	6	39	1.15	35.8	K	ENGELLPILRGEN	-	2642.94
		100.0	6	6	39	1.15	35.8	K	GELVGGLDIVK	E	56217.6
		100.0	6	6	39	1.15	35.8	R	LDGAHAPELTK	K	26523.3
		100.0	6	6	39	1.15	35.8	K	LEAEGVPEVSEK	Y	34681.5
		100.0	6	6	39	1.15	35.8	K	LTHAAPCMLFMK	G	49361.4
		100.0	6	6	39	1.15	35.8	K	YEISSVPTFLFFK	N	4106.09
39_82	Mannose-6-phosphate	100.0	13	14	43	1.36	35.0	K	DTFNGNLPFLFK	V	8184.40
	isomerase	100.0	13	14	43	1.36	35.0	K	FIDVPTLCEMLSYTPSSSK	D	1425.43
	OS=Homo sapiens	100.0	13	14	43	1.36	35.0	K	GDCVECMACSDNTVR	A	6210.76
	GN=MPI PE=1 SV=2	100.0	13	14	43	1.36	35.0	R	GGVLFIGANESVSLK	L	9357.02
	MPI_HUMAN	100.0	13	14	43	1.36	35.0	K	KVVVEQLNLLVK	R	5765.92
	46657.0	100.0	13	14	43	1.36	35.0	K	LTEPKDLLIFR	A	14803.0
		100.0	13	14	43	1.36	35.0	K	TEVPGSVTEYK	V	30317.3
		100.0	13	14	43	1.36	35.0	K	TLSQWIAENQDSLGSK	V	2321.24
		100.0	13	14	43	1.36	35.0	R	VFPLSCAVQQYAWGK	M	4449.28
		100.0	13	14	43	1.36	35.0	K	VLSVETPLSIQAHPNK	E	2923.94
		100.0	13	14	43	1.36	35.0	K	VLSVETPLSIQAHPNKELAEK	L	10221.5
		100.0	13	14	43	1.36	35.0	K	VVVEQLNLLVK	R	12973.6
		100.0	13	14	43	1.36	35.0	K	VVVEQLNLLVKR	I	12002.2
39_87	Mannose-6-phosphate	100.0	7	7	20	0.589	23.4	K	DTFNGNLPFLFK	V	4878.37
	isomerase	100.0	7	7	20	0.589	23.4	K	FIDVPTLCEMLSYTPSSSK	D	1568.72
	OS=Homo sapiens	100.0	7	7	20	0.589	23.4	R	GGVLFIGANESVSLK	L	5637.54
	GN=MPI PE=1 SV=2	100.0	7	7	20	0.589	23.4	K	TEVPGSVTEYK	V	14485.3
	MPI_HUMAN	100.0	7	7	20	0.589	23.4	K	TLSQWIAENQDSLGSK	V	2804.71
	46657.0	100.0	7	7	20	0.589	23.4	R	VFPLSCAVQQYAWGK	M	3138.64
		100.0	7	7	20	0.589	23.4	K	VVVEQLNLLVK	R	11501.1
41_82	Elongation factor 1-δ	100.0	5	5	11	0.433	24.2	M	ATNFLAHEK	I	10531.9
	OS=Homo sapiens	100.0	5	5	11	0.433	24.2	R	FYEQMNGPVAGASR	Q	1929.77
	GN=EEF1D PE=1 SV=5	100.0	5	5	11	0.433	24.2	R	IASLEVENQSLR	G	13696.1
	EF1D_HUMAN	100.0	5	5	11	0.433	24.2	K	LVPVGYGIR	K	9828.11

	31121.9	100.0	5	5	11	0.433	24.2	K	SLAGSSGPGASSGTSGDHGELVVR	I	3230.44
43_82	Serpin B6	100.0	3	5	447	7.34	89.9	K	ADFSGMSQTDLSLSK	V	357769
	OS=Homo sapiens	100.0	3	5	447	7.34	89.9	K	DNSKNVFFSPMSMSCALAMVYMGAK	G	6903.36
	GN=SERPINB6 PE=1	100.0	3	5	447	7.34	89.9	K	ELNMIIMLPDETTDLR	T	135787
	SV=3	100.0	3	5	447	7.34	89.9	R	FCADHPFLFFIQHSK	T	53323.5
	SPB6_HUMAN	100.0	3	5	447	7.34	89.9	R	FKLEESYDMESVLR	N	219542
	42622.9	100.0	3	5	447	7.34	89.9	K	FYQAEMEELDFISAVEK	S	75150.7
		100.0	3	5	447	7.34	89.9	K	FYQAEMEELDFISAVEKSR	K	12711.4
		100.0	3	5	447	7.34	89.9	K	GNTAAQMAQILSFNK	S	424810
		100.0	3	5	447	7.34	89.9	R	GNWDEQFDK	E	11423.1
		100.0	3	5	447	7.34	89.9	R	GNWDEQFDKENTEER	L	64159.2
		100.0	3	5	447	7.34	89.9	K	HINTWVAEK	T	43330.2
		100.0	3	5	447	7.34	89.9	K	HINTWVAEKTEGK	I	15172.8
		100.0	3	5	447	7.34	89.9	K	IAELLSPGSVDPLTR	L	921273
		100.0	3	5	447	7.34	89.9	R	KHINTWVAEK	T	9154.99
		100.0	3	5	447	7.34	89.9	R	KHINTWVAEKTEGK	I	5814.99
		100.0	3	5	447	7.34	89.9	R	LDMMDEEEVEVSLPR	F	51882.5
		100.0	3	5	447	7.34	89.9	K	LEESYDMESVLR	N	46767.4
		100.0	3	5	447	7.34	89.9	R	LFGEKSCDFLSSFR	D	5841.51
		100.0	3	5	447	7.34	89.9	R	LVLVNAVYFR	G	870207
		100.0	3	5	447	7.34	89.9	R	MANRLFGEK	S	19635.0
		100.0	3	5	447	7.34	89.9	-	MDVLAEANGTFALNLLK	T	5075.08
		100.0	3	5	447	7.34	89.9	K	NEEKPVQMMFK	Q	47879.2
		100.0	3	5	447	7.34	89.9	R	NLGMTDAFELGK	A	669641
		100.0	3	5	447	7.34	89.9	K	NVFFSPMSMSCALAMVYMGAK	G	105445
		100.0	3	5	447	7.34	89.9	K	SCDFLSSFR	D	668626
		100.0	3	5	447	7.34	89.9	K	SCDFLSSFRDSCQK	F	1108.86
		100.0	3	5	447	7.34	89.9	K	SFVEVNEEGTEAAAATAAIMMMR	C	106068
		100.0	3	5	447	7.34	89.9	K	SGGGGDIHQGFQSLLTEVNK	T	40399.6
		100.0	3	5	447	7.34	89.9	K	TEGKIAELLSPGSVDPLTR	L	29511.8
		100.0	3	5	447	7.34	89.9	K	TGTQYLLR	M	829961
		100.0	3	5	447	7.34	89.9	K	TNGILFCGR	F	589212
		100.0	3	5	447	7.34	89.9	K	TNGILFCGRFSSP	-	9893.47
		100.0	3	5	447	7.34	89.9	R	TVEKELTYEK	F	323036
		100.0	3	5	447	7.34	89.9	R	TVEKELTYEKFVEWTR	L	3647.12
		100.0	3	5	447	7.34	89.9	K	VSKNEEKPVQMMFK	Q	26307.9
		100.0	3	5	447	7.34	89.9	K	VVHKSFVEVNEEGTEAAAATAAIMMMR	C	1476.72
43_87	Serpin B6	100.0	25	45	189	4.44	80.9	K	ADFSGMSQTDLSLSK	V	91376.9
	OS=Homo sapiens	100.0	25	45	189	4.44	80.9	K	ADFSGMSQTDLSLSKVVHK	S	3217.00
	GN=SERPINB6 PE=1	100.0	25	45	189	4.44	80.9	K	ELNMIIMLPDETTDLR	T	50369.7
	SV=3	100.0	25	45	189	4.44	80.9	R	FCADHPFLFFIQHSK	T	20376.8
	SPB6_HUMAN	100.0	25	45	189	4.44	80.9	R	FKLEESYDMESVLR	N	48312.5
	42622.9	100.0	25	45	189	4.44	80.9	K	FYQAEMEELDFISAVEK	S	28319.4
		100.0	25	45	189	4.44	80.9	K	GNTAAQMAQILSFNK	S	65165.2
		100.0	25	45	189	4.44	80.9	R	GNWDEQFDK	E	6671.37
		100.0	25	45	189	4.44	80.9	R	GNWDEQFDKENTEER	L	8983.26
		100.0	25	45	189	4.44	80.9	K	HINTWVAEK	T	6190.94
		100.0	25	45	189	4.44	80.9	K	HINTWVAEKTEGK	I	5321.76
		100.0	25	45	189	4.44	80.9	K	IAELLSPGSVDPLTR	L	220175
		100.0	25	45	189	4.44	80.9	R	LDMMDEEEVEVSLPR	F	32774.3
		100.0	25	45	189	4.44	80.9	K	LEESYDMESVLR	N	18941.4
		100.0	25	45	189	4.44	80.9	R	LVLVNAVYFR	G	385640
		100.0	25	45	189	4.44	80.9	-	MDVLAEANGTFALNLLK	T	4140.42
		100.0	25	45	189	4.44	80.9	K	NEEKPVQMMFK	Q	7475.39
		100.0	25	45	189	4.44	80.9	R	NLGMTDAFELGK	A	159004
		100.0	25	45	189	4.44	80.9	K	NVFFSPMSMSCALAMVYMGAK	G	30573.9
		100.0	25	45	189	4.44	80.9	K	SCDFLSSFR	D	211899
		100.0	25	45	189	4.44	80.9	K	SFVEVNEEGTEAAAATAAIMMMR	C	29174.1
		100.0	25	45	189	4.44	80.9	K	SGGGGDIHQGFQSLLTEVNK	T	13967.7
		100.0	25	45	189	4.44	80.9	K	TGTQYLLR	M	250123
		100.0	25	45	189	4.44	80.9	K	TNGILFCGR	F	114746
		100.0	25	45	189	4.44	80.9	R	TVEKELTYEK	F	77960.5
44_81	Hepatoma-derived	100.0	7	8	19	0.551	30.0	R	AGDLLEDSPK	R	17803.6
	growth factor	100.0	7	8	19	0.551	30.0	K	CGDLVFAK	M	65739.7
	OS=Homo sapiens	100.0	7	8	19	0.551	30.0	K	EAATLEVERPLPMEVEK	N	4050.34
	GN=HDGF PE=1 SV=1	100.0	7	8	19	0.551	30.0	K	EAENPEGEEKEAATLEVERPLPMEVEK	N	2727.63
	HDGF_HUMAN	100.0	7	8	19	0.551	30.0	K	GFSEGLWEIENNPTVK	A	4149.36
	26788.6	100.0	7	8	19	0.551	30.0	R	IDEMPEAAVK	S	37872.3
		100.0	7	8	19	0.551	30.0	R	RAGDLLEDSPK	R	3220.70
44_81	Cluster of Endoplasmin	100.0	4	4	8	0.232	6.49	K	ADLINNLGTIAK	S	6376.52
	OS=Homo sapiens	100.0	4	4	8	0.232	6.49	R	ELISNASDALDK	I	3444.79
	GN=HSP90B1 PE=1	100.0	4	4	8	0.232	6.49	K	IDIIPNPQER	T	15484.7
	SV=1	100.0	4	4	8	0.232	6.49	R	TLTLVDTGIGMTK	A	9316.94
	ENPL_HUMAN	100.0	4	4	8	0.232	6.49	K	ADLINNLGTIAK	S	6376.52

	83284.3	100.0	4	4	8	0.232	6.49	R	ELISNASDALDK	I	3444.79
		100.0	4	4	8	0.232	6.49	K	IDIIPNPQER	T	15484.7
		100.0	4	4	8	0.232	6.49	R	TLTLVDTGIGMTK	A	9316.94
		100.0	4	4	8	0.232	6.49	K	ADLINNLGTIAK	S	6376.52
		100.0	4	4	8	0.232	6.49	R	ELISNASDALDK	I	3444.79
		100.0	4	4	8	0.232	6.49	K	IDIIPNPQER	T	15484.7
		100.0	4	4	8	0.232	6.49	R	TLTLVDTGIGMTK	A	9316.94
		100.0	4	4	8	0.232	6.49	K	ADLINNLGTIAK	S	6376.52
		100.0	4	4	8	0.232	6.49	R	ELISNASDALDK	I	3444.79
		100.0	4	4	8	0.232	6.49	K	IDIIPNPQER	T	15484.7
		100.0	4	4	8	0.232	6.49	R	TLTLVDTGIGMTK	A	9316.94
		100.0	4	4	8	0.232	6.49	K	ADLINNLGTIAK	S	6376.52
		100.0	4	4	8	0.232	6.49	R	ELISNASDALDK	I	3444.79
		100.0	4	4	8	0.232	6.49	K	IDIIPNPQER	T	15484.7
		100.0	4	4	8	0.232	6.49	R	TLTLVDTGIGMTK	A	9316.94
		100.0	4	4	8	0.232	6.49	K	ADLINNLGTIAK	S	6376.52
		100.0	4	4	8	0.232	6.49	R	ELISNASDALDK	I	3444.79
		100.0	4	4	8	0.232	6.49	K	IDIIPNPQER	T	15484.7
		100.0	4	4	8	0.232	6.49	R	TLTLVDTGIGMTK	A	9316.94
44_82	Hepatoma-derived growth factor OS=Homo sapiens GN=HDGF PE=1 SV=1 HDGF_HUMAN 26788.6	100.0	17	22	55	1.18	70.4	R	AGDLLEDSPK	R	53377.6
		100.0	17	22	55	1.18	70.4	R	AGDLLEDSPKRPK	E	25124.8
		100.0	17	22	55	1.18	70.4	K	CGDLVFAK	M	422279
		100.0	17	22	55	1.18	70.4	K	DLFPYEESK	E	61814.2
		100.0	17	22	55	1.18	70.4	K	EAATLEVERPLPMEVEK	N	33660.3
		100.0	17	22	55	1.18	70.4	K	EAENPEGEEKEAATLEVERPLPMEVEK	N	13273.8
		100.0	17	22	55	1.18	70.4	K	GFSEGLWEIENNPTVK	A	42879.1
		100.0	17	22	55	1.18	70.4	K	GNAEGSSDEEGKLVIDEPAK	E	5667.21
		100.0	17	22	55	1.18	70.4	K	GNAEGSSDEEGKLVIDEPAKEK	N	2760.38
		100.0	17	22	55	1.18	70.4	R	GPPQEEEEEEDEEEEATKEDAE-APGIRDHESL	-	10187.5
		100.0	17	22	55	1.18	70.4	R	IDEMPEAAVK	S	289552
		100.0	17	22	55	1.18	70.4	R	KGFSEGLWEIENNPTVK	A	35039.7
		100.0	17	22	55	1.18	70.4	K	LVIDEPAK	E	17403.0
		100.0	17	22	55	1.18	70.4	K	MKGYPHWPAR	I	9069.07
		100.0	17	22	55	1.18	70.4	R	RAGDLLEDSPK	R	7489.41
		100.0	17	22	55	1.18	70.4	R	RAGDLLEDSPKRPK	E	9037.33
		100.0	17	22	55	1.18	70.4	K	SCVEEPEPEPEAAEGDGDKK	G	4517.75
44_82	Cluster of Endoplasmin OS=Homo sapiens GN=HSP90B1 PE=1 SV=1 ENPL_HUMAN 83284.3	100.0	6	11	60	1.29	18.5	K	ADLINNLGTIAK	S	279062
		100.0	6	11	60	1.29	18.5	K	EDQTEYLEER	R	6727.49
		100.0	6	11	60	1.29	18.5	R	ELISNASDALDK	I	132316
		100.0	6	11	60	1.29	18.5	R	ELISNASDALDKIR	Y	28659.7
		100.0	6	11	60	1.29	18.5	K	ELKIDIIPNPQER	T	53086.5
		100.0	6	11	60	1.29	18.5	K	HNDDEQYAWESSAGGSFTVR	A	4666.45
		100.0	6	11	60	1.29	18.5	K	HSQFIGYPITLYLEK	E	10546.9
		100.0	6	11	60	1.29	18.5	K	IDIIPNPQER	T	409089
		100.0	6	11	60	1.29	18.5	K	IRYESLTDPSK	L	10043.3
		100.0	6	11	60	1.29	18.5	K	IRYESLTDPSKLDSGK	E	6810.25
		100.0	6	11	60	1.29	18.5	R	TLTLVDTGIGMTK	A	265784
		100.0	6	11	60	1.29	18.5	K	VILHLKEDQTEYLEER	R	9211.93
		100.0	6	11	60	1.29	18.5	K	VILHLKEDQTEYLEERR	V	13129.0
		100.0	6	11	60	1.29	18.5	R	YESLTDPSK	L	86734.4
		100.0	6	11	60	1.29	18.5	R	YESLTDPSKLDSGK	E	69032.6
		100.0	6	11	60	1.29	18.5	K	YIDQEELNK	T	123108
		100.0	6	11	60	1.29	18.5	K	YIDQEELNKTKPIWTR	N	9865.42
		100.0	6	11	60	1.29	18.5	K	ADLINNLGTIAK	S	279062
		100.0	6	11	60	1.29	18.5	K	EDQTEYLEER	R	6727.49
		100.0	6	11	60	1.29	18.5	R	ELISNASDALDK	I	132316
		100.0	6	11	60	1.29	18.5	R	ELISNASDALDKIR	Y	28659.7
		100.0	6	11	60	1.29	18.5	K	ELKIDIIPNPQER	T	53086.5
		100.0	6	11	60	1.29	18.5	K	HNDDEQYAWESSAGGSFTVR	A	4666.45
		100.0	6	11	60	1.29	18.5	K	HSQFIGYPITLYLEK	E	10546.9
		100.0	6	11	60	1.29	18.5	K	IDIIPNPQER	T	409089
		100.0	6	11	60	1.29	18.5	K	IRYESLTDPSK	L	10043.3
		100.0	6	11	60	1.29	18.5	K	IRYESLTDPSKLDSGK	E	6810.25
		100.0	6	11	60	1.29	18.5	R	TLTLVDTGIGMTK	A	265784
		100.0	6	11	60	1.29	18.5	K	VILHLKEDQTEYLEER	R	9211.93
		100.0	6	11	60	1.29	18.5	K	VILHLKEDQTEYLEERR	V	13129.0
		100.0	6	11	60	1.29	18.5	R	YESLTDPSK	L	86734.4
		100.0	6	11	60	1.29	18.5	R	YESLTDPSKLDSGK	E	69032.6
		100.0	6	11	60	1.29	18.5	K	YIDQEELNK	T	123108
		100.0	6	11	60	1.29	18.5	K	YIDQEELNKTKPIWTR	N	9865.42
		100.0	6	11	60	1.29	18.5	K	ADLINNLGTIAK	S	279062
		100.0	6	11	60	1.29	18.5	K	EDQTEYLEER	R	6727.49
		100.0	6	11	60	1.29	18.5	R	ELISNASDALDK	I	132316
		100.0	6	11	60	1.29	18.5	R	ELISNASDALDKIR	Y	28659.7

		100.0	6	11	60	1.29	18.5	K	ELKIDIIPNPQER	T	53086.5
		100.0	6	11	60	1.29	18.5	K	HNDDEQYAWESSAGGSFTVR	A	4666.45
		100.0	6	11	60	1.29	18.5	K	HSQFIGYPITLYLEK	E	10546.9
		100.0	6	11	60	1.29	18.5	K	IDIIPNPQER	T	409089
		100.0	6	11	60	1.29	18.5	K	IRYESLTDPSK	L	10043.3
		100.0	6	11	60	1.29	18.5	K	IRYESLTDPSKLDSGK	E	6810.25
		100.0	6	11	60	1.29	18.5	R	TLTLVDTGIGMTK	A	265784
		100.0	6	11	60	1.29	18.5	K	VILHLKEDQTEYLEER	R	9211.93
		100.0	6	11	60	1.29	18.5	K	VILHLKEDQTEYLEERR	V	13129.0
		100.0	6	11	60	1.29	18.5	R	YESLTDPSK	L	86734.4
		100.0	6	11	60	1.29	18.5	R	YESLTDPSKLDSGK	E	69032.6
		100.0	6	11	60	1.29	18.5	K	YIDQEELNK	T	123108
		100.0	6	11	60	1.29	18.5	K	YIDQEELNKTKPIWTR	N	9865.42
		100.0	6	11	60	1.29	18.5	K	ADLINNLGTIAK	S	279062
		100.0	6	11	60	1.29	18.5	K	EDQTEYLEER	R	6727.49
		100.0	6	11	60	1.29	18.5	R	ELISNASDALDK	I	132316
		100.0	6	11	60	1.29	18.5	R	ELISNASDALDKIR	Y	28659.7
		100.0	6	11	60	1.29	18.5	K	ELKIDIIPNPQER	T	53086.5
		100.0	6	11	60	1.29	18.5	K	HNDDEQYAWESSAGGSFTVR	A	4666.45
		100.0	6	11	60	1.29	18.5	K	HSQFIGYPITLYLEK	E	10546.9
		100.0	6	11	60	1.29	18.5	K	IDIIPNPQER	T	409089
		100.0	6	11	60	1.29	18.5	K	IRYESLTDPSK	L	10043.3
		100.0	6	11	60	1.29	18.5	K	IRYESLTDPSKLDSGK	E	6810.25
		100.0	6	11	60	1.29	18.5	R	TLTLVDTGIGMTK	A	265784
		100.0	6	11	60	1.29	18.5	K	VILHLKEDQTEYLEER	R	9211.93
		100.0	6	11	60	1.29	18.5	K	VILHLKEDQTEYLEERR	V	13129.0
		100.0	6	11	60	1.29	18.5	R	YESLTDPSK	L	86734.4
		100.0	6	11	60	1.29	18.5	R	YESLTDPSKLDSGK	E	69032.6
		100.0	6	11	60	1.29	18.5	K	YIDQEELNK	T	123108
		100.0	6	11	60	1.29	18.5	K	YIDQEELNKTKPIWTR	N	9865.42
		100.0	6	11	60	1.29	18.5	K	ADLINNLGTIAK	S	279062
		100.0	6	11	60	1.29	18.5	K	EDQTEYLEER	R	6727.49
		100.0	6	11	60	1.29	18.5	R	ELISNASDALDK	I	132316
		100.0	6	11	60	1.29	18.5	R	ELISNASDALDKIR	Y	28659.7
		100.0	6	11	60	1.29	18.5	K	ELKIDIIPNPQER	T	53086.5
		100.0	6	11	60	1.29	18.5	K	HNDDEQYAWESSAGGSFTVR	A	4666.45
		100.0	6	11	60	1.29	18.5	K	HSQFIGYPITLYLEK	E	10546.9
		100.0	6	11	60	1.29	18.5	K	IDIIPNPQER	T	409089
		100.0	6	11	60	1.29	18.5	K	IRYESLTDPSK	L	10043.3
		100.0	6	11	60	1.29	18.5	K	IRYESLTDPSKLDSGK	E	6810.25
		100.0	6	11	60	1.29	18.5	R	TLTLVDTGIGMTK	A	265784
		100.0	6	11	60	1.29	18.5	K	VILHLKEDQTEYLEER	R	9211.93
		100.0	6	11	60	1.29	18.5	K	VILHLKEDQTEYLEERR	V	13129.0
		100.0	6	11	60	1.29	18.5	R	YESLTDPSK	L	86734.4
		100.0	6	11	60	1.29	18.5	R	YESLTDPSKLDSGK	E	69032.6
		100.0	6	11	60	1.29	18.5	K	YIDQEELNK	T	123108
		100.0	6	11	60	1.29	18.5	K	YIDQEELNKTKPIWTR	N	9865.42
		100.0	6	11	60	1.29	18.5	K	ADLINNLGTIAK	S	279062
		100.0	6	11	60	1.29	18.5	K	EDQTEYLEER	R	6727.49
		100.0	6	11	60	1.29	18.5	R	ELISNASDALDK	I	132316
		100.0	6	11	60	1.29	18.5	R	ELISNASDALDKIR	Y	28659.7
		100.0	6	11	60	1.29	18.5	K	ELKIDIIPNPQER	T	53086.5
		100.0	6	11	60	1.29	18.5	K	HNDDEQYAWESSAGGSFTVR	A	4666.45
		100.0	6	11	60	1.29	18.5	K	HSQFIGYPITLYLEK	E	10546.9
		100.0	6	11	60	1.29	18.5	K	IDIIPNPQER	T	409089
		100.0	6	11	60	1.29	18.5	K	IRYESLTDPSK	L	10043.3
		100.0	6	11	60	1.29	18.5	K	IRYESLTDPSKLDSGK	E	6810.25
		100.0	6	11	60	1.29	18.5	R	TLTLVDTGIGMTK	A	265784
		100.0	6	11	60	1.29	18.5	K	VILHLKEDQTEYLEER	R	9211.93
		100.0	6	11	60	1.29	18.5	K	VILHLKEDQTEYLEERR	V	13129.0
		100.0	6	11	60	1.29	18.5	R	YESLTDPSK	L	86734.4
		100.0	6	11	60	1.29	18.5	R	YESLTDPSKLDSGK	E	69032.6
		100.0	6	11	60	1.29	18.5	K	YIDQEELNK	T	123108
		100.0	6	11	60	1.29	18.5	K	YIDQEELNKTKPIWTR	N	9865.42
46_85	Complement component 1 Q subcomponent-binding protein, mitochondrial OS=Homo sapiens GN=C1QBP PE=1 SV=1 C1QBP_HUMAN 31362.6	100.0	3	4	18	0.675	22.0	K	AFVDFLSDEIK	E	11564.8
		100.0	3	4	18	0.675	22.0	K	AFVDFLSDEIKEER	K	6291.33
		100.0	3	4	18	0.675	22.0	R	EVSFQSTGESEWK	D	6168.76
		100.0	3	4	18	0.675	22.0	K	MSGGWELELNGTEAK	L	8880.89
		100.0	3	4	18	0.675	22.0	K	VEEQEPELTSTPNFVVEVIK	N	5266.94
46N85	Complement component 1 Q subcomponent-	100.0	4	4	10	0.447	20.9	K	AFVDFLSDEIK	E	9885.33
		100.0	4	4	10	0.447	20.9	R	EVSFQSTGESEWK	D	11777.6

	binding protein,	100.0	4	4	10	0.447	20.9	K	MSGGWELELNGTEAK	L	6993.95
	mitochondrial	100.0	4	4	10	0.447	20.9	K	VEEQEPELTSTPNFVVEVIK	N	298.271
	OS=Homo sapiens										
	GN=C1QBP PE=1 SV=1										
	C1QBP_HUMAN										
	31362.6										
46_86	Complement component	100.0	4	5	15	0.617	20.9	K	AFVDFLSDEIK	E	13226.9
	1 Q subcomponent-	100.0	4	5	15	0.617	20.9	R	EVSFQSTGESEWK	D	9026.41
	binding protein,	100.0	4	5	15	0.617	20.9	K	MSGGWELELNGTEAK	L	13058.0
	mitochondrial	100.0	4	5	15	0.617	20.9	K	VEEQEPELTSTPNFVVEVIK	N	3155.20
	OS=Homo sapiens										
	GN=C1QBP PE=1 SV=1										
	C1QBP_HUMAN										
	31362.6										
46N86	Complement component	100.0	7	7	15	0.624	33.7	K	AFVDFLSDEIK	E	9199.15
	1 Q subcomponent-	100.0	7	7	15	0.624	33.7	K	AFVDFLSDEIKEER	K	1040.27
	binding protein,	100.0	7	7	15	0.624	33.7	K	ALVLDCHYPEDEVGQEDEAESDIFSIR	E	1341.53
	mitochondrial	100.0	7	7	15	0.624	33.7	R	EVSFQSTGESEWK	D	7185.91
	OS=Homo sapiens	100.0	7	7	15	0.624	33.7	K	MSGGWELELNGTEAK	L	9999.48
	GN=C1QBP PE=1 SV=1	100.0	7	7	15	0.624	33.7	K	VEEQEPELTSTPNFVVEVIK	N	940.487
	C1QBP_HUMAN	100.0	7	7	15	0.624	33.7	K	VEEQEPELTSTPNFVVEVIKNDDGKK	A	8452.63
	31362.6										
46_87	Complement component	100.0	7	10	39	1.10	33.7	K	AFVDFLSDEIK	E	20156.5
	1 Q subcomponent-	100.0	7	10	39	1.10	33.7	K	AFVDFLSDEIKEER	K	24915.7
	binding protein,	100.0	7	10	39	1.10	33.7	K	ALVLDCHYPEDEVGQEDEAESDIFSIR	E	14346.5
	mitochondrial	100.0	7	10	39	1.10	33.7	R	EVSFQSTGESEWK	D	73030.2
	OS=Homo sapiens	100.0	7	10	39	1.10	33.7	K	MSGGWELELNGTEAK	L	74365.0
	GN=C1QBP PE=1 SV=1	100.0	7	10	39	1.10	33.7	K	VEEQEPELTSTPNFVVEVIK	N	23742.8
	C1QBP_HUMAN	100.0	7	10	39	1.10	33.7	K	VEEQEPELTSTPNFVVEVIKNDDGKK	A	5283.89
	31362.6										
47_81	NADH dehydrogenase	100.0	3	4	37	0.872	36.2	R	EPATINYPFEK	G	81449.1
	[ubiquinone] iron-sulfur	100.0	3	4	37	0.872	36.2	R	GLGMTLSYLFR	E	19602.8
	protein 8. mitochondrial	100.0	3	4	37	0.872	36.2	K	LCEAICPAQAITIEAEPR	A	49554.7
	OS=Homo sapiens	100.0	3	4	37	0.872	36.2	R	TLLWTELFR	G	23464.3
	GN=NDUFS8 PE=1	100.0	3	4	37	0.872	36.2	R	TTRYDIDMTK	C	67786.9
	SV=1	100.0	3	4	37	0.872	36.2	R	YDIDMTK	C	30838.0
	NDUS8_HUMAN	100.0	3	4	37	0.872	36.2	K	YVNMQDPEMDMK	S	23379.1
	23705.9	100.0	3	4	37	0.872	36.2	K	YVNMQDPEMDMKSVTDR	A	6999.90
		100.0	3	4	37	0.872	36.2	R	EPATINYPFEK	G	81449.1
		100.0	3	4	37	0.872	36.2	R	GLGMTLSYLFR	E	19602.8
		100.0	3	4	37	0.872	36.2	K	LCEAICPAQAITIEAEPR	A	49554.7
		100.0	3	4	37	0.872	36.2	R	TLLWTELFR	G	23464.3
		100.0	3	4	37	0.872	36.2	R	TTRYDIDMTK	C	67786.9
		100.0	3	4	37	0.872	36.2	R	YDIDMTK	C	30838.0
		100.0	3	4	37	0.872	36.2	K	YVNMQDPEMDMK	S	23379.1
		100.0	3	4	37	0.872	36.2	K	YVNMQDPEMDMKSVTDR	A	6999.90
		100.0	3	4	37	0.872	36.2	R	EPATINYPFEK	G	81449.1
		100.0	3	4	37	0.872	36.2	R	GLGMTLSYLFR	E	19602.8
		100.0	3	4	37	0.872	36.2	K	LCEAICPAQAITIEAEPR	A	49554.7
		100.0	3	4	37	0.872	36.2	R	TLLWTELFR	G	23464.3
		100.0	3	4	37	0.872	36.2	R	TTRYDIDMTK	C	67786.9
		100.0	3	4	37	0.872	36.2	R	YDIDMTK	C	30838.0
		100.0	3	4	37	0.872	36.2	K	YVNMQDPEMDMK	S	23379.1
		100.0	3	4	37	0.872	36.2	K	YVNMQDPEMDMKSVTDR	A	6999.90
		100.0	3	4	37	0.872	36.2	R	EPATINYPFEK	G	81449.1
		100.0	3	4	37	0.872	36.2	R	GLGMTLSYLFR	E	19602.8
		100.0	3	4	37	0.872	36.2	K	LCEAICPAQAITIEAEPR	A	49554.7
		100.0	3	4	37	0.872	36.2	R	TLLWTELFR	G	23464.3
		100.0	3	4	37	0.872	36.2	R	TTRYDIDMTK	C	67786.9
		100.0	3	4	37	0.872	36.2	R	YDIDMTK	C	30838.0
		100.0	3	4	37	0.872	36.2	K	YVNMQDPEMDMK	S	23379.1
		100.0	3	4	37	0.872	36.2	K	YVNMQDPEMDMKSVTDR	A	6999.90
47_86	NADH dehydrogenase	100.0	2	2	10	0.319	23.8	R	GLGMTLSYLFR	E	23654.7
	[ubiquinone] iron-sulfur	100.0	2	2	10	0.319	23.8	K	LCEAICPAQAITIEAEPR	A	5852.74
	protein 8. mitochondrial	100.0	2	2	10	0.319	23.8	R	TLLWTELFR	G	4773.92
	OS=Homo sapiens	100.0	2	2	10	0.319	23.8	K	YVNMQDPEMDMK	S	1417.27
	GN=NDUFS8 PE=1	100.0	2	2	10	0.319	23.8	R	GLGMTLSYLFR	E	23654.7
	SV=1	100.0	2	2	10	0.319	23.8	K	LCEAICPAQAITIEAEPR	A	5852.74
	NDUS8_HUMAN	100.0	2	2	10	0.319	23.8	R	TLLWTELFR	G	4773.92
	23705.9	100.0	2	2	10	0.319	23.8	K	YVNMQDPEMDMK	S	1417.27
		100.0	2	2	10	0.319	23.8	R	GLGMTLSYLFR	E	23654.7
		100.0	2	2	10	0.319	23.8	K	LCEAICPAQAITIEAEPR	A	5852.74
		100.0	2	2	10	0.319	23.8	R	TLLWTELFR	G	4773.92
		100.0	2	2	10	0.319	23.8	K	YVNMQDPEMDMK	S	1417.27

		100.0	2	2	10	0.319	23.8	R	GLGMTLSYLFR	E	23654.7
		100.0	2	2	10	0.319	23.8	K	LCEAICPAQAITIEAEPR	A	5852.74
		100.0	2	2	10	0.319	23.8	R	TLLWTELFR	G	4773.92
		100.0	2	2	10	0.319	23.8	K	YVNMQDPEMDMK	S	1417.27
101_82	Sequestosome-1	100.0	16	24	74	1.59	49.3	R	AGEARPGPTAESASGPSEDPSVNFLK	N	60100.5
	OS=Homo sapiens	100.0	16	24	74	1.59	49.3	M	ASLTVKAYLLGK	E	20486.8
	GN=SQSTM1 PE=1	100.0	16	24	74	1.59	49.3	M	ASLTVKAYLLGKEDAAR	E	14885.4
	SV=1	100.0	16	24	74	1.59	49.3	K	AYLLGKEDAAR	E	162315
	SQSTM_HUMAN	100.0	16	24	74	1.59	49.3	K	CSVCPDYDLCSVCEGK	G	20560.1
	47687.4	100.0	16	24	74	1.59	49.3	K	EAALYPHLPPEADPR	L	36034.1
		100.0	16	24	74	1.59	49.3	K	EVDPSTGELQSLQMPESEGPSS-LDPSQEGPTGLK	E	257.713
		100.0	16	24	74	1.59	49.3	R	FSFCCSPEPEAEAEAAAGPGPCER	L	10536.5
		100.0	16	24	74	1.59	49.3	Y	LLGKEDAAR	E	20710.9
		100.0	16	24	74	1.59	49.3	R	LTPVSPESSSTEEK	S	34451.9
		100.0	16	24	74	1.59	49.3	R	NMVHPNVICDGCNGPVVGTR	Y	31226.4
		100.0	16	24	74	1.59	49.3	K	NYDIGAALDTIQYSK	H	46595.0
		100.0	16	24	74	1.59	49.3	R	RFSFCCSPEPEAEAEAAAGPGPCER	L	1939.83
		100.0	16	24	74	1.59	49.3	R	SRLTPVSPESSSTEEK	S	5391.87
		100.0	16	24	74	1.59	49.3	K	SSSQPSSCCSDPSKPGGNVEGAT-QSLAEQMR	K	10764.0
		100.0	16	24	74	1.59	49.3	R	YKCSVCPDYDLCSVCEGK	G	11255.8
101_82	Programmed cell death	100.0	11	12	31	0.664	24.7	R	AALDKATVLLSMSK	G	5944.67
	protein 4	100.0	11	12	31	0.664	24.7	R	APQLVGQFIAR	A	39625.6
	OS=Homo sapiens	100.0	11	12	31	0.664	24.7	K	ATVLLSMSK	G	19425.0
	GN=PDCD4 PE=1 SV=2	100.0	11	12	31	0.664	24.7	R	AVGDGILCNTYIDSYK	G	5462.91
	PDCD4_HUMAN	100.0	11	12	31	0.664	24.7	K	DLPELALDTPR	A	12264.4
	51736.4	100.0	11	12	31	0.664	24.7	R	FVEECFQAGIISK	Q	13998.8
		100.0	11	12	31	0.664	24.7	K	LLSDLCGTVMSTTDVEK	S	9790.79
		100.0	11	12	31	0.664	24.7	K	MILDLLK	S	14072.2
		100.0	11	12	31	0.664	24.7	R	SGLTVPTSPK	G	23556.9
		100.0	11	12	31	0.664	24.7	R	SGLTVPTSPKGR	L	2632.95
		100.0	11	12	31	0.664	24.7	K	SGVPVLAVSLALEGK	A	11548.4
101_87	Sequestosome-1	100.0	13	19	44	1.09	43.6	R	AGEARPGPTAESASGPSEDPSVNFLK	N	39068.0
	OS=Homo sapiens	100.0	13	19	44	1.09	43.6	M	ASLTVKAYLLGK	E	4220.69
	GN=SQSTM1 PE=1	100.0	13	19	44	1.09	43.6	K	AYLLGKEDAAR	E	56161.0
	SV=1	100.0	13	19	44	1.09	43.6	K	CSVCPDYDLCSVCEGK	G	5353.20
	SQSTM_HUMAN	100.0	13	19	44	1.09	43.6	K	EAALYPHLPPEADPR	L	36890.5
	47687.4	100.0	13	19	44	1.09	43.6	R	FSFCCSPEPEAEAEAAAGPGPCER	L	5999.15
		100.0	13	19	44	1.09	43.6	R	LTPVSPESSSTEEK	S	7382.70
		100.0	13	19	44	1.09	43.6	R	NMVHPNVICDGCNGPVVGTR	Y	9012.58
		100.0	13	19	44	1.09	43.6	K	NYDIGAALDTIQYSK	H	40160.4
		100.0	13	19	44	1.09	43.6	R	SRLTPVSPESSSTEEK	S	3561.56
		100.0	13	19	44	1.09	43.6	K	SSSQPSSCCSDPSKPGGNVE-GATQSLAEQMRK	I	9673.36
		100.0	13	19	44	1.09	43.6	R	VAALFPALR	P	19387.2
		100.0	13	19	44	1.09	43.6	R	YKCSVCPDYDLCSVCEGK	G	3340.46
104_81	Vimentin	100.0	7	11	150	3.27	73.0	R	DGQVINETSQHHDDLE	-	20551.8
	OS=Homo sapiens	100.0	7	11	150	3.27	73.0	R	DNLAEDIMR	L	5591.69
	GN=VIM PE=1 SV=4	100.0	7	11	150	3.27	73.0	R	EEAENTLQSFR	Q	11541.0
	VIME_HUMAN	100.0	7	11	150	3.27	73.0	R	EEAENTLQSFRQDVDNASLAR	L	5741.14
	53652.7	100.0	7	11	150	3.27	73.0	R	EMEENFAVEAANYQDTIGR	L	7615.23
		100.0	7	11	150	3.27	73.0	R	ETNLDSLPLVDTHSK	R	28706.5
		100.0	7	11	150	3.27	73.0	R	ETNLDSLPLVDTHSKR	T	1010.13
		100.0	7	11	150	3.27	73.0	R	EYQDLLNVK	M	58292.8
		100.0	7	11	150	3.27	73.0	K	FADLSEAANR	N	151503
		100.0	7	11	150	3.27	73.0	K	FADLSEAANRNNDALR	Q	73184.7
		100.0	7	11	150	3.27	73.0	R	FANYIDK	V	13483.3
		100.0	7	11	150	3.27	73.0	R	FANYIDKVR	F	68358.4
		100.0	7	11	150	3.27	73.0	R	HLREYQDLLNVK	M	20655.6
		100.0	7	11	150	3.27	73.0	K	ILLAELEQLK	G	35358.1
		100.0	7	11	150	3.27	73.0	K	ILLAELEQLKGQGK	S	91779.7
		100.0	7	11	150	3.27	73.0	R	ISLPLPNFSSLNLR	E	34738.2
		100.0	7	11	150	3.27	73.0	R	KVESLQEEIAFLK	K	9024.14
		100.0	7	11	150	3.27	73.0	R	KVESLQEEIAFLKK	L	27108.7
		100.0	7	11	150	3.27	73.0	R	LGDLYEEEMR	E	47301.8
		100.0	7	11	150	3.27	73.0	R	LGDLYEEEMRELR	R	33056.2
		100.0	7	11	150	3.27	73.0	R	LLQDSVDFSLADAINTEFK	N	841.728
		100.0	7	11	150	3.27	73.0	R	LQDEIQNMKEEMAR	H	6945.24
		100.0	7	11	150	3.27	73.0	K	LQEEMLQR	E	6732.17
		100.0	7	11	150	3.27	73.0	K	LQEEMLQREEAENTLQSFR	Q	8517.23
		100.0	7	11	150	3.27	73.0	K	MALDIEIATYR	K	82745.7
		100.0	7	11	150	3.27	73.0	K	MALDIEIATYRK	L	53692.5
		100.0	7	11	150	3.27	73.0	R	MFGGPGTASR	P	6677.57
		100.0	7	11	150	3.27	73.0	R	MFGGPGTASRPSSSR	S	17234.2

		100.0	7	11	150	3.27	73.0	K	NLQEAEEWYK	S	24412.3
		100.0	7	11	150	3.27	73.0	K	NLQEAEEWYKSK	F	1378.16
		100.0	7	11	150	3.27	73.0	R	QDVDNASLAR	L	9228.12
		100.0	7	11	150	3.27	73.0	R	QMREMEENFAVEAANYQDTIGR	L	13425.0
		100.0	7	11	150	3.27	73.0	R	QVQSLTCEVDALK	G	12906.5
		100.0	7	11	150	3.27	73.0	R	QVQSLTCEVDALKGTNESLER	Q	21303.9
		100.0	7	11	150	3.27	73.0	K	SKFADLSEAANR	N	1918.23
		100.0	7	11	150	3.27	73.0	R	SLYASSPGGVYATR	S	238187
		100.0	7	11	150	3.27	73.0	R	SSVPGVR	L	3597.07
		100.0	7	11	150	3.27	73.0	R	TLLIKTVETR	D	2629.34
		100.0	7	11	150	3.27	73.0	R	TNEKVELQELNDR	F	18247.4
		100.0	7	11	150	3.27	73.0	K	TVETRDGQVINETSQHHDDLE	-	1730.31
		100.0	7	11	150	3.27	73.0	R	TYSLGSALRPSTSR	S	271798
		100.0	7	11	150	3.27	73.0	K	VELQELNDR	F	32897.2
		100.0	7	11	150	3.27	73.0	K	VESLQEEIAFLK	K	5480.90
		100.0	7	11	150	3.27	73.0	R	VEVERDNLAEDIMR	L	68942.6
105_81	Vimentin	100.0	6	10	142	3.93	70.6	R	DGQVINETSQHHDDLE	-	2584.34
	OS=Homo sapiens	100.0	6	10	142	3.93	70.6	R	DVRQQYESVAAK	N	2589.96
	GN=VIM PE=1 SV=4	100.0	6	10	142	3.93	70.6	R	EEAENTLQSFR	Q	18266.9
	VIME_HUMAN	100.0	6	10	142	3.93	70.6	R	EKLQEEMLQR	E	2611.25
	53652.7	100.0	6	10	142	3.93	70.6	R	EMEENFAVEAANYQDTIGR	L	7675.48
		100.0	6	10	142	3.93	70.6	R	ETNLDSLPLVDTHSK	R	29221.4
		100.0	6	10	142	3.93	70.6	R	ETNLDSLPLVDTHSKR	T	5108.11
		100.0	6	10	142	3.93	70.6	R	EYQDLLNVK	M	59825.1
		100.0	6	10	142	3.93	70.6	K	FADLSEAANR	N	118787
		100.0	6	10	142	3.93	70.6	K	FADLSEAANRNNDALR	Q	94761.1
		100.0	6	10	142	3.93	70.6	R	FANYIDK	V	14920.1
		100.0	6	10	142	3.93	70.6	R	FANYIDKVR	F	13960.5
		100.0	6	10	142	3.93	70.6	R	HLREYQDLLNVK	M	10444.8
		100.0	6	10	142	3.93	70.6	K	ILLAELEQLK	G	11081.2
		100.0	6	10	142	3.93	70.6	K	ILLAELEQLKGQGK	S	31181.3
		100.0	6	10	142	3.93	70.6	R	ISLPLPNFSSLNLR	E	19030.3
		100.0	6	10	142	3.93	70.6	R	KVESLQEEIAFLK	K	6389.43
		100.0	6	10	142	3.93	70.6	R	LGDLYEEEMR	E	57213.3
		100.0	6	10	142	3.93	70.6	R	LQDEIQNMK	E	7382.85
		100.0	6	10	142	3.93	70.6	R	LQDEIQNMKEEMAR	H	6123.52
		100.0	6	10	142	3.93	70.6	K	LQEEMLQR	E	14327.5
		100.0	6	10	142	3.93	70.6	K	LQEEMLQREEAENTLQSFR	Q	15902.0
		100.0	6	10	142	3.93	70.6	K	MALDIEIATYR	K	47744.1
		100.0	6	10	142	3.93	70.6	K	MALDIEIATYRK	L	48182.6
		100.0	6	10	142	3.93	70.6	R	MFGGPGTASRPSSSR	S	62780.1
		100.0	6	10	142	3.93	70.6	K	NLQEAEEWYK	S	31288.3
		100.0	6	10	142	3.93	70.6	K	NLQEAEEWYKSK	F	2368.80
		100.0	6	10	142	3.93	70.6	R	QMREMEENFAVEAANYQDTIGR	L	10973.9
		100.0	6	10	142	3.93	70.6	R	QVQSLTCEVDALK	G	17067.2
		100.0	6	10	142	3.93	70.6	R	QVQSLTCEVDALKGTNESLER	Q	28712.5
		100.0	6	10	142	3.93	70.6	K	SKFADLSEAANR	N	2629.38
		100.0	6	10	142	3.93	70.6	K	SKFADLSEAANRNNDALR	Q	4466.86
		100.0	6	10	142	3.93	70.6	R	SLYASSPGGVYATR	S	407718
		100.0	6	10	142	3.93	70.6	R	SSVPGVR	L	7419.84
		100.0	6	10	142	3.93	70.6	R	SYVTTSTR	T	4392.21
		100.0	6	10	142	3.93	70.6	R	TLLIKTVETR	D	4684.80
		100.0	6	10	142	3.93	70.6	R	TNEKVELQELNDR	F	20165.2
		100.0	6	10	142	3.93	70.6	R	TYSLGSALRPSTSR	S	380043
		100.0	6	10	142	3.93	70.6	K	VELQELNDR	F	24764.9
		100.0	6	10	142	3.93	70.6	K	VESLQEEIAFLK	K	9409.40
		100.0	6	10	142	3.93	70.6	R	VEVERDNLAEDIMR	L	51827.2
112_82	Perilipin-3	100.0	16	24	74	1.62	52.1	K	DTVATQLSEAVDATR	G	19613.4
	OS=Homo sapiens	100.0	16	24	74	1.62	52.1	R	GLDKLEENLPILQQPTEK	V	5148.61
	GN=PLIN3 PE=1 SV=3	100.0	16	24	74	1.62	52.1	R	IATSLDGFDVASVQQQR	Q	68100.7
	PLIN3_HUMAN	100.0	16	24	74	1.62	52.1	K	LEENLPILQQPTEK	V	3022.67
	47073.6	100.0	16	24	74	1.62	52.1	K	LEPQIASASEYAHR	G	5355.40
		100.0	16	24	74	1.62	52.1	R	LGQMVLSGVDTVLGK	S	38142.7
		100.0	16	24	74	1.62	52.1	R	QEQSYFVR	L	74155.8
		100.0	16	24	74	1.62	52.1	K	QLQGPEKEPPKPEQVESR	A	3032.47
		100.0	16	24	74	1.62	52.1	M	SADGAEADGSTQVTVEEPVQQ-PSVVDR	V	15400.3
		100.0	16	24	74	1.62	52.1	K	SEEWADNHLPLTDAELAR	I	13438.3
		100.0	16	24	74	1.62	52.1	K	SVVTGGVQSVMGSR	L	156550
		100.0	16	24	74	1.62	52.1	R	TLTAAAVSGAQPILSK	L	26775.8
		100.0	16	24	74	1.62	52.1	R	VASMPLISSTCDMVSAAYASTK	E	7180.51
		100.0	16	24	74	1.62	52.1	K	VLADTKELVSSK	V	17439.1
		100.0	16	24	74	1.62	52.1	K	VSGAQEMVSSAK	D	7962.10
		100.0	16	24	74	1.62	52.1	K	VSGAQEMVSSAKDTVATQLSEAVDATR	G	10291.5
112_85	Perilipin-3	100.0	3	5	129	2.81	50.5	K	DTVATQLSEAVDATR	G	54174.7

	OS=Homo sapiens	100.0	3	5	129	2.81	50.5	L	EPQIASASEYAHR	G	2528.70
	GN=PLIN3 PE=1 SV=3	100.0	3	5	129	2.81	50.5	R	GAVQSGVDKTKSVVTGGVQSVMGSR	L	9143.95
	PLIN3_HUMAN	100.0	3	5	129	2.81	50.5	R	GLDKLEENLPILQQPTEK	V	21853.0
	47073.6	100.0	3	5	129	2.81	50.5	R	IATSLDGFDVASVQQQR	Q	112354
		100.0	3	5	129	2.81	50.5	K	LEENLPILQQPTEK	V	14038.3
		100.0	3	5	129	2.81	50.5	K	LEPQIASASEYAHR	G	2807.69
		100.0	3	5	129	2.81	50.5	R	LGQMVLSGVDTVLGK	S	193266
		100.0	3	5	129	2.81	50.5	E	PQIASASEYAHR	G	7138.59
		100.0	3	5	129	2.81	50.5	R	QEQSYFVR	L	411483
		100.0	3	5	129	2.81	50.5	M	SADGAEADGSTQVTVEEPVQQ-PSVVDR	V	3754.01
		100.0	3	5	129	2.81	50.5	K	SEEWADNHLPLTDAELAR	I	37765.8
		100.0	3	5	129	2.81	50.5	K	SVVTGGVQSVMGSR	L	492880
		100.0	3	5	129	2.81	50.5	R	TLTAAAVSGAQPILSK	L	111255
		100.0	3	5	129	2.81	50.5	R	VASMPLISSTCDMVSAAYASTK	E	38330.7
		100.0	3	5	129	2.81	50.5	K	VLADTKELVSSK	V	151855
		100.0	3	5	129	2.81	50.5	K	VSGAQEMVSSAK	D	22946.1
		100.0	3	5	129	2.81	50.5	K	VSGAQEMVSSAKDTVATQLSEAVDATR	G	25459.7
115_81	Elongation factor 1-δ	100.0	4	4	7	0.435	15.7	M	ATNFLAHEK	I	38047.5
	OS=Homo sapiens	100.0	4	4	7	0.435	15.7	R	FYEQMNGPVAGASR	Q	2222.31
	GN=EEF1D PE=1 SV=5	100.0	4	4	7	0.435	15.7	R	IASLEVENQSLR	G	8043.97
	EF1D_HUMAN	100.0	4	4	7	0.435	15.7	K	LVPVGYGIR	K	45355.6
	31121.9										
115_82	Elongation factor 1-δ	100.0	8	10	56	2.43	50.2	R	ATAPQTQHVSPMRQVEPPAK	K	15871.8
	OS=Homo sapiens	100.0	8	10	56	2.43	50.2	M	ATNFLAHEK	I	484485
	GN=EEF1D PE=1 SV=5	100.0	8	10	56	2.43	50.2	R	FYEQMNGPVAGASR	Q	51977.0
	EF1D_HUMAN	100.0	8	10	56	2.43	50.2	R	GVVQELQQAISK	L	15633.1
	31121.9	100.0	8	10	56	2.43	50.2	R	IASLEVENQSLR	G	111963
		100.0	8	10	56	2.43	50.2	K	LVPVGYGIR	K	688549
		100.0	8	10	56	2.43	50.2	K	LVPVGYGIRK	L	13889.8
		100.0	8	10	56	2.43	50.2	R	QENGASVILR	D	86197.3
		100.0	8	10	56	2.43	50.2	R	QENGASVILRDIAR	A	55535.0
		100.0	8	10	56	2.43	50.2	R	RFYEQMNGPVAGASR	Q	4081.67
		100.0	8	10	56	2.43	50.2	R	SIQLDGLVWGASK	L	46536.5
		100.0	8	10	56	2.43	50.2	K	SLAGSSGPGASSGTSGDHGELVVR	I	144343
		100.0	8	10	56	2.43	50.2	K	VGTDLLEEEITK	F	4112.10